ISSN 1300 - 6045
e-ISSN 1309 - 2251

KAFKAS ÜNİVERSİTESİ VETERİNER FAKÜLTESİ DERGİSİ

Journal of the Faculty of Veterinary Medicine, Kafkas University

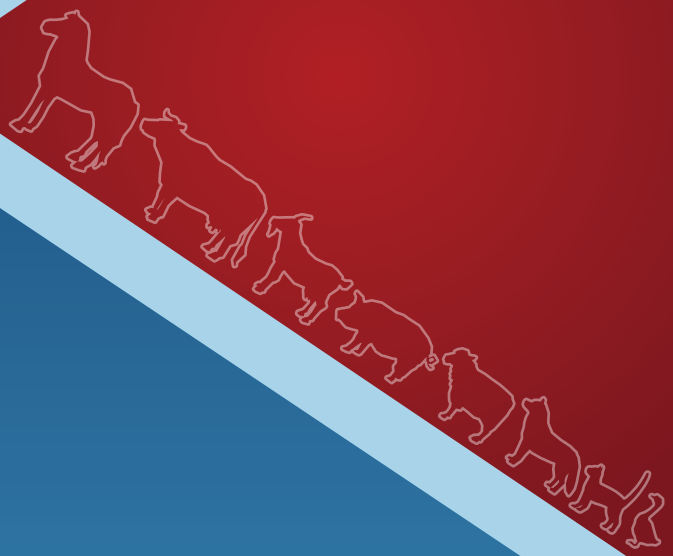

http://vetdergi.kafkas.edu.tr

Online Submission
http://submit.vetdergikafkas.org

Volume: 27
Issue: 3 (May - June)
Year: 2021

ISSN 1300 - 6045
e-ISSN 1309 - 2251

KAFKAS ÜNİVERSİTESİ VETERİNER FAKÜLTESİ DERGİSİ

Journal of the Faculty of Veterinary Medicine, Kafkas University

Published Bi-monthly

Volume: 27
Issue: 3 (May - June)
Year: 2021

ISSN (Print): 1300-6045 **ISSN (Electronic): 1309-2251**

This journal is published bi-monthly, by the Faculty of Veterinary Medicine, University of Kafkas, Kars - Turkey

This journal is indexed and abstracted in:

- Web of Science Core Collection: Science Citation Index Expanded (since 2007)
- Additional Web of Science Indexes: Essential Science Indicators - Zoological Record
- CABI - Veterinary Science Database
- DOAJ
- EBSCO - Academic Search Premier
- Elsevier - SCOPUS
- Elsevier - EMBASE
- Index Copernicus
- SOBİAD Atıf Dizini
- TÜBİTAK/ULAKBİM TR-Dizin
- Türkiye Atıf Dizini

Print

ESER OFSET MATBAACILIK
BOSNAHERSEK CAD. ALTUNALEM YAPI KOOP. ZEMİN KAT - ERZURUM
Tel: +90 442 2334667 E-mail: eserofset25@hotmail.com

Address for Correspondence

Kafkas Üniversitesi Veteriner Fakültesi Dergisi Editörlüğü 36040, Kars - TÜRKİYE
Phone: +90 474 2426807-2426836/5228 Fax: +90 474 2426853
E-mail: vetdergi@kafkas.edu.tr

Electronic Edition http://vetdergikafkas.org

Online Submission http://submit.vetdergikafkas.org

The Referees List of This Issue *(in alphabetical order)*

Abdullah KARASU	Van Yüzüncü Yıl Üniversitesi Veteriner Fakültesi
Ahmet Cumhur AKIN	Burdur Mehmet Akif Ersoy Üniversitesi Veteriner Fakültesi
Akiko UEMURA	Tokyo University of Agriculture and Technology, Faculty of Veterinary Medicine, Japan
Aytaç AKÇAY	Ankara Üniversitesi Veteriner Fakültesi
Bilal AKYÜZ	Erciyes Üniversitesi Veteriner Fakültesi
Bilal DİK	Selçuk Üniversitesi Veteriner Fakültes
Bülent EKİZ	İstanbul Üniversitesi-Cerrahpaşa Veteriner Fakültesi
Damla BİNNETOĞLU	Kafkas Üniversitesi Tıp Fakültesi
Ekin Emre ERKILIÇ	Kafkas Üniversitesi Veteriner Fakültesi
Elham HASSAN	Cairo University Faculty of Veterinary Medicine, Egypt
Elif DOĞAN	Kastamonu Üniversitesi Veteriner Fakültesi
Elmas ULUTAŞ	Yozgat Bozok Üniversitesi Veteriner Fakültesi
Erdoğan UZLU	Balıkesir Üniversitesi Veteriner Fakültesi
Evren ESİN	Çukurova Üniversitesi Ceyhan Veteriner Fakültesi
Fatma Bahar SUNAY	Balıkesir Üniversitesi Tıp Fakültesi
Funda YİĞİT	İstanbul Üniversitesi-Cerrahpaşa Veteriner Fakültesi
Gökmen ERASLAN	Erciyes Üniversitesi Veteriner Fakültesi
Hamidreza FATTAHIAN	Islamic Azad University, Faculty of Specialized Veterinary Sciences, Iran
Hasan ERDOĞAN	Aydın Adnan Menderes Üniversitesi Veteriner Fakültesi
Hasan Tarık ATMACA	Kırıkkale Üniversitesi Veteriner Fakültesi
Haydar ÖZPINAR	Altınbaş Üniversitesi/Uygulamalı Bilimler Fakültesi
Hikmet Yeter ÇOGUN	Çukurova Üniversitesi Ceyhan Veteriner Fakültesi
Hülya YALÇINTAN	İstanbul Üniversitesi-Cerrahpaşa Veteriner Fakültesi
İbrahim CEMAL	Aydın Adnan Menderes Üniversitesi Ziraat Fakültesi
İlker ÇAMKERTEN	Aksaray Üniversitesi Veteriner Fakültesi
İrem ERGİN	Ankara Üniversitesi Veteriner Fakültesi
Kor YERELİ	Manisa Celal Bayar Üniversitesi Tıp Fakültesi
Kozet AVANUS	İstanbul Üniversitesi-Cerrahpaşa Veteriner Fakültesi
Lora KOENHEMSİ	İstanbul Üniversitesi-Cerrahpaşa Veteriner Fakültesi
Musa SARICA	Ondokuz Mayıs Üniversitesi Ziraat Fakültesi
Musa TATAR	Burdur Mehmet Akif Ersoy Üniversitesi Veteriner Fakültesi
Mustafa HİTİT	Kastamonu Üniversitesi Veteriner Fakültesi
Mükremin Özkan ARSLAN	Kafkas Üniversitesi Tıp Fakültesi
Nail Tekin ÖNDER	Kafkas Üniversitesi Veteriner Fakültesi
Nazire MİKAİL	Siirt Üniversitesi Ziraat Fakültesi
Necati TİMURKAAN	Fırat Üniversitesi Veteriner Fakültesi
Nihal Y. GÜL SATAR	Bursa Uludağ Üniversitesi Veteriner Fakültesi
Nihat YUMUŞAK	Harran Üniversitesi Veteriner Fakültesi
Özden ÇOBANOĞLU	Bursa Uludağ Üniversitesi Veteriner Fakültesi
Özgür KURT	Acıbadem Mehmet Ali Aydınlar Üniversitesi Tıp Fakültesi
Özlem GÜZEL	İstanbul Üniversitesi-Cerrahpaşa Veteriner Fakültesi
Pavel HYRSL	Masaryk University, Faculty of Science, Czech Republic
Raziye IŞIK	Tekirdağ Namık Kemal Üniversitesi Ziraat Fakültesi
Savaş ÖZTÜRK	Kafkas Üniversitesi Veteriner Fakültesi
Savaş SARIÖZKAN	Erciyes Üniversitesi Veteriner Fakültesi
Semih ALTAN	Dicle Üniversitesi Veteriner Fakültesi
Seray TÖZ	Ege Üniversitesi Tıp Fakültesi
Serkan Kemal BÜYÜKÜNAL	İstanbul Üniversitesi-Cerrahpaşa Veteriner Fakültesi
Sırrı KAR	Tekirdağ Namık Kemal Üniversitesi Fen Edebiyat Fakültesi
Tolga KAHRAMAN	İstanbul Üniversitesi-Cerrahpaşa Veteriner Fakültesi
Volkan KOŞAL	Van Yüzüncü Yıl Üniversitesi Veteriner Fakültesi
Yurdakul Deniz FIRAT	Sağlık Bilimleri Üniversitesi Bursa Yüksek İhtisas EAH

Kafkas Universitesi Veteriner Fakultesi Dergisi
ISSN: 1300-6045 e-ISSN: 1309-2251
Journal Home-Page: http://vetdergikafkas.org

Kafkas Univ Vet Fak Derg
27 (3): 271-277, 2021
DOI: 10.9775/kvfd.2020.24894

RESEARCH ARTICLE

Evaluation of Homocysteine Levels in Neonatal Calves with Diarrhea

Süleyman KOZAT [1,a (*)] Cumali ÖZKAN [1,b] Eda Nur OKMAN [1,c]

[1] Department of Internal Medicine, Faculty of Veterinary Medicine, University of Yuzuncu Yil, TR-65080 Van - TURKEY
ORCIDS: [a] 0000-0001-5089-2623; [b] 0000-0001-8502-6987; [c] 0000-0001-9016-9739

Article ID: KVFD-2020-24894 Received: 26.08.2020 Accepted: 24.05.2021 Published Online: 26.05.2021

Abstract

The aim of this study was to investigate the relationship between serum homocysteine (HCY), and creatinine, urea, venous blood gas and electrolytes values in neonatal calves with diarrhea. The study was conducted on a total of 30 calves, 20 with diarrhea and 10 healthy (control), with diarrhea complaints, of different races, sexes and ages ranging from 2-24 days. According to the venous blood gas results, the pCO_2 and base deficit values of calves with diarrhea were significantly higher ($P<0.001$) compared to the control group values, while pH, pO_2 and HCO_3 values were significantly lower ($P<0.001$). While serum Na^+ and Cl^- concentrations in diarrheic calves did not show any statistical change when compared to the control group ($P>0.05$), serum K^+ concentrations were statistically higher ($P<0.001$). Serum HCY, folate and vitamin B_{12} concentration values of diarrheic calves were significantly higher ($P<0.001$) when compared to the control group. As a result; in neonatal calves with diarrhea, it has been concluded that homocystein excretion is disrupted by low renal excretion due to decrease in glomerular filtration rate that caused hyperhomocysteine. In addition, it is thought that this study will shed light on studies that will reveal the effect of hyperhomocysteinemia in the cardiovascular system in diarrheic calves.

Keywords: *Homocysteine, Neonatal calf, Diarrhea*

Yenidoğan İshalli Buzağılarda Homosistein Düzeylerinin Değerlendirilmesi

Öz

Bu çalışmanın amacı ishalli yenidoğan buzağılarda serum homosistein (HCY) ile kreatinin, üre, venöz kan gazı ve elektrolit değerleri arasındaki ilişkiyi araştırmaktır. Araştırma, ishal şikayeti olan, farklı ırk ve cinsiyette ve yaşları 2-24 gün arasında değişen 20 ishalli ve 10 sağlıklı (kontrol) olmak üzere toplam 30 buzağı üzerinde yürütüldü. Venöz kan gazı sonuçlarına göre, ishalli buzağıların pCO_2 ve baz açığı değerleri kontrol grubu değerlerine göre önemli ($P<0.001$) düzeyde yüksek belirlenirken, pH, pO_2 ve HCO_3 değerleri anlamlı ($P<0.001$) düzeyde düşük saptandı. İshalli buzağılarda Na^+ ve Cl^- elektrolit konsantrasyonlarının seviyeleri kontrol grubuna göre anlamlı bulunmazken, serum K^+ elektrolit konsantrasyon seviyeleri kontrol grubuna göre önemli düzeyde ($P<0.001$) yüksek tespit edildi. İshalli buzağıların serum HCY, folat ve vitamin B_{12} konsantrasyon değerleri kontrol grubuna göre anlamlı olarak yüksek ($P<0.001$) bulundu. Sonuç olarak; yenidoğan ishalli buzağılarda sıvı kaybına bağlı olarak dolaşımdaki sıvı hacmi azalmakta ve böbreklerin glomüler filtrasyon hızı düşmektedir. Böbreklerde düşen glomüler filtrasyon hızına bağlı olarak homosisteinin böbrek yoluyla atılımı aksamakta ve sonucunda da hiperhomosisteine neden olmaktadır. Ayrıca ishal vakalarında artan homosistein konsantrasyonlarının kardiyovasküler sistemde bozukluklara neden olup olmadığına yönelik yapılacak araştırmalara ışık tutacaktır.

Anahtar sözcükler: *Homosistein, Yenidoğan buzağı, İshal*

INTRODUCTION

Calf scour remains one of the most important problems faced by livestock industry [1] despite all the developments in the field of prophylaxis and treatment of calf scour. It is still common today and is directly related to deaths; it also leads to indirect economic losses with development pause and treatment expenses [2,3]. It is reported that diarrhea affects 90-100% of neonatal calves in some livestock farming [1], diarrhea related death in calves is more common than those of other reasons and causes great economic losses in Turkey livestock economy. The loss of fluid and electrolyte in diarrhea occurs mainly from the extracellular compartment in the body (intravascular + extravascular fluid) and as a result dehydration develops [2]. High fluid loss causes a decrease in plasma volume (hypovolemia),

How to cite this article?

Kozat S, Özkan C, Okman EN: Evaluation of homocysteine levels in neonatal calves with diarrhea. *Kafkas Univ Vet Fak Derg,* 27 (3): 271-277, 2021. DOI: 10.9775/kvfd.2020.24894

(*) Corresponding Author

Tel: +90 533 5525466
Fax: +90 432 2251127
E-mail: skozat@hotmail.com (S. Kozat)

hemoconcentration and low blood pressure. Decreased arterial blood pressure leads to decreased renal function and prerenal azotemia and H^+ excretion, on the other hand, increase anaerobic metabolism with decreased tissue perfusion [1-3].

Homocysteine (HCY) is a sulfurous amino acid that does not participate in proteins formed by methionine metabolism [4-7]. Plasma HCY is metabolised by remethylation and transsulfuration mechanisms [5,8]. S-adenosyl homocysteine (SAH) is formed by using S-adenosylmethionine (SAM) as a methyl donor by transmethylation. By hydrolyzing SAH, homocysteine and adenosine are formed [9]. Homocysteine is converted to methionine by remethylation where N5-methyltetrafolate is the methyl donor and vitamin B_{12} is cofactor [6]. In the remethylation pathway, methionine synthase and N5-methyltetrafolate reductase enzymes act as catalysts. In addition, remethylation takes place in the liver and kidney by using the betaine methyl donor and the betaine-homocysteine methyltransferase enzyme, independent of vitamin B_{12} and folic acid [10]. Vitamin B_6 is used as a cofactor in the transsulfuration pathway in the kidneys. Homocysteine is combined with serine and cystathionine is synthesized with the enzyme B-cystathionine synthase. Cystathionine is also converted into cysteine with the enzyme cystathionesis. Cysteine is either excreted directly from the kidneys or converted into glutathione and sulfate [4,6,11].

Increases in plasma total homocysteine levels are reported to be caused by N5-methyltetrahydrofolate reductase and cystathionine B synthetase enzyme defects, or dietary deficiencies of enzyme cofactors B_{12}, B_6 and folic acid [6]. Plasma homocysteine levels increase with creatine due to renal failure [12]. The increase in total homocysteine levels, ie, hyperhomocysteinemia, has been shown to cause cardiovascular system disease as a result of its role in atherogenesis, atherosclerosis and thrombosis [10]. Hyperhomocysteinemia causes direct vascular endothelial damage, changes the anticoagulant effect of the endothelium to procoagulant and causes proliferation in smooth muscle cells [10,13]. Present information clarifies that the accurate renal function play basic role in homocysteine clearance. This vitnessing and the reverse connection between homocysteine amounts and glomerular filtration rate (GFR) signifies that the kidneys play important role in HCY metabolism [6]. Although plasma folic acid levels are normal in kidney failure in many studies, decreasing plasma total homocysteine levels with folic acid supplementation have increased the possibility of relative intracellular vitamin deficiency [14]. This situation is reported to be related to the disorder in the conversion of folate to metabolically appropriate form [6]. Homocysteine is an intermediate of methionine metabolism. Hyperhomocysteinemia (HHCY) can be caused by a deficiency in enzymes or vitamin cofactors required for HCY metabolism, or from kidney disease [4,6,12,14].

Research has shown that there is a close relationship between plasma HCY and GFR. HCY is cleared from the body by urinary excretion after glomerular filtration, just like creatinine. It has been presented that kidney plays a major role in the maintenance of HCY plasma homeostasis in rats [15]. Decreased kidney function in chronic uremic patients, which is one of the causes of hyperhomocysteinemia, is an important determinant for plasma homocysteine concentration and there is a close relationship between decreased kidney reserve and homocysteine levels [14]. Homocysteine levels increase at least three to four times in patients with renal failure compared to normal individuals [16].

In this study was investigated the relationship between serum HCY and creatinine, urea, venous blood gas and electrolyte values in newborn calves with diarrhea. Fluid volume and glomerular filtration rate decreases as a result of dehydration in neonatal calves with diarrhea. The homocysteine transsulfuration mechanism is thought to be impaired as a result of the decreased GFR. Based on this equation, homocysteine will cause an increase in the total plasma homocysteine level as a result of disruption of transsulfuration mechanism in homocysteine. It was aimed to reveal whether there is a change in homocysteine levels in dehydrated calves, especially due to decreased kidney function.

Material and Methods

This research was approved (28/12/2017 and 27552122-604.01.02-E.91873) by the Animal Research Ethical Committee of Van Yuzuncu Yil University, Local Ethics Committee.

Animal

The animal material of this experiment consisted of 2-24 days old 30 calves from different races and genders brought to the Veterinary Faculty of Animal Hospital. Thirty calves were divided into 2 groups as twenty calves were diarrheic and ten calves were healthy (control). All calves in the control and experimental groups were examined on physical examination. The diarrheic calves were assessed by evaluating; defecation frequency (>4 times per day), fecal consistency (color and content), intensity (mucous, bloody an abundant), body temperature, heart frequencies, skin elasticity, position of the eye in the orbit, body retention, suction reflex examination and duration of diarrhea [17]. Calves were classified as having diarrhea after being evaluated according to clinical examination.

Laboratory Analysis

Blood samples were taken from *v. jugularis* in accordance with the technique for the analysis of hematological and biochemical parameters in diarrheic calves and healthy calves.

Hematological Analysis

In order to analyse the hematological parameters, blood samples were taken from *v. jugularis* into anticoagulated tubes (3 mL EDTA) in accordance with the blood samples technique. Hemoglobin concentration (HB), hematocrit value (HCT), leukocyte count (LEU), erythrocytes (RBC), platelet count (PLT), lymphocytes (LYM), monocytes (Mon), neutrophil (NEU), eosinophil (EO) and mean corpuscular hemoglobin concentration (MCHC) values were measured from the blood samples taken in anticoagulated tubes with the Veterinary Hemogram device (Veterinary MS4-s-Melet Schloesing Laboratories in France).

Blood Gas Analysis

Whole blood from the vena jugularis of the calves with dry lithium heparin content (2 mL, 22G × 11 / 4) were taken for blood gas analysis and blood gas analysis were performed for 3 min. Blood gases (pH, pCO_2, pO_2, HCO_3 and base deficit), Na^+ (mmol/L), K^+ (mmol/L) and Cl^- (mmol/L) concentrations of diarrheic and healthy calves were measured with the blood gases analyser (Radiometer ABL80, Denmark).

Biochemical Analysis

Blood samples were taken from *v. jugularis* to gel biochemical serum tubes (10 mL) to analyze biochemical parameters. Serum tubes were centrifuged for 15 min at 3000 rpm (rate per minute) and serum sample were taken into eppendorfs. The serum samples were kept at -20°C until biochemical parameters analysis. In serum samples obtained, total protein, albumin, urea and creatinine levels of diarrheic and healthy calves were measured with the autoanalyzer (BS-120 Vet-Mindray, China) device. Serum homocysteine levels of diarrheic and healthy calves were measured using the ELISA device (Biotek Elx800) as specified in the procedure of the homocysteine commercial test kits (Axis® Homocysyeine EIA-UK). Serum vitamin B_{12} and folate levels of diarrheic and healthy calves were measured with the autoanalyzer (Elecyc 2010 Roche Hitachi-Japan).

Statistical Analysis

Descriptive statistics for the results were expressed as mean and standard deviation. Independent samples t-test was used to compare two groups (diarrhea and healthy). Pearson Correlation was used to some variables in calves with diarrhea. SPPS 21 (IBM, USA) package program was used for necessary statistical analysis.

Results

Hematological Findings

In the statistical analysis; WBC, HCT, EO MCV, MCH and HB values of calves with diarrhea were significantly higher than those of the control group (P<0.001) and PLT value was found to be significantly lower (P<0.001) *(Table 1)*.

Biochemical Findings

In the statistical analysis of biochemical parameters; urea, creatinine and total protein levels of diarrheic calves were significantly higher when compared with the same parameters of the control group (P<0.001, P<0.05) *(Table2)*.

According to the statistical analysis; while the pCO_2 value of calves with diarrhea was found to be significantly higher compared to the control group (P<0.001), pH, pO_2, HCO_3 and base deficit values of calves with diarrhea were significantly lower than those of the control group *(Table 3)*.

The concentrations of Na^+ and Cl^- electrolytes in calves with diarrhea were not significantly different from than those of the control group, however, the concentration levels of K^+ in diarrheic calves were significantly higher compared to the control group (P<0.001) *(Table 4)*.

Table 1. *Hematological parameters in healthy calves and dehydrated calves with diarrhoea*

Parameter	Healthy Calves (n=10) X ± SD	Diarrhoeic Calves (n=20) X ± SD	P Value
Age (day)	12.80±4.32	12.90±5.54	0.374
WBC (m/mm³)	10.37±1.03	15.86±7.39*	0.028
RBC (m/mm³)	9.01±0.90	8.87±1.79	0.822
HCT (%)	28.36±2.73	40.07±4.94*	0.001
LYM (m/mm³)	6.92±1.49	7.89±5.76	0.608
MON (m/mm³)	0.58±0.11	0.76±0.41	0.164
NEU(m/mm³)	4.53±1.34	5.55±3.76	0.415
EO (m/mm³)	0.38±0.13	0.84±0.69*	0.049
PLT (m/mm³)	699.70±278.35	336.95±169.83*	0.001
MCV (fl)	29.06±3.151	34.23±3.77*	0.001
MCH (pg)	12.31±1.36	13.61±1.49*	0.028
HB (g/dL)	10.11±1.23	12.79±2.66*	0.005

WBC: *White blood cell;* ***RBC:*** *red blood cell;* ***HCTt:*** *hematocrit;* ***LYM:*** *lymphocyte;* ***MON:*** *monocyte;* ***NEU:*** *neutrophil;* ***EO:*** *eosinophil;* ***PLT:*** *platelet;* ***MVC:*** *mean corpuscular volume;* ***MCH:*** *mean corpuscular hemoglobin;* ***HB:*** *hemoglobin;* ******* *Means in the same row with different superscripts are significantly different (P<0.05)*

Table 2. *Biochemical parameters in healthy calves and dehydrated calves with diarrhoea*

Parameter	Healthy Calves (n=10) X ± SD	Diarrhoeic Calves (n=20) X ± SD	P Value
Albumin (g/dL)	2.64±0.64	2.88±0.36	0.293
TP (g/dL)	5.81±0.96	6.80±1.10*	0.021
Creatinine (mg/dL)	0.74±0.07	2.68±1.40*	0.001
Urea (mg/dL)	17.03±5.87	62.87±22.35*	0.001

TP: *total protein;* ******* *Means in the same row with different superscripts are significantly different (P<0.05)*

Table 3. *Blood gas parameters in healthy calves and dehydrated calves with diarrhoea*

Parameter	Healthy Calves (n=10) X ± SD	Diarrhoeic Calves (n=20) X ± SD	P Value
pH	7.33±0.05	7.15±0.09*	0.001
pCO_2 (mm/Hg)	33.94±3.91	39.37±4.28*	0.002
pO_2 (mm/Hg)	39.90±4.63	28.40±6.51*	0.001
HCO_3^- (mmol/L)	21.66±4.67	15.57±6.19*	0.011
Base deficit (mmol/L)	18.01±3.02	-1.08±8.23*	0.001

pO_2: *partial pressure of oxygen;* ***pCO_2:*** *partial pressure of carbondioxyde; * Means in the same row with different superscripts are significantly different (P<0.05)*

Table 4. *Serum electrolyte concentrations in healthy calves and dehydrated calves with diarrhoea*

Parameter	Healthy Calves (n=10) X ± SD	Diarrhoeic Calves (n=20) X ± SD	P Value
Na^+ (mmol/L)	137.20±3.01	134.10±7.75	0.236
K^+ (mmol/L)	4.99±0.25	6.55±1.23*	0.001
Cl^- (mmol/L)	99.90±4.70	97.60±8.10	0.411

** Means in the same row with different superscripts are significantly different (P<0.05)*

Table 5. *Homocysteine, vitamin B_{12} and folate concentrations in healthy calves and dehydrated calves with diarrhoea*

Parameter	Healthy Calves (n=10) X ± SD	Diarrhoeic Calves (n=20) X ± SD	P Value
HCY (µmol/L)	0.87±0.22	1.43±0.32*	0.001
Vitamin B_{12} (pg/mL)	149.57±28.58	248.50±101.41*	0.006
Folate (ng/mL)	4.66±3.28	12.08±7.61*	0.007

HCY: *homocysteine; * Means in the same row with different superscripts are significantly different (P<0.05)*

Serum homocysteine, folate, and vitamin B_{12} concentration values of diarrheic calves were significantly higher (P<0.001) compared to the control group *(Table 5)*.

In the statistical analysis of the correlations of some variables of neonatal calves with diarrhea, a positive correlation was found between serum HCY, creatinine, and urea levels (r=0.95, P<0.001; r=0.97, P<0.001, respectively) *(Fig.1)*.

Discussion

It has been reported that significant changes in hematological parameters are detected depending on the degree of dehydration in fluid losses due to diarrhea [2,17-19]. There is a positive relationship between the degree of dehydration and Hct value in calves with diarrhea and the severity of dehydration can be determined from the HCT value [2]. Increased HCT value, RBC count, WBC, NEU count and HB values have been reported in neonatal calves with diarrhea [1,2]. It is reported that it occurs as a result of the reaction of the body against leukocytosis, gastro-intestinal infection in cases with diarrhea [1]. In this study, WBC, HCT, EO, MCV and MCH values of diarrheic calves were found to be significantly higher when compared with the same parameters of the control group (P<0.001), while the PLT value was found to be significantly lower. Some researchers [1,20] reported changes in hematological parameters in calves with diarrhea. Also in this study, increases in MCV and MCH results from the increase in hemoglobin concentration.

In many studies, in general, a decrease in bicarbonate concentration in calves with diarrhea is considered as a marker of acidosis [21]. In calves with diarrhea, metabolic acidosis initially results in bicarbonate with feces, as well as the presence of unidentified organic acids in plasma [22,23] and a decrease in glomerular filtration rate in response to

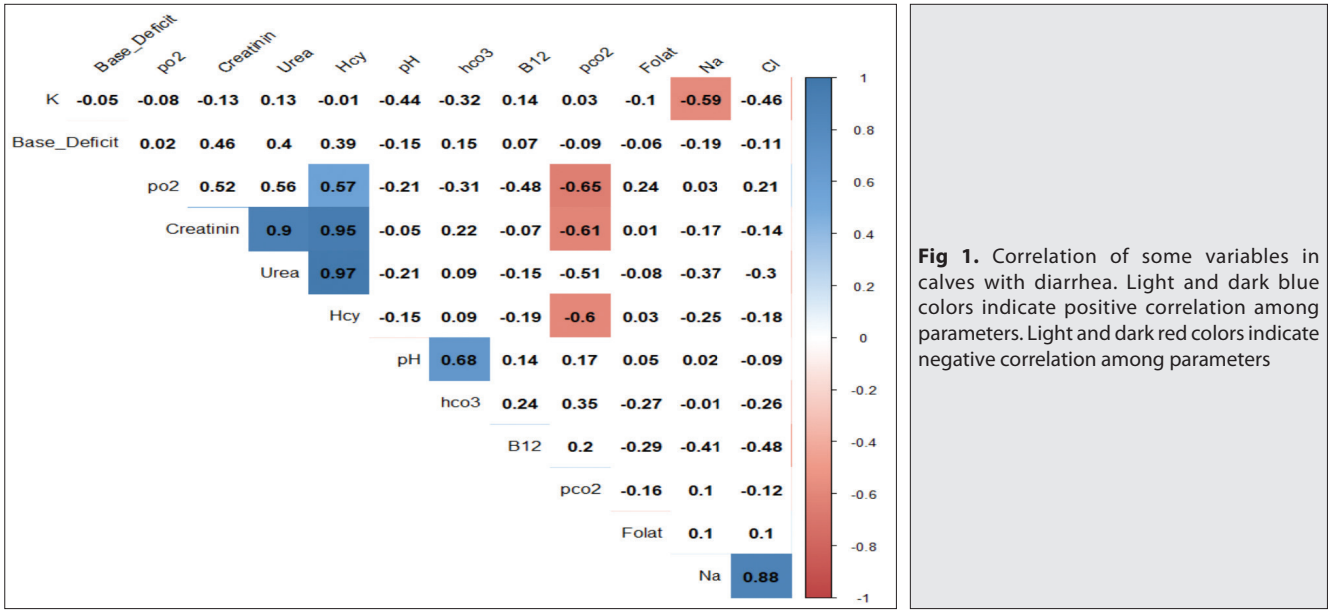

Fig 1. Correlation of some variables in calves with diarrhea. Light and dark blue colors indicate positive correlation among parameters. Light and dark red colors indicate negative correlation among parameters

severe dehydration [18]. In calves with diarrhea, pH<7.28 and HCO_3^- concentration of 20.0 mmol/L are reported, which reflects metabolic acidosis [3,19]. In another study, researchers found the mean base excess to calves with 4-8% dehydrated and moderately metabolic acidosis: –9.6 mEq/L, average pCO_2: 43 mmHg, average pO_2: 39 mmHg and average pH: 7.21 [24]. In this study, pH of calves with diarrhea was determined as 7.15±0.10, pCO_2: 39.37±4.28, pO_2: 28.40±6.51, HCO_3^-:15.57±6.19 and base deficit: -1.08±8.23 mmol/L. The values of the blood gas parameters obtained in our study are similar to the findings of many researchers [3,18,19,24].

In calves with diarrhea, arterial blood pressure and glomerular filtration rate (GFR) decreases as a result of hypovolemia [2,19,25], urine and creatinine retention increase, and serum concentrations of these nitrogenous substances increase [2]. In this study; while control group calves had urea: 17.03±5.87 mg/dL and creatinine:0.74±0.07 mg/dL, calves with diarrhea were determined to have urea: 62.87±22.35 mg/dL and creatinine: 2.68±1.40 mg/dL. However, urea and creatinine levels of calves with diarrhea were significantly higher than the control group (P<0.001). The urea and creatinine data of calves with diarrhea support the data of the previous studies [2,21]. The buffering required eliminating diarrhea-induced acidemia results in hyperkalemia as a result of K^+. Hyperkalemia results from the direct electrochemical exchange of potassium for protons across the cell membrane [2,18]. Therefore, H^+ in the extracellular fluid enters the intracellular fluid, whereas K^+ in the intracellular fluid enters the extracellular fluid [19]. Strongest relations were described between plasma K^+ and indices dehydration, emphasizing the importance of decreased glomerular filtration rate for the development of hyperkalemia [2,19,21]. In this study, the increase in serum K^+ concentrations in calves with diarrhea supports the researchers' data and hypotheses [2,19,25].

Several studies in different diseases have been conducted in the fields of human and veterinary medicine regarding the plasma and serum homocysteine [5,9-15,26]. However, there was no research on whether there was a change in HCY concentrations in patients with fluid loss due to diarrhea. There is a direct relationship between homocysteine and reduction in glomerular filtration and serum creatinine reduction in kidneys impairment. Creatinine concentration level in individuals is between 150-500 µmol/L, typically homocysteine values are between 20-30 µmol/L in human medicine [27]. In kidney dysfunction, this mechanism does not work and accordingly an increase in the total amount of homocysteine in plasma is observed [10]. Hyperhomocysteine is existent in individuals with declining kidney function, so that this alteration can be considered as a major factor in the progression of kidney diseases [28]. Vascular complications related to hyperhomocysteinemia may also occur in uremic pediatric patients [26]. There is highly correlated GFR (r= -0.70, P<0.001) plasma homocysteine as a result of decreased kidney function in moderate renal failure [29]. In determining GFR, serum homocysteine level plays a key role in early diagnosis of kidney diseases compared to serum creatinine level [16,29]. Serum creatinine and blood urea nitrogen measurements are easy for indirect symptoms of GFR [30]. Increased protein catabolism due to fasting, other than prerenal insufficiency, exacerbates the increase in serum urea concentration in calves with diarrhea [2]. In a study, it has been reported that there is a positive correlation between plasma homocysteine concentration and creatinine level and negative correlation with creatinine clearance [14]. In this study, a positive correlation was found between creatinine levels and HCY concentrations of diarrheic calves. Serum HCY concentration levels were high in cases with high creatinine concentrations. These data support the data of many researchers who reveal the relationship between creatinine, HCY and kidney function [14,27-29].

Other amino acids and intermediates involved in homocysteine metabolism are also affected in patients with uremia. Patients have normal levels of methionine, whereas transsulfurization metabolites such as cystationin and cysteine are high. It has been shown that plasma concentration of intermediates such as S-adenosyl methionine (Ado-Met) and S-adenosyl homocysteine (Ado-HCY) increase, the increase in Ado-HCY is more pronounced, and accordingly the Ado-Met/Ado-HCY ratio decreases. Increased plasma and erythrocyte homocysteine in uremic patients have been found to cause the accumulation of Ado-HCY, a toxic component in erythrocytes [16]. It is stated that plasma cysteine-homocysteine mixed disulfide levels have a positive correlation between creatinine levels in patients with renal failure [26]. In our study, the increase in HCY concentrations of diarrhea calves and the higher vitamin B_{12} and folate levels compared to the control group supports the data of the researchers [16,26]. Plasma HCY concentrations did not decrease although homocysteine metabolism increased in favor of transsulphration due to the disruption of remethylation pathway in uremic patients [15,16]. In many studies, plasma HCY levels have been reported to be significantly increased in patients with moderate renal impairment and HCY level has increased significantly in the last stage of kidney disease [11]. An increase in plasma HCY level in kidney diseases may result from an increased production rate (i.e. transmethylation), a reduced rate of extraction from transsullation or remethylation, or a decrease in HCY excretion [31]. In human medicine, HCY is used to evaluate complications of kidney, cardiovascular and other diseases [11,15,26]. HCY has been shown to be an independent risk factor for cardiovascular disease in kidney patients. It has been reported that there is a positive correlation between plasma HCY levels and GFR and serum creatinine [32]. Current evidence suggests that the main mechanism for hyperhomocysteinemia in kidney failure is a reduction in HCY removal from the body. However, it

is argued whether the increase in homocysteine level is a result of a decrease in kidney metabolic clearance or a result of extrarenal metabolic changes [31]. Kidneys play a major role in removing a large number of aminotiol or HCY-related compounds from the circulation (i.e cysteine-glycine, glutathione, AdoMet and AdoHCY) in human medicine [15]. However, the glomerular filtration of HCY appears to be limited due to protein binding. Besides of the glomerular filtration, it can remove normal kidney HCY by plasma flow and peritubular uptake. Although it is in the absolutely low normal range, if it is associated with HCY levels in uremia, flow decreases along the transsulfuration path; In addition, the remethylation path is impaired and HCY increases in mild to moderate renal failures [31]. Because there is a tight relationship between plasma flow and GFR, and decreasing GFR causes an increase in plasma HCY levels [11]. In this study, urea, creatinine and HCY levels of diarrheic calves were found to be significantly higher than those of the control group. In addition, in the statistical analysis of the correlations of some variables of diarrheic calves, positive correlation was found between HCY and creatinine and urea concentrations (respectively r= 0.95, P<0.001; r=0.97, P<0.001). It is known that the increase in HCY levels in calves with diarrhea may be due to decreased glomerular filtration. The study supports the hypotheses suggested by the researchers [11,15,31,32] in the increase of HCY levels of the related diarrheic calves.

As a result, in this study, significant changes were detected in urea and creatinine concentrations, which are important markers in the evaluation of glomerular filtration rate or kidney function in diarrheic calves. Hyperhomcysteinemia caused by glomerular filtration rate of kidneys decreases resulting from fluid volume decreases as a result of fluid loss in neonatal calves with diarrhea. The increase in HCY level in calves with diarrhea; HCY may be caused by an increased production rate (i.e. transmethylation), reduction from remethylation or transsulfuration rate of homocysteine, or a decrease in HCY excretion. It is concluded that hyperhomocysteinemia in diarrhea cases will shed light on the studies to be conducted about whether it causes disorders in the cardiovascular system.

Conflict of Interest

The authors have no competing or conflict of interests in submitting this article.

Financial Support

This study was supported by the Scientific Research Project Directory of the University of Yuzuncu Yil, Van, Turkey (Project No. TSA-2019-7946). We would like to thank to the Scientific Research Directory of the University of Yuzuncu Yil for their financial support on this study.

Author Contributions

SK and CÖ designed the project. ENO provided samples. SK, CÖ and ENO performed statistical analysis of data. All authors also contributed to the preparation of the manuscript.

References

1. Shekhar S, Ranjan R, Singh CV, Kumar P: Prevalence, clinicohaemato-biochemical alterations in colibacillosis in neonatal calves. *Int J Curr Microbiol Appl Sci,* 6 (9): 3192-3198, 2017. DOI: 10.20546/ijcmas.2017.609.393

2. Kozat S, Voyvoda H: İshalli buzağılarda kristalloid (laktatlı ringer) ve kolloid+kristalloid (%6 dekstran-70+ laktatlı Ringer) infüzyon solüsyonlarının rehidratasyon etkinliği. *Van Sağ Bil Derg,* 9, 139-151, 2006.

3. Zeybek S, Civelek T: The time dependent effects of intravenous administration of isotonic sodium bicarbonate on venous acid-base status and renal function in neonatal calves with acute diarrhea. *Kocatepe Vet J,* 7, 39-46, 2014. DOI: 10.5578/kvj.7375

4. Blom HJ, Smulders Y: Overview of homocysteine and folate metabolism. with special references to cardiovascular disease and neural tube defects. *J Inherit Metab Dis*, 34 (1): 75-81, 2011. DOI: 10.1007/s10545-010-9177-4

5. Çayır C, Kozat S: Investigation of homocysteine levels in healthy dogs. *J Vet Sci Anim Husb,* 4 (3): 305, 2016. DOI: 10.15744/2348-9790.4.305

6. Kozat S, Okman EN: Homocystein: A new biochemical marker in livestock sector. *J Adv Vet Anim Res*, 4, 319-332, 2017. DOI: 10.5455/javar.2017.d230

7. Özkan C, Kozat S, Kaya A, Akgül Y: Serum homocysteine, vitamin B_{12} and folate levels in healthy Turkish Van Cats. *J Adv Vet Anim Res,* 4, 58-64, 2017. DOI: 10.5455/javar.2017.d191

8. Bostom AG, Lathrop L: Hyperhomocysteinemia in end stage renal disease: Prevalence, etiology, and potential relationship to atherosclerotic outcomes. *Kidney Int*, 52, 10-20, 1997. DOI: 10.1038/ki.1997.298

9. Kılıçkap A, Kozat S: Research of serum homocysteine levels in healthy cows. *J Vet Sci Anim Husb*, 5 (1): 103, 2017. DOI: 10.15744/2348-9790.5.103

10 Kim J, Kim H, Roh H, Kwon Y: Causes of hyperhomocysteinemia and its pathological significance. *Arch Pharm Res*, 41, 372-383, 2018. DOI: 10.1007/s12272-018-1016-4

11. Amin HK, El-Sayed MIK, Leheta OF: Homocysteine as a predictive biomarker in early diagnosis of renal failure susceptibility and prognostic diagnosis for end stages renal disease. *Ren Fail,* 38 (8): 1267-1275, 2016. DOI: 10.1080/0886022X.2016.1209382

12. Stamler JS, Osborne JA, Jaraki O, Rabbani LE, Mullins M, Singel D, Loscalzo, J: Adverse vascular effects of homocysteine are modulated by endothelium-derived relaxing factor and related oxides of nitrogen. *J Clin Invest,* 91, 308-318, 1993. DOI: 10.1172/JCI116187

13. Temel İ, Özerol E: Homosistein metabolizma bozuklukları ve vasküler hastalıklarla ilişkisi. *İnönü Üniv Tıp Fak Derg,* 9, 149-157, 2002.

14. Chauveau P, Chadefaux B, Coude M, Aupetit J, Hannedouche T, Kamoun P, Jungers P: Hyperhomocysteinemia, a risk factor for atherosclerosis in chronic uremic patients. *Kidney Int Suppl*, 41, 72-77, 1993.

15. Long Y, Nie J: Homocysteine in renal injury. *Kidney Dis*, 2, 80-87, 2016. DOI: 10.1159/000444900

16. Van Guldener C, Stam F, Stehouwer CDA: Homocysteine metabolism in renal failure. *Kidney Int*, 59 (Suppl. 78): S234-S237, 2001. DOI: 10.1046/j.1523-1755.2001.59780234.x

17. Gultekin M, Voyvoda H, Ural K, Erdogan H, Balikci C, Gultekin G: Plasma citrulline, arginine, nitric oxide, and blood ammonia levels in neonatal calves with acute diarrhea. *J Vet Intern Med,* 33, 987-998, 2019. DOI: 10.1111/jvim.15459

18. Constable PD, Stampli HR, Navetat H, Berchtold J, Schelcher F:

Use of a quantitative strong ion approach to determine the mechanism for acid-base abnormalities in sick calves with or without diarrhoea. *J Vet Intern Med*, 19, 581-589, 2005. DOI: 10.1111/j.1939-1676.2005.tb02731.x

19. Öcal N, Yasa Duru S, Yağcı BB, Gazyağci S: İshalli buzağılarda asit-baz dengesi bozukluklarının saha şartlarında tanı ve sağaltımı. *Kafkas Univ Vet Fak Derg*, 12, 175-183, 2006.

20. Özkan C, Akgül Y: Neonatal ishalli buzağılarda hematolojik, biyokimyasal ve elektrokardiyografik bulgular. *YYU Vet Fak Derg,* 15, 123-129, 2004.

21. Constable PD: Clinical assessment of acid-base status: Comparison of the henderson hasselbalch and strong ion approaches. *Vet Clin Pathol*, 29 (4): 115-128, 2000. DOI: 10.1111/j.1939-165X.2000.tb00241.x

22. Erdogan H, Voyvoda H: Effects of rapid and ultra-rapid fluid resuscitation guided by blood lactate clearance rate in diarrheic calves. *J Hellenic Vet Med Soc*, 70, 1413-1420, 2019. DOI: 10.12681/jhvms.20349

23. Özaydın İ, Erkılıç EE, Kılıç E, Yayla S, Baran V: Yenidoğan buzağılarda sıvı-elektrolit sağaltımı. **In,** Baran V (Ed): Ruminantlarda Neonatal Cerrahi. Ankara, Türkiye Klinikleri, 105-110, 2019.

24. Güzelbektaş H, Çoskun A, Şen İ: Relationship between the degree of dehydration and the balance of acid-based changes in dehydrated calves with diarrhoea. *Bull Vet Inst Pulawy*, 51, 83-85, 2007.

25. Constable PD, Grünberg W: Hyperkalemia in diarrheic calves: Implications for diagnosis and treatment. *Vet J,* 195, 271-272, 2013. DOI: 10.1016/j.tvjl.2012.11.002

26. Merouani A, Genest J, Rozen, R, Lambert M, Mitchell GA, Dubois J, Robitaille P: Cerebral vascular complications in a cystinotic uremic child. *Pediatr Nephrol*, 13, 73-76, 1999. DOI: 10.1007/s004670050567

27. Still RA, McDowell IF: Clinical implications of plasma homocysteine measurement in cardiovascular disease. *J Clin Pathol,* 51, 183-188, 1998. DOI: 10.1136/jcp.51.3.183

28. Martella BM, Veiga GRL, Alves BCA, Azzalis LA, Junqueira VBC, Gehrkei FS, Fonseca FLA, Bacci MR: The importance of homocysteine levels in the prognosis of patients with chronic renal disease and in hemodialysis patients. *J Bras Patol Med Lab*, 54**,** 170-176, 2018. DOI: 10.5935/1676-2444.20180030

29. Arnadotir M, Hultberg B, Nilsson-Ehle P, Thysel H: The effect reduced glomerular filtration rate on plasma total homocysteine concentration. *Scand J Clin Lab Invest*, 56, 41-46, 1996. DOI: 10.3109/00365519609088586

30. Braun JP, Lefebvre HP, Watson ADJ: Creatinine in the dog: A review. *Vet Clin Pathol*, 32 (4): 162-179, 2003. DOI: 10.1111/j.1939-165X.2003.tb00332.x

31. Garibotto G, Sofia A, Valli A, Tarroni A, Di Martino M, Cappelli V, Aloisi F, Procopio V: Causes of hyperhomocysteinemia in patients with chronic kidney diseases. *Semin Nephrol*, 26 (1): 3-7, 2006. DOI: 10.1016/j.semnephrol.2005.06.002

32. Rossi S, Rossi G, Giordano A, Paltrinieri S: Homocysteine measurement by an enzymatic method and potential role of homocysteine as a biomarker in dogs. *J Vet Diagn Invest,* 20, 644-649, 2008. DOI: 10.1177/104063870802000520

Kafkas Universitesi Veteriner Fakultesi Dergisi
ISSN: 1300-6045 e-ISSN: 1309-2251
Journal Home-Page: http://vetdergikafkas.org

Kafkas Univ Vet Fak Derg
27 (3): 279-284, 2021
DOI: 10.9775/kvfd.2020.24981

RESEARCH ARTICLE

MicroRNA-200c Mediates the Mechanism of MAPK8 Gene Regulating Follicular Development in Sheep [1]

Ying NAN [1,a] Yifan XIE [1,b] Menting ZHU [1,3,c] Heng YANG [2,d] Zongsheng ZHAO [1,e (*)]

[1] *The research was supported by NSFC (No. 31260537) (No. 31802065) and State Key Laboratory of Sheep Genetic Improvement and Healthy Production (No. MYSKLKF201902)*

[1] Shihezi University, College of Animal Science and Technology, Shihezi, CHINA
[2] Southwest University, College of Animal Science, Chongqing, CHINA
[3] State Key Laboratory of Sheep Genetic Improvement and Healthy Production, Xinjiang Academy of Agricultural and Reclamation Science, Shihezi, CHINA

ORCIDs: [a] 0000-0002-8674-112 X; [b] 0000-0003-3327-8482; [c] 0000-0002-1153-6914; [d] 0000-0002-2072-0713; [e] 0000-0002-0953-5365

Article ID: KVFD-2020-24981 Received: 23.09.2020 Accepted: 09.04.2021 Published Online: 12.04.2021

Abstract

Most sheep breeds are seasonal estrus and single birth animals. In order to improve pastoral area economy and lambing rate, In order to improve pastoral area economy and lambing rate, and It is very important to study the key genes affecting sheep reproductive traits at the molecular level. On the basis of early verification of the relationship between miR-200c and MAPK8 gene target. In this experiment, after over-expression of miR-200c in ovarian granulosa cells, the expression of mitogen-activated protein kinase 8 (MAPK8), frizzled class receptor 3 (FZD3), G protein subunit alphaq (GNAQ), jun proto-oncogene (JUN), protein kinase C beta (PRKCB) in estrus-related pathway genes was detected by qRT-PCR, and the expression of estradio (E_2) and progesterone (P_4) in reproductive stimulation was detected by ELISA. The relationship between MAPK8 gene and follicular ovulation was analyzed. The results showed that up-regulated corpus follicular mRNA expressions of FZD3, GNAQ ($P<0.01$), and down-regulated mRNA expressions of MAPK8, PRKCB ($P<0.05$) and JUN ($P<0.01$). The secretion of E_2 first increased and then decreased with the passage of time, while the secretion of P_4 first increased and then returned to the normal level with the passage of time, which was consistent with the development of follicles in mammalian estrus. In summary, miR-200c-mediated MAPK8 gene has a strong promoting effect on E_2 secretion and a certain regulating effect on P_4, suggesting that miR-200c-mediated target gene MAPK8 plays a regulating role in follicular development.

Keywords: *Kazakh sheep, miR-200c, MAPK8, Ovulatory number*

MicroRNA-200c Koyunda MAPK8 Gen Düzenleyici Foliküler Gelişim Mekanizmasına Aracılık Eder

Öz

Koyun ırklarının çoğu mevsimsel östrus gösteren ve tek doğum yapan hayvanlardır. Kırsal alan ekonomisini iyileştirmek ve kuzulama oranını artırmak için, miR-200c ve MAPK8 gen hedefleri arasındaki ilişkinin erken doğrulanması temelinde koyun üreme özelliklerini etkileyen önemli genleri moleküler düzeyde incelemek oldukça önemlidir. Bu çalışmada, yumurtalık granüloza hücrelerinde miR-200c'nin aşırı ekspresyondan sonra, östrusla ilişkili yolak genlerinden Mitojen Aktiveli Protein Kinaz 8 (MAPK8), Frizzled sınıf reseptör 3 (FZD3), G Protein Altünite Alfa Q (GNAQ), Jun Protoonkogen (JUN), Protein Kinaz C Beta (PRKCB) ekspresyonu QT-PCR ile ve üreme stimülasyonunda östradiol (E_2) ve progesteron (P_4) ekspresyasyonu ELISA ile saptandı. MAPK8 geni ile foliküler ovulasyon arasındaki ilişki incelendi. Sonuçlar, FZD3, GNAQ'nın korpus foliküler mRNA ekspresyonlarının arttığını ($P<0.01$) ve MAPK8, PRKCB ($P<0.05$) ve JUN ($P<0.01$)'un mRNA ekspresyonlarının ise azaldığını gösterdi. Memeli östrusundaki folikül gelişim ile uyumlu olarak E_2 salgısı başlangıçta arttı sonra zamanla azalırken, P_4 salgısı başlangıçta arttı ve daha sonra zamanla normal seviyeye döndü. Özetle, miR-200c aracılı MAPK8 geninin E_2 salgılanması üzerinde güçlü bir teşvik edici etkisi ve P_4 üzerinde belirli bir düzenleyici etkisi vardır, bu da miR-200c aracılı hedef gen MAPK8'in foliküler gelişimde düzenleyici bir rol oynadığını düşündürmektedir.

Anahtar sözcükler: *Kazak koyunu, miR-200c, MAPK8, Yumurtlama sayısı*

How to cite this article?

Nan Y, Xie Y, Zhu M, Yang H, Zhao Z: MicroRNA-200c mediates the mechanism of MAPK8 gene regulating follicular development in sheep. *Kafkas Univ Vet Fak Derg,* 27 (3): 279-284, 2021.
DOI: 10.9775/kvfd.2020.24981

(*) Corresponding Author

Tel: +86 1356 5735767
E-mail: zhaozongsh@shzu.edu.cn (Z. Zhao)

Introduction

The breeding characteristics of sheep are closely related to the production cost and efficiency of breeding industry. However, increasing the number of lambs born is the main measure to improve the economic benefits of sheep field. In order to improve the utilization efficiency, increasing twin or multiple birth rate, of Jining grey goat, more study can be done on molecular genetics [1]. It is very important to study the molecular genetic mechanism of non-degenerate multiple fetuses in sheep. In the endocrine reproductive system, pregnancy and lactation are regulated by reproductive hormones since the endocrine hormones and reproduction are closely related [2]. The oogenesis and folliculogenesis are closely linked and occur simultaneously in the growing ovarian follicles. Granulosa cells are highly complex and depend on many factors, including intercellular communication. Studies have shown that the hypothalamic-pituitary-gonadal axis (HPG) is related to multiple births, in which hormone regulation is particularly important. Released by the hypothalamus, gonadotropin-releasing hormone (GnRH) to stimulate the pituitary gland synthesis and follicle-stimulating hormone (FSH) and luteinizing hormone (LH) secretion [3], thereby promote follicle maturation and ovulation, so reach the role of adjusting the estrus cycle [4]. Follicle development involves multiple regulatory factors and complex regulatory networks formed by signaling pathways, such as FSH, LH and E_2, and prostaglandin (PGs), which play an important role in regulating the estrus cycle [5]. There is also new evidence in recent years that the transforming growth factor-β (TGF-β) superfamily plays an important role in early follicular development, granulosa cell proliferation, and differentiation [6]. These factors act on the granulosa cells on the follicular membrane and regulate the proliferation, differentiation and apoptosis of follicular granulosa cells. Studies have shown that estrogen can negatively regulate the secretion of GnRH and LH by upstream hypothalamic-pituitary tissues, its signal transduction is achieved by activating the MAPK signal transduction system. In addition, PRKCB is also found to indirectly affect MAPK cascade and follicular ovulation [7-9]. Further studies found that plasma concentrations of P_4 and E_2 in high-fecundity sheep were higher than that of low-fecundity sheep, and were significantly positively correlated with ovulation [10]. A study showed that FSH, LH and 17β-E_2 were secreted for many times under their synergism, and LH receptors were produced in follicular granulosa cells. Under the action of LH, more follicles matured and ovulated, which was the main cause of multiple fetters [11,12].

The role and transcription level of miRNA in transcriptional regulation of gene expression have attracted extensive attention from scientists, who have found that miRNA can regulate follicular development in sheep. For example, miR-200 is expressed in tumors and is highly expressed in bladder and cervical cancers, related to the proliferation of tumor cells [13,14] suggested that the expression of miR-200c in the serum of heavy calcium carbonate (HCC) patients was down-regulated, which was associated with tumor size and tumor node metastasis (TNM) staging. At the same time, Zhang et al.[15] found that miR-200c can specifically inhibit the activity of Rho E 3'-UTR reporter gene, which suggested that miR-200c may have an inhibitory effect on Rho E and affect the occurrence and development of gastric cancer. In addition, Kuang et al.[16] found that miR-200c contain similar oncogenic and anti-tumor genes in the development and progression of epithelial ovarian cancer. At present, the research on follicular development regulation is still at the primary stage. However, the miR-200c play a very important role in regulating follicular development, but its role in follicular development has not been proven.

In the early stage, we have predicted the differential expression of miRNA using Targetscan and RNAhybrid software, analyzed the target genes through GO enrichment analysis and DAVID's KEGG pathway analysis, screened out the differentially expressed gene miR-200c, and confirmed the negative regulatory relationship between miR-200c and the target gene MAPK8. In this study, the effects of miR-200c on ovarian granulocyte cells and some estrus-related genes were investigated to determine the role of MAPK8 gene in follicular development, providing a theoretical basis for the study of seasonal estrus and reproductive performance of sheep.

Material and Methods

Sample Collection

Kazakh ewes were raised in the animal laboratory of Shihezi University animal experiment station. Upon confirmation of their reproductive status, these ewes were injected with sodium pentobarbital. After slaughter, the uterus was taken out and the ovary in follicular phase was screened out, and placed in a sampling bucket containing 1% PBS, and transferred to a laboratory ultra-clean station for ovarian granulosa cell culture within 30 min.

Culture and Identification of Cells

Ovaries were recovered at slaughter and transported to the laboratory at 38°C in 1% PBS within 30 min. The ovaries of each animal were placed in 1% PBS supplemented with fetal bovine serum (FBS, Sigma-Aldrich Co, St.Louis, MO, USA). After that, single preovulatory large follicles, with an estimated diameter greater than 5 mm, were opened into a sterile Petri dish by puncturing with a 5 mL syringe and 20-G needle. The culture medium consisted of Dulbecco's Modified Eagle medium F12 (DMEM-F12, Sigma-Aldrich, USA), 10% fetal calf serum (FCS; increased concentration required to maintain adequate cell viability in culture) (PAA, Linz, Austria), 1% penicillin and streptomycin (Invitrogen, USA). The cells were cultured at 38.5°C under aerobic

conditions (5% CO_2). The medium was changed every 48 h.

Screening of cell growth density is more than 80% of the cells in a petri dish typically increases, at room temperature in 4% paraformaldehyde fixed solution after 15 min. After incubation at room temperature with 3% H_2O_2 for 10 min to eliminate internal peroxidase activity, after incubation with 0.1% tritonx-100 (Sigma-Aldrich, China) at room temperature for 20 min, after blood was discarded, 10% goat serum (Gibco, China) was incubated at room temperature for 1 h without washing. 2 mL monoclonal antibody (Anti-JNK1+JNK2 (T183+Y185 phosphate), the working fluid concentration is 1:200, Shanghai biological engineering co, LTD, China) was added and incubated at 4°C for 12 h. After that, FITC label, diluted 1:200, at 37°C for 1 h, and later with the same amount of DAPI (Sigma-Aldridge, China) dye solution at room temperature for 15 min were applied. Fluorescent anti-quench seal solution (Sigma-Aldrich, China) was added to avoid light. Cell staining was observed under an inverted confocal fluorescence microscope.

Oligonucleotide Transfection of Sheep Ovarian Granulocytes

Cells were transfected with 100 nmol/L of miR-200c mimics. Single-strand oligonucleotides were designed to specifically bind and inhibit endogenous miRNAs. Ovarian granulocytes were inoculated in a 6-well plate and upon reaching to 70-80% confluency, these were transfected using Lipofectamine™ 2000 (sigma-Aldrich, China) according to the manufacturer's instructions. NC is the blank group, miR-200c is the interference group, and miR-200c Inhibitor is the interference control group.

QT-PCR and ELISA were Used to Detect the Effect of miRNA-200c on Estrus Related Genes and Hormones

Total RNA of the cells collected was extracted by the Trizol reagent (Thermo Fisher Scientific, China), cDNA was synthesized by Takara-PrimeScript™ RT reagent Kit. Expression value of related reproductive gene was verified by quantitative Real-time polymerase chain reaction (QT-PCR). The primers used were listed in *Table 1*. The PCR instrument was ABI PRISM 7500 (Applied Biosystems, Carlsbad, California). This was done using the QuantStudio 7 Flex fluorescent quantitative PCR instrument (Applied Biosystems, USA). PCR amplification was performed in 20 μL of reaction mixture that contained 10 μL SYBR Premix EX Taq II (TAKARA Bio Inc., Dalian, China), 1 μL of each forward and reverse primer, 7 μL RNase-Free ddH_2O, and 2 μL cDNA (200 ng/μL). PCR amplification was performed in triplicate wells using the following conditions: initial denaturation at 95°C for 5 min, followed by 40 cycles of 95°C for10 sec, and 60°C for 30 sec. The dissociation curve was analyzed after amplification. A melting temperature (Tm) peak at Tm±0.8°C on the dissociation curve was used to determine the specificity of PCR amplification. Sheep β-actin gene was selected as housekeeping genes.

Collect groups of 6 h and 24 h after transfection cell culture. Samples were stored separately at -20ºC to maintain protein activity and avoided repeated freezing. E_2 and P_4 levels were detected according to the ELISA kit instructions (Ovine E_2 ELIA kit, Ovine P_4 ELISA kit, BLUEGENE, China).

Analysis of Data

Results were analysed using SPSS17.0. $2^{-\Delta\Delta Ct}$ was used to calculate the relative expression level. $P<0.05$ was considered significantly different, and $P<0.01$ was accepted highly significantly different.

Results

Ovarian Granulosa Cell Identification

Ovarian granulosa cells were identified after DAPI staining, and the nucleus of the ovarian granulosa cells was seen blue *(Fig. 1-A)*, and the cytoplasm was mainly green, and the immune response product of the target gene *MAPK8* was distributed in the cytoplasm, as indicated by the red arrow *(Fig. 1-B)*. When A and B were observed in combination, the cytoplasm was fluorescent green and the nucleus was blue *(Fig. 1-C)*, the results showed that the transfection was successful and the follow-up experiments could be carried out.

Table 1. *Primer information for qRT-PCR*

Gene	Primers for QT-PCR	Tm (°C)	Product Length (bp)
FZD3	F: TACCTTCATGCCCAATCTTCTG R: CGAGGATACGGCTCATCACAAT	60.29	288
GNAQ	F: AGACAATGAGAACCGAATGGAG R: GAAATAGTCAACTAGGTGGGAATACA	58.00	151
JUN (C-Jun)	F: ACGACCTTCTACGACGATGCCCTCA R: ACGAAGCCCTCGGCGAATCCCT	68.25	326
MAPK8	F: AGCAGTGACCAGTGGCTCTCAG R: CAGCCGACGCTTCTAGACTGC	64.21	119
PRKCB	F: GGCGTCCTGCTGTATGAGATGTTG R: AGCCACGTTGTGTTCCATGATCG	63.78	96
β-actin	F: TCGTTGTAGAAGGTGTGGT R: AGAGCAAGAGAGGCATCC	55.96	103

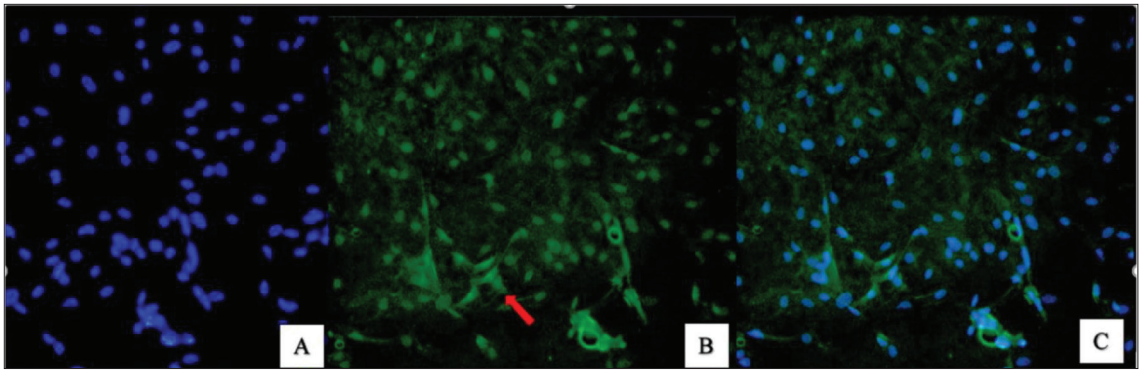

Fig 1. Immunohistochemical identification of cells

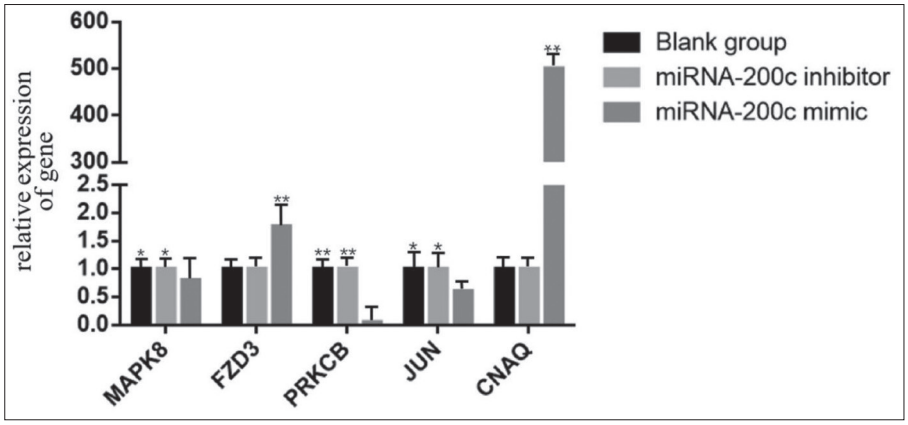

Fig 2. Expression levels of related genes after transfection of miR-200c. The significant results with a P-values lower than 0.01 and 0.05 are given two asterisks (**) and one asterisk (*), respectively

Fig 3. Contents of E_2 and P_4 in ovarian granulosa cell culture medium after transfection for 6 h and 24 h (A is the content of E_2 in ovarian granulosa cell culture medium after transfection for 6 h and 24 h; B is the content of P_4 in ovarian granulosa cell culture medium after transfection for 6 h and 24 h. The significant results with a P-values lower than 0.01 and 0.05 are given two asterisks (**) and one asterisk (*), respectively)

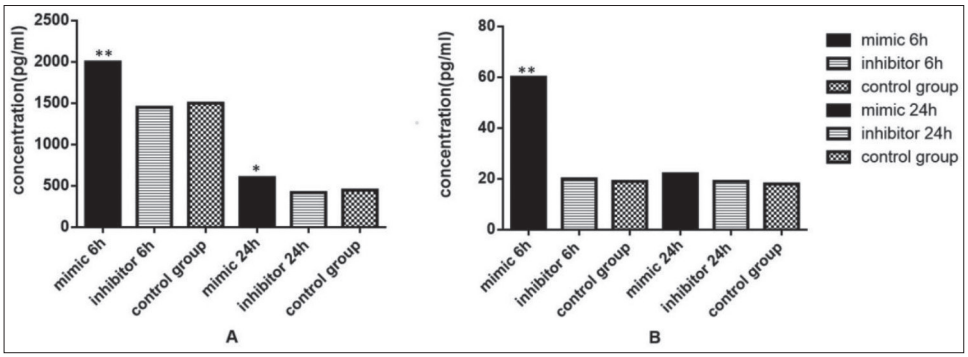

QT-PCR was Used to Detect Changes in Estrus Related Genes

In order to further study the regulation effect of miRNA on the 3'UTR region of target gene MAPK8 and other esturation-related genes, mRNA expression levels of target gene MAPK8 and other esturation-related genes in ovarian granulocytes of Kazak sheep were detected by QT-PCR. In this study, MAPK8 upstream and downstream genes in esturation-related *GnRH* signaling pathway and Wnt signaling pathway were selected for expression verification. After the overexpression of miR-200c *(Fig. 2)*, the expression of MAPK8 gene was significantly down-regulated ($P<0.05$), and the upstream FZD3 gene was significantly up-regulated ($P<0.01$). The expression of PRKCB gene was very significantly down-regulated ($P<0.01$), the expression of downstream *JUN* gene was significantly down-regulated ($P<0.05$), and the expression of miR-200b target gene GNAQ in our research group was highly significantly up-regulated ($P<0.01$).

ELISA Detection Results of E_2 and P_4

After transfection for 6 h, E_2 level in the mimic group was significantly higher than that in the inhibitor group and control group ($P<0.01$). Twenty-four h after transfection, E_2 level in the mimic group was significantly higher than that in the inhibitor group and control group ($P<0.05$) *(Fig. 3-A)*. The results indicated that E_2 level increased after transfection with miR-200c mimetic.

After transfection for 6 h, the level of P_4 in the mimic group was significantly higher than that in the inhibitor

group and control group (P<0.01). Twenty-four h after transfection, E_2 level in the mimic group was significantly higher than that in the inhibitor group and control group (P<0.05) *(Fig. 3-B)*. P4 level increased 6 h after transfection of miR-200c mimetic, but did not change significantly at 24 h after transfection.

The results indicated that miR-200c-mediated MAPK8 gene could promote E_2 secretion and regulate P_4.

Discussion

Early by our team, miR-200a/b/c was found to have different expressions in hypothalamus, pituitary, ovary, uterus, uterine horn, and fallopian tube. We analyzed the tissue expression profile of miR-200a/b/c in Kazakh sheep. The results suggested that miR-200a/b/c may be involved in the regulation of estrus by regulating different target genes in animals [14,17].

In experiments on sheep hypothalamus cells, it was found that miR-200b could regulate the expression of GnRH by down-regulating GNAQ, thus affecting the estrus of sheep [18]. Studies have shown that follicular ovulation can be affected and follicular development further regulated by interfering with the expression of the PLA2G4D gene (the down-regulated gene of PRKCB) [19]. The results of this experiment showed that after the overexpression of miR-200c, the expression of PRKCB and MAPK8 genes were significantly down-regulated. To sum up, MAPK8, as a down-regulation gene, would feedback and regulate the expression of follicle development-related genes in GnRH synthesis pathway and Wnt signaling pathway. We speculated that MAPK8 was an important gene promoting follicular development. Related studies have shown that binding of C-Jun amino-terminal kinase MAPK8 and transcription factor ATF2 upon phosphorylation of C-Jun amino-terminal kinase MAPK8 results in phosphorylation of the binding region, which binds to AP-'1 on the gene promoter to promote cell proliferation and cell differentiation [20]. When the expression of MAPK8 stagnated in the morula stage, a cavity was formed, leading to incomplete oocyte development. In addition, Wang et al.[21] found that the JNK signaling pathway was blocked after MAPK8 was silenced and activated after MAPK8 overexpression, suggesting that MAPK8 may inhibit follicular development. Other studies have shown that up-regulation of FZD3/5 and activation of Wnt signaling pathway can reduce oxidative stress injury of neurons in Alzheimer's disease model in mice and inhibit cell apoptosis [22]. This is consistent with the results of our experiment, with the over-expression of miR-200c and the significantly down-regulated downstream gene JUN.

The researchers also found that FSH and estrogen, combined with increased LH and FSH receptors in follicular granulosa cells, combined with the ovary further stimulated the follicle to produce more estrogen [23]. Similar studies have shown that the development of sheep reproductive system is positively correlated with E_2 secretion in LH and follicular cells. E_2 increases in early stage and estrogen gradually increases. Total follicular growth was positively correlated with E_2 content in plasma [24]. Nogueira et al.[25] believed that the high content of P_4 and low content of E_2 in the non-breeding season were important factors leading to anorexia in sheep. Instead, reducing P_4 levels and increasing E_2 levels during the non-breeding season may promote estrus, where higher P_4 levels lead to higher levels of pituitary follicle stimulating hormone, which further retards follicular development. The lower the level of P_4, the lower the release of LH and the weaker the inhibitory effect of pituitary, leading to increased FSH, which further stimulates follicular development.

In our studies, enzyme-linked immunosorbent assay was used to detect the content of reproductive hormones (E_2 and P_4) at different stages after the overexpression of miR-200c. The results showed that the levels of E_2 and P_4 increased after transfection of miR-200c mimetic. Especially, P_4 level increased 6 h after transfection of miR-200c mimetic, but did not change significantly 24 h after transfection, which was consistent with follicular development in estrus of mammals. In short, MAPK8 ACTS as a down-regulated gene, regulating the expression of genes related to follicular development in GnRH synthesis pathway and Wnt signaling pathway. It can be concluded that MAPK8 gene mediated by miR-200c has a strong promoting effect on E_2 secretion and a certain regulatory effect on P_4.

In conclusion, we found that MAPK8 gene was significantly down-regulated after miR-200c overexpressed in ovarian granulosa cells, which indirectly affected the expression of other genes related to follicular development and comprehensively regulated follicular development. Moreover, MAPK8 gene mediated by miR-200c has a strong role in promoting E_2 secretion, and E_2 has a certain regulatory effect on P_4, thus promoting follicular ovulation. We can conclude that MAPK8, a target gene mediated by miR-200c, plays an important role in follicular development, providing a theoretical basis for improving the yield and number of young sheep.

Author Contributions

NY is the executor of the experimental design and experimental research of this study. NY and JY finished data analysis and writing the first draft of the paper. YH and ZM participated in experimental design and analysis of experimental results. ZZ is the designer and leader of the project, guiding experimental design, data analysis, thesis writing and revision. All the authors have read and agreed to the final text.

References

1. Zhang GX, Chu MX, Wang JY, Fang L, Ye SC: Polymorphism of exon 10 of prolactin receptor gene and its relationship with prolificacy of

Jining Grey goats. *Hereditas,* 29, 329-336, 2007. DOI: 10.3321/j.issn:0253-9772.2007.03.014

2. Rezaei R, Wu ZL, Hou YQ, Fuller WB, Wu GY: Amino acids and mammary gland development: Nutritional implications for milk production and neonatal growth. *J Anim Sci Biotechnol,* 7:20, 2016. DOI: 10.1186/s40104-016-0078-8

3. Haziak K, Herman, AP, Wojtulewicz K, Pawlina B, Paczesna K, Bochenek J, Tomaszewska-Zaremba D: Effect of CD14/TLR4 antagonist on GnRH/LH secretion in ewe during central inflammation induced by intracerebroventricular administration of LPS. *J Anim Sci Biotechnol,* 9:52, 2018. DOI: 10.1186/s40104-018-0267-8

4. Huang HY, Li L, Ye HH, Feng B, Li S: Identification and distribution of gonadotropin-releasing hormone-like peptides in the brain of horseshoe crab *Tachypleus tridentatus. Chin J Oceanol Limnol,* 31, 384-390, 2013. DOI: 10.1007/s00343-013-2067-5

5. Ning HM, Ge YM, Su J, Zhang WL, Yao Y, Yang GH, Lei ZH: Effects of orexin A on mRNA expression of various neuropeptides in the hypothalamus and pituitary, and on serum LH levels in ovariectomized gilts. *Agric Sci China*, 9, 1362-1371, 2010. DOI: 10.1016/S1671-2927(09)60227-3

6. Fournet N, Weitsman SR, Zachow RJ, Magoffin DA: Transforming growth factor-beta inhibits ovarian 17 alpha-hydroxylase activity by a direct noncompetitive mechanism. *Endocrinology*, 137, 166-174, 1996. DOI: 10.1210/endo.137.1.8536609

7. Kang SK, Tai CJ, Cheng KW, Leung PCK: Gonadotropin-releasing hormone activates mitogen-activated protein kinase in human ovarian and placental cells. *Mol Cell Endocrinol,* 170, 143-151, 2000. DOI: 10.1016/S0303-7207(00)00320-8

8. Patergnani S, Marchi S, Rimessi A, Bonora M, Giorgi C, Mehta KD, Pinton P: PRKCB/protein kinase C, beta and the mitochondrial axis as key regulators of autophagy. *Autophagy*, 9, 1367-1385, 2013. DOI: 10.4161/auto.25239

9. Mugami S, Dobkin Bekman M, Rahamim Ben Navi L, Naor Z: Differential roles of PKC isoforms (PKCs) in GnRH stimulation of MAPK phosphorylation in gonadotrope derived cells. *Mol Cell Endocrinol*, 463, 97-105, 2018. DOI: 10.1016/j.mce.2017.04.004

10. An XP, Hou JX, Zhao HB, Li G, Bai L, Peng JY, Yan QM, Song YX, Wang JG, Cao BJ: Polymorphism identification in goat GnRH1 and GDF9 genes and their association analysis with litter size. *Anim Genet*, 44, 234-238, 2013. DOI: 10.1111/j.1365-2052.2012.02394.x

11. An XP, Han P, Hou JX, Zhao HB, Yan Y, Ma T, Fang F, Meng FX, Song YX, Wang JG, Cao BY: Molecular cloning and characterization of KISS1 promoter and effect of KISS1 gene mutations on litter size in the goat. *Genet Mol Res*, 12, 4308-4316, 2013. DOI: 10.4238/2013.February.28.13

12. Carletti MZ, Christenson LK: Rapid effects of LH on gene expression in the mural granulosa cells of mouse periovulatory follicles. *Reproduction*, 137, 843-855, 2009. DOI: 10.1530/REP-08-0457

13. Ravasi T, Suzuki H, Pang KC, Katayama S, Furuno M, Okunishi R, Fukuda S, Ru K, Frith MC, Gongora MM, Grimmond SM, Hume DA, Hayashizaki Y, Mattick JS: Experimental validation of the regulated expression of large numbers of non-coding RNAs from the mouse genome. *Genome Res*, 16, 11-19, 2006. DOI: 10.1101/gr.4200206

14. Kuang YQ, Cao JX, Xu FF, Chen Y: Duplex-specific nucleasenuclease-mediated amplification strategy for mass spectrometry quantification of miRNA-200c in breast cancer stem cells. *Anal Chem,* 91, 8820-8826, 2019. DOI: 10.1021/acs.analchem.8b04468

15. Zhang LQ, Lu N: Status and prospect of the role of miR-200c in early diagnosis of gastric cancer. *World Chin J Digestol,* 6, 382-388, 2019.

16. Zhang L, Wang K, Wu Q, Jin L, Lu H, Shi Y, Liu L, Yang L, Lv L: Let-7 inhibits the migration and invasion of extravillous trophoblast cell via targeting MDM4. *Mol Cell Probes,* 45, 48-56, 2019. DOI: 10.1016/j.mcp.2019.05.002

17. Shi J, Ye Q, Zhou Z, Zhou XC, Di W: Expression of miRNA-200c in IIIc stage ovarian serous cystadenocarcinoma and its role in metastasis. *Mod Trends Immunol,* 1, 36-41, 2016.

18. Romerowicz-Misielak M, Koziorowski M: The gonadotropins subunits, GnRH and GnRH receptor gene expression and role of carbon monoxide in seasonal breeding animals. *Ann Anim Sci,* 12, 15-23, 2012. DOI: 10.2478/v10220-012-0002-x

19. Mélanie V, Olivier K, Nathalie H, Edith C, Yann LP, Yves C, Jean M, Porcher, Francois B: 17α-Ethinylestradiol and nonylphenol affect the development of for ANrain GnRH neurons through an estrogen receptors-dependent pathway. *Reprod Toxicol*, 33, 198-204, 2012. DOI: 10.1016/j.reprotox.2011.04.005

20. Barutcu SA, Girnius N, Vernia S, Davis RJ: Role of the MAPK/c-Jun NH2-terminal kinase signaling pathway in starvation-induced autophagy. *Autophagy*, 14, 1586-1595. 2018. DOI: 10.1080/15548627.2018.1466013

21. Wang Y, Bi Y, Zuo Q, Zhang W, Li D, He N, Cheng S, Zhang Y, Li B: MAPK8 regulates chicken male germ cell differentiation through JNK signaling pathway. *J Cell Biochem,* 119, 1548-1557, 2018. DOI: 10.1002/jcb.26314

22. Zhang L, Fang Y, Cheng X, Lian YJ, Xu HL: Silencing of long noncoding RNA SOX21-AS1 relieves neuronal oxidative stress injury in mice with Alzheimer's disease by upregulating FZD3/5 via the Wnt signaling pathway. *Mol Neurobiol*, 56, 3522-3537, 2019. DOI: 10.1007/s12035-018-1299-y

23. Li J, Gao H, Tian Z, Wu Y, Wang Y, Fang Y, Lin L, Han Y, Wu S, Haq I, Zeng S: Effects of chronic heat stress on granulosa cell apoptosis and follicular atresia in mouse ovary. *J Anim Sci Biotechnol,* 7:57, 2016, DOI: 10.1186/s40104-016-0116-6

24. Wang MX, Shao XG: The serum progesterone level in superovulation was increased. *Chin J Pract,* 24, 1004-3845, 2015.

25. Nogueira DM, Cavalieri J, Fitzpatrick LA, Gummow B, Blache D, Parker AJ: Effect of hormonal synchronisation and/or short-term supplementation with maize on follicular dynamics and hormone profiles in goats during the non-breeding season. *Anim Reprod Sci,* 171, 87-97, 2016. DOI: 10.1016/j.anireprosci.2016.06.003

Kafkas Universitesi Veteriner Fakultesi Dergisi
ISSN: 1300-6045 e-ISSN: 1309-2251
Journal Home-Page: http://vetdergikafkas.org

Kafkas Univ Vet Fak Derg
27 (3): 285-289, 2021
DOI: 10.9775/kvfd.2020.25064

RESEARCH ARTICLE

Association of BMPR-1B Gene 3'-UTR Region Polymorphism with Litter Size in Tibetan Sheep

Jianlei JIA [1,2,a] Dejuan XIE [1,b] Yingying ZHANG [1,c] Huaixia ZHANG [1,d]
Liping ZHANG [2,e] Shengzhen HOU [1,f] Qian CHEN [1,g (*)]

[1] College of Agriculture and Animal Husbandry, Qinghai University, Xining, Qinghai, 810016, PR CHINA
[2] College of Animal Science and Technology, Gansu Agricultural University, Lanzhou, Gansu, 730070, PR CHINA
ORCIDs: [a] 0000-0001-5843-1709; [b] 0000-0002-6204-8486; [c] 0000-0002-5022-7233; [d] 0000-0003-1987-6777; [e] 0000-0001-8365-3530
[f] 0000-0001-2345-6789; [g] 0000-0002-5523-3659

Article ID: KVFD-2020-25064 Received: 11.10.2020 Accepted: 26.02.2021 Published Online: 08.03.2021

Abstract

Bone Morphogenetic Protein Receptor-1B (BMPR-1B) is considered as the primary gene in sheep for follicular development and litter size trait. It has been defined as the most major candidate gene for genetic markers of sheep reproductive performance. In our study, polymorphisms in the BMPR-1B gene 3'-UTR region were investigated in 363 Tibetan sheep (119 Plateau-type Tibetan sheep, 141 Valley-type Tibetan sheep, and 103 Oula-type Tibetan sheep) by DNA sequencing analysis. Two single nucleotide polymorphisms (SNPs) were identified, which were G1339A and A1354G. The frequencies of SNPs were in Hardy-Weinberg equilibrium (Chi-square test, P>0.05). AA and AG genotypes were found in the A1354G variant of the 3'UTR region, that AA and A were the preponderant genotype and allele, respectively. The $\chi 2$ independence test analyses indicated that the A1354G variant of BMPR-1B gene 3'UTR region polymorphisms was significantly correlated with litter size in all-types Tibetan sheep (P<0.05). These results demonstrate that the BMPR-1B gene 3'-UTR region might be a potential candidate gene for marker-assisted selection (MAS).

Keywords: *Tibetan sheep, BMPR-1B gene, 3'-UTR region, Polymorphism, Litter size*

Tibet Koyunlarında BMPR-1B Geni 3'-UTR Bölgesi Polimorfizmi İle Batın Genişliği İlişkisi

Öz

Kemik Morfogenetik Protein Reseptörü-1B (BMPR-1B), koyunlarda foliküler gelişim ve batın genişliği özelliği için birincil gen olarak kabul edilir. Bu gen, koyunlarda üreme performansının genetik belirteçleri için en önemli aday gen olarak tanımlanmıştır. Çalışmamızda, 363 Tibet koyununda (119 plato tipi Tibet koyunu, 141 vadi tipi Tibet koyunu ve 103 Oula tipi Tibet koyunu) BMPR-1B geninin 3'-UTR bölgesindeki polimorfizmler DNA dizi analizi ile araştırıldı. G1339A ve A1354G adlı iki single nükleotid polimorfizm (SNP) saptandı. SNP'lerin frekansları Hardy-Weinberg dengesi içerisindeydi (Ki-kare testi, P>0.05). 3'UTR bölgesinin A1354G varyantında AA ve AG genotipleri saptandı ve AA ve A sırasıyla baskın genotip ve aleldi. $\chi 2$ bağımsızlık testi analizleri, BMPR-1B geni 3'UTR bölgesi polimorfizmlerinden A1354G varyantının, tüm Tibet koyun türlerinde batın genişliği ile yakından ilişkili olduğunu gösterdi (P <0.05). Bu sonuçlar, BMPR-1B geni 3'-UTR bölgesinin, markör destekli seleksiyon (MAS) için potansiyel bir aday gen olabileceğini göstermektedir.

Anahtar sözcükler: *Tibet koyunu, BMPR-1B geni, 3'-UTR bölgesi, Polimorfizm, Batın genişliği*

INTRODUCTION

Bone Morphogenetic Protein Receptor-1B (BMPR-1B) is a member of transforming growth factor-β family, which plays an imperative role in sheep follicular development and reproductive traits and is called as fecundity (Fec) gene for its function in additive effect on sheep litter size and ovulation rate [1]. BMPR-1B is upon binding with BMP ligands, BMPR-2B transphosphorylates the GS domain of the BMPR-1B, which leads to the activation of downstream cascades and the inactivation of the partial receptor, then Smads state of expression and phosphorylation is changed, the synthesis of estradiol by FSH induction is promoted, the synthesis and secretion of progesterone is inhibited, granular cell differentiation of A746G mutation ewes and follicular maturation are accelerated, and ovulation is increased [2,3].

How to cite this article?

Jia J, Xie D, Zhang Y, Zhang H, Zhang L, Hou S, Chen Q: Association of BMPR-1B gene 3'-UTR region polymorphism with litter size in Tibetan sheep. *Kafkas Univ Vet Fak Derg,* 27 (3): 285-289, 2021.
DOI: 10.9775/kvfd.2021.25064

(*) Corresponding Author

Tel: +86 890 9710194 Fax: +86 0971 5318423
E-mail: 95862583@qq.com (Q. Chen)

Several studies confirm that A746G mutation led to the loss-of-function in BMPR-1B gene, and changes protein conformation that promotes steroid production, increases ovulation rate and litter size in sheep. BMPR-1B had been proved for additive effects on ewe ovulation rate, and it could inhibit granulosa cell apoptosis, prevented follicular atresia, and promote litter size [4]. This may be a primary physiological mechanism for BMPR1B to affect ewe fecundity [5]. The research showed that the higher ovulation rate of Small Tail Han sheep related to mitochondrial oxidation BMPR-1B protein expressions, and it could provide an advanced recognition of the molecular mechanism for sheep high prolificacy [6].

BMPR-1B gene was widely expressed in some tissues such as ovary, testes, ear, hypothalamus and blood, mostly in ovary tissue, which regulated the release of gonadotropin hormones (FSH and LH) [7]. Based on the breed and biological properties in ruminant, we hypothesized that BMPR-1B was a major candidate gene for genetically improving reproductive performance in sheep [8]. Tibetan sheep was one of the original sheep breeds in China, and known as excellent adaptability in Tibetan plateau, however, Tibetan ewes were a low reproduction rate breed, which twin rate was only 3~5 percent [9]. To date, there are few reports on the effects of the association of BMPR-1B gene polymorphisms with litter size trait in Tibetan sheep. In present study, we performed extensive BMPR-1B gene 3′-UTR region screening by DNA sequencing methods to detect polymorphisms, we present 2 genetic polymorphisms found in BMPR-1B gene 3′-UTR region in Tibetan sheep and examined A1354G variant of 3′UTR regionassociation with litter size trait.

Material and Methods

The study protocol and experimental animals were approved by the National Administration of Qinghai University (China, 2016).

Animals Collection

Three hundred and sixty three ewes (80 Singletons Plateau-type Tibetan ewes, 39 Twins Plateau-type Tibetan ewes, 70 Singletons Valley-type Tibetan ewes, 71 Twins Valley-type Tibetan ewes with twins, 51 Singletons Oula-type Tibetan ewes and 52 Twins Oula-type Tibetan ewes) were selected under grazing conditions on natural grasslands in Haibei Tibetan Autonomous Prefecture (Qinghai, China).

All experimental ewes were 3-4 years old, which had a clear lambing record, raising conditions (NRC 2007), and the same breeding ewes bodyweight was no significant difference.

Genomic DNA Extraction and Genotyping

Five mL jugular blood samples of each ewes were collected in single-use evacuated tubes containing heparin sodium as anticoagulant. Genomic DNA was extracted from whole samples using the Blood DNA Kit (TaKaRa, Dalian, China). The quality and quantity of extracted DNA samples were measured by Nanodrop ND-1000 spectrophotometer (Thermo Fisher Scientific, Wilmington, DE, USA). Genomic DNA samples were diluted to 50 ng/uL and stored at -20°C for subsequent analysis.

PCR primers were designed from BMPR-1B gene 3′-UTR region (1145bp-1500bp) sequence available at GenBank (GenBank accession number: NM_001009431.1) using the Primer Premier Software (Version 3.0). Genomic DNA was amplified using primer sequences (F: 5′-GGAACAGCAG AGGAATG-3′ and R: 5′-CACAGTCAGGAAGTAAAT-3′). DNA was pooled from 180 random samples in 6 types Tibetan sheep and amplified by PCR. PCR amplification product was a 20 μL mixture composed of 1 μL of each primer, 1 μL dNTP, 10 μL 2xTaq MIX (TaKaRa, Dalian, China), and 7 μL RNase-free dd H_2O. The cycling protocol was as follows: an initial denaturation for 3 min at 94°C; 35 cycles of 94°C for 30 s; annealing at 52°C for 30 s, extension at 72°C for 30 s, and the final extension was performed at 72°C for 10 min. All PCR products were sequenced using an ABI 3730 sequencer (ABI, Foster City, CA, USA).

Data Analysis

Allele and genotype frequencies were estimated after sequence alignment by direct counting. Chi-square test for Hardy-Weinberg equilibrium (HWE) was applied to assess the deviations in the number of observed versus expected genotypes. Population genetic indexes, including heterozygosity (HE) and polymorphism information content (PIC) were calculated according to Nei's methods [10].

The association between A1354G variant of BMPR-1B gene 3′UTR region polymorphism and litter size trait in Tibetan sheep (the phenotype was directly treated as category) was analyzed using the $\chi 2$ independence test. Tests of hypotheses were done using t-tests at $P<0.05$ with $P<0.10$ considered a trend.

Results

Genomic DNA extraction and Amplification

The extracted genomic DNA samples were detected by 1% agarose gel, which all samples were good integrity. The amplifications resulted in a product size of 355-bp on 2.5% agarose gel electrophoresis when visualized under the UV transilluminator in all ewes. This product was directly used for DNA sequencing.

SNP Discovery and Genotyping of Selected SNPs

The sheep BMPR1-B gene maps to chromosome 6. In the current study, the constructed DNA pools were used to amplify the 3′UTR of the BMPR1-B cDNA sequence. The PCR product was sequenced, and two SNPs were identified:

g.3004 G>A (G1339A) and g.3019 A>G (A1354G) *(Fig. 1)*.

The χ^2 independence test analysis showed that A1354G mutation of BMPR-1B gene 3'UTR were significantly correlated with litter size in all-types of Tibetan sheep. The effects of genotypes on mRNA secondary structure of BMPR-1B gene 3'UTR was analyzed via RNA fold Web Server on-line prediction software *(Fig. 2)*. The A1354G mutation affected the mRNA secondary structure of BMPR-1B 3'UTR between AA and AG genotypes.

Population Genetic Variability Analyses

The genotype distribution, allelic and genotypic frequencies of A1354G variant of BMPR-1B gene 3'UTR region was calculated in *Table 1*. The results revealed AA and AG genotypes for PCR products by DNA sequencing analysis, and AA type was the preponderant genotype, A was the preponderant allele in all Tibetan sheep. GG genotype could not be detected among the animals examined.

The heterozygosity (He), Hard-Weinberg Equilibrium (HWE), and Polymorphism Information Content (PIC) value of A1354G variant of BMPR-1B gene 3'UTR region were given in *Table 2*. The convention for classifying PIC is that a value less than 0.250 indicates low polymorphism, 0.250 to 0.500 indicates intermediate polymorphism, and greater than 0.500 indicates high polymorphism. In present study, PIC values ranged from 0.03 to 0.21, which showed that the loci had low genetic diversity, but PIC value of twins Tibetan sheep was significantly greater than that of singletons Tibetan sheep ($P<0.05$). The χ^2 test showed that Tibetan sheep were in HWE ($P>0.05$), and P value of twins Tibetan sheep was significantly lower than that of singletons Tibetan sheep ($P<0.05$).

Genotype Frequencies Analysis and Association Analysis

The χ^2 independence test was used to analyze the association of genotypic frequency and litter size traits within Tibetan sheep type. For A1354G variant of BMPR-1B gene 3'UTR region, the results showed that differences between the singletons and twins Tibetan sheep in AA and AG genotypic frequency were significant ($\chi^2 = 29.3788$, $P<0.0001$). There were no significant differences in different Tibetan sheep type between AA genotype and AG genotype ($\chi^2 = 0.0753$ and $P=0.9631$). There were statistically significant differences in litter size traits for different genotype × types of Tibetan sheep, this meant that G allele frequency promoted the Tibetan sheep litter size ($\chi^2 = 31.2004$, $P<0.0001$).

Discussion

BMPR-1B was a member of TGF-β super family and played an important role in ewe follicle development and litter size [11]. The studies identified the BMPR-1B gene was a major gene associated with litter size traits in Australian Merino sheep, Cambridge sheep and Small Tail Han sheep [12]. BMPR-1B gene were reported of 22 single nucleotide polymorphisms *(http://www.ncbi.nlm.nih.gov/gene/443454)* [13]. Previous research on the A746G of BMPR-1B gene found that the additive effect on BMP

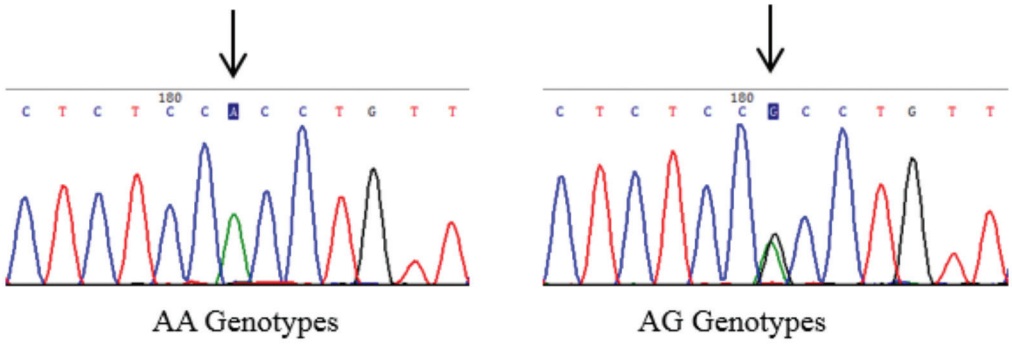

Fig 1. Sequencing blast of 1354 loci in sheep BMPR-IB gene 3'-UTR

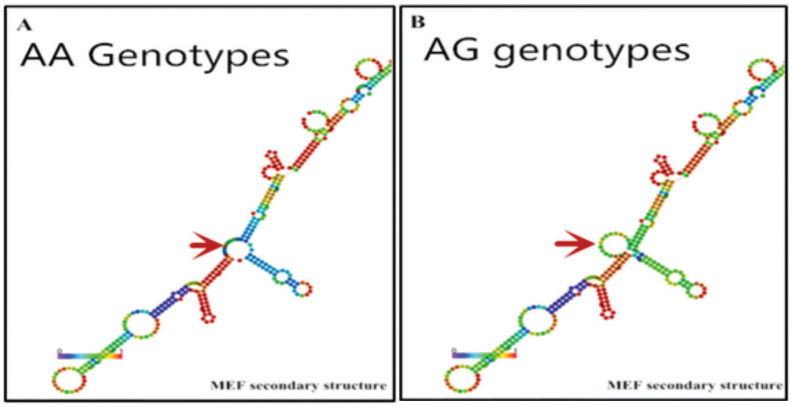

Fig 2. Secondary structure prediction of different genotypes of mRNA in BMPR-IB gene 3'-UTR

Table 1. *Genotype distribution, allelic and genotypic frequencies of 1354 loci of BMPR-1B gene 3'UTR*

Group	Samples	Genotypic Frequency [a,b]		Allelic Frequency [c]	
		AA	AG	A	G
Singletons Plateau-type Tibetan sheep	80	0.95 (76)	0.05 (4)	0.975	0.025
Twins Plateau-type Tibetan sheep	39	0.72 (28)	0.28 (11)	0.86	0.14
Singletons Valley-type Tibetan sheep	70	0.97 (68)	0.03 (2)	0.985	0.015
Twins Valley-type Tibetan sheep	71	0.77 (55)	0.23 (16)	0.885	0.115
Singletons Oula-type Tibetan sheep	51	0.96 (49)	0.04 (2)	0.98	0.02
Twins Oula-type Tibetan sheep	52	0.81 (42)	0.19 (10)	0.905	0.095

Note: a- *AA was wild-type of 1354 loci of BMPR-1B gene 3'UTR, AG was mutation-type of 1354 loci of BMPR-1B gene 3'UTR;* ***b-*** *Numbers in parentheses are numbers of individuals that belong to the respective genotypes;* ***c-*** *Mutant allele for 1354 loci of BMPR-1B gene 3'UTR (G), wild type allele for 1354 loci of BMPR-1B gene 3'UTR (*A)

Table 2. *Genetic diversity index of 1354 loci of BMPR-1B gene 3'UTR*

Group	PIC	He	Ne	P-value	χ^2
Singletons Plateau-type Tibetan sheep	0.05	0.28	1.323	0.82	0.06
Twins Plateau-type Tibetan sheep	0.21	0.24	1.451	0.31	1.05
Singletons Valley-type Tibetan sheep	0.03	0.36	1.278	0.91	0.02
Twins Valley-type Tibetan sheep	0.18	0.29	1.454	0.29	1.14
Singletons Oula-type Tibetan sheep	0.04	0.23	1.413	0.87	0.02
Twins Oula-type Tibetan sheep	0.16	0.31	1.357	0.45	0.59

signal pathway during follicle development led to increase average ovulation [14]. However, there are few reports on the effects of the non-coding region SNPs, especially in 3' untranslated region and 5' promoter region. Recent evidence indicated that gene UTR region could regulate mRNA location and protein abundance by affecting the mRNA stability or translation [15]. The genetic information which stored in gene 3'UTR could be transferred to proteins through protein-protein interaction to affect protein expression [16]. In Dorset, Mongolian, and Small Tail Han sheep reported synonymous mutation could activate the native splicing donor site, which resulted the premature stop codon or yielding a shorter mRNA, and affected sheep ovarian specific expressions of follicular oocyte cells and granulosa cells under the unusual condition [17,18]. Here, we detected 2 SNPs (g.3004 G>A and g.3019 A>G) in 3'UTR of BMPR-1B gene. Data analysis revealed that A1354G variant of BMPR-1B gene 3'UTR region (g.3019 A>G) was associated with litter size traits in Tibetan sheep.

As a low heritability trait, litter size was controlled by a major gene and some minor polygenes, then, screening the SNPs of target genes was very important to sheep breeding [19]. Sequence alignment demonstrated that A1354G variant located in the 3'UTR did not result in changes of amino acid sequence, but the genotype distribution of different Tibetan sheep type and litter size traits ewes (singletons ewes and twins ewes) had significant differences. There was a significantly association between a C/T polymorphism in the BMPR-1B gene 3'UTR and litter size traits in Small Tail Han sheep, Gansu Alpine Merino sheep [20]. There were only two genotypes (AA and AG) without GG genotype in Tibetan sheep, and the causes of this situation could be that i) the allelic frequency of G was too low to be detected in this study as the sample sizes were too small. ii) allele G was a recessive lethal gene and GG genotype Tibetan sheep could not survive.

The twins lambs rate in Tibetan sheep was very low, which was solely 3~5 percent. However, since sheep numbers were particularly important in pasture safe grazing capacity, to explore those traits would greatly promote the development of sheep industry [21]. BMPR-1B gene plays an important role in sheep reproductive endocrine, ovary development, litter size, organ development and body mass. BMPR-1B promoted steroid production, changed the Smad state of expression and phosphorylation, thereby expediting follicular maturation and increasing sheep litter size [22]. Many studies demonstrated that BMPR-1B gene levels of transcripts had an additive effect on litter size and ovulation rate, but has negative effects on fetal growth and development and body mass during gestation [23,24]. Based on these results, BMPR-1B appears to be litter size regulatory factor, especially in ruminant species. Combined with the results of our study, we suggest that A1354G variant of BMPR-1B gene 3'UTR region may directly or indirectly mediate Tibetan sheep litter size trait.

In this paper, the polymorphisms of BMPR-1B gene 3'UTR in Tibetan sheep were analyzed. Genotype association

analysis with litter size trait in Tibetan sheep were performed, which will provide information for the early MAS in Tibetan sheep. Further research with a larger sample size and additional expression analyses of this gene are necessary to support our results.

Conflicts of Interest

The authors declare no conflict of interest.

Acknowledgments

The authors are grateful to all the participants who took part in this study.

This work was supported by National Natural Science Foundation of China (No.31660662) and National Natural Science Foundation of Qinghai Province (2020-ZJ-735). The funders have no role in study design, data collection, analysis, decision to publish or preparation of the manuscript.

Author Contributions

J. JIA and D. XIE Conceptualization; Y. ZHANG and H. ZHANG Data curation; J. JIA, Y. ZHANG. and L.g ZHANG Formal analysis; S. HOU Funding acquisition; Q. CHEN Investigation; S. HOU Methodology; H. ZHANG and Q. CHEN Project administration; S. HOU Resources; D. XIE Software; Q. CHEN Supervision; Y. ZHANG Validation; H. ZHANG. and L. ZHANG Visualization; J. JIA Writing - original draft; D. XIE, L. ZHANG and Q. CHEN Writing - review & editing.

Reference

1. Jia JL, Chen Q, Gui LS, Jin JP, Li YY, Ru QH, Hou SZ: Association of polymorphisms in bone morphogenetic protein receptor-1B gene exon-9 with litter size in Dorset, Mongolian, and Small Tail Han ewes. *Asian Australas J Anim Sci,* 32 (7): 949-955, 2019. DOI: 10.5713/ajas.18.0541

2. Zhang XM, Li WR, Wu YS, Peng XR, Lou B, Wang LQ, Liu MJ: Disruption of the sheep *BMPR-1B* gene by CRISPR/Cas9 in *in vitro*-produced embryos. *Theriogenology*, 91, 163-172.e2, 2017. DOI: 10.1016/j.theriogenology.2016.10.025

3. Jia JL, Jin JP, Chen Q, Yuan Z, Li HQ, Bian JH, Gui LS: Eukaryotic expression, Co-IP and MS identify BMPR-1B protein-protein interaction network. *Biol Res,* 53:24, 2020. DOI: 10.1186/s40659-020-00290-7

4. Ahlawat S, Sharma R, Maitra A, Tantia MS: Current status of molecular genetics research of goat fecundity. *Small Ruminant Res,* 125, 34-42, 2015. DOI: 10.1016/j.smallrumres.2015.01.027

5. Maskur M, Tapaul R, Kasip L: Genetic polymorphism of bone morphogenetic protein receptor 1B (BMPR-1B) gene and its association with litter size in Indonesian fat-tailed sheep. *Afr J Biotechnol,* 15, 1315-1319, 2016. DOI: 10.5897/AJB2015.15093

6. Carreira AC, Alves GG, Zambuzzi WF, Sogayar MC, Granjeiro JM: Bone morphogenetic proteins: Structure, biological function and therapeutic applications. *Arch Biochem Biophys*, 561, 64-73, 2014. DOI: 10.1016/j.abb.2014.07.011

7. Polley S, De S, Batabyal S, Kaushik R, Yadav P, Arora JS, Chattopadhyay S, Pan S, Brahma B, Datta TW, Goswami SL: Polymorphism of fecundity genes *(BMPR1B, BMP15* and *GDF9)* in the Indian prolific Black Bengal goat. *Small Ruminant Res,* 85, 122-129, 2009. DOI: 10.1016/j.smallrumres.2009.08.004

8. Crispo M, Vilariño M, Santos-Neto PC, Nunez-Olivera R, Cuadro F, Barrera N, Mulet AP, Nguyen TH, Anegon I, Menchaca A: Embryo development, fetal growth and postnatal phenotype of eGFP lambs generated by lentiviral transgenesis. *Transgenic Res*, 24, 31-41, 2015. DOI: 10.1007/s11248-014-9816-x

9. Zhou JW, Guo YM, Kang JP, Degen AA, Titgemeyer EC, Jing XP, Wang WJ, Shang ZH, Li ZP, Yang G, Long RJ: Tibetan sheep require less energy intake than small-tailed Han sheep for N balance when offered a low protein diet. *Anim Feed Sci Technol,* 248, 85-94, 2019. DOI: 10.1016/j.anifeedsci.2019.01.006

10. Nei M: Estimation of average heterozygosity and genetic distance from a small number of individuals. *Genetics*, 89 (3): 583-590, 1978.

11. Lin Y, Jiang WG: Bone morphogenetic proteins in tumour associated angiogenesis and implication in cancer therapies. *Cancer Lett*, 380, 586-597, 2016. DOI: 10.1016/j.canlet.2015.10.036

12. Jia JL, Zhang LP, Ding Q, Yang ZW: Correlation between polymorphism of *BMPR-1B* gene exon7 and lambing performance of sheep. *JNWAFU*, 44 (1): 7-13, 2016. DOI: 10.13207/j.cnki.jnwafu.2016.01.002

13. Du L, Zhang LP, Zhang XY, Zhu SH, Ma XM. The Correlation analysis between polymorphism and fecundity of 1113 locus in *BMPR-1B* gene CDS area of three sheep *(Ovis aries)* varieties. *J Agric Biotechnol,* 25 (12): 1989-1997, 2017.

14. Ma XM, Zhang LP, Zhu SH, Di L, Zhang XY. Analysis of polymorphism at 864 locus of *BMPR-1B* gene CDS region and its relationship with litter size in four sheep breeds. *GAB*, 36 (10): 4116-4124, 2017. DOI: 10.13417/j.gab.036.004116

15. Zhu SH, Zhang LP, Ma XM, Di L, Zhang XY: Analysis and differences of sheep BMP-15 gene expression in ewes with different lambing traits. *Genomics Appl Biol,* 37 (05): 1853-1858, 2018. DOI: 10.13417/j.gab.037.001853

16. Zhao YZ: Application of quantitative genetics in sheep breeding. **In,** Chinese Sheep Science. 384, China Agriculture Press, Beijing, 2013.

17. Chen CY, Chen ST, Juan HF, Huang HC: Lengthening of 3'UTR increases with morphological complexity in animal evolution. *Bioinformatics*, 28, 3178-3181, 2012. DOI: 10.1093/bioinformatics/bts623

18. Berkovits BD, Mayr C: Alternative 3' UTRs act as scaffolds to regulate membrane protein localization. *Nature*, 522, 363-367, 2015. DOI: 10.1038/nature14321

19. Mayr C: What are 3' UTRs doing. *Cold Spring Harb Perspect Biol*, 11:a034728, 2018. DOI: 10.1101/cshperspect.a034728

20. Chu MX, Jia LH, Zhang YJ, Jin M, Chen HQ, Fang L, Di R, Cao GL, Feng T, Tang QQ, Ma HY, Li K: Polymorphisms of coding region of *BMPR-1B* gene and their relationship with litter size in sheep. *Mol Biol Rep*, 38, 4071-4076, 2011. DOI: 10.1007/s11033-010-0526-z

21. Liu HJ, Xu TW, XU SX, Ma L, Han XP, Wang XG, Zhang XL, Hu LY, Zhao N, Chen YW, Pi L, Zhao XQ: Effect of dietary concentrate to forage ratio on growth performance, rumen fermentation and bacterial diversity of Tibetan sheep under barn feeding on the Qinghai-Tibetan plateau. *PeerJ*, 7:e7462, 2019. DOI: 10.7717/peerj.7462

22. Chu MX, Zhao XH, Zhang YJ, Jin M, Wang JY, Di R, Cao GL, Feng T, Fang L, Ma YH, Li K: Polymorphisms of *BMPR-1B* gene and their relationship with litter size in goats. *Mol Biol Rep*, 37 (8): 4033-4039, 2010. DOI: 10.1007/s11033-010-0062-x

23. Mu FF, Wang X, Xu WJ, Liu EY, Ci RQZ, Zhang L: Correlation between BMP15 and BMPR-IB gene mutations in Pengbo semi-fine wool sheep and their lambing. *Journal of Huaibei Normal University (Natural Sciences)*, 40 (3): 49-54, 2019. DOI: 10.3969/j.issn.2095-0691.2019.03.010

24. Antebi YE, Linton JM, Klumpe H, Bintu B, Gong M, Su C, McCardell R, Elowitz MB: Combinatorial signal perception in the bmp pathway. *Cell*, 170, 1184-1196, 2017. DOI: 10.1016/j.cell.2017.08.015

Kafkas Universitesi Veteriner Fakultesi Dergisi
ISSN: 1300-6045 e-ISSN: 1309-2251
Journal Home-Page: http://vetdergikafkas.org

Kafkas Univ Vet Fak Derg
27 (3): 291-299, 2021
DOI: 10.9775/kvfd.2020.25124

RESEARCH ARTICLE

Comparative Efficacy of Yohimbine and Tolazoline for Antagonism of Ketamine-Xylazine Induced Sedation in Captive Wild Felids

Ameer Hamza RABBANI [1,a (*)] Yasir Razzaq KHAN [2,b] Omer NASEER [2,c] Kashif HUSSAIN [2,d] Ahmad ALI [2,e] Abdul WAHEED [3,f] Muhammad SHAHID [1,g] Hareem AFZAL [4,h]

[1] Department of Surgery, Faculty of Veterinary Sciences, Cholistan University of Veterinary and Animal Sciences, 63100, Bahawalpur, PAKISTAN
[2] Department of Medicine, Faculty of Veterinary Sciences, Cholistan University of Veterinary and Animal Sciences, 63100, Bahawalpur, PAKISTAN
[3] Institute of Continuing Education & Extension, Cholistan University of Veterinary and Animal Sciences, 63100, Bahawalpur, PAKISTAN
[4] Veterinary Officer, Bahria Town, 46220, Rawalpindi, PAKISTAN
ORCIDs: [a] 0000-0001-7105-7694; [b] 0000-0002-9031-0306; [c] 0000-0002-5388-4917; [d] 0000-0002-0594-8023; [e] 0000-0002-2539-606X
[f] 0000-0002-9242-6329; [g] 0000-0002-9443-8462; [h] 0000-0002-9044-972X

Article ID: KVFD-2020-25124 Received: 03.11.2020 Accepted: 01.03.2021 Published Online: 02.03.2021

Abstract

This study was conducted to investigate the comparative efficacy of yohimbine and tolazoline for antagonism of ketamine-xylazine induced sedation in captive wild felids in Pakistan. It included 16 tigers (Panthera tigris), 22 lions (Panthera leo) and 16 leopards (Panthera pardus), aged between 2-10 years, weighing approximately 190.6±12.4 kg, 161.6±16.6 kg, and 50.5±6.9 kg respectively. A total of 54 anesthetic inductions were carried out on clinical patients from all species dividing them into two groups KX-T and KX-Y receiving 0.15 mg/kg tolazoline and 0.15 mg/kg yohimbine as antagonists, respectively. Body temperature, pulse and respiration rate (TPR) were recorded at ten-minute intervals for thirty minutes in either groups. These physiological norms differed significantly only in Tigers at 10min and 20min intervals. Furthermore, onset of arousal and recovery time in animals receiving yohimbine was evidently shorter, ranging between 2.8±0.76 to 8.42±0.33 min. ALT, AST, Urea and Creatinine were significantly elevated in groups administered with Tolazoline when compared to Yohimbine as well. Hence, yohimbine at described dosage effectively antagonized ketamine and xylazine anesthesia by significant reduction in reversal times for all the species under consideration, bearing nominal deleterious effects on physiological, hepatic and renal parameters. So, this study concludes yohimbine to be a superior antagonist for ketamine-xylazine anesthetic reversal than tolazoline.

Keywords: *Leopard, Lion, Reversal, Tiger, Tolazoline, Yohimbine*

Kafeste Tutulan Yabani Kedigillerde Ketamin-Ksilazin İle İndüklenen Sedasyon Antagonizmi İçin Yohimbin ve Tolazolinin Karşılaştırmalı Etkinliği

Öz

Bu çalışma, Pakistan'da kafeste tutulan yabani kedigillerde ketamin-ksilazin kaynaklı sedasyon antagonizmi için yohimbin ve tolazolinin karşılaştırmalı etkinliğinin araştırılması için yapıldı. Çalışmada, yaşları 2 ile 10 arası değişen 190.6±12.4 kg ağırlığında 16 kaplan (Panthera tigris), 161.6±16.6 kg ağırlığında 22 aslan (Panthera leo) ve 50.5±6.9 kg ağırlığında 16 leopar (Panthera pardus) yer aldı. Tüm hayvan türlerinden klinik hastalara toplam 54 anestezik indüksiyonu gerçekleştirildi ve antagonist olarak sırasıyla 0.15 mg/kg tolazolin ve 0.15 mg/kg yohimbin verilerek KX-T ve KX-Y adlı iki gruba ayrıldı. Her iki gruptaki hayvanların vücut ısısı, nabız ve solunum sayıları (TPR) on dakika aralıklarla otuz dakika süreyle kaydedildi. Bu fizyolojik normlar, yalnızca kaplanlarda 10. dakika ve 20. dakikada önemli ölçüde farklılık gösterdi. Ayrıca, yohimbin uygulanan hayvanlarda ayılma ve derlenme süresinin başlaması, 2.8±0.76 ile 8.42±0.33 dakika ile belirgin olarak daha kısaydı. Tolazolin uygulanan grupta ALT, AST, üre ve kreatinin seviyesi, yohimbin ile karşılaştırıldığında önemli ölçüde daha yüksekti. Dolayısı ile, bildirilen dozda yohimbin kullanımı, fizyolojik, hepatik ve renal parametreler üzerinde önemsiz zararlı etkileri ile söz konusu tüm hayvan türlerinin anesteziden uyanma sürelerinde önemli bir azalma sağlayarak ketamin ve ksilazin anestezisini etkili bir şekilde antagonize etti. Bu nedenle bu çalışmada, ketamin-ksilazin anestezisinden uyanmada yohimbinin, tolazolinden daha üstün bir antagonist olduğu sonucuna varıldı.

Anahtar sözcükler: *Aslan, Kaplan, Leopar, Tolazolin, Uyanma, Yohimbin*

How to cite this article?

Rabbani AH, Khan YR, Naseer O, Hussain K, Ali A, Waheed A, Shahid M, Afzal H: Comparative efficacy of yohimbine and tolazoline for antagonism of ketamine-xylazine induced sedation in captive wild felids. *Kafkas Univ Vet Fak Derg,* 27 (3): 291-299, 2021.
DOI: 10.9775/kvfd.2021.25124

(*) Corresponding Author

Tel: +90 464 6127317
E-mail: ameerhamzarabbani@cuvas.edu.pk (A. H. Rabbani)

Introduction

Lions, tigers and leopards have been classified as vulnerable or endangered species on the International Union for Conservation of Nature (IUCN) Red List, forecasting a dreary future for their survival [1]. These days, most of the lions and wild tigers live in sparsely and sporadically distributed populaces, thereby increasing the probability of inbreeding [2-4]. Unlike tigers and lions, leopards are indigenous to varied regions in the Indian subcontinent [5]. They were once seen across almost all terrains of Pakistan. But these days, Indian subspecies of *Panthera pardus* may only be seen running wild around metropolitan edges of Islamabad to certain mountain ranges in the north [6]. Considering such a scenario, the survival of wild carnivorous felids largely depends upon captive breeding in zoos and wildlife reserves. Therefore, it has become imperative that scientific inquiries are undertaken to gain information about physiology, pathology and treatment of diseases that afflict these species [7]. Sedative and fast-acting anesthetics are pre-requisites in the field of wildlife medicine [8]. Their use has become ever more frequent in the last five decades [9]. Research and management of feral species require a reliable immobilization protocol that can easily be reversed and poses the least amount of hazard to the physiology of that animal [10]. Captive felids regularly need chemical restraining or tranquilization to assist in clinical examination, vaccination, sample collection, administration of medication and minor surgeries [11]. These animals are generally tranquilized using remote delivery devices such as pole syringes or darts. Monitoring of animals in tranquilized state is usually not possible in field settings so the drugs used must have a broad safety margin and must not incur resounding deleterious effects on vital parameters [12]. Ketamine-xylazine tranquilization is widely practiced in zoo settings and has been used effectively to immobilize several wild felids including lions, leopards and tigers [13]. The sedative and relaxing effects of xylazine counteract pressor and cataleptic effects of ketamine [14,15]. Nevertheless, alpha-2 agonists have been observed to cause bradycardia, ventricular arrhythmias, hypertension and hypotension in tigers and leopards [16,17]. Consequently, a suitable antagonist for speedy recovery of tranquilized patient is greatly needed to avoid cardiovascular instability [17]. Both yohimbine and tolazoline are alpha-2 adrenergic antagonists [9]. Tolazoline is capable of ameliorating respiratory depression and muscle relaxation attributed to xylazine [9,18,19]. Upon recovery, a marked lack of co-ordination may also be resolved by tolazoline administration [20]. Yohimbine, similar to tolazoline has been reported to significantly shorten recovery from sedation [21]. Effects of alpha-2 adrenergic antagonists such as atipamezole, yohimbine, and tolazoline have been extensively studied in ruminants to antagonize anesthetic effects of ketamine-xylazine combination [21,22]. Moreover, studies in domestic cats, lions, Bengal tigers and leopards have proposed that yohimbine and tolazoline could accelerate the recovery from ketamine-xylazine anesthesia [23]. The present study was undertaken to compare the ability of yohimbine and tolazoline in antagonizing the anesthetic effects of ketamine-xylazine in three endangered large felids (lions, leopards and tigers).

Material and Methods

Selection of Animals

This study included wild felids that had to be anesthetized for clinical or minor surgical procedures. All captive tigers *(Panthera tigris),* leopards *(Panthera pardus)* and lions *(Panthera leo)* included in this study were male, aged between 2-10 years. The study was undertaken during years 2018 and 2019 at day and night zoo, Bahria town Karachi and amongst some privately kept animals at farm-houses around the adjoining areas of Lahore. A total of 54 anesthetic inductions were carried out on 16 male tigers, 22 male lions and 16 male leopards *(Table 1)*. The mean body weight (mean ± SD) of these wild felids were; male tigers 190.6±12.4 kg (range 173.6-210 kg), male lions 161.6±16.6 kg (range 134.3-189.2 kg), and male leopards 50.5±6.9 kg (range 42.6-64.2 kg) respectively. All animals selected for this study were adequately de-wormed and vaccinated previously. Nutritional requirements were fulfilled by beef along with weekly calcium and vitamin supplementation. Wild felids inducted into this study were allowed to consume water freely during day or night. This study included animals that had to be sedated for clinical or managerial functions at privately owned zoos and farm houses in Pakistan. All procedures were conducted in line with prescribed guidelines of "The prevention of cruelty to animals act, 1890" and "The Punjab wildlife act, 1974" of Pakistan.

Anesthetic Procedure

All animals were kept off feed 8 h before the anesthetic procedure, to avoid any complications. All animals were anesthetized in the early hours of the day, between 09:00-12:00 hours with a combination of 2.6 mg/kg ketamine HCl (Ketarol® 50 mg/mL, Global Pharmaceuticals) and 1.3 mg/kg xylazine HCl (Xylaz® 20 mg/mL, Farvet). The combination of anesthetic drugs was loaded into a 5ml dart syringe equipped with a 35-mm needle. Thigh or the shoulder region were targeted using a blowpipe to inject these drugs intramuscularly with a plastic projectile dart. We preferred using projectile darts as opposed to squeeze cages, because wild felids had to be lured with

Table 1. *Number of tigers, leopards and lions involved in anesthetic trial*

Zoo	Tigers	Leopards	Lions
	Male	Male	Male
Danzoo, Bahria town Karachi	9	10	14
Privately kept wild felids at farm houses around Lahore	7	6	8

food to go into them. However, to avoid any iatrogenic problems, animals had to be kept off-feed 6-8 h before tranquilization when xylazine has to be employed. As xylazine is commonly associated with emesis in felines if the animal has fed recently [24]. Therefore, feeding them immediately prior to anesthetic administration might have caused drenching of vomitus during transportation or recumbency. After the animals were darted, they were left undisturbed and were monitored from an adequately safe distance until they showed signs of anesthetic induction. Anesthetic induction time was judged by oropharyngeal tone, sedation, incoordination and pupillary dilation. After being completely anesthetized, the feline species were moved on a stretcher in lateral recumbency to another cage for the required procedure. To avoid any iatrogenic problems, ophthalmic ointments were administered on cornea and conjunctiva as anesthetized cats lose control of their palpebral muscles. Furthermore, while transportation their eyes were covered to protect them from bright sunlight. It was observed by Sontakke et al.[20] that duration of immobilization in wild felids can range up to 31-40 min after a single loading dose of xylazine and ketamine combination. A maintenance dose of ketamine and xylazine was not required to prolong anesthesia. The overall duration of anesthesia included the duration of induction and immobilization similar to prior investigations. Parameters, such as pulse, rectal temperature and respiratory rates were monitored immediately after anesthetic induction at every 10-min interval until anesthetic recovery.

Reversal of Anesthesia

The procedures performed on subjects were minor and mostly diagnostic in nature therefore did not take more than 15 min. Consequently, all wild felids were administered with either yohimbine or tolazoline irrespective of the species differences 20 min after induction of anesthesia. Within each species, anesthetized animals were divided into two groups: Group KX-T received an intravenous injection of 0.15 mg/kg tolazoline (Tolazine®, Akorn Animal Health) while the second group namely KX-Y received an intravenous injection of 0.15 mg/kg Yohimbine (Antagozil®, Troy Laboratories). The time duration that elapsed from the point of reversal administration (tolazoline/yohimbine) to the animal being able to stand was deemed as Standing/Recovery time. Individuals were monitored for up to 12 h after recovery to identify any signs of stupor or sedation.

Effect of Anesthesia on Liver and Renal Function

One day before the procedure each animal was restrained in a squeeze cage and phlebotomy was performed via the coccygeal route for blood sample collection. The blood sample was transferred from the syringe to the serum gel vacutainer and labeled appropriately. The values of liver function test (LFT) and renal function test (RFT) obtained from this blood sample, established the baseline values. A second sample of blood was collected from individuals in both groups (i.e., tolazoline and yohimbine) 12 h after the completion of the procedure for serum analysis. Liver function test (LFT) included evaluation of aspartate amino-transferase (AST) and alanine transaminase (ALT) while renal function test (RFT) involved biochemical assessment of blood serum concentrations for urea and creatinine.

Ethical Considerations

This study was conducted under the proposed guidelines outlined by Pakistan's Prevention of Cruelty to Animals Act (1890) and is in compliance with the Guide for the Care and Use of Agricultural Animals in Research and Teaching.

Statistical Analysis

All data analyses were performed using GraphPad Prism (Ver. 8.4.3 for Windows; GraphPad Software, La Jolla California, USA). Data are presented as mean ± SD. An unpaired t-test analyzed the efficacy of two drugs as reversal agents against anesthesia. One-way ANOVA followed by a Tukey test was used for evaluation of blood chemistry parameters while two-way ANOVA analysis followed by the Sidak test was employed to compare the effects of two drugs on respiration, pulse and body temperature at different time intervals. A probability of $P<0.05$ was considered to be the minimum level of significance.

Results

Induction of Anesthesia

Anesthetic induction using a combination of 2.6 mg/kg ketamine and 1.3 mg/kg xylazine produced effective sedation. Loss of muscular tone, pupillary dilatation and absence of oropharyngeal reflex within twenty minutes of darting indicated adequate analgesia and deep sedation. As ataxia started to set in, and the animal became recumbent laterally, the time of anesthetic induction was tallied. The induction times in the tiger and lion were comparable but leopards took a significantly shorter period of time to get sedated *(Table 2)*. Ear twitch and palpebral reflexes were checked to monitor the depth of anesthesia. The animals involved in this study were anesthetized either to transfer them from one site to another or to perform wound management. The procedures were thereafter completed and animals were transferred to their housing pens for recovery from anesthesia.

Table 2. *Time to induction of anesthesia (minutes) in the captive tigers, lions and leopards*

Sr. No	Specie	Gender	Number of Animals	Induction Time
1	Tiger	Male	16	18.17±1.177[a]
2	Lion	Male	22	18.39±1.8[3]a
3	Leopard	Male	16	13.93±1.1[3]b

Values are represented as mean ± SD. Different superscripts in a column within a species differ significantly whereby P<0.05

Table 3. *Average respiration rates (breaths per min), average pulse rates (beats per min) and average body temperature (°F) at different time intervals for male tigers, lions and leopards during immobilization administered with Tolazoline and Yohimbine*

Specie	Antagonist	Average Respiration Rates at Different Time Durations			Average Pulse Rates at Different Time Durations			Average Body Temperature at Different Time Durations		
		10	20	30	10	20	30	10	20	30
Tiger	Tolazoline	18.87±1.45^a	20±1.41^a	20.5±2.56^a	67.5±3.16^a	59.25±2.5^a	52.8±1.6^a	102.4±0.2^a	101.85±0.24^a	101.05±0.24^a
	Yohimbine	23.125±2.47^b	23.5±2.67^b	21.625±2.5^a	58.75±1.6^b	72.5±1.19^b	65.8±2.58^b	102.35±0.24^a	104.2±0.48^b	103.05±0.24^b
Lion	Tolazoline	20.45±3.32^a	21.90±4.06^a	21.54±2.16^a	65.81±3.31^a	57±3.84^a	53.45±2.06^a	102.50±0.34^a	102±0.33^a	101.2±0.33^a
	Yohimbine	22.63±1.91^a	22.45±2.50^a	21±2.04^a	62.5±6.12^a	70.6±2.73^b	65.63±4.08^b	101.43±1.03^b	102.61±1.81^a	102.25±0.92^b
Leopard	Tolazoline	19.62±1.30^a	20.62±2.06^a	21.37±1.99^a	71.5± 2^a	67.62±4.47^a	64.62±6.69^a	101.66±0.88^a	101.16±0.84^a	100.55±0.70^a
	Yohimbine	22.5±2.20^b	21.12±2.9^a	19.25±1.48^a	67±3.54^b	72.12±1.12^a	69.37±2.82^a	101.66±0.33^a	102.52±0.83^b	102.21±0.41^b

Values are represented as mean ± SD. Different superscripts in a column within a species differ significantly whereby P<0.05

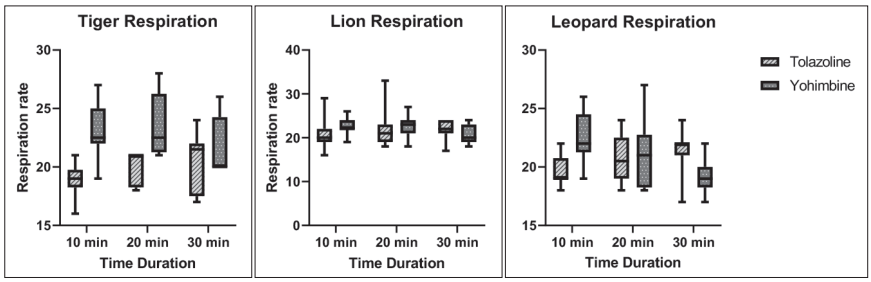

Fig 1. Interleaved Box and Whisker plots (GraphPad Prism Ver. 8.4.3) depicting comparative respiratory rates after tolazoline and yohimbine administration in Tiger, Lion and Leopard immobilized with ketamine-xylazine anesthesia at 10 min, 20 min, 30 min time intervals

Fig 2. Interleaved Box and Whisker plots (GraphPad Prism Ver. 8.4.3) depicting comparative Pulse rates after tolazoline and yohimbine administration in Tiger, Lion and Leopard immobilized with ketamine-xylazine anesthesia at 10 min, 20 min, 30 min time intervals

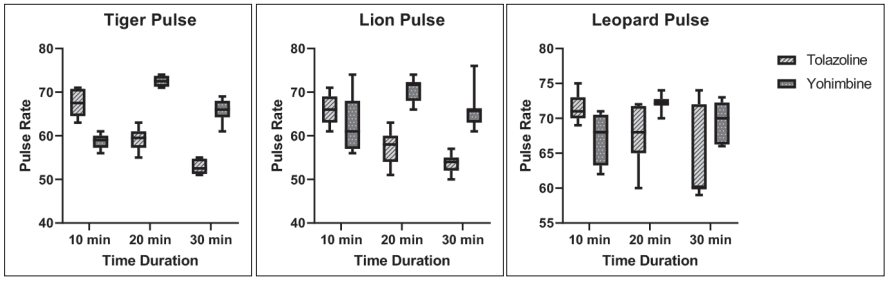

Values for Physiological Norms

As reversal was injected in either group receiving tolazoline or yohimbine intravenously, physiological parameters such as respiration, pulse and body temperature were recorded at 10 min intervals for a period of thirty minutes *(Table 3)*.

In tigers, respiration rates differed significantly at 10 min (P=0.0014) and 20 min (P=0.0098) post tolazoline or yohimbine administration, however, the difference became insignificant by 30th min (P=0.6882). Respiration rates were insignificant in case of lions while these values differed only at 10th min (P=0.0253) interval during the reversal procedure for leopards *(Fig. 1)*.

Average pulse rates were significantly different throughout the thirty-minute interval in the case of tigers whereby P<0.0001. However, in the case of lions pulse rates were significantly different by 20th and 30th min intervals despite being similar in the beginning. While pulse rates in leopards were significant only at 10 min mark (P=0.0285) *(Fig. 2)*.

Initially at 10-min interval body temperature in tigers was nonsignificant between either of the groups, yet their values differed significantly by 20th (P<0.0001) and 30th (P<0.0001) min intervals. Lions of both groups experienced a differing body temperature at 10 and 20 min (P<0.0001), howbeit it was significant at 20 (P=0.0176) and 30 (P=0.0003) min interval intervals in case of leopards *(Fig. 3)*.

Recovery from Anesthesia

Sixteen Tigers, twenty-two lions and sixteen leopards were involved in the comparative study of two anesthetic reversals i.e., tolazoline and yohimbine. All individuals studied in reversal trials were male of their respective species. Wild felids were randomly and equally divided into two groups whereby each received either of the reversal agents, post ketamine-xylazine induction. Following tolazoline (0.15 mg/kg) or yohimbine (0.15 mg/kg) administration, the onset of arousal from anesthesia was identified and elapsed time was noted by the presence of oropharyngeal reflex. Afterward, the animal started to show pedal reflex, lifted its head and moved into sternal recumbency. Finally, the time it took for the animal to stand unaided from sternal recumbency was termed to

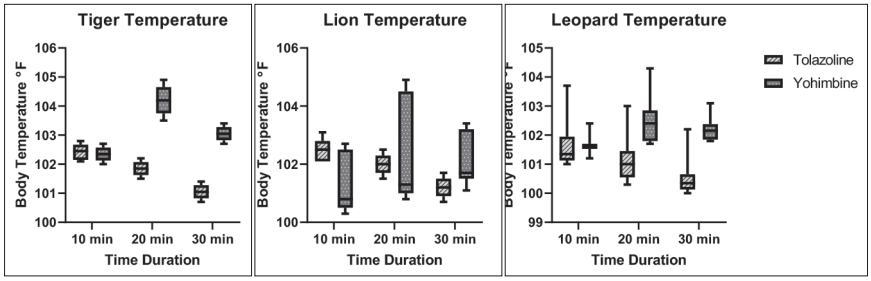

Fig 3. Interleaved Box and Whisker plots (GraphPad Prism Ver. 8.4.3) depicting comparative Body temperatures (°F) after tolazoline and yohimbine administration in Tiger, Lion and Leopard immobilized with ketamine-xylazine anesthesia at 10 min, 20 min, 30 min time intervals

Table 4. *Comparative efficacy of tolazoline and yohimbine for anesthetic reversal in captive male tigers, lions and leopards*

Species	Antagonist	Number of Animals	Stages of Induced Reversal		
			Onset of Arousal (min)	Sternal Recumbency (min)	Standing/Recovery Time (min)
Tiger	Tolazoline	8	3.65±0.44[a]	7.95±0.24[a]	12.1±0.48[a]
	Yohimbine	8	1.04±0.16[a]	4.5±0.31[b]	6.3±0.58[b]
Lion	Tolazoline	11	2.4±0.33[a]	4.4±0.33[a]	7.5±0.66[a]
	Yohimbine	11	0.97±0.28[b]	1.2±0.63[b]	2.8±0.76[b]
Leopard	Tolazoline	8	6.1±0.48[a]	10.3±0.97[a]	16.45±0.73[a]
	Yohimbine	8	2.2±0.47[b]	6.5±0.82[b]	8.42±0.33[b]

Values are represented as mean ± SD. Different superscripts in a column within a species differ significantly whereby P<0.05

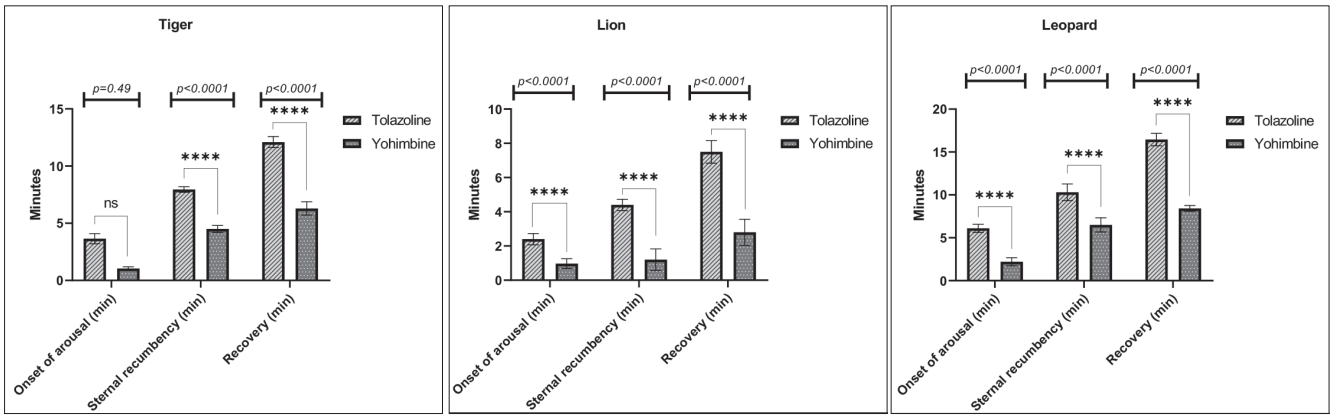

Fig 4. Interleaved Bar Chart (GraphPad Prism Ver. 8.4.3) depicting comparative efficacy of reversals i.e., Tolazoline and Yohimbine in tiger, lion and leopard immobilized with ketamine-xylazine anesthesia. Values are represented as mean ± SD. Significant differences (P<0.05) among groups are indicated in GP style: 0.1234 (ns), 0.0332 (*), 0.0021 (**), 0.0002 (***), <0.0001 (****)

be standing or recovery time. All these time intervals for all the species involved in the trial were collected and statistically analyzed *(Table 4)*.

The onset of arousal was significantly improved in lions (P<0.0001) and leopards (P<0.0001) while sternal recumbency and standing recovery were improved significantly for all wild felid groups administered with yohimbine. The shortest recovery period with tolazoline was observed in lions (7.5±0.66) while sternal recumbency varied between 4.4±0.33 to 10.3±0.97. However, the shortest recovery period was observed in lions administered with yohimbine (2.8±0.76). Moreover, tiger and leopards followed suite with values 6.3±0.58 and 8.42±0.33 respectively *(Fig. 4)*. In groups administered with tolazoline, although time intervals from normal unassisted recovery periods were significantly improved, however it still took much longer for tigers (12.1±0.48), lions (7.5±0.66) and leopards (16.45±0.73) in this group to recover.

Liver and Renal Function

All animals involved in the trial had their blood sampled and evaluated before anesthetic administration for AST, ALT, urea and creatinine levels to establish a baseline. Groups administered with tolazoline and yohimbine had their blood sampled 12 h after the recovery to determine the deleterious effects of these drugs and compare their voracity *(Table 5)*.

In tigers, AST (P<0.0045), ALT (P<0.0072) and urea (P<0.0001)

Table 5. *Comparative values of liver function test (LFT) and renal function test (RFT) in groups of captive male tigers, lions and leopards administered with Tolazoline or Yohimbine*

Species	Values	LFT		RFT	
		AST (µ/L)	ALT (µ/L)	Urea (mg/dL)	Creatinine (mg/dL)
Tiger	Normal	62.07±15.93[a]	76.55±25.04[a]	32.73±10.66[a]	3.03±0.94[a]
	Tolazoline	82.01±18.96[b]	99.36±9.76[b]	49.47±7.03[b]	6.98±1.04[b]
	Yohimbine	67.19±15.2[a]	82.07±22.53[a]	36.54±8.98[a]	4.04±0.43[c]
Lion	Normal	33.26±2.6[a]	42.32±3.8[a]	33.24±1.54[a]	2.39±0.17[a]
	Tolazoline	55.83±7.06[b]	66.7±6.88[b]	55.31±7.45[b]	4.13±0.57[b]
	Yohimbine	39.48±4.82[c]	47.18±3.99[c]	37.10±2.91[c]	2.68±0.31[c]
Leopard	Normal	54.66±15.99[a]	55.46±15.07[a]	34.8±8.76[a]	1.23±0.57[a]
	Tolazoline	87.97±18.12[b]	84.45±11.07[b]	56.09±8.13[b]	2.21±0.16[b]
	Yohimbine	61.23±12.31[a]	63.26±10.02[a]	39.63±9.49[a]	1.44±0.43[a]

Values are represented as mean ± SD. Different superscripts in a column within a species differ significantly whereby P<0.05

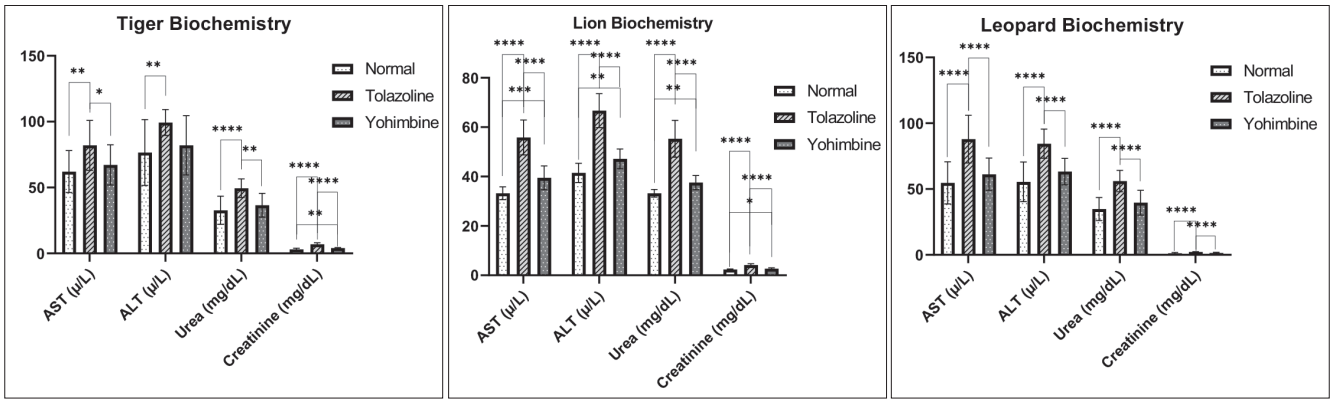

Fig 5. Interleaved Bar Chart (GraphPad Prism Ver. 8.4.3) depicting comparative AST, ALT, Urea and Creatinine values after Tolazoline and Yohimbine administration in tiger, lion and leopard immobilized with ketamine-xylazine anesthesia. Values are represented as mean ± SD. Significant differences (P<0.05) among groups are indicated in GP style: 0.1234 (ns), 0.0332 (*), 0.0021 (**), 0.0002 (***), <0.0001 (****)

were significantly elevated due to tolazoline from baseline values, whereas creatinine levels were significantly increased by both of the reversal agents. In lions, all the biochemical parameters were significantly different within the groups whereby values of the tolazoline group were highest in that regard. However, these values were found to be significantly greater in tolazoline when within a group post hoc analysis was performed. Similar to tigers, values in leopards when analyzed revealed that AST (P<0.0001), ALT (P<0.0001), urea (P<0.0001) and creatinine (P<0.0001) were significantly greater in animals administered with Tolazoline from normal baseline values *(Fig. 5)*.

Discussion

The present study illustrates the efficacy of tolazoline and yohimbine for antagonizing the anesthetic effects of ketamine-xylazine combination used to immobilize lions, tigers and leopards in Pakistan. The anesthetic combinations currently being used, have shown deleterious side-effects when administered persistently. Succinyl choline hydrochloride was found to cause respiratory paralysis, while ketamine hydrochloride and phencyclidine hydrochloride had prolonged recovery periods [25]. Similar to lions, tigers exhibited unwanted side effects in response to these drugs as well. A combination of zolazepam and tiletamine has been found effective in tranquilizing wild felids, however, use in tigers has been limited as it was found to cause severe cardiopulmonary complications [26]. In certain cases, medetomidine has also been used in combination with ketamine to sedate tigers but information regarding its safe usage and effectiveness has been limited [22]. Currently, immobilization and anesthetic induction protocol of wild felids include intramuscular administration of an alpha-2 adrenergic receptor agonist, such as xylazine, medetomidine or dexmedetomidine in combination with Neuraminidase Adenine Dinucleotide (NMDA) receptor antagonist namely ketamine [11,15,19]. Ketamine is not recommended to be used as a tranquilizer or anesthetic agent separately, but only in combination with a potent sedative. It has demonstrated some side-effects such as ataxia, dysphoria, hypersalivation and hypoalgesia during induction and recovery from anesthesia. In prior studies, these side-effects have been rectified

using benzodiazepines [11]. Administration of an alpha-2 adrenergic receptor agonist in combination with ketamine allows for a reduction in the dose of anesthetic agents, thereby lowering the probability of seizures [5,27]. Cardiovascular stability also improved as lower doses of anesthetic agents were administered [28]. Consequently, in our study, animals were anesthetized with a combination of 2.6 mg/kg ketamine and 1.3 mg/kg xylazine. The efficacy of aforementioned combination is quite ubiquitous. So instead of investigating efficaciousness of these agents, previously reported dose rates were implemented. Events of overdose or contraindications were not observed amongst individuals inducted into this study. In spite of ketamine-xylazine efficacy, stimulation of alpha-2 adrenoreceptors have been found to cause increase in plasma potassium concentrations progressively. Thereby causing, hypo-insulinemia by inhibiting insulin secretion from pancreatic beta cells in feline species [9]. This hyperkalemic shift has been known to cause tachycardia initially, followed by sudden bradycardia leading to cardiac arrest and death in exotic felids [29]. Uncontrollable and unpredictable anesthetic regimens are problematic in wildlife research [30]. Consequently, this study has focused on mitigating the imperative need for reliable anesthetic antagonists in wild and captive felids. Prior studies in Bengal tiger and domestic cats have suggested the efficacy of alpha-2 antagonists in assisting the recovery of ketamine-xylazine induced anesthesia. The use of alpha-2 antagonists such as Tolazoline, yohimbine and atipamezole have been found effective in the reversal of xylazine based anesthetic regimens. Cardiac arrhythmia, tachycardia, diarrhea and vomiting and orthostatic hypotension are reported to be severe side-effects [18]. Tolazoline should be stored in cool, dark conditions as it is light-sensitive and unstable at high ambient temperatures [31]. Yohimbine, similar to tolazoline is also a potent alpha-2 adrenergic antagonist and has been employed as a reversal against ketamine-xylazine-induced sedation in wild cats [23] body weight 105-211 kg. In lions, atipamezole has also been used however the recovery period was prolonged and varied while tigers recovered within half an hour of drug administration [32,33].

In the present study, 0.15 mg/kg body weight tolazoline and yohimbine were administered intravenously in equally distributed groups of tigers, lions and leopards. The physiological parameters (temperature, pulse and respiration) were recorded immediately after the administration of reversal administration. These parameters in groups administered with tolazoline and yohimbine were consistent with previous reports [34]. Review of prior investigations into the effect of yohimbine and tolazoline antagonism on physiological norms has been corroborated by our findings whereby 10 min after its administration respiration significantly increased in all wild felids except lions [5,20,35] *(Fig. 1)*. However, pulse rates were observably lower than reported in wild felids administered with yohimbine than the ones treated with tolazoline, relating to its pronounced cardiovascular impact that has been reported previously in wolves [18,36] *(Fig. 2)*. But as time continued to elapse yohimbine, possessing greater potency, longevity and affinity in wild felids caused significant elevation in vital parameters. Improvement in respiratory rates, pulse rates and body temperature observed amongst tigers and leopards by 20th min of yohimbine administration as opposed to tolazoline could be justified by lower affinity of tolazoline to bind with alpha-2 adrenergic receptors [31]. Howbeit, temperature did not significantly differ in case of lions at 20 min interval, indicating physiological variation amongst different species. As most individuals continued to recover by 30th min, respiratory rates became non-significant amongst either of the groups. Yet, pulse rates and body temperature continued to remain significantly elevated in lions and tigers treated with yohimbine indicating greater efficacy in said species [20]. Better metabolic rate in leopards deduced from shorter recovery durations might be attributed to non-significant pulse rates at 30-min interval post reversal administration [5] *(Fig. 3)*.

When tolazoline was administered, a significant reduction in immobilization time was achieved in all cases. It allowed a return to mobility within 20-22 min of injection. Comparatively, onset of arousal was significantly improved in lions and leopards only, while sternal recumbency and standing recovery were improved significantly for all groups of species administered with yohimbine *(Fig. 4)*. The values of induced reversal stages in terms of minutes were consistent with earlier findings for antagonism with tolazoline and yohimbine [18,20]. In free-ranging animals, a quick reversal from anesthesia is imperative and the effectiveness of both reversal agents is quite consequential. Moderate return to sedation has been recorded by different authors after reversal administration [37]. But such a phenomenon was not observed in the present study, thereby indicating the doses of tolazoline and yohimbine used in our study were sufficient to antagonize the drug effects.

The adverse effects of tolazoline and yohimbine were evaluated by analyzing effects on AST, ALT, urea and creatinine. Prior studies regarding the hematological and biochemical analysis of wild felids indicated hyperglycemia and glycosuria. Both yohimbine and tolazoline have been linked to elevated levels of liver enzymes. Their adverse effects have been previously associated with hepatotoxicity and nephrotoxicity in several domestic and pet animal species [31]. But data pertaining to their impact in wild species is rather limited. Most of the prior findings have studied the impact of ketamine-xylazine combination and attributed post-anesthetic aberrations in haemato-biochemical values to xylazine rather than alpha-2 antagonist usage [24,38–40]. Nevertheless, there have been studies whereby tolazoline, yohimbine or atipamezole were employed to reverse anesthetic effects in wild felids [5,12,21,41-43].

Some of these studies have related elevated AST, ALT, urea and creatinine values with yohimbine or tolazoline usage. Similarly, we have observed pronounced effects of tolazoline on AST, ALT and urea of tiger and leopards inducted into this study as compared to yohimbine. Concomitantly, our findings in lions were vexing as both tolazoline and yohimbine significantly affected AST, ALT and urea values. Such findings in free ranging African lions have been previously reported [33]. It was suggested that higher liver enzyme values indicated liver injury while elevated serum urea and creatinine were attributed to poor clearance by kidneys [34]. Considering this fact, we can assume that just because the values were far greater when tolazoline was employed as reversal rather than yohimbine, the deleterious impact on liver and kidney was more pronounced due to tolazoline usage *(Fig. 5)*.

In the current paradigm, ketamine and xylazine combination is being used to anesthetize wild felid species in Pakistan for relocation or minor clinical procedures. This combination used in adequate dosage renders successful ataxia and effective loss of sensation. In our study we have reported that yohimbine can radically shorten the recovery period after anesthesia. The deleterious effects of yohimbine on liver and kidney function 12 h after administration were much lower than that of tolazoline.

In summary, considering the fact that yohimbine produced shorter duration for onset, sternal and standing recovery along with lower serum biochemistry values. It can therefore be concluded, that yohimbine is a far more efficacious and safer antagonist than tolazoline when used as a reversal agent in wild felids.

Acknowledgments

The authors would like to thank Dr. Taimoor Saleem for his help in sample and data collection.

Financial Support

This research did not receive any specific grant from funding agencies in the public, commercial, or not-for-profit sectors.

Conflict of Interest

There are no conflicts of interest in our present study.

Author Contributions

Experimental Design was conceived by A.H. Rabbani,, Y.R. Khan and K. Hussain. Data was collected by A.H. Rabbani, A. Waheed and H. Afzal. Statistical analysis was conducted by O. Naseer, M. Shahid and A. Ali. Original draft was written by A.H. Rabbani, O. Naseer and Y.R. Khan. All authors have contributed to the revision and final proof-reading of the manuscript.

References

1. Hussain S: Producing wilderness predators. **In,** Sivaramakrishnan K (Ed): The Snow Leopard and the Goat: Politics of Conservation in the Western Himalayas. 40-57, University of Washington Press, 2019.

2. Cardillo M, Purvis A, Sechrest W, Gittleman JL, Bielby J, Mace GM: Human population density and extinction risk in the world's carnivores. *PLoS Biol*, 2 (7): e197, 2004. DOI: 10.1371/journal.pbio.0020197

3. Bauer H, Van Der Merwe S: Inventory of free-ranging lions *Panthera leo* in Africa. *Oryx*, 38 (1): 26-31, 2004. DOI: 10.1017/S0030605304000055

4. Wikramanayake E, Dinerstein E, Seidensticker J, Lumpkin S, Pandav B, Shrestha M, Mishra H, Ballou J, Johnsingh AJT, Chestin I, Sunarto S, Thinley P, Thapa K, Jiang G, Elagupillay S, Kafley H, Pradhan NMB, Jigme K, Teak S, Cutter P, Aziz MA, Than U: A landscape-based conservation strategy to double the wild tiger population. *Conserv Lett*, 4 (3): 219-227, 2011. DOI: 10.1111/j.1755-263X.2010.00162.x

5. Deka K, Athreya V, Odden M, Linnell J: Chemical immobilization of leopard *Panthera pardus* in the wild for collaring in Maharashtra, India. *J Bombay Nat Hist Soc*, 109 (3): 153-157, 2012.

6. Lodhi A: Conservation of leopards in Ayubia National Park, Pakistan. *MSc Thesis,* The University of Montana, 2007.

7. Larsson MHMA, Coelho FM, Oliveira VMC, Yamaki FL, Pereira GG, Soares EC, Fedullo JDL, Pereira RC, Ito FH: Electrocardiographic parameters of captive lions *(Panthera leo)* and tigers *(Panthera tigris)* immobilized with ketamine plus xylazine. *J Zoo Wildl Med*, 39 (3): 314-319, 2008. DOI: 10.1638/2007-0028.1

8. Pavlova EV, Alekseeva GS, Erofeeva MN, Vasilieva NA, Tchabovsky AV, Naidenko SV: The method matters: The effect of handling time on cortisol level and blood parameters in wild cats. *J Exp Zool Part A*, 329 (3): 112-119, 2018. DOI: 10.1002/jez.2191

9. Seal US, Armstrong DL, Simmons LG: Yohimbine hydrochloride reversal of ketamine hydrochloride and xylazine hydrochloride immobilization of Bengal tigers and effects on hematology and serum chemistries. *J Wildl Dis*, 23 (2): 296-300, 1987. DOI: 10.7589/0090-3558-23.2.296

10. Jalanka H: Medetomidine-and ketamine-induced immobilization of snow leopards *(Panthera uncia):* Doses, evaluation, and reversal by atipamezole. *J Zoo Wildl Med*, 20 (2): 154-162, 1989.

11. Clark-Price SC, Lascola KM, Schaeffer DJ: Physiological and biochemical variables in captive tigers *(Panthera tigris)* immobilized with dexmedetomidine and ketamine or dexmedetomidine, midazolam and ketamine. *Vet Rec*, 177 (22): 570, 2015. DOI: 10.1136/vr.103526

12. Semjonov A, Andrianov V, Raath JP, Orro T, Venter D, Laubscher L, Pfitzer S: Evaluation of BAM (butorphanol-azaperone-medetomidine) in captive African lion *(Panthera leo)* immobilization. *Vet Anaesth Analg*, 44 (4): 883-889, 2017. DOI: 10.1016/j.vaa.2017.02.001

13. Sharma D: Ketamine-xylazine anaesthesia in snow leopard *(Uncia uncia). Zoos' Print J*, 22 (11): 2895, 2007.

14. Bharathidasan M, Thirumurugan R, William BJ, George RS, Arunprasad A, Kannan TA, Viramuthu S: Xylazine-ketamine immobilization and propofol anesthesia for surgical excision of sebaceous adenoma in a jaguar *(Panthera onca). Vet World*, 7 (11): 986-990, 2014. DOI: 10.14202/vetworld.2014.986-990

15. Cistola AM, Golder FJ, Centonze LA, McKay LW, Levy JK: Anesthetic and physiologic effects of tiletamine, zolazepam, ketamine, and xylazine combination (TKX) in feral cats undergoing surgical sterilization. *J Feline Med Surg*, 6 (5): 297-303, 2004. DOI: 10.1016/j.jfms.2003.11.004

16. Jimenez IA, Militana EA, Martin-Flores M: General anaesthesia of a black leopard *(Panthera pardus)* with alfaxalone, ketamine and isoflurane. *Vet Rec Case Rep*, 8 (2): e001009, 2020. DOI: 10.1136/vetreccr-2019-001009

17. Grassman Jr LI, Austin SC, Tewes ME, Silvy NJ: Comparative immobilization of wild felids in Thailand. *J Wildl Dis*, 40 (3): 575-578, 2004. DOI: 10.7589/0090-3558-40.3.575

18. Kreeger TJ, Seal US, Faggella AM: Xylazine hydrochloride-ketamine hydrochloride immobilization of wolves and its antagonism by tolazoline hydrochloride. *J Wildl Dis*, 22 (3): 397-402, 1986. DOI: 10.7589/0090-3558-22.3.397

19. Di Cesare F, Cagnardi P, Ravasio G, Capasso M, Magnone W, Villa R: Pharmacokinetics of ketamine and norketamine following intramuscular administration combined with dexmedetomidine in tigers *(Panthera tigris). Int J Health Anim Sci Food Saf*, 5 (1s): 85-86, 2018. DOI: 10.13130/2283-3927/10062

20. Sontakke SD, Umapathy G, Patil MS, Shivaji S: Tolazoline antagonises ketamine-xylazine anaesthesia in an endangered Black buck *(Antilope cervicapra). Eur J Wildl Res*, 55 (4): 357-361, 2009. DOI: 10.1007/s10344-009-0251-x

21. Sontakke SD, Umapathy G, Shivaji S: Yohimbine antagonizes the anaesthetic effects of ketamine-xylazine in captive Indian wild felids. *Vet Anaesth Analg*, 36 (1): 34-41, 2009. DOI: 10.1111/j.1467-2995.2008.00427.x

22. Curro TG, Okeson D, Zimmerman D, Armstrong DL, Simmons LG: Xylazine-midazolam-ketamine versus medetomidine-midazolam-ketamine anesthesia in captive Siberian tigers *(Panthera tigris altaica). J Zoo Wildl Med*, 35 (3): 320-327, 2004. DOI: 10.1638/03-049

23. Fahlman Å, Loveridge A, Wenham C, Foggin C, Arnemo JM, Nyman G: Reversible anaesthesia of free-ranging lions *(Panthera leo)* in Zimbabwe. *J S Afr Vet Assoc*, 76 (4): 187-192, 2005. DOI: 10.4102/jsava.v76i4.424

24. Kolahian S: Efficacy of different antiemetics with different mechanism of action on xylazine induced emesis in cats. *Iran J Vet Surg*, 9 (1): 9-16, 2014.

25. Bush M, Custer H, Smeller J, Bush LM, Seal US, Barton R: The acid-base status of lions, *Panthera leo,* immobilized with four drug combinations. *J Wildl Dis*, 14 (1): 102-109, 1978. DOI: 10.7589/0090-3558-14.1.102

26. Spear BV: Lions, tigers and bears beware: The decline of environmental protection. *North Ill Univ Law Rev*, 18, 553-574, 1998.

27. Kaur M, Singh PM: Current role of dexmedetomidine in clinical anesthesia and intensive care. *Anesth Essays Res*, 5 (2): 128-133, 2011. DOI: 10.4103/0259-1162.94750

28. Aroni F, Iacovidou N, Dontas I, Pourzitaki C, Xanthos T: Pharmacological aspects and potential new clinical applications of ketamine: Reevaluation of an old drug. *J Clin Pharmacol*, 49 (8): 957-964, 2009. DOI: 10.1177/0091270009337941

29. Steeil J, Ramsay EC, Marin M, Molsey C, Reilly S, Seddighi MR: Hyperkalemia in exotic felids anesthetized with alpha-2 adrenoceptor agonist, ketamine and isoflurane. **In,** *Proc. Annual Conference AAZV,* 2013. http://www.tigerhaven.org/reference/files/Steeil%20Hyperkalemia%20in%20cats%202013.pdf; *Accessed:* 17 Jun 2020.

30. Ramsay EC: Felids. **In,** West G, Heard DJ, Caulkett N (Eds): Zoo Animal and Wildlife Immobilization and Anesthesia. 2nd ed., 635-646, Wiley-Blackwell, United Kingdom, 2014. DOI: 10.1002/9781118792919

31. Muir WW, McDonell WN, Kerr CL, Grimm KA, Lemke KA, Branson KR, Lin H-C, Steffey EP, Mama KR, Martinez EA: Anesthetic physiology and pharmacology. **In,** Grimm KA, Tranquilli WJ, Lamont LA (Eds): Essentials of Small Animal Anesthesia and Analgesia. 2nd ed., 15-82, Wiley-Blackwell, United Kingdom, 2011.

32. Miller M, Weber M, Neiffer D, Mangold B, Fontenot D, Stetter M: Anesthetic induction of captive tigers *(Panthera tigris)* using a medetomidine-ketamine combination. *J Zoo Wildl Med*, 34 (3): 307-308, 2003. DOI: 10.1638/02-036

33. Jacquier M, Aarhaug P, Arnemo JM, Bauer H, Enriquez B: Reversible immobilization of free-ranging African lions *(Panthera leo)* with medetomidine-tiletamine-zolazepam and atipamezole. *J Wildl Dis*, 42 (2): 432-436, 2006. DOI: 10.7589/0090-3558-42.2.432

34. Herbst LH, Packer C, Seal US: Immobilization of free-ranging African lions *(Panthera leo)* with a combination of xylazine hydrochloride and ketamine hydrochloride. *J Wildl Dis*, 21 (4): 401-404, 1985. DOI: 10.7589/0090-3558-21.4.401

35. Seal US, Armstrong DL, Simmons LG: Yohimbine hydrochloride reversal of ketamine hydrochloride and xylazine hydrochloride immobilization of Bengal tigers and effects on hematology and serum chemistries. *J Wildl Dis*, 23 (2): 296-300, 1987. DOI: 10.7589/0090-3558-23.2.296

36. Kreeger TJ, Arnemo JM, Raath JP: Emergency treatment - Animal. **In,** Handbook of Wildlife Chemical Immobilization. 3rd ed., 80-97, Wildlife Pharmaceuticals Inc., Colorado USA, 1999.

37. Tyler NJC, Hotvedt R, Blix AS, Sørensen DR: Immobilization of Norwegian reindeer *(Rangifer tarandus tarandus)* and Svalbard Reindeer *(R. t. platyrhynchus)* with medetomidine and medetomidine-ketamine and reversal of immobilization with atipamezole. *Acta Vet Scand*, 31 (4): 479-488, 1990. DOI: 10.1186/BF03547531

38. Symonds HW: The effect of xylazine upon hepatic glucose production and blood flow rate in the lactating dairy cow. *Vet Rec*, 99 (12): 234-236, 1976.

39. Hickman MA, Cox SR, Mahabir S, Miskell C, Lin J, Bunger A, McCall RB: Safety, pharmacokinetics and use of the novel NK-1 receptor antagonist maropitant (CereniaTM) for the prevention of emesis and motion sickness in cats. *J Vet Pharmacol Ther*, 31 (3): 220-229, 2008. DOI: 10.1111/j.1365-2885.2008.00952.x

40. Kanda T, Hikasa Y: Neurohormonal and metabolic effects of medetomidine compared with xylazine in healthy cats. *Can J Vet Res*, 72, 278-286, 2008.

41. Stander PE, Morkel PB: Field immobilization of lions using disassociative anaesthetics in combination with sedatives. *Afr J Ecol*, 29 (2): 137-148, 1991. DOI: 10.1111/j.1365-2028.1991.tb00994.x

42. Van Wyk TC, Berry HH: Tolazoline as an antagonist in free-living lions immobilized with a ketamine-xylazine combination. *J S Afr Vet Assoc,* 57, 221-224, 1986.

43. Forsyth SF, Machon RG, Walsh VP: Anaesthesia of a sumatran tiger on eight occasions with ketamine, medetomidine and isoflurane. *N Z Vet J*, 47 (3): 105-108, 1999. DOI: 10.1080/00480169.1999.36123

Kafkas Universitesi Veteriner Fakultesi Dergisi
ISSN: 1300-6045 e-ISSN: 1309-2251
Journal Home-Page: http://vetdergikafkas.org

Kafkas Univ Vet Fak Derg
27 (3): 301-306, 2021
DOI: 10.9775/kvfd.2020.25170

RESEARCH ARTICLE

Oxidative Impact of Dietary Triclabendazole in *Galleria mellonella*

Ender BÜYÜKGÜZEL [1,a (*)] Kemal BÜYÜKGÜZEL [2,b]

[1] Department of Molecular Biology and Genetics, Faculty of Science and Arts, Zonguldak Bülent Ecevit University, TR-67100 Zonguldak - TURKEY
[2] Department of Biology, Faculty of Science and Arts, Zonguldak Bülent Ecevit University, TR-67100 Zonguldak - TURKEY
ORCIDs: [a] 0000-0002-4442-5081; [b] 0000-0002-6959-8480

Article ID: KVFD-2020-25170 Received: 22.11.2020 Accepted: 23.03.2021 Published Online: 02.04.2021

Abstract

Recent studies have shown that anthelmintic and antifungal agents are recommended as alternative agents in chemical control of insect pests. In this study, first instar larvae of the greater wax moth, *Galleria mellonella,* were reared on artificial diets containing 0.001, 0.01, and 0.1 g/100 g of triclabendazole, an anthelmintic benzimidazole. The effects of these triclabendazole concentrations on the lipid peroxidation product, malondialdehyde (MDA) and glutathione-S-transferase (GST) activity were investigated in all G. mellonella developmental stages, as well as in the midgut tissue of the insect. Compared to controls, the highest triclabendazole concentration (0.1%) increased MDA content from 0.182±0.03 to 0.415±0.04 nmol/mg protein in the larvae, from 0.190±0.04 to 0.626±0.06 nmol/mg protein in the pupae, and from 0.354±0.06 to 0.451±0.04 nmol/mg protein in the adults. MDA content was determined to be 0.141±0.02 to 0.835±0.13 nmol/mg protein in the midgut. The highest concentration of triclabendazole was found to significantly increase GST activity in the larvae, pupae, adults, and in the midgut tissue of *G. mellonella* in comparison to controls. The three dietary concentrations of triclabendazole resulted in a high degree of oxidative stress and an increase in the activity of the detoxification enzyme GST following an increase in MDA levels in the midgut and in all developmental stages of G. mellonella.

Keywords: *Galleria mellonella, Oxidative stress, Triclabendazole, Malondialdehyde, Glutathione-S- transferase*

Triklabendazolün *Galleria mellonella*'daki Oksidatif Etkisi

Öz

Son çalışmalarda, antihelmintik ve antifungal ajanların, böcek zararlılarının kimyasal kontrolünde alternatif kimyasallar olarak önerildiğini görülmektedir. Bu çalışmada, büyük bal mumu güvesi, *Galleria mellonella,* birinci evre larvaları 0.001, 0.01 ve 0.1 g/100 g benzimidazol grubu bir antihelmintik olan triklabendazol içeren yapay besinler ile beslendi. Belirlenen konsantrasyonların böceğin farklı gelişme evrelerinde (7. evre larva, pup ve ergin) ve orta bağırsağında oksidatif stresin önemli bir belirteci olan lipid peroksidasyonu ürünü malondialdehit (MDA) miktarı ve bir detoksifikasyon enzimi olan glutatyon-S-transferaz (GST) aktivitesi üzerine etkileri araştırıldı. Kontrol grubu ile en yüksek triklabendazol konsantrasyonu (0.1%) karşılaştırıldığında MDA miktarını böceğin larval evresinde 0.182±0.03'ten 0.415±0.04 nmol/mg proteine, pupal evrede 0.190±0.04'ten 0.626±0.06 nmol/mg proteine, ergin bireylerde 0.354±0.06'dan 0.451±0.04 nmol/mg proteine yükseldi. Orta bağırsağında MDA miktarı 0.141±0.02'den 0.835±0.13 nmol/mg protein olarak belirlendi. Triklabendazolün en yüksek konsantrasyonu kontrol grubuna göre böceğin larva, pup, ergin evreleri ve orta bağırsağında GST aktivitesini arttırdığı tespit edildi. Elde edilen bu sonuçlar ile triklabendazolun üç farklı konsantrasyonunun bulunduğu yapay besinler ile beslenen *G. mellonella*'nın tüm gelişme evrelerinde ve orta bağırsağında oksidatif stres belirteci MDA miktarındaki artışa bağlı olarak yüksek derecede oksidatif stres meydana geldiği ve detoksifikasyon enziminin aktivitesinin arttığı belirlendi.

Anahtar sözcükler: *Galleria mellonella, Oksidatif stres, Triklabendazol, Malondialdehit, Glutatyon-S- transferaz*

INTRODUCTION

A number of physical, chemical, and biological techniques are used to protect crops from pest insects and increase crop yields [1,2]. However, the use of insecticides in agricultural fields poses a threat to other, non-target organisms, as well as to the environment. Therefore, the use of effective and environmentally sensitive chemicals as an alternative to traditional insecticides has increased. It has contributed to the growing interest in alternative pest control of

How to cite this article?

Büyükgüzel E, Büyükgüzel K: Oxidative impact of dietary triclabendazole in *Galleria mellonella*. *Kafkas Univ Vet Fak Derg,* 27 (3): 301-306, 2021.
DOI: 10.9775/kvfd.2020.25170

(*) Corresponding Author

Tel: +90 372 2574010/1405
E-mail: endericen@hotmail.com (E. Büyükgüzel)

clinically important drugs, including anthelmintics [3]. *Galleria mellonella* is a model organism, easy to rearing in laboratory conditions, used in many biological studies including physiological, genetic, and toxicological research areas in recent years [4,5]. Recent laboratory studies have shown that next-generation chemicals have negative effects on *G. mellonella* [6-10]. In a study by Çalık et al.[3], the sub-lethal effects of mebendazole, an anthelmintic in the benzimidazole group, on the biology of this model organism was investigated by observing survival, growth, adult longevity, fecundity, and hatchability and was found to have a deleterious effect on its physiology.

Insects are exposed to numerous stresses throughout their lives, especially physical (radiation, temperature, etc.) and chemical (pesticides, heavy metals, etc.) factors [11]. These factors may cause free radical formation, oxidative stress and, subsequently, cellular damage [11-13]. Malondialdehyde (MDA) is a widely used marker of oxidative stress [13,14], and an increase in free radicals causes the overproduction of MDA. However, there are antioxidant enzyme systems in insects that work against these free radicals [6,15-17]. In particular, glutathione S-transferases (GSTs) are multi-functional antioxidant enzymes involved in the detoxification process via a number of different mechanisms. They are evolutionarily conserved enzymes that are important in the detoxification of many xenobiotic compounds [15,18].

The midgut, where digestive enzymes are secreted and nutrients absorbed, is an important tissue of insects [19]. One study that investigated the effects of *Bacillus thuringiensis* (a bio-insecticide used for agricultural pest management) on antioxidant capacity and lipid peroxidation in *G. mellonella* found that it contributed to cell death by increasing the effect of oxidative stress in the midgut [20]. Recently, a number of other studies have indicated that anthelmintic and antifungal agents should be used as alternatives for insect management [3,6-10,21,22]. In one study, the effects of terbinafine (an antifungal agent) on MDA and protein carbonyl (PCO) contents, which are oxidative stress biomarkers in the midgut of *G. mellonella*, and glutathione S-transferase (GST) activity, a detoxification enzyme, were examined. It was determined that terbinafine increased the MDA content in the midgut tissue when compared to a control group, and similarly increased PCO content and GST enzyme activity with in a dose-dependent manner [22].

Triclabendazole is a benzimidazole anthelmintic known to be effective against the larval and adult stages of parasites *(Fasciola hepatica, Fasciola gigantica* and *Fascioloides magna)* that cause infections in humans and animals [23,24]. In a previous study that our laboratory conducted, we showed that triclabendazole also negatively affects the biology of *G. mellonella*. However, insect survival parameters are important criteria for investigating and understanding the appropriate use of triclabendazole as an insecticide [3]. Therefore, in this study, the oxidative effects of triclabendazole on the midgut tissue of *G. mellonella,* and at different development stages, was examined at increasing concentrations in an artificial diet.

Material and Methods

Galleria mellonella Culture

A stock culture was obtained by rearing *G. mellonella* (Lepidoptera: Pyralidae) pupae and adults at Zonguldak Bülent Ecevit University, Department of Molecular Biology and Genetics, Insect Culture Laboratory. Newly hatched first instar larvae were reared on an artificial diet consisting of 420 g wheat bran, 150 mL liquid honey, 150 mL glycerin, 20 g ground dark honeycombs, and 30 mL distilled water [25]. The insect culture was maintained in a Nüve FN 400 incubator (Nüve A.Ş., Ankara, Turkey) that was set to 28±2°C, 65±5% relative humidity, and in continuous darkness. The final larval stage, as well as the pupae, adults, and midguts were used for biochemical analysis.

Triclabendazole Concentrations

Triclabendazole [($C_{14}H_9Cl_3N_2OS$) (5-kloro-6-(2,3-dikloro-fenoksi)-2-(metil-tiyo)-1*H*-benzimidazol)] was obtained from Merck, Darmstadt, Germany. The triclabendazole concentrations used in this study were determined as gram quantity supplemented to 100 grams of diet. Three different concentrations of 0.001, 0.01 and 0.1% were used. A control group reared on a diet without triclabendazole was included. The experimental triclabendazole concentrations were based on our previous study investigating the effects of triclabendazole on the development and life parameters of *G. mellonella* [3].

Midgut Isolation

Last larval stage of *G. mellonella* were kept on ice for 5 min and disinfected with 95% ethanol. They were then fixed in a paraffin-filled petri dish and cut from the front of the first pair of thoracic legs to the third pair of abdominal legs along the mid-axis with dissection scissors. The midguts were retrieved using fine-tipped forceps under a stereo-microscope (Olympus SZ61; Olympus, Tokyo, Japan) and separated from the anterior and hindgut. The fat body, malpighian tubules, and gut contents were also removed. The midguts were placed in Eppendorf tubes containing cold homogenization buffer (w/v 1.15% KCl, 25 mM K_2HPO_4, 5 mM EDTA, 2 mM PMSF, 2 mM DTT, pH 7.4) and stored at -80°C.

Determination of MDA Content and GST Activity

Malondialdehyde content, which reacts to thiobarbituric acid at 532 nm, was measured based on the method by Jain and Levine [26] with a dial beam spectrophotometer (Shimadzu 1700 UV/Vis, Kyoto, Japan) and calculated using a coefficient of 1.56 x 105 $M^{-1}cm^{-1}$. Results are given as nmol/mg protein. GST (EC 2.5.1.18) activity was assayed

by measuring the formation of glutathione (GSH) and 1-chloro-2,4-dinitrobenzene conjugate [27] with a dial beam spectrophotometer (Shimadzu 1700 UV/Vis, Kyoto, Japan). The specific activity of the enzyme is given as µmol/mg protein/min. Protein concentrations were determined according to Lowry et al.[28] and bovine serum albumin was used as a quantitative standard.

Data Analysis

One-way analysis of variance (ANOVA) was used to analyze MDA content and GST activity in the midgut, seventh instar larvae, pupae, and adult *G. mellonella* treated with different concentrations of triclabendazole in an artificial diet. To determine significant differences between mean values, the least significant differences test was used. Statistical significance was assessed at P<0.05. SPSS statistical software (version 15.0 for windows; SPSS Inc., Chicago, IL, USA) was used for the analyses [29].

Results

At the highest triclabendazole concentration (0.1%), MDA content was significantly higher than in the control group. It increased from 0.182±0.03 to 0.415±0.04 nmol/mg protein in the larvae, 0.190±0.04 to 0.626±0.06 nmol/mg protein in the pupae, and from 0.354±0.06 to 0.451±0.04 nmol/mg protein in the adult stage of the insect *(Fig. 1, Fig. 2, Fig. 3)*. Furthermore, when compared with the control group, the amount of MDA in the mid-intestinal tissue at the highest triclabendazole concentration increased approximately 6-fold, from 0.141±0.02 to 0.835±0.13 nmol/mg protein *(Fig. 4)*.

The effects of triclabendazole on GST activity showed statistically significant increases for all of the different triclabendazole concentrations at all developmental stages, and in the midgut tissue. At the larval stage, GST activity in the control group was 145.90±27.89 µmol/mg protein/min. However, this value was 329.76±32.51 µmol/mg protein/min at the highest triclabendazole concentration *(Fig. 5)*. While GST activity at the pupal stage was 36.25±6.82 in the control group, it was found to be 104.67±12.39 µmol/mg protein/min at 0.1% of triclabendazole *(Fig. 6)*.

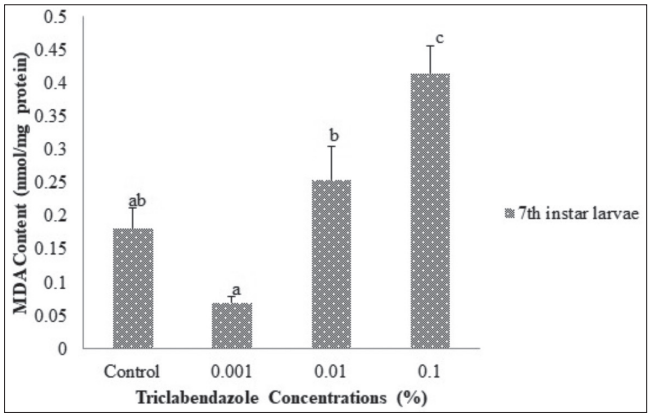

Fig 1. Effects of dietary triclabendazole on MDA content in 7th instar larvae of *G. mellonella*. Bars represent the means ± SE of four replicates. Means followed by different letter are significantly different (P<0.05, LSD test)

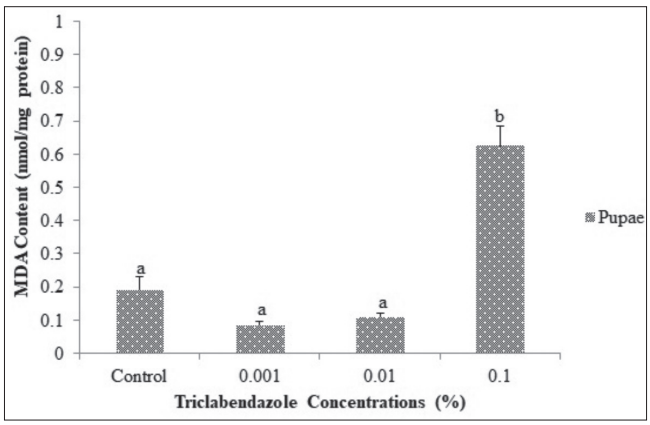

Fig 2. Effects of dietary triclabendazole on MDA content in pupae of *G. mellonella*. Bars represent the means ± SE of four replicates. Means followed by different letter are significantly different (P<0.05, LSD test)

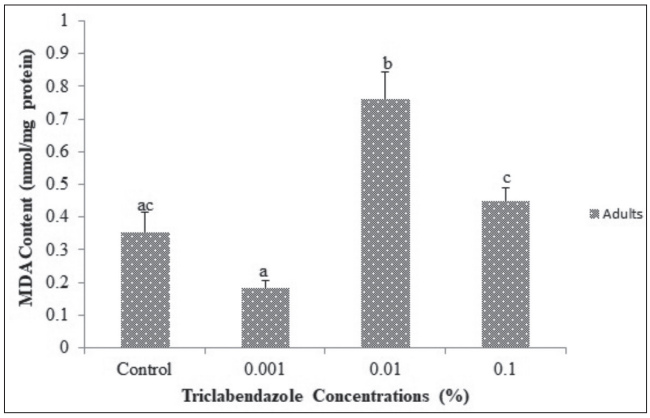

Fig 3. Effects of dietary triclabendazole on MDA content in adults of *G. mellonella*. Bars represent the means ± SE of four replicates. Means followed by different letter are significantly different (P<0.05, LSD test)

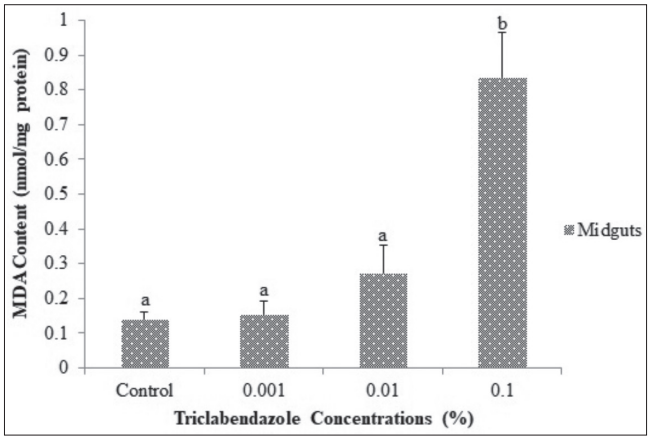

Fig 4. Effects of dietary triclabendazole on MDA content in midguts of *G. mellonella*. Bars represent the means ± SE of four replicates. Means followed by different letter are significantly different (P<0.05, LSD test)

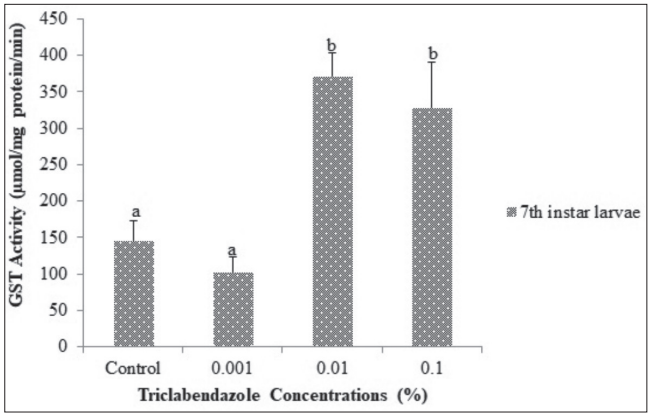

Fig 5. Effects of dietary triclabendazole on GST activity in 7th instar larvae of *G. mellonella*. Bars represent the means ± SE of four replicates. Means followed by different letter are significantly different (P<0.05, LSD test)

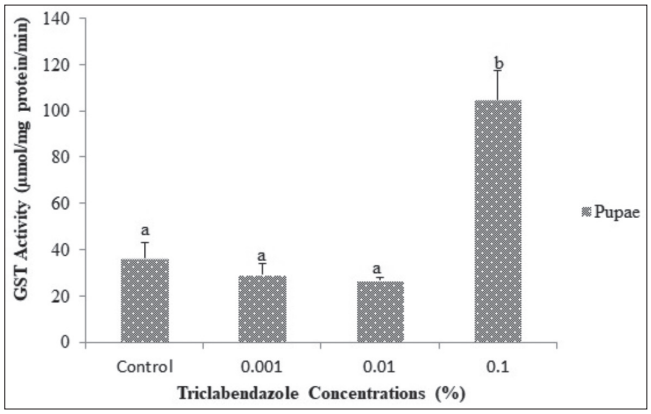

Fig 6. Effects of dietary triclabendazole on GST activity in pupae of *G. mellonella*. Bars represent the means ± SE of four replicates. Means followed by different letter are significantly different (P<0.05, LSD test)

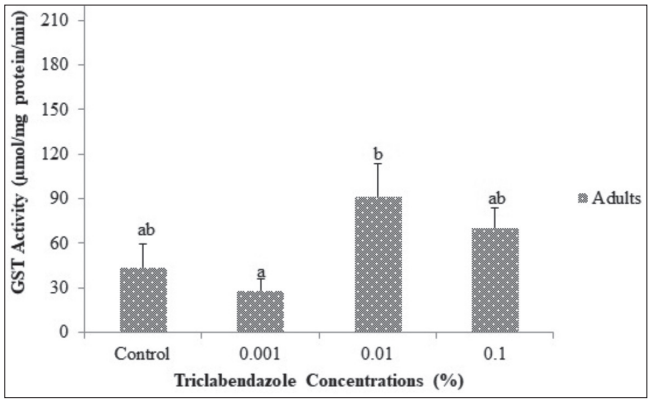

Fig 7. Effects of dietary triclabendazole on GST activity in adults of *G. mellonella*. Bars represent the means ± SE of four replicates. Means followed by different letter are significantly different (P<0.05, LSD test)

The GST activity of the adults was 44.13±15.27 in the control group and 91.62±21.57 µmol/mg protein/min at 0.01% of triclabendazole *(Fig. 7)*. A statistically significant increase was recorded in the GST activity in the midgut tissue as well, which increased approximately 9-fold

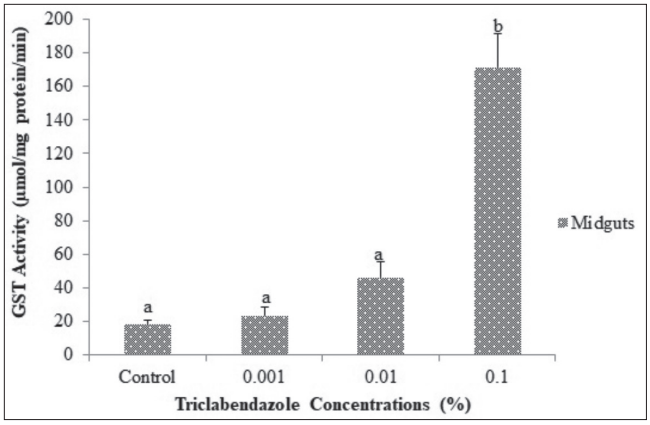

Fig 8. Effects of dietary triclabendazole on GST activity in midguts of *G. mellonella*. Bars represent the means ± SE of four replicates. Means followed by different letter are significantly different (P<0.05, LSD test)

(from 18.31±2.34 µmol/mg protein/min in the control group to 171.29±20.33 µmol/mg protein/min at 0.1% of triclabendazole) *(Fig. 8)*.

Discussion

Insect lipid reserves are affected by a number of factors including nutritional status, developmental stage, environmental variables, the diaphragm, migration flight, and energy metabolism [30]. Diet quality during the larval stage is especially important for the other development stages [7,31]. The effect of triclabendazole on the biology of *G. mellonella* has also been investigated by Kılıç et al.[7] who determined that the chemical negatively affected survival rates and developmental time. Our results support those of Kılıç et al.[7] and further show a statistically significant increase in MDA content and GST activity at all developmental stages, as well as in the midgut tissue of *G. mellonella,* at the highest dietary concentration of triclabendazole. This indicates that increased MDA content at high triclabendazole concentrations induces oxidative stress in response to free radical formation. However, additional studies are needed to determine the mechanisms (other than dietary interaction, life parameter) that underlie how triclabendazole affect on *G. melloenlla*.

Numerous investigations have shown that different anti-fungal and antibacterial agents have deleterious effects on the survival parameters of *G. mellonella,* and that high concentrations of these substances reduce the quality of artificial diets and cause free radical formation [10,18,32-34]. In a study using niclosamide, an anthelmintic in the salicylanilide group, it was found that a concentration of 0.1% increased MDA content and GST activity in the midgut of *G. mellonella* by 4-fold and 2-fold, respectively [6]. These results are similar to ours, where high concentrations of triclabendazole increased MDA content and GST activity in the larva, pupa, and adult stages of *G. mellonella*, as well as in the midgut tissue. Antioxidant enzymes are known

to be highly sensitive to reactive molecules that occur under oxidative stress. GST is a detoxifying and antioxidant enzyme that removes lipid peroxidation products or the hydroperoxides of cells [35]; therefore, the free radicals that occurred with high concentrations of triclobendazole may have been removed by increasing GST activity.

Insects require essential biomolecules such as proteins, carbohydrates, lipids, enzymes, and vitamins for growth, development, and reproduction [36]. In a study investigating the antihelmintic oxyclozanide that was added to the artificial diet of *G. mellonella*, the authors found that it increased the amount of total protein; although, it had a negative effect on the survival rate in the larvae, pupae, and adult stages. The researchers suggested that the chemical reduced diet quality and consequently decreased the consumption of diet. On the other hand, they also suggested that the chemical increased the amount of total protein, which may have been caused by the developing tolerance of insect by using this substance in an effective way [10]. In another study, triclabendazole was added to the artificial diet of *G. mellonella*. The anthelmintic affected the chemical and physical components of the diet and possibly altered the feeding behavior of the larvae, which may have led to the biological characteristics of the insect being adversely affected [7]. In our study, we believe that high concentrations of triclabendazole had a negative effect on the diet quality of the insect, which led to increased MDA content and GST activity. In a similar study, terbinafine was provided to *G. mellonella* at concentrations of 0.001, 0.01, 0.1, and 1% and was found to adversely affect survival and development. Moreover, MDA and PCO content in the midgut tissue increased, and consequently, GST enzyme activity increased [22]. In another study, the effects of gemifloxacin (at concentrations of 150, 300, 600, and 900 mg/L) on *Drosophila melanogaster* was investigated. The authors found that the survival and development of the insect was adversely affected in a dose-dependent manner, and both MDA content and GST enzyme activity were increased, especially at a dose of 300 mg/L, as a result of oxidative damage in the eggs of the insect [18]. In a study by Güneş and Büyükgüzel [17] four different concentrations of boric acid (10, 100, 200 and 300 mg/L), was added to the artificial diet of *D. melanogaster*, which significantly increased MDA content in the final larval stage of the insect. The authors also reported that MDA and GST activity significantly increased in eggs collected from female individuals.

The larval midgut epithelium of *G. mellonella* is an area that is constantly renewed by via apoptosis, and a new epithelium is formed during the transition from the larval stage to the pupal stage [19,32,37,38]. The intestines of Lepidoptera insects are alkaline, with wide reduction-oxidation potential, which are sensitive to oxidative injury during digestion [34]. Hence, the effect of reactive oxygen species -stimulated oxidative stress in the midgut can occur by disrupting the antioxidant defense system [38]. In this study, it appears that the increase in MDA content in the midgut tissue of *G. mellonella* initiated increased GST activity.

Numerous studies have been conducted to evaluate the effect of xenobiotics, including triclabendazole, on the survival, development, and other biological aspects of different insect species [6-10,18,21,34]. In addition to how chemicals with different mechanisms of action and clinical significance effect these parameters, information regarding the stress mechanisms and antioxidant enzyme capacities in insects have been investigated. According to the literature review, this is the new study to investigate the oxidative effects of different concentrations of triclabendazole fed to *G. mellonella* at three different developmental stages, as well as its effects on the midgut tissue. Our results demonstrate that oxidative stress occurs in *G. mellonella* at high concentrations of triclabendazole and affects its detoxification capacity. According to our results, we may be recommended the 0.1% triclabendazole concentration for use in the field. However, before applying in the field, its effects on other non-target creatures should also be considered. We believe these results will contribute to bodies of research that investigate new, environmentally-friendly, alternative chemicals in insect pest management and on its use as antimicrobial agent in artificial diet conducted under laboratory conditions.

Conflict of Interest

The authors have declared that no competition interests.

Acknowledgement

Authors thank the Research Fund of ZBEU, Project No: 2013-73769380-01 for supporting this study.

Author Contributions

EB and KB planned and designed the research procedure. EB performed the biochemical analysis and the *Galleria mellonella* culture. EB and KB carried out the statistical analysis. The manuscript was written by EB and KB. KB contributed to the language editing of the final manuscript. Both authors have interpreted the data, revised the manuscript for contents, and approved the final version.

References

1. Kılınçer N, Yiğit A, Kazak C, Er MK, Kurtuluş A, Uygun N: Teoriden pratiğe zararlılarla biyolojik mücadele. *Türk Biyo Müc Derg*, 1 (1): 15-60, 2010.

2. Ayubi A, Moravvej G, Karimi J, Jooyandeh A: Lethal effects of four insecticides on immature stages of *Chrysoperla carnea* (Stephens) (Neuroptera: Chrysopidae) in laboratory conditions. *Turk Entomol Derg*, 37 (4): 399-407, 2013.

3. Çalık G, Büyükgüzel K, Büyükgüzel E: Reduced fitness in adults from larval, *Galleria mellonella* (Lepidoptera: Pyralidae) reared on media amended with the antihelmintic, mebendazole. *J Econ Entomol*, 109 (1): 182-187, 2016. DOI: 10.1093/jee/tov305

4. Pereira, TC, de Barros PP, Fugisaki LRO, Rossoni RD, Ribeiro FC, de Menezes RT, Jungueira JC, Scorzoni L: Recent advances in the use of *Galleria mellonella* model to study immune responses against human pathogens. *J Fungi (Basel),* 4:128, 2018. DOI: 10.3390/jof4040128

5. Hernandez, RJ, Hesse E, Dowling AJ, Coyle NM, Feil EJ, Gaze WH, Vos M: Using the wax moth larva *Galleria mellonella* infection model to detect emerging bacterial pathogens. *Peer J*, 6:e6150, 2019. DOI: 10.7717/peerj.6150

6. Büyükgüzel E, Kayaoğlu S: Niklozamidin *Galleria mellonella* L. (Lepidoptera: Pyralidae)'nın bazı biyolojik ve fizyolojik özelliklerine etkisi. *Turk Entomol Derg*, 38 (1): 83-99, 2014. DOI: 10.16970/ted.87976

7. Kılıç A, Büyükgüzel K, Büyükgüzel E: Antihelmintik triklabendazolun yapay besin ile beslenen *Galleria mellonella* (Lepidoptera: Pyralidae) larvalarının yaşama ve gelişimine etkisi. *Kafkas Univ Vet Fak Derg*, 21 (6): 841-847, 2015. DOI: 10.9775/kvfd.2015.13731

8. Sugeçti S, Büyükgüzel K: Effects of oxfendazole on metabolic enzymes in hemolymph of *Galleria mellonella* L. (Lepidoptera: Pyralidae) larvae reared on artificial diet. *Karaelmas Fen Müh Derg*, 8 (2): 590-594, 2018. DOI: 10.7212%2Fzkufbd.v8i2.1380

9. Sefer NE, Büyükgüzel K: Piperazinin *Galleria mellonella*'nın yaşama ve gelişimi üzerine etkisi. *Karaelmas Fen Müh Derg*, 8 (1): 365-372, 2018. DOI: 10.7212%2Fzkufbd.v8i1.1248

10. Çelik C, Büyükgüzel K, Büyükgüzel E: The effects of oxyclozanide on survival, development and total protein of *Galleria mellonella* L. (Lepidoptera: Pyralidae). *J Entomol Res Soc*, 21 (1): 95-108, 2019.

11. Farooqui T, Farooqui AA: Oxidative stress in vertebrates and invertebrates: Molecular Aspects of Cell Signaling. 261-270, John Wiley & Sons Inc., New Jersey, 2012.

12. Halliwell B, Gutteridge JM: Free Radicals in Biology and Medicine. 5th ed., 199-283, Oxford University Press, New York, 2015.

13. Özcan O, Erdal H, Çakırca G, Yönden Z: Oksidatif stres ve hücre içi lipit, protein ve DNA yapıları üzerine etkileri. *J Clin Exp Invest,* 6 (3): 331-336, 2015. DOI: 10.5799/ahinjs.01.2015.03.0545

14. Kodrík D, Bednářová A, Zemanová M, Krishnan N: Hormonal regulation of response to oxidative stress in insects-an update. *Int J Mol Sci*, 16 (10): 25788-25816, 2015. DOI: 10.3390/ijms161025788

15. Büyükgüzel E, Kalender Y: Exposure to streptomycin alters oxidative and antioxidative response in larval midgut tissues of *Galleria mellonella*. *Pestic Biochem Physiol*, 94 (2-3): 112-118, 2009. DOI: 10.1016/j.pestbp.2009.04.008

16. Altuntaş H, Demirci SN, Duman E, Ergin E: Toxicological and physiological effects of ethephon on the model organism, *Galleria mellonella* L. 1758 (Lepidoptera: Pyralidae). *Turk Entomol Derg*, 40 (4): 413-423, 2016. DOI: 10.16970/ted.00995

17. Güneş E, Büyükgüzel E: Oxidative effects of boric acid on different developmental stages of *Drosophila melanogaster* Meigen, 1830 (Diptera: Drosophilidae). *Turk Entomol Derg*, 41 (1): 3-15, 2017. DOI: 10.16970/ted.59163

18. Aslan N, Büyükgüzel E, Büyükgüzel K: Oxidative effects of gemifloxacin on some biological traits of *Drosophila melanogaster* (Diptera: Drosophilidae). *Environ Entomol*, 48 (3): 667-673, 2019. DOI: 10.1093/ee/nvz039

19. Miguel-Aliaga I, Jasper H, Lemaitre B: Anatomy and physiology of the digestive tract of *Drosophila melanogaster*. *Genetics*, 210 (2): 357-396, 2018. DOI: 10.1534/genetics.118.300224

20. Dubovskiy IM, Martemyanov VV, Vorontsova YL, Rantala MJ, Gryzanova EV, Glupov VV: Effect of bacterial infection on antioxidant activity and lipid peroxidation in the midgut of *Galleria mellonella* L. larvae (Lepidoptera, Pyralidae). *Comp Biochem Physiol C Toxicol*, 148 (1): 1-5, 2008. DOI: 10.1016/j.cbpc.2008.02.003

21. Ustundag G, Buyukguzel K, Buyukguzel E: The effect of niclosamide on certain biological and biochemical properties of *Drosophila melanogaster*. *Eur J Biol*, 78 (1): 29-39, 2019. DOI: 10.26650/EurJBiol.2019.0003

22. Kastamonuluoğlu S, Büyükgüzel K, Büyükgüzel E: The use of dietary antifungal agent terbinafine in artificial diet and its effects on some biological and biochemical parameters of the model organism *Galleria mellonella* (Lepidoptera: Pyralidae). *J Econ Entomol*, 113 (3): 1110-1117, 2020. DOI: 10.1093/jee/toaa039

23. Calvopina HM, Guderian RH, Paredes WY, Cooper PJ: Comparison of two single day regimens of triclabendazole for the treatment of human pulmonary paragonimiasis. *Trans R Soc Trop Med Hyg*, 97, 451-454, 2003. DOI: 10.1016/S0035-9203(03)90088-5

24. Yüksek N, Altuğ N, Gül A: Koyunlarda endoparazit enfeksiyonlarında triklabendazol - levamizol kombinasyonunun tedavi etkinliği. *Van Vet J*, 18 (1): 19-24, 2007.

25. Bronskill J: A cage to simplify the rearing of the greater wax moth, *Galleria mellonella* (Pyralidae). *J Lepid Soc*, 15 (2): 102-104, 1961.

26. Jain SK, Levine SN: Elevated lipid peroxidation and vitamin E quinine levels in heart ventricles of streptozoticin-treated diabetic rats. *Free Radic Biol Med*, 18 (2): 337-341, 1995. DOI: 10.1016/0891-5849(94)00114-Y

27. Habig WH, Pabst MJ, Jakoby WB: Glutathione-S-transferases: The first enzymatic step in mercapturic acid formation. *J Biol Chem*, 249, 7130-7139, 1974.

28. Lowry OH, Rosebroug NJ, Farr AL, Randall RJ: Protein measurement with the folin phenol reagent. *J Biol Chem*, 193, 265-275, 1951.

29. SPSS Inc: User's Manual. Version 15.0 for Windows; SPSS Inc., Chicago, IL, USA, 2006.

30. Arrese EL, Soulages JL: Insect fat body: Energy, metabolism, and regulation. *Annu Rev Entomol,* 55, 207-225, 2010. DOI: 10.1146/annurev-ento-112408-085356

31. van Schoor T, Kelly ET, Tam N, Attardo GM: Impacts of dietary nutritional composition on larval development and adult body composition in the yellow fever mosquito *(Aedes aegypti). Insects,* 11 (8): 535, 2020. DOI: 10.3390/insects11080535

32. Büyükgüzel E, Kalender Y: Penicillin-induced oxidative stress: Effects on antioxidative response of midgut tissues in larval instars of *Galleria mellonella*. *J Econ Entomol*, 100 (5): 1533-1541, 2007. DOI: 10.1093/jee/100.5.1533

33. Büyükgüzel E, Kalender Y: *Galleria mellonella* survivorship, development and protein content in response to dietary antibiotics. *J Entomol Sci*, 43 (1): 27-40, 2008. DOI: 10.18474/0749-8004-43.1.27

34. Harmancı C, Büyükgüzel K, Büyükgüzel E: The effect of neomycin on survival and development of *Pimpla turionellae* L. (Hymenoptera: Ichneumonidae) reared on a natural host. *J Econ Entomol*, 112 (3): 1081-1088, 2019. DOI: 10.1093/jee/toy419

35. Dmochowska-Ślęzak K, Giejdasz K, Fliszkiewicz M, Żołtowska K: Variations in antioxidant defense during the development of the solitary bee *Osmia bicornis*. *Apidologie*, 46, 432-444, 2015. DOI: 10.1007/s13592-014-0333-y

36. Ventrella E, Adamski Z, Chudzińska E, Miądowicz-Kobielska M, Marciniak P, Buyukguzel E, Buyukguzel K, Erdem M, Falabella P, Scrano L, Bufo SA: *Solanum tuberosum* and *Lycopersicon esculentum* leaf extracts and single metabolites affect development and reproduction of *Drosophila melanogaster*. *Plos One*, 11 (5): e0155958, 2016. DOI: 10.1371/journal.pone.0155958

37. Uwo MF, Ui-Tei K, Park P, Takeda M: Replacement of midgut epithelium in the greater wax moth, *Galleria mellonela*, during larval-pupal moult. *Cell Tissue Res*, 308 (2): 319-331, 2002. DOI: 10.1007/s00441-002-0515-1

38. Tettamanti G, Grimaldi A, Pennacchio F, de Eguileor M: *Toxoneuron nigriceps* parasitization delays midgut replacement in fifth-instar *Heliothis virescens* larvae. *Cell Tissue Res*, 332 (2): 371-379, 2008. DOI: 10.1007/s00441-008-0579-7

Kafkas Universitesi Veteriner Fakultesi Dergisi
ISSN: 1300-6045 e-ISSN: 1309-2251
Journal Home-Page: http://vetdergikafkas.org

Kafkas Univ Vet Fak Derg
27 (3): 307-314, 2021
DOI: 10.9775/kvfd.2020.25194

RESEARCH ARTICLE

Anti-leakage Effect of Bacterial Cellulose Cover Used in Colonic Anastomosis in Rats

Kenan BINNETOGLU [1,a (*)] Ahmet MIDI [2,b]

[1] Kafkas University, Faculty of Medicine, Department of General Surgery, TR-36000 Kars - TURKEY
[2] Bahcesehir University, Faculty of Medicine, Department of Pathology, TR-34000 Istanbul - TURKEY
ORCIDs: [a] 0000-0001-7517-5970; [b] 0000-0002-6197-7654

Article ID: KVFD-2020-25194 Received: 30.11.2020 Accepted: 05.04.2021 Published Online: 11.04.2021

Abstract

In surgical operations, anastomoses are often preferred for the functionality of the gastrointestinal tract. It has been well known that anastomotic leakages are one of the most serious complications causing high mortality and morbidity. In this experimental study, bacterial cellulose was used to prevent leakage after colon anastomosis as a wound healing agent. The preventive effects of bacterial cellulose, which is often preferred in surgical interventions, on colon leakage were investigated. In our study, colonic anastomosis was performed on 20 Sprague-Dawley rats. In the control group, primary anastomosis was performed on 10 animals. In the experimental group, primary anastomosis followed by cellulose cover along the anastomosis line was performed on 10 animals. After 7 days, anastomotic bursting pressure was measured and histopathological examinations were performed. According to the findings of our study, the bursting pressure increased with bacterial cellulose application. On the other hand, histopathological examinations, bacterial cellulose group showed a significant increase in the fibroblast density, eosinophil density, and collagen density. As a result, bacterial cellulose has been shown to accelerate wound healing mechanically and histopathologically. In our study, it has been demonstrated that bacterial cellulose can be used as a physical barrier with biological properties to prevent leakage after colon anastomosis. Besides, our study will shed light on the advanced clinical studies to be conducted on the effect of bacterial cellulose preventing anastomotic leakage, and we claim that bacterial cellulose may be used for this purpose in the near future.

Keywords: *Anastomosis, Bacterial cellulose, Colonic leakage, Rat*

Ratlarda Kolon Anastomozunda Bakteriyel Selüloz Örtüsünün Kaçak Önleyici Etkisi

Öz

Cerrahi uygulamalarda mide barsak sistemin işlevselliği için anastomozlar cerrahlar tarafından sık olarak tercih edilmektedir. Bunun yanı sıra anastomoz kaçakları yüksek mortalite ve morbiditeye neden olan en ciddi komplikasyonlardan biri olduğu bilinmektedir. Bu çalışmada biyolojik yara iyileştirici olarak artan şekilde popülerliğe sahip olan bakteriyel selüloz, kolon anastomozu sonrası kaçağı önleyici olarak kullanılmıştır. Özellikle cerrahi müdahalelerde sıklıkla tercih edilen bakteriyel selülozun kolon kaçağı üzerine koruyucu etkileri bu çalışmada araştırılmıştır. Materyal ve metot; Yaptığımız bu çalışmada deney hayvanı olarak 20 adet Spraque-Dawley cinsi rat kullanılmıştır. Kontrol grubunda 10 adet deney hayvanına primer anastomoz uygulaması yapılmıştır. Deney grubunda ise 10 adet deney hayvanına primer anastomoz uygulaması yapılarak sütur hattına bakteriyel selüloz örtüsü serilmiştir. Anastomoz uygulamasından 7 gün sonra anastomoz patlama basıncı ölçülerek histopatolojik analizler yapılmıştır. Çalışmamızın sonuçlarına göre bakteriyel selüloz uygulamasının patlama basıncını arttırdığı görülmüştür. Diğer yandan histopatolojik analiz sonuçlarına göre ise bakteriyel selüloz grubunda fibroblast yoğunluğunun, eizinofil yoğunluğunun ve kollojen yoğunluğunun önemli derecede arttığı görülmüştür. Sonuç olarak bakteriyel selülozun mekanik ve histolojik olarak yara iyileştirmesinin hızlandırdığı gösterilmiştir. Bakteriyel selülozun anastomoz sonrası kolon kaçağını önlemek amacı ile biyolojik özellikte fiziksel bir bariyer olarak kullanılabileceği bizim çalışmamızda ortaya konmuştur. Buna ilaveten çalışmamız bakteriyel selülozun anastomoz kaçağını engelleyici etkisi ile ilgili yapılacak olan ileri klinik araştırmalara ışık tutarak, yakın zamanda bakteriyel selüozun bu amaçla klinik kullanıma girebileceğini düşünmekteyiz.

Anahtar sözcükler: *Anastomoz, Bakteriyel selüloz, Kolon kaçağı, Rat*

How to cite this article?

Binnetoglu K, Midi A: Anti-leakage effect of bacterial cellulose cover used in colonic anastomosis in rats. *Kafkas Univ Vet Fak Derg,* 27 (3): 307-314, 2021.
DOI: 10.9775/kvfd.2020.25194

(*) Corresponding Author

Tel: +90 464 6127317
E-mail: kenanbinnet@hotmail.com (K. Binnetoğlu)

Introduction

Anastomotic separation is a serious postoperative complication and the risk of anastomotic leakage is higher in colon surgery than in other gastrointestinal tract (GIT) anastomoses [1]. Anastomotic leakages are one of the most serious complications causing high mortality and morbidity. It is reported that colorectal surgery cases have more frequent mortality and morbidity rates than other anastomoses in the GIT [2]. The size of an anastomotic leakage varies from a tiny point opening to wide clefts and to complete separation [3]. Moreover, it is known that there are leakages due to technical problems [4].

Anastomotic leakages and resulting morbidity/mortality increase towards the distal. Leakage rates vary in the literature. Parameters affecting the leakage rate can be listed as emergency or elective treatment of the patient, definition of leakage and its diagnosis. It is known that the rate is between 3-5% after elective surgery and between 10-15% after emergency surgery [3]. Based on certain reasons such as perforation and mechanical intestinal obstruction, applying emergency surgery on cases with colorectal cancer is still controversial today. Opting for resection and primary anastomosis in such cases ends up with a 10% risk of mortality, and it is assumed that 4-6% of this rate is due to anastomotic leakage [5]. In preventing anastomotic leakages, certain methods are applied today such as applying different anastomotic techniques, antibiotic prophylaxis, pre-operative intestinal cleansing, and fecal diversion with proximal ostomies [6].

The basic producers of cellulose are the plants; as per bacterial cellulose (BC), it is the form of cellulose that is generated by microorganisms. Although BC has the same chemical formula as vegetable cellulose, it stands out with its different physical properties and purity, as well as its potential, particularly in the medical field thanks to the improvements in the biomedical and cell-tissue culture techniques in recent years [7,8]. It has been known for many years that cellulose, which forms the basic structural matrix of the cell walls of almost all plants, some fungi and algae species, is synthesized by *Acetobacter xylinum* [9]. BC has a high biocompatibility owing to its resemblance to extra cellular matrix and its non-toxic structure. It is largely non-immunogenic in that it has a carbohydrate structure, not a protein structure [10]. BC is widely used in various treatments of human and animals. Owing to its high biocompatibility and low inflammatory response, it is applied in humans, especially in the treatment of ulcers, burns and dental implants [11,12]. Today, studies are being carried out for new areas of application for BC, which has a use expanding each passing day. BC has been previously used with satisfactory results in different areas of experimental surgery such as in the scarring of cutaneous wounds, as well as in the grafting used in vascular surgery. BC's biocompatibility has also been well demonstrated in experimental and clinical studies [13]. In this context, research on biological materials is very important to prevent anastomotic leakages. Therefore, we aimed at investigating possible effects of BC on anastomotic leakage.

Material and Methods

Animals and Ethics Approval

The study was carried out on 20 Albino Wistar female rats weighing 250-350 grams. Ethical approval (045.2016.mar) was obtained on 04.04.2016 from the Experimental Animal Ethics Committee of Marmara University. The animals were fed with dry food without any nutrient restriction, each in separate steel cages, in an environment where the temperature was fixed at 23°C degrees. A 12-h light/12-h dark cycle was maintained.

Experimental Groups

The rats were randomly divided into 2 groups as experimental and control groups. In the control group, primary anastomosis was performed on 10 animals. In the experimental group primary anastomosis followed by cellulose cover along the anastomosis line (10 animals) was performed.

Applying BC to Anastomosis Line

Bacterial cellulose was produced in the form of a cover in the laboratories of Immunology Department using *Acetobacter xylinum*. Sterilization was made with ethylene oxide [14].

In the research, anesthesia of the experimental animals was conducted through anesthetic 100 mg/kg ketamine and 30-50 mg/kg chlorpromazine. The abdomens of all rats to be used in the study were shaved and laid on the surgical table in supine position. Following a 4 cm incision on the mid-line of the abdomen, a 4 cm colon segment was resected from 3 cm above the peritoneal reflex *(Fig. 1)*. Subsequently, anastomosis was performed with 5/0 prolene using a single-layer continuous suture technique. The abdomens of the experimental animals were closed in the primary anastomosis group, while BC was laid on the suture line of the other group and the abdomens were closed with 4-0 silk *(Fig. 2)*. Normal saline (0.5 mL) was administered subcutaneously to all animals during surgery as fluid resuscitation. The mice were placed on heating pads to keep them warm during and after surgery and protect animals from hypothermia. At the end of the 7th day following the anastomosis intervention, the rats were euthanized with anesthetic overdose.

Mechanical Measurement of Anastomosis Recovery

Mechanical measurement is often used to assess anastomosis recovery [15]. In our research, the bursting pressure was measured in the postoperative 7th day. In order to measure the bursting pressure, a catheter was advanced 3-4 cm

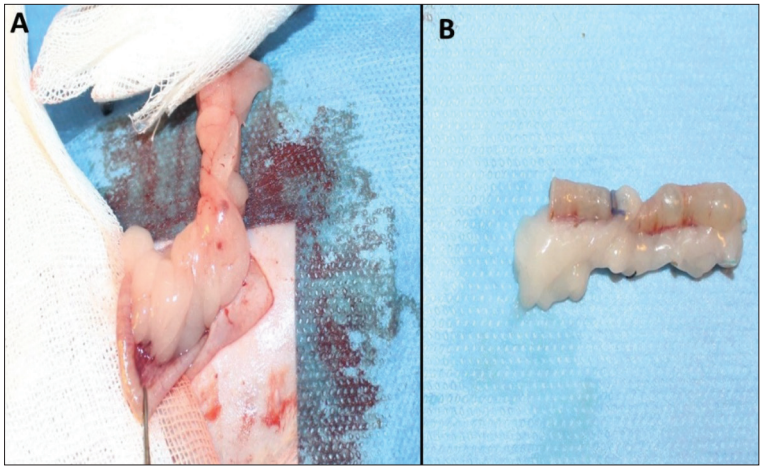

Fig 1. A: Taking the colon out of the abdomen, **B:** Resection of the colon segment

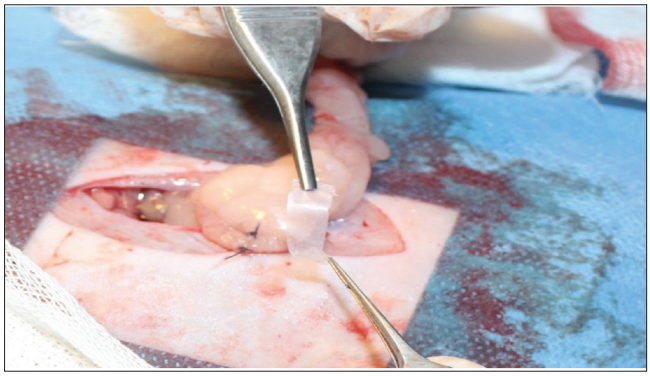

Fig 2. Fixating the bacterial cellulose that covers the anastomosis line

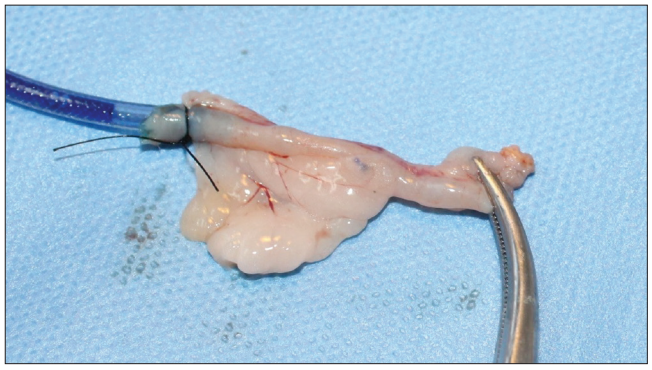

Fig 3. Measuring the burst pressure by injecting the methylene blue

through the anus, and was placed so that its tip came closest to the anastomosis mid-line. After filling the abdomen with saline, 2 cm below and 2 cm above the colon anastomosis were ligated with 2/0 silk. The colon segment connected to the two ends with an inserted catheter was inflated with isotonic colored methylene blue *(Fig. 3)* using an infusion pump at an infusion rate of 4 mL/min; during the inflation process, the pressure values were monitored with the help of a pressure transducer and the bursting pressure was measured. Subsequently, the colon anastomosis line was excised and histopathological examinations were started.

Histopathologic Evaluation

Materials were fixed for five days in 10% formaldehyde. After fixation, the samples were sampled to receive the anastomosi suture line and placed in the cassettes for tissue follow-up. The samples were labeled according to the number sent to the laboratory without knowing which group they belonged to. Then, automatic tissue tracking device (Shandenexelsior ES] was followed for 13 h. In this procedure, tissues were exposed to 2 times 30 min formaldehyde, 6 times 60 min alcohol, 3 times 60 min xylene, once 60 min and two times 80 min paraffin respectively. After the follow-up, 2-micron thick sections were taken from the paraffin-embedded tissues and stained with Hematoxylin & Eosin (H&E). Investigation of the sections was performed by a pathologist in a blind manner under the light microscope (The Olympus Bx 50, Olympus Optical). Active and chronic inflammation, angiogenesis, microabscess, fibrosis, collogen and eosinophil density were the parameters to assess the degree of healing. Histopathological staging of the anastomosis line was performed according to the Ehrlich Hunt model [16,17]. Criteria for staging is as follows 1: There is a small amount but scattered, 2: There is a small amount in every area, 3: Large amount, scattered, 4: Large amount, every area.

Statistical Analysis

In statistical evaluation of the data obtained in the study, IBM 20.00 SPSS package program was used. A nonparametric test was used in examining two different groups in terms of certain variables, the student t-test was used for bursting pressure, and Mann Whitney U test was used for examining the group as the source of difference in histopathological analyses. $P<0.05$ was accepted as the statistical significance limit.

Results

During and after the operation phase, one animal from the control group and one animal from the BC group died. Died animals were excluded from the study. During the

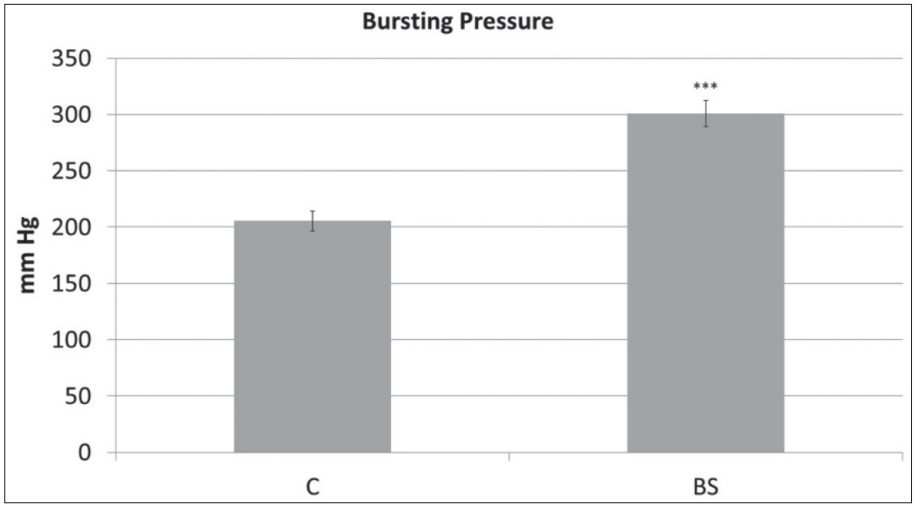

Fig 4. Colon Bursting Pressure (mmHg) ** P<0.05

Fig 5. Histopathologic findings according to Ehrlich-Hunt model. **C:** Control, **BC:** Bacterial cellulose, **Fd:** Fibroblast density, **Cici:** Chronic inflammatory cell infiltration, **Aici:** Acute inflammatory cell infiltration, **Ed:** Eosinophil density, **Af:** Abscess formation, **Cd:** Collagen Density, **A:** Angiogenesis. * P<0.05, *** P<0.005

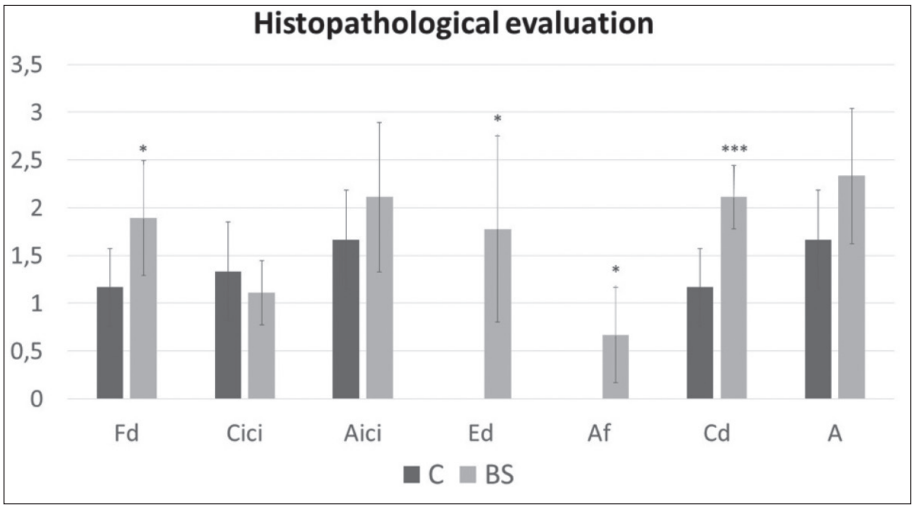

measurement of anastomosis pressure, the anastomoses of the subjects in all groups exploded, and the average bursting pressures were found to be 205.5±8.77 mm Hg in the control group and 300.92±11.8 mm Hg in the BC group *(Fig. 4)*. Based on the anastomosis bursting pressure values obtained from the groups, the application of BC increased the bursting pressure, creating a statistically significant difference compared to the control group (P<0.05).

In the histopathological staging conducted in line with the Ehrlich-Hunt model to evaluate the regeneration of the anastomosis line, it was observed that all parameters in the control group were mild (0-1-2), while particularly acute inflammatory cell infiltration was intense (2-3) in the BC group. Moreover, fibroblast density, which is an indicator of wound healing rate, increased with the application of BC, demonstrating a statistically significant difference compared to the control group (P=0.02). However, no statistically significant change was observed in the acute inflammatory cell infiltration and chronic inflammatory cell infiltration. It was also evaluated that eosinophil density demonstrated a statistically significant increase compared to the control group (P=0.05). The abscess formation was evaluated to be increased with a statistically significant difference (P=0.05). Collagen density values demonstrated the most significant increase in the BC group compared to the control group (P=0.003). On the other hand, angiogenesis parameters increased with the application of BC in comparison to the control group; however, this increase was not statistically significant *(Fig. 5)*. Microscopic images of the histopathological examination are shown in *Fig. 6*.

Discussion

Anastomotic leakage, a significant complication in colorectal surgery, occurs due to problems in the colon healing process [18]. When anastomotic leak occurs in the colon, the postoperative hospital stay increases two times. In order to prevent leakage in colon anastomoses, there should be a healthy bowel, tightness in the anastomosis line and sufficient blood flow Apart from that, anastomosis healing starts with hemostasis and then an inflammatory response occurs. The inflammatory response continues with the release of mediators that increase collagen production and mucosal reepithelization. One of the best indicators of anastomosis healing is increased angiogenesis. If the blood

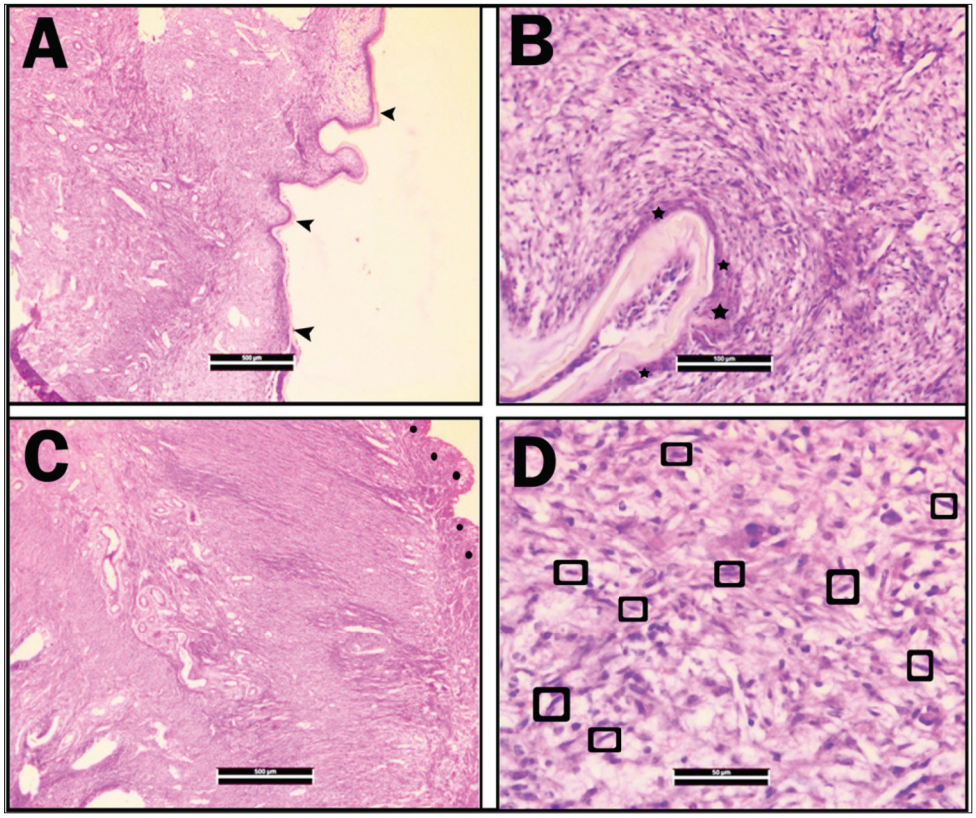

Fig 6. Microscopic images of the histopathological examination of colon tissue. **A:** Complete integration in the serosal surface in the cellulose group *(Arrow)* H&E X40, **B:** Dense fibroblast proliferation around the cellulose material to the cellulose group *(Star)* H&E X100, **C:** Healed appearance of the defect area with thick fibrous tissue in the primary group *(Round)* H&E X40, **D:** Intensive fibroblast proliferation in the primary group *(Square)* H&E X400

supply is good, anastomosis recovery will be faster [19]. In order to prevent colonic anastomotic leakages and to support the anastomosis mechanically, a wide variety of substances have been used such as sheep's intestines, cartilage plaques, goose trachea, and raw hide. Additionally, various drugs, surgical techniques, prosthetics, and adhesives have also been tried [20]. There is an ongoing quest for the most appropriate technique in order to reduce mortality and morbidity rates in anastomoses. Examining the literature, it is observed that numerous experimental research studies have been conducted based on the idea to support with prosthetic materials (patch supporting anastomosis, sponges) for the perfect manual single-layer colonic anastomosis [6].

After a surgery in the GIT, a healing wound demonstrates different characteristics. There are many different characteristics such as a large pool of microorganisms contained in the lumen, the effect of serosa on closing the suture line, vascular nutrition specific to the GIT, whose perfusion decreases in the case of hypovolemia. Under normal conditions and unlike the skin wounds, in bowel wounds smooth muscle cells synthesize collagen in addition to fibroblasts. This synthesis is regulated by different mechanisms. GIT wound healing mainly involves the stages of inflammation, proliferation, fibroplasia and maturation. It is the most important source of tensile strength in the intact mucosa and it is the principal layer on which the sutures that connect the anastomotic tips cling. The accumulation of collagen in the layer determines the mechanical resistance of the wound and its capacity to carry sutures. The tensile strength of the healed suture line reflects the level of recovery in quality and quantity [18]. In our study, with the application of BC in changes that were histopathalogically detected, a significant increase was observed in the amount of collagen. This increase created a statistically significant difference. Studies on bowel anastomoses reported a significant decrease in bowel anastomosis strength within the first 3-4 days. It was thought that this condition was due to increased collagenase activity in the wound area, however, it was observed that there was no decrease in the amount of collagen in reality. Thus, it was admitted that the decrease in anastomosis strength was due to a deficiency in the enzymatic structure of the collagen fibers. In a different study, it was suggested that proteases and free oxygen radicals released from neutrophils temporarily arriving at the wound area can cause a decrease in tensile strength by altering the extracellular matrix. After the 4th day, collagen production and accumulation in the wound area begins to become apparent, and an increase in anastomosis strength occurs with an increase in the amount of collagen. Accordingly, based on our study findings, it can be said that there is an increase in anastomosis strength with the application of BC. Numerous methods and material applications are being tried to obtain a stronger anastomosis line in GIT anastomoses [21,22]. In recent years, the number of studies has been increasing that are recommending the use of surgical tissue adhesive to improve the safety of anastomosis. The most important

examples of these adhesives are fibrin tissue adhesive, bioglue and cyanoacrylate [23].

In determining the quantitative degree of anastomosis recovery, histological, mechanical and biochemical parameters are used, but the value of each one alone is limited. Mechanical parameters are the tools that most reliably reflect anastomosis recovery. Therefore, anastomosis bursting pressure and tensile strength are often applied. Anastomosis bursting pressure is a method of evaluating anastomosis recovery at an early stage after surgery [24]. Since the anastomosis bursting pressure is lowest in the postoperative 3rd day and increases in the 7th, it is usually accepted as the appropriate time to measure the bursting pressure in the 7th postoperative day [15]. According to the results of mechanical measurements in our study, it is observed that BC strengthens the anastomosis line and increases the bursting pressure. Another method that can be used to evaluate the recovery in the anastomosis line caused by cellulose is the histological examination. Among the most frequently applied methods is the examination of cellular infiltration and fibroblastic activity in the anastomosis line with light microscopy [16]. In our study, in evaluating the degree of recovery, active and chronic inflammatory status around the anastomosis, angiogenesis and fibrosis were parametrically evaluated [17]. According to our histopathological findings, it was determined that there were statistically significant increases in the fibroblast density, acute inflammation and eosinophil density with the BC application compared to the control group. There were also significant increases in the chronic inflammation, abscess formation, collagen density and angiogenesis with the application of BC; however, these increases were not statistically significant. Unlike plant cellulose, BC bears several unique characteristics such as high level crystallinity, high purity, high water retention, high mechanical strength, and enhanced biocompatibility. With these exceptional properties, BC can serve as the ideal biomass for the improvement of various industrial products [25]. Both *in vivo* and *in vitro* studies have been conducted to investigate biocompatibility. As an example for its biocompatibility, in an in vivo study, Cai et al. prepared BC-collagen composites by immersing a BC membrane in collagen solution. Fibroblast cells were kept in incubation for 48 hours on a planted BC surface, after which the cells showed healthy adherence and proliferation [26]. In another study, it was observed that human vascular endothelial cells incubated in the BC structure grew in both horizontal and vertical directions and performed cell migration for neovascularization. However, due to the gradient difference in oxygen distribution, it was found that cell penetration and adhesion were weakened on BC membranes with a thickness of 5 mm [27]. In another study, in which BC film was used as a graft for bile duct repair, it was asserted that it was a bio-compatible material that provides a complete healing process and bile flow continuity [28]. BC can be sterilized, it is tissue-compatible, porous, elastic, and easy to be held by hand, it contains moisture to an extent since it absorbs water which ensures a faster recovery for the wounds, and additionally, it prevents the development of secondary infections in the injured area, reduces pain by absorbing the heat in the burnt area and inhibits the growth of the wound in the tissue [29,30]. BC has been used in the treatment of skin injuries such as carcinoma/skin graft with basal cells, severe body burns, facial peeling, sutures, dermal abrasion, skin lesions, chronic ulcers, and skin grafts in both donor and recipient areas [12]. In the recent reports, it has been stated that applying wound grafts made of cellulose in the treatment of chronic wounds has superior effects compared to other existing wound-healing materials. Kucharzewski et al.[30], compared BC with Unna hydrocolloid to treat chronic venous ulcers, and demonstrated that BC was more effective. There are many studies on the wound-healing effect of BC. When the literature was searched, it was found that BC was not investigated in colon anastomosis before. In our study, it is observed that BC accelerates wound healing with both histopathological and mechanical measurements. In a study conducted to determine the effectiveness of BC in closing the pharyngocutaneous fistula, fibroblast and inflammatory cell storage significantly increased, but no significant difference was observed in angiogenesis [14]. Promising results were also obtained in another study examining the effects of BC on facial nerve regeneration [31]. Moon Hwa Kwaka confirmed the effectiveness of BC for 15 days on healing burn wounds. At the end of the 15 days, when the skin regeneration was evaluated and the relationship of angiogenesis was examined, it was demonstrated that BC accelerated the wound healing process on the skin of burn injuries of rats through angiogenesis and regulation of connective tissue formation without stimulating any special toxicity to the liver and kidney. In this study, the thickness of the epidermis and dermis and the number of blood vessels were higher in the group treated with BC, while the skin healing severity score was lower in the group treated with BC compared to the group covered with gause patch [32]. In our study, it is observed that histopathologically angiogenesis had a small increase in the application of BC, but this was not a statistically significant difference. In another study, Helenius et al.[33], implanted subcutaneous BC on rats for 1, 4, and 12 weeks, and they evaluated through chronic inflammation, foreign reaction, cell growth and angiogenesis, histology, immunohistochemistry and electron microscopy. In the study, it did not cause any acute or chronic inflammatory reactions. No signs of microscopic or macroscopic inflammation were observed. Angiogenesis was observed at all periods and it was also seen that new blood vessels grew in the implanted cellulose. In our study, parallel to that study, there was an increase in angiogenesis, however, it was not statistically significant. Additionally, in our study, fibroblast density was observed to increase to a level that would create a statistically significant difference. Moreover, an increase was not observed in chronic

inflammatory cell infiltration, while a small increase was recorded in acute inflammatory cell infiltration. As a conclusion, our study demonstrated that in rat colon anastomosis, the application of BC in the anastomosis line was better than in the primary anastomosis group in mechanical evaluation. Although fibroblast density, eosinophil density and collagen density were significantly higher in the BC group than in the primary suture. Eosinophils are known to be distributed frequently in the lamina propria within the GIS and to a lesser extent in the epithelium. The density of increased eosinophils tissue is not entirely defined. Eosinophils that coalesce in the epithelium or exhibit intense degranulation are always considered abnormal. In this context, eosinophilic inflammation is usually defined as a hypersensitivity reaction. Moreover, eosinophil density increases in some infections, gastroesophageal reflux disease, autoimmune gastritis, specific drug reactions, and inflammatory bowel disease and radiation enteritis. This study histopathologically examined eosinophil density as an indicator of hypersensitivity reaction to BC [34]. However statistical results on fibroblast density showed similar results with the findings in the literature about the effect of BC on wound healing, and an increased collagen formation was observed. It was observed that BC, which is highly biocompatible and can be used as a tissue graft and accelerates wound healing, could be used in preventing anastomotic leakage, which is one of the most important complications of anastomosis. In our study, it has been demonstrated that bacterial cellulose can be used as a physical barrier with biological properties to prevent colon leakage after anastomosis. Besides, our experimental study will shed light on the advanced clinical studies to be conducted on the effect of bacterial cellulose preventing anastomotic leakage.

Acknowledgements

Bacterial Cellulose was produced by Assoc. Prof. Ishak Ozel Tekin in the Laboratories of the Immunology Department of the Medical Faculty of Bulent Ecevit University. Thanks to Ishak Ozel Tekin for contribution.

Financial Support

This research did not receive any specific grant from funding.

Conflict of Interest

The authors declared no conflict of interest.

Author Contributions

KB- Study design, data collections, data analysis, writing. AM- Study design, data collections, data analysis

References

1. Despoudi K, Mantzoros I, Ioannidis O, Cheva A, Antoniou N, Konstantaras D, Symeonidis S, Pramateftakis MG, Kotidis E, Angelopoulos S, Tsalis K: Effects of albumin/glutaraldehyde glue on healing of colonic anastomosis in rats. *World J Gastroenterol*, 23 (31): 5680-5691, 2017. DOI: 10.3748/wjg.v23.i31.5680

2. Ho YH, Ashour MA: Techniques for colorectal anastomosis. *World J Gastroenterology*, 16 (13): 1610-1621, 2010. DOI: 10.3748/wjg.v16.i13.1610

3. Üreyen O, İlhan E, Dadalı E, Gökçelli U, Alay D, Bağrıaçık Altıntaş S, Tekeli MT: Evaluation of factors associated with anastomotic leakage in colorectal surgery. *Turk J Colorectal Dis*, 28 (3): 129-135, 2018. DOI: 10.4274/tjcd.53386

4. Fischer EJ: Master of surgery. **In,** Özmen MM (Ed): Master of Surgery. 5th ed., 769-700, Güneş Tıp Kitabevi, Ankara, 2011.

5. Deans GT, Krukowski ZH, Irwin ST: Malignant obstruction of the left colon. *Br J Surg*, 81 (9): 1270-1276, 1994. DOI: 10.1002/bjs.1800810905

6. Aysan E, Dincel O, Bektas H, Alkan M: Polypropylene mesh covered colonic anastomosis. Results of a new anastomosis technique. *Int J Surg*, 6 (3): 224-229, 2008. DOI: 10.1016/j.ijsu.2008.04.001

7. Hornung M, Ludwig M, Gerrard AM, Schmauder HP: Optimizing the production of bacterial cellulose in surface culture: Evaluation of product movement influences on the bioreaction. *Eng Life Sci*, 6 (6): 546-551, 2006. DOI: 10.1002/elsc.200620163

8. Jozala AF, Lencastre-Novaes LC, Lopes AM, Santos-Ebinuma VC, Mazzola PG, Pessoa A, Grotto D, Gerenutti M, Chaud MV: Bacterial nanocellulose production and application: A 10-year overview. *Appl Microbiol Biotechnol*, 100 (5): 2063-2072, 2016. DOI: 10.1007/s00253-015-7243-4

9. Ye J, Zheng S, Zhang Z, Yang F, Ma K, Feng Y, Zheng J, Mao D, Yang X: Bacterial cellulose production by *Acetobacter xylinum* ATCC 23767 using tobacco waste extract as culture medium. *Bioresour Technol*, 274, 518-524, 2019. DOI: 10.1016/j.biortech.2018.12.028

10. Petersen N, Gatenholm P: Bacterial cellulose-based materials and medical devices: Current state and perspectives. *Appl Microbiol Biotechnol*, 91 (5): 1277-1286, 2011. DOI: 10.1007/s00253-011-3432-y

11. Jonas R, Farah LF: Production and application of microbial cellulose. *Polym Degrad Stab*, 59 (1-3): 101-106, 1998. DOI: 10.1016/S0141-3910(97)00197-3

12. Fontana JD, De Souza AM, Fontana CK, Torriani IL, Moresch JC, Gallotti BJ, De Souza SJ, Narcisco GP, Bichara JA, Farah LFX: Acetobacter cellulose pellicle as a temporary skin substitute. *Appl Biochem Biotechnol*, 24, 253-264, 1990. DOI: 10.1007/BF02920250

13. Silveira RK, Coelho ARB, Pinto FCM, De Albuquerque AV, De Melo Filho DA, De Andrade Aguiar JL: Bioprosthetic mesh of bacterial cellulose for treatment of abdominal muscle aponeurotic defect in rat model. *J Mater Sci Mater Med,* 27:129, 2016. DOI: 10.1007/s10856-016-5744-z

14. Demir B, Sarı M, Binnetoglu A, Yumusakhuylu AC, Filinte D, Tekin İÖ, Bağlam T, Batman AÇ: Comparison of pharyngocutaneous fistula closure with and without bacterial cellulose in a rat model. *Auris Nasus Larynx*, 45 (2): 301-305, 2018. DOI: 10.1016/j.anl.2017.04.005

15. Jilborn H, Ahonen J, Zedeerfeldt B: Healing of experimental colonic anastomoses I. Bursting strength of the colon after left colon resection and anastomoses. *Am J Surg*, 136 (5): 587-594, 1978. DOI: 10.1016/0002-9610(78)90315-X

16. Philips JD, Kim CS, Fonkalsrud EW, Zeng H, Dindar H: Effects of chronic corticosteroids and vitamin A on the healing of intestinal anastomoses. *Am J Surg,* 163, 71-77, 1992.

17. Ehrlich HP, Tarver H, Hunt TK: Effects of vitamin A and glucocorticoids upon inflammation and collagen synthesis. *Ann Surg*, 177 (2): 222-227, 1973. DOI: 10.1097/00000658-197302000-00017

18. Thornton FJ, Barbul A: Healing in the gastrointestinal tract. *Surg Clin North Am*, 77 (3): 549-573, 1997. DOI: 10.1016/s0039-6109(05)70568-5

19. Küçükkartallar T, Tekin A, Belviranlı M, Aksoy F, Vatansev C:

Eritropoetinin kemoterapi uygulanan ratlarda kolon anastomozlarının iyileşmesi üzerine etkisi. *Selçuk Tıp Derg*, 23, 131-138, 2007.

20. Kanellos I, Mantzoros I, Demetriades H, Kalfadis S, Sakkas L, Kelpis T, Betsis D: Suturless colonic anastomosis in the rat: A randomized controlled study. *Tech Coloproctol*, 6 (3): 143-146, 2002. DOI: 10.1007/s101510200033

21. Mast BA: Healing in other tissues. *Surg Clin North Am,* 77 (3): 529-547, 1997. DOI: 10.1016/s0039-6109(05)70567-3

22. Oxlund H, Chritensen H, Seyer-Hansen M, Andreasses TT: Collagen deposition and mechanical strength of colon anastomoses and skin incisional wounds of rats. *J Surg Res,* 66 (1): 25-30, 1996. DOI: 10.1006/jsre.1996.0367

23. Venâncio SA, Henrique CMV, Anania PR, Evaldo M, Querino TJ, Abel SCV, Daniel P: Evaluation of tensile strength of tissue adhesives made of fibrin and cyanoacrylate used as reinforcement of colon suture in "ex vivo" swine. *J Coloproctol, 38 (1): 13-17, 2018.* DOI: 10.1016/j.jcol.2017.09.415

24. Vakalopoulos KA, Wu Z, Kroesea LF, Jeekel J, Kleinrensink GJ, Dodou D, Lam KH, Lange JF: Sutureless closure of colonic defects with tissue adhesives: An in vivo study in the rat. *Am J Surg,* 213 (1): 151-158, 2017. DOI: 10.1016/j.amjsurg.2016.05.009

25. Parte FGB, Santoso SP, Chou CC, Verma V, Wang HT, Ismadji S, Cheng KC: Current progress on the production, modification, and applications of bacterial cellulose. *Crit Rev Biotechnol*, 40 (3): 397-414, 2020. DOI: 10.1080/07388551.2020.1713721

26. Cai Z, Chen P, Jin HJ, Kim J: The effect of chitosan content on the crystallinity, thermal stability, and mechanical properties of bacterial cellulose: Chitosan composites. *Proc Inst Mech Eng Pt C J Mechan Eng Sci,* 223, 2225-2230, 2009. DOI: 10.1243/09544062JMES1480

27. Fink H, Ahrenstedt L, Bodin A, Brumer H, Gatenholm P, Krettek A, Risberg B: Bacterial cellulose modified with xyloglucan bearing the adhesion peptide RGD promotes endothelial cell adhesion and metabolism-a promising modification for vascular graft. *J Tissue Eng Regen Med,* 5 (6): 454-463, 2011. DOI: 10.1002/term.334

28. Abreu GFS, Batista LL, Adeodato DCN, Albuquerque AV, Ferraz-Carvalho RS, Lima RP, Souza VSB Carvalho GL, Aguiar JLA: Use of bacterial cellulose film for repair of bile duct injury in pigs. *J Biomater Appl*, 35, 331-341, 2020. DOI: 10.1177/0885328220928221

29. Biskin S, Damar M, Oktem SN, Sakalli E, Erdem D, Pakir O: A new graft material for myringoplasty: Bacterial cellulose. *Eur Arch Otorhinolaryngol*, 273, 3561-3565, 2016. DOI: 10.1007/s00405-016-3959-8

30. Kucharzewski M, Slezak A, Franek A: Topical treatment of non-healing venous ulcers by cellulose membrane. *Phlebologie*, 32 (6): 147-151, 2003. DOI: 10.1055/s-0037-1621462

31. Binnetoglu A, Demir B, Akakin D, Kervancioglu Demirci E, Batman C: Bacterial cellulose tubes as a nerve conduit for repairing complete facial nerve transection in a rat model. *Eur Arch Otorhinolaryngol*, 277 (1): 277-283, 2020. DOI: 10.1007/s00405-019-05637-9

32. Kwak MH, Kim JE, Go J, Koh EK, Song SH, Son HJ, Kim HS, Yun YH, Jung YJ, Hwang DY: Bacterial cellulose membrane produced by *Acetobacter* sp. A10 for burn wound dressing applications. *Carbohydr Polym*, 122, 387-398, 2015. DOI: 10.1016/j.carbpol.2014.10.049

33. Helenius G, Bäckdahl H, Bodin A, Nannmark U, Gatenholm P, Risberg B: *In vivo* biocompatibility of bacterial cellulose. *J Biomed Mater Res A*, 76A (2): 431-438, 2006. DOI: 10.1002/jbm.a.30570

34. Yantiss RK: Eosinophils in the GI tract: How many is too many and what do they mean? *Mod Pathol*, 28, S7-S21, 2015. DOI: 10.1038/modpathol.2014.132

Kafkas Universitesi Veteriner Fakultesi Dergisi
ISSN: 1300-6045 e-ISSN: 1309-2251
Journal Home-Page: http://vetdergikafkas.org

Kafkas Univ Vet Fak Derg
27 (3): 315-322, 2021
DOI: 10.9775/kvfd.2021.25359

RESEARCH ARTICLE

The Effects of the Basil *(Ocimum sanctum)* Treatment on the Tumor Necrosis Factor-α and Interleukin 1β Release in the Kidney Tissue of the Diabetic Rats [1][2]

Sevda ELİŞ YILDIZ [1,a (*)] Buket BAKIR [2,b] Hasan ASKER [3,c] Ebru KARADAĞ SARI [4,d]

[1] *This study was supported by a grant from the Kafkas University, BAP (Project No: 2017-TS-33)*
[2] *Presented at the International Eurasian Conference on Biotechnology and Biochemistry as an oral presentation, 16-18 December 2020 Ankara, Turkey*

[1] Department of Midwifery, Faculty of Health Sciences, Kafkas University, TR-36100 Kars - TURKEY
[2] Department of Histology and Embryology, Faculty of Veterinary Medicine, Namik Kemal University, TR-59030 Tekirdag, - TURKEY
[3] Department of Histology and Embryology, Faculty of Medicine, Uşak University, Uşak - TURKEY
[4] Department of Histology and Embryology, Faculty of Veterinary Medicine, Kafkas University, TR-36040 Kars - TURKEY
ORCIDs: [a] 0000-0002-3585-6648; [b] 0000-0003-3637-3688; [c] 0000-0002-5703-2164; [d] ORCID:0000-0001-7581-6109

Article ID: KVFD-2021-25359 Received: 02.01.2021 Accepted: 08.04.2021 Published Online: 08.04.2021

Abstract

This study aims to examine the changes of the *Ocimum sanctum* treatment on the tumor necrosis factor alpha (TNF-α) and interleukin 1β (IL-1β) in the kidney tissue of the rats, in which the experimental diabetes was induced with streptozotocin (STZ). Forty *Sprague Dawley* male rats were divided into 5 groups: Diabetes, Diabetes + *Ocimum sanctum, Ocimum sanctum,* Control, and Sham. The immunohistochemical localization of TNF-α and IL-1β in the kidney tissue was determined by using the streptavidin-biotin-peroxidase method. Strong TNF-α immunoreactivity was determined in the renal cortex of the rats in the Diabetes and Diabetes + *Ocimum sanctum* groups on 14th days, low immunoreactivity was determined in the rats in *Ocimum sanctum*, Sham, and Control groups. While strong IL-1β immunoreactivity was observed in the renal cortex of the Diabetes group, moderate IL-1β immunoreactivity was observed in the renal cortex of the Diabetes + *Ocimum sanctum* and low immunoreactivity was determined in the *Ocimum sanctum,* Sham, and Control groups. In this study, it was assessed how the polymorphisms, occurring in the cytokine genes of *Ocimum sanctum* in the rats, in which experimental diabetes was induced, and TNF-α and IL-1β, which was demonstrated to have an important role in the complication development in the diabetic patients affected the renal tissue.

Keywords: *Diabetes, Ocimum sanctum, Tumor Necrosis Factor Alpha, Interleukin, Kidney*

Diyabetik Ratlarda Fesleğen *(Ocimum sanctum)* Uygulamasının Böbrek Dokusunda Tümör Nekrozis Faktör-α ve İnterlökin 1β Salınımı Üzerine Etkileri

Öz

Bu çalışmada, fesleğen *(Ocimum sanctum)* uygulamasının, streptozotocin (STZ) ile deneysel diyabet oluşturulan ratların böbrek dokusunda tümör nekrozis faktör alfa (TNF-α) ve interlökin 1β (IL-1β) üzerine meydana getirdiği değişikleri incelemek amaçlanmıştır. Çalışmamızda toplam 40 adet *Spraque Dawley* cinsi erkek rat kullanıldı. Ratlar, Diyabet, Diyabet + *Ocimum sanctum, Ocimum sanctum,* Kontrol ve Sham olmak üzere 5 gruba ayrıldı. TNF-α ve IL-1β'in böbrek dokusundaki immunohistokimyasal lokalizasyonu streptavidin-biotin peroxidaz yöntemi ile belirlendi. Diyabet ve Diyabet + *Ocimum sanctum* uygulanmış grubun dışındaki grupların böbrek korteksinde zayıf düzeyde TNF-α immunoreaktivitesi tespit edildi. Diyabet grubunun böbrek korteksinde güçlü, Diyabet + *Ocimum sanctum* grubunda ise böbrek korteksinde orta düzeyde IL-1β immunoreaktivitesi tespit edilmesine rağmen *Ocimum sanctum,* Sham ve Kontrol grubundaki ratlarda ise zayıf düzeyde immunoreaktivite tespit edildi. Bu çalışma ile deneysel olarak diyabet oluşturulmuş ratlarda *Ocimum sanctum*'un sitokin genlerinde oluşan polimorfizmlerin diyabetli hastalarda komplikasyon gelişiminde önemli rol oynadıkları gösterilen TNF-α ve IL-1β'in böbrek dokusu üzerine ne kadar etkili olduğu değerlendirildi.

Anahtar sözcükler: *Şeker Hastalığı, Fesleğen, Tümör Nekrozis Faktör Alfa, İnterlökin, Böbrek*

How to cite this article?

Eliş Yildiz S, Bakır B, Asker H, Karadağ Sarı E: The effects of the basil *(Ocimum sanctum)* treatment on the tumor necrosis factor-α and interleukin 1β release in the kidney tissue of the diabetic rats. *Kafkas Univ Vet Fak Derg,* 27 (3): 315-322, 2021.
DOI: 10.9775/kvfd.2021.25359

(*) **Corresponding Author**

Tel: +90 474 225 1567 Fax : +90 474 225 1265
E-mail: sevdaelis36@hotmail.com (S. Eliş Yıldız)

Introduction

Diabetes mellitus (DM) is a common metabolic disorder that involves glucose, amino acids, and fatty acids. Either insulin deficiency or insulin resistance may cause diabetes and partial deficiency of the insulin or insulin resistance in the peripheral tissues [1]. The reactive oxygen species (ROS) increase as a result of the oxidative stress and insulin resistance develops with the cytokines secretions from the activated macrophage and monocytes in large amounts [2]. The cytokines play a significant role in both the natural and specific inflammatory response. Most of the polymorphisms that will be able to show up in the cytokine genes are in the form of single nucleotide polymorphism (SNP) in the regulatory regions. These variations increase the sensitivity against various diseases by affecting the cytokine genes expression levels [3,4]. The cytokines detection is important for prognosis and diagnosis of different diseases related with inflammation, immunology and atherosclerosis and the most important ones are interleukins (ILs) and TNF-α [5]. TNF-α is produced as a pro-hormone substance constituting 233 amino acids and is a strong cytokine taking place among Type 1 proinflammatory cytokines secreted by the macrophage and T lymphocytes. The TNF-α has important functions such as stimulating growth, cytotoxicity, and angiogenesis in Type 2 diabetes and its microvascular complications [6]. It was specified by various studies performed that amount of the proinflammatory cytokines such as IL-1β and TNF-α was correlated with increased complications in diabetic patients [3,4].

The interest to use plants for treatments progressively is in increase and treatment with plants is become prevalent. The tendency to the pharmacological and toxicological studies related to plants started to increase in our country. *Ocimum sanctum* has fertility prevention, anticancer, antidiabetic, antifungal and antimicrobial influences [7]. The basil leaf exhibits antidiabetic activity, as was revealed in one study, it was observed that aqueous extract of Tulsi significantly lowered the blood glucose level in diabetic rats [8]. The basil leaf pulverized by foods was given to healthy and diabetic rats for one week, it was observed that the basil decreased the fasting blood glucose [9]. In a clinical trial in which the basil was acquired, it was determined that it had positive influences on the serum glucose level after both the preprandial and postprandial in 40 Type 2 diabetic patients since it was made by mixing water and fresh leaf powder and used as a support product for 4 weeks [10]. Medicinal plants are increasingly being used as a DM management strategy. In this context, traditional herbal medicine is used across the world for disease treatment [11]. It is argued as a result of the studies performed that gene polymorphisms of the cytokines such as TNF-α and IL-1β are associated with the complication development in diabetic patients.

We investigated the immunohistochemical localization of TNF-α and IL-1 β in the kidneys of healthy and diabetic rats to which *Ocimum sanctum* had been administered. We also investigated the effects of *Ocimum sanctum* on structural changes in the kidney.

Material and Methods

Animals

Approval was received by the Animal Experiments Local Ethics Committee of Kafkas University (Decision no: KAU-HADYEK/2016-108). In this study, 40 male rats, aged 4 to 5 month weighing 200-300 g, that were not copulated previously and used in any study, were used. The rats used in the study were harbored in a standard cage in 12 h light and 12 h dark environment at 22±2°C ambient temperature and fed by *ad-libitum* and tap water.

Preparation of Ocimum Sanctum Extract

Ten g of basil in powder form was taken and dissolved in 100 mL of ethanol. The mixture obtained was left to shake on shaker for 24 h at room temperature. After the time expired, the mixture was filtered with the help of filter paper. The solvent content was removed in a Rotary evaporator at low pressure and low temperature. Extracts were stored at -20°C until experiment [12].

Experiment Groups

1. Control Group (n=8): No application was made.

2. Sham Group (n=8): Sodium citrate solution was administered as 50 mg/kg intraperitoneal injection.

3. *Ocimum Sanctum* Group (n=8): *Ocimum sanctum* extract was administered as 200 mg/kg for through the oral gavage 14 days [13].

4. Diabetes Group (n=8): Experimental diabetes was induced by intraperitoneal injection of 50 mg/kg STZ dissolved in 0.1 M citrate buffer, pH 4.5 [14].

5. Diabetes + *Ocimum sanctum* Group (n=8): Experimental diabetes was induced by intraperitoneal injection of 50 mg/kg STZ dissolved in 0.1 M citrate buffer, pH 4.5 and *Ocimum sanctum* extract was administered as 200 mg/kg for 14 days through the oral gavage for the group in which diabetes was created.

Then, cervical dislocation was performed under anesthesia to the rats in each group and kidney tissues samples were taken up for histology and immunohistochemistry.

Determination of Blood Glucose Levels

The blood samples were taken from the tail vein of the animals left hungry for 8 hours before starting to the study (0^{th} day) by using a glucometer (Yasee, GLM-76, Taiwan) in order to determine the preprandial blood glucose levels. Those, of which glucose levels were at the level of 200 mg/dL, were included in the study by measuring the

preprandial blood glucose levels for 8 h on the 3rd day of the STZ practice. *Ocimum sanctum* extract was given by the oral gavage for 14 days starting from the 3rd day of the STZ practice.

Statistical Evaluation

The blood glucose measurements of the rats in all groups were taken on the 0th, 3rd and 14th days. Statistical Package for Social Sciences 20.0 program was used to compare statistically the blood glucose levels between the groups. ANOVA (Variance analysis) and T-test were applied for probable differences. The confidence interval was specified as 0.05 in the statistical analyses. Kolmogorov Smirnov test was performed to measure the normality of the distribution. Since the P value was >0.05, the distrubition was said to be normal.

Histopathological Examination

The kidney tissue samples taken from all experimental animals were fixed in a 10% formaldehyde solution. The tissue sections were taken at thickness of 5 µm from the paraffin blocks prepared. Sections were stained with Crossman's triple staining [15]. Slides were evaluated under a light microscope (Olympus BX51; Olympus Optical Co., Osaka, Japan) and microscopic photos were taken.

Immunohistochemical Examination

The streptavidin-biotin-peroxidase technique, one of the indirect methods, was used to the sections taken to the lams coated by chrome aluminum gelatin. The sections were then incubated in 3% H_2O_2 prepared in 0.1M PBS for 15 min to prevent the endogenous peroxidase activity by agitating in the PBS (0.1 M, Ph, 7.2) after the deparaffinization and rehydration processes. They were then applied heat at the maximum temperature in a microwave oven for 10 min (800 watt) in the citrate buffer solution to bring antigens into the open after washing with the PBS. The blocking solution A was dripped to prevent the nonspecific binding (Histostain-Plus IHC Kit, HRP, broad-spectrum Ref.) after washed by PBS. The anti-TNF-α (Santa Cruz, it was diluted at the rate of 1/500) and anti-IL-1β primary antibody (Santa Cruz, it was diluted at the rate of 1/250) were applied on the sections in a humid environment at the ambient temperature for 1 h. The Broad Spectrum Antibody was dripped on the sections since it was against the type produced by the primary antibody. The HRP streptavidin was incubated at the ambient temperature for 15 min after washing with PBS. The 3,3'-Diaminobenzidine tetrahydrochloride (DAB) substrate solution was added for the chromogen practice and then, Mayer's hemotoxilen was used for the back-groud staining. The slides were examined in a research microscope and their photos were taken. Rabbit serum without primer antibody served as the negative control. The immunohistochemical evaluation was made by considering staining characteristic and staining density of the target cells. The evaluation was made by two independent observers by giving values from 0 to 3 in accordance with the characteristics including nonstaining (-), weak staining (+), moderate staining (++), and severe staining (+++) [16-18].

Results

Blood Glucose Levels

When the groups were compared, significant differences were observed between diabetes and diabetes + *Ocimum sanctum* groups and control, sham and *Ocimum sanctum* groups in 3rd-day. The significant differences were also observed on the 14th day between diabetes and diabetes + *Ocimum sanctum* groups and control, sham and *Ocimum sanctum* groups. When the diabetes and diabetes + *Ocimum sanctum* group was compared, no significant difference was statistically determined on the 3rd and 14th days *(Table 1)*.

Histopathological Results

The kidney tissue samples taken from the rats in all groups were semi-quantitatively evaluated in terms of the tissue damage. Bowman cavities (urinary cavity) were determined as either very decreased or removed as a result of the increased cellularity in the glomerular mesangium in some glomerulus in the kidney tissues of the rats, by which diabetes created. No thickening was seen in the glomerular basal membranes. The casts were specified in some tubulus lumens. It was determined that there was a hydropic and balloony degeneration in some collector (collecting) and distal tubulus epithelium *(Fig. 1-a)*. A vacuolization was observed in the tubulus epithelium cells in the cortical regions.

Bowman cavities were specified as either very decreased or removed as a result of the increased cellularity in the

Table 1. *Statistical evaluations of the rats fasting blood glucose level in accordance with the groups*

Days	Sham	Control	*Ocimum sanctum*	Diabetes	Diabetes + *Ocimum sanctum*
0	87.375 ± 9.66^{aA}	76.000 ± 5.66^{aA}	68.250 ± 7.29^{aA}	81.625 ± 6.21^{aA}	74.875 ± 8.43^{aA}
3	77.125 ± 4.32^{aA}	75.875 ± 5.74^{aA}	67.750 ± 6.94^{aA}	361.500 ± 11.39^{bB}	284.630 ± 41.30^{cB}
14	89.000 ± 10.17^{aA}	79.125 ± 5.11^{aA}	61.375 ± 9.13^{aA}	353.250 ± 26.39^{bB}	261.750 ± 37.83^{cB}

^{a,b,c} The differences between the averages shown by the different letter in the same line are statistically important ($P<0.05$); ^{A,B,C} The differences between the averages shown by the different letter in the column are statistically important ($P<0.05$)

glomerular mesangium in diabetes + *Ocimum sanctum* group rats' kidney tissues. Not any thickening was seen in the glomerular basal membranes. It was specified that the proximal and distal tubules were normal *(Fig. 1-b)*.

The control, sham and *Ocimum sanctum* group rats kidney tissues were determined to be in normal histological form on the 14th day *(Fig. 1-c,d)*.

Immunohistochemical Results

Tumor necrosis factor alpha and IL-1β immunoreactivity were specifically seen on the 14th day in the rats kidney tissues in all groups. TNF-α immunoreactivity was determined at a strong level in the kidney cortex of the diabetes and diabetes + *Ocimum sanctum* groups and at a weak level in the *Ocimum sanctum,* sham and control groups. Although a strong TNF-α immunoreactivity was in the tubulus proximalis and tubulus distalis epithelial cells in diabetes *(Fig. 2-a)* and diabetes + *Ocimum sanctum (Fig. 2-b)* groups, it was determined at a weak level in the *Ocimum sanctum (Fig. 2-c)*, control *(Fig. 2-d)* and sham *(Fig. 2-e)* groups on the 14th day in the rats. TNF-α immunoreactivity was not encountered in glomerulus and vessel endothelium in the kidney tissues in all groups. The semiquantitative analysis results of intergroup for TNF-α immunohistochemical staining were summarized in *Table 2*.

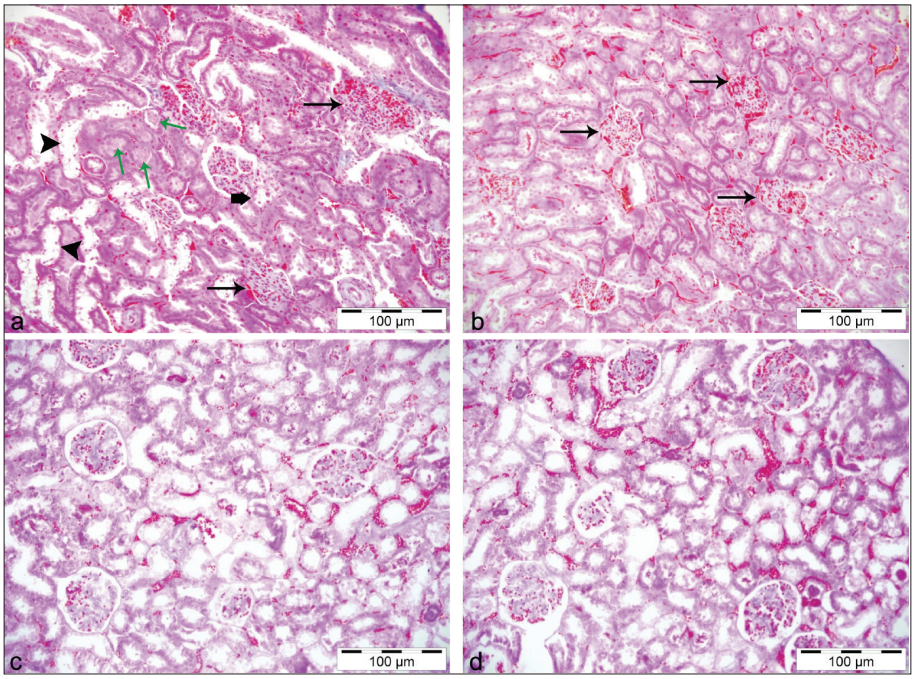

Fig 1. Rat kidney tissues. **a-** Diabetes group. Bowman cavities: *black arrows,* tubulus lumens: *green arrows.* Hydropic and balloony degeneration in some collector (collecting): *arrowhead* and distal tubulus epithelium: *thick arrow;* **b-** Diabetes + *Ocimum sanctum* group. Bowman cavities: *black arrows;* **c-** Control group; **d-** *Ocimum sanctum* group. Triple Staining

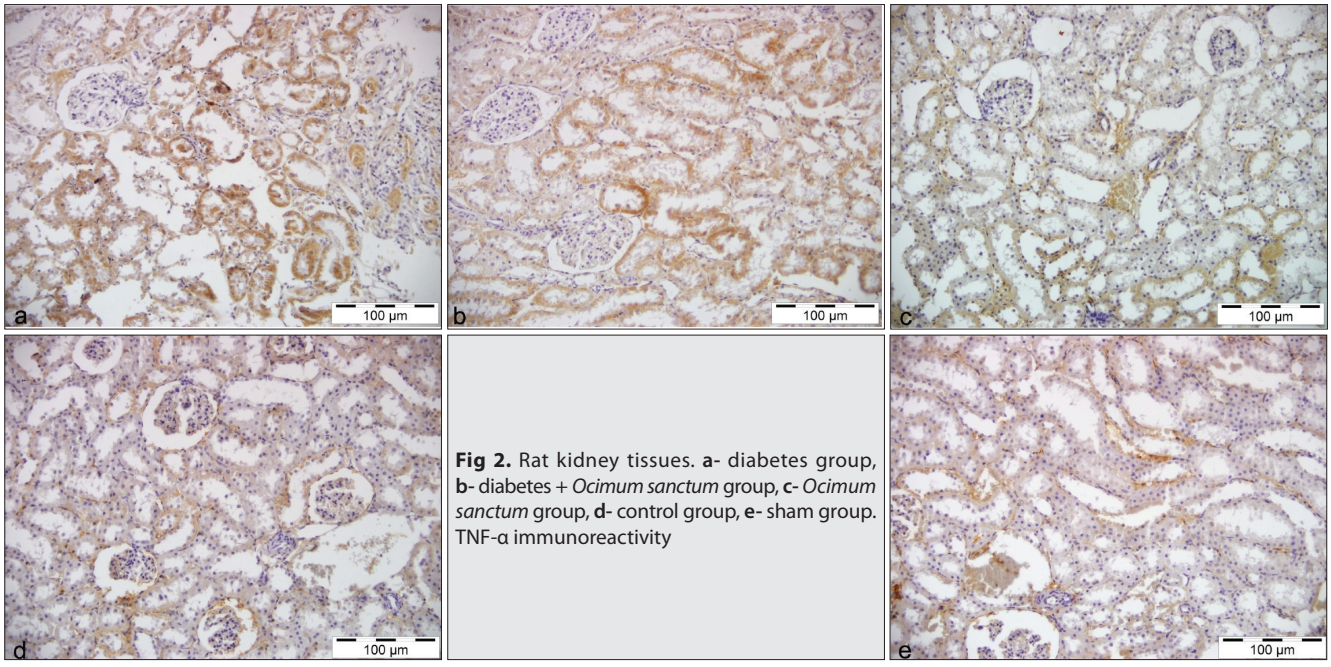

Fig 2. Rat kidney tissues. **a-** diabetes group, **b-** diabetes + *Ocimum sanctum* group, **c-** *Ocimum sanctum* group, **d-** control group, **e-** sham group. TNF-α immunoreactivity

Table 2. *The semiquantitative analysis results of intergroup TNF-α immunoreactivity on the 14th day*					
Cell Type	**Diabetes Group**	**Diabetes + *Ocimum sanctum* Group**	***Ocimum sanctum* Group**	**Sham Group**	**Control Group**
Tubulus proximalis	+++	+++	+	+	+
Tubulus distalis	+++	+++	+	+	+
Glomerulus	-	-	-	-	-
Vessel Endothelium	-	-	-	-	-

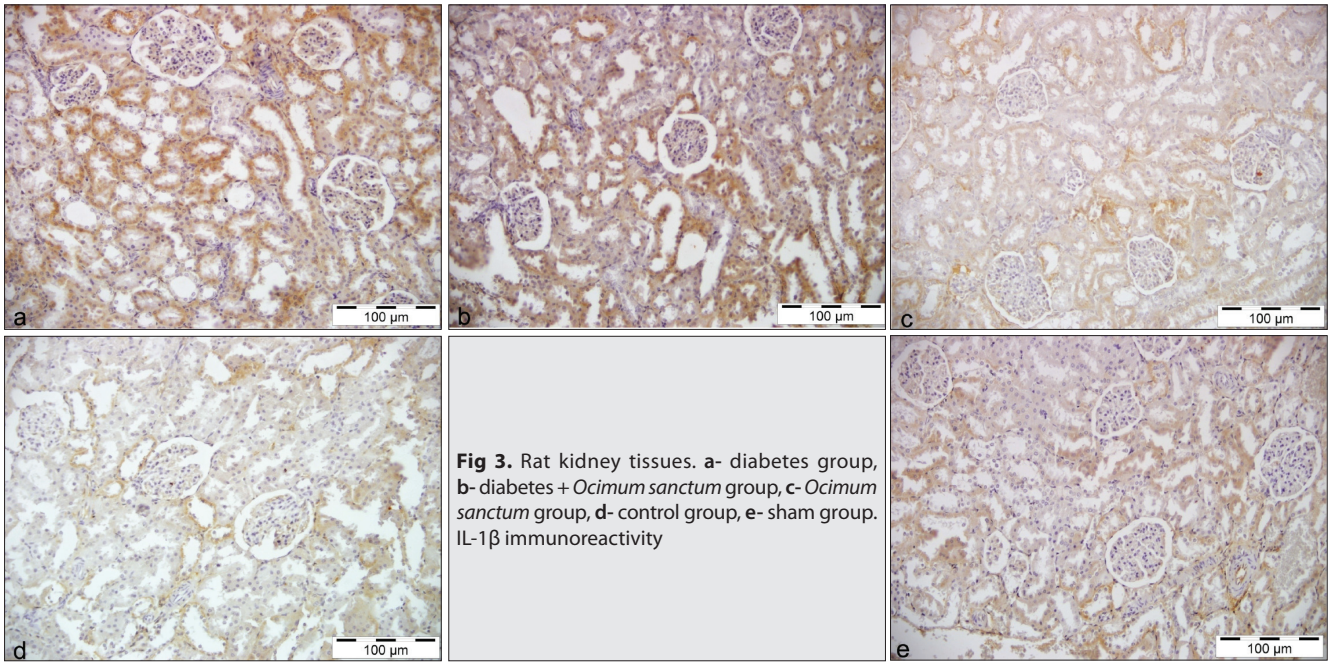

Fig 3. Rat kidney tissues. **a-** diabetes group, **b-** diabetes + *Ocimum sanctum* group, **c-** *Ocimum sanctum* group, **d-** control group, **e-** sham group. IL-1β immunoreactivity

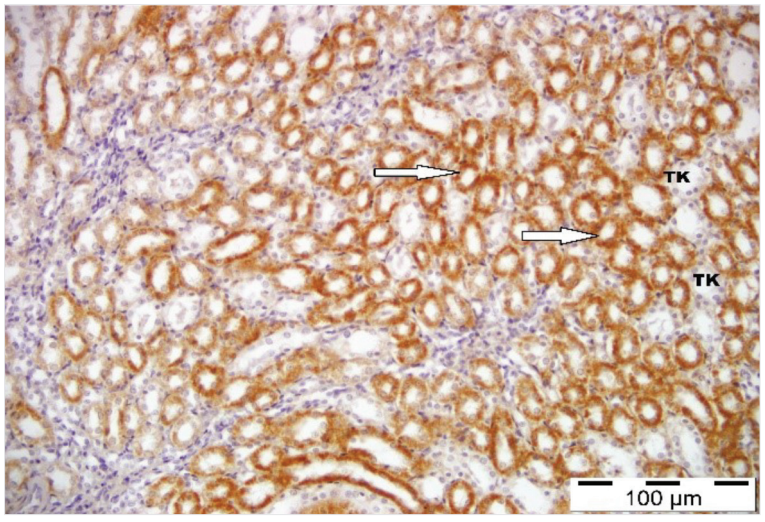

Fig 4. Rat kidney tissues in the diabetes group. *Arrow:* Loop of Henle, TK: Tubulus Collectivus. IL-1β immunoreactivity

Interleukin 1β immunoreactivity was determined at a strong level in diabetes groups kidney cortex and at a moderate level in diabetes + *Ocimum sanctum* groups kidney cortex. Although a strong immunoreactivity was determined in the rats tubulus proximalis and tubulus distalis in diabetes group on the 14th day *(Fig. 3-a)*, the immunoreactivity was at a moderate level in diabetes + *Ocimum sanctum* group *(Fig. 3-b)* and at a weak level in the rats in the *Ocimum sanctum (Fig. 3-c)*, control *(Fig. 3-d)* and sham *(Fig. 3-e)* groups. Strong immunoreactivity was determined in the rats loop of henle cells in diabetes group on the 14th day *(Fig. 4)*. No IL-1β immunoreactivity was detected in the glomeruli and vessel endothelium in the kidney of rats in all groups. The semiquantitative analysis results of intergroup for IL-1β immunohistochemical staining were summarized in *Table 3*.

Table 3. *The semiquantitative analysis results of intergroup IL-1β immunoreactivity on the 14th day*

Cells	Diabetes Group	Diabetes + *Ocimum sanctum* Group	*Ocimum sanctum* Group	Sham Group	Control Group
Tubulus proximalis	+++	++	+	+	+
Tubulus distalis	+++	++	+	+	+
Loop of Henle	+++	++	+	+	+
Vessel endothelium	-	-	-	-	-
Glomerulus	-	-	-	-	-

Discusion

Ocimum sanctum had an influence of decreasing high blood glucose, regulating lipid metabolism and suppressing blood sugar and would be able to have a therapeutical role in Type 2 diabetes disease by showing an influence like insulin in the rats [19,20]. Antora et al.[21] applied *Ocimum sanctum* extract to diabetic rats and they prepared that the application of *Ocimum sanctum* extract had an oral hypoglycemic activity. Leaf extract of *Ocimum sanctum* significantly decreases blood glucose in glucose induced hyperglycemic and STZ-induced diabetic rats [22]. In our study no significant difference was found in blood glucose on the 14th day in the diabetes + *Ocimum sanctum* group. Not being a statistical difference even though the blood glucose decreased in the *Ocimum sanctum* + diabetes group in our study to the contrary of the studies performed [23,24] make us think that it showed up depending on the dose, gender and day.

Lee et al.[25] specified that diabetes created glomerular enlargement, sclerosis and tubulointerstitial fibrosis in the rat kidney. Also, the glomerular and tubular basal membrane thickenings occurred by the accumulation of extracellular matrix components in nephropathy in the experimental diabetic and pathologic cases were emphasized various researchers [26,27]. In our study, Bowman cavities (urinary cavity) were determined as either very decreased or removed as a result of the increased cellularity in the glomerular mesangium in some glomerulus of the kidney tissues of the rats, for which diabetes created. No thickening was seen in the glomerular basal membranes. The casts were specified in some tubulus lumens. It was determined that there was a hydropic and balloony degeneration in some collector (collecting) and distal tubulus epithelium. Vacuolization was observed in the tubulus epithelium cells in the cortical regions. Bowman cavities (urinary cavity) were specified as either very decreased or removed as a result of the increased cellularity in the glomerular mesangium in diabetes + *Ocimum sanctum* group rats' kidney tissues. No thickening was seen in the glomerular basal membranes. It was specified that the proximal and distal tubules were normal. The tubulus lumens enlargement due to the necrosis occurred in the epithelium cells of the proximal, distal and collector tubules that we followed up in diabetic group to which the STZ was given, relieving in diabetes group to which the *Ocimum sanctum* was applied and prevention of the pathologic changes showed up by diabetes in the *Ocimum sanctum* make us think that it will be able to be related to the characteristics of stabilizing the cell membrane and protecting the components from any damage by means of the high lipophilic nature.

The TNF-α is a cytokine causing immune, metabolic and inflammatory events and playing a role in the insulin resistance development [28]. TNF-α is thought to play a role in various diseases including Type 2 diabetes [28] and is an important cytokine in diabetes pathogenesis [29]. The TNF-α's regulating role, especially in the lipid and glucose metabolism, gains importance in the metabolic syndrome and diabetes since it plays a key role in energy metabolism [29]. It was specified in many studies performed that the TNF-α levels increased after the STZ injection and TNF-α played a role in the complications development in diabetes [30,31]. In our study, the TNF-α immunoreactivity was determined at a strong level in the rats kidney cortex in diabetes and diabetes + *Ocimum sanctum* groups and at a weak level in the *Ocimum sanctum,* sham and control groups kidney cortex in parallel with the studies performed. Although a strong immunoreactivity was determined on the 14th day in the rats tubulus proximalis and tubulus distalis cells in diabetes and diabetes+*Ocimum sanctum* groups, the TNF-α immunoreactivity was observed at a weak level in the *Ocimum sanctum*, sham and control groups. In our study, the TNF-α may make us think that it played an important role in diabetic nephropathys pathogenesis since the TNF-α immunohistochemically increased in the rats kidney tissues in diabetes and diabetes + *Ocimum sanctum* groups.

It was specified that the IL-1β and TNF-α are the central inflammatory cytokines and their amounts are correlated with the increased complications in diabetic patients [32]. Although the cytokines influence was not exactly revealed on diabetic nephropathy, there are some data that they have important influences in some experimental studies performed [32,33]. In the immunohistochemical study we performed, the IL-1β immunoreactivity was determined at a strong level in the rats kidney cortex in diabetes group and at a moderate level in diabetes + *Ocimum sanctum* groups kidney cortex. Although a strong immunoreactivity

was determined on the 14th day in the henle loop, tubulus proximalis and tubulus distalis cells in diabetes group in the rats. The immunoreactivity was detected at a moderate level in diabetes + *Ocimum sanctum* group and at a weak level in the *Ocimum sanctum*, control and sham groups for the rats. Although a strong IL-1β immunoreactivity was determined in the rats kidney tissues in diabetes group, detecting the IL-1-β immunoreactivity at a moderate level in diabetes + *Ocimum sanctum* groups kidney tissues is in nature that it supports the studies performed for being an antidiabetic influence [34,35].

In conclusion, although the *Ocimum sanctum* application did not make a statistically significant influence on the blood glucose, it was observed that it caused an observable decrease and reduced the kidney damage caused by diabetes in the rats, to which STZ was applied. However, it was determined that it did not immunohistochemically show an influence on the TNF-α secretion but made an influence on IL-1β. The plants use in the treatment of many diseases will be able to be encouraging for the future and long-term uses and further studies are required in order to show the *Ocimum sanctum's* positive influence on diabetic complications.

Acknowledgements

Histopathological results was evaluation Prof. Dr. Mahmut Sözmen in the patology Depertment Faculty of Veterinary Medicine, Ondokuz Mayıs University. Thanks to Mahmut Sözmen for contribution.

Author Contribution

S.E.Y. and E.K.S. conceived the original idea, designed and supervised the project. S.E.Y, B.B and H.A performed experiments. All authors wrote the manuscript.

Declaration of Interest

The authors report no conflicts of interest.

References

1. Adeva-Andany MM, Funcasta-Calderón R, Fernández-Fernández C, Castro-Quintela E, Carneiro-Freire N: Metabolic effects of glucagon in humans. *J Clin Transl Endocrinol*, 15, 45-53, 2019. DOI: 10.1016/j.jcte.2018.12.005

2. Elmarakby AA, Sullivan JC: Relation ship between oxidative stres and inflammatory cytokines in diabetic nephropathy. *Cardiovasc Ther*, 30 (1): 49-59 2012. DOI: 10.1111/j.1755-5922.2010.00218.x

3. Luotola K, Paakkönen R, Alanne M, Lanki T, Moilanen L, Surakka I, Pietilä A, Kähönen M, Nieminen MS, Antero Kesäniemi Y, Peters A, Jula A, Perola M, Salomaa V: Association of variation in the Interleukin-1 gene family with diabetes and glucose homeostasis. *J Clin Endocrinol Metab,* 94, 4575-4583, 2009. DOI: 10.1210/jc.2009-0666

4. Szoke D, Molnar B, Solymosi N, Racz K, Gergics P, Blasko B, Vasarhelyi B, Vannay A, Mandy Y, Klausz G, Gyulai Z, Galamb O, Spisak S, Hutkai B, Somogyi A, Berta K, Szabo A, Tulassay T, Tulassay Z: Polymorphisms of the ApoE, HSD3B1, IL-1β and p53 genes are associated with the development of early uremic complications in diabetic patients: Results of A DNA Resequencing Array Study. *Int J Mol Med,* 23 (2): 217-227, 2009. DOI: 10.3892/ijmm_00000120

5. Sánchez-Tirado E, Salvo C, González-Cortés A, Yáñez-Sedeño P, Langa F, Pingarrón JM: Electrochemical immunosensor for simultaneous determination of interleukin-1 beta and tumor necrosis factor alpha in serum and saliva using dual screen printed electrodes modified with functionalized double-walled carbon nanotubes. *Anal Chim Acta*, 959, 66-73, 2017. DOI: 10.1016/j.aca.2016.12.034

6. Liu C, Feng X, Li Q, Wang Y, Li Q, Hua M: Adiponectin, TNF-α and inflammatory cytokines and risk of type 2 diabetes: A systematic review and meta-analysis. *Cytokine,* 86, 100-109, 2016. DOI: 10.1016/j.cyto.2016.06.028

7. Prakash P, Gupta N: Therapeuticuses of *Ocimum sanctum* Linn (Tulsi) with a note on eugenol and its pharmacological actions: A short review. *Indian J Physiol Pharmacol*, 49 (2): 125-131, 2005.

8. Bano N, Ahmed A, Tanveer M, Khan GM, Ansari MT: Pharmacological evaluation of *Ocimum sanctum. J Bioequivalenc Bioavailab,* 9 (3): 387-392, 2017. DOI: 10.4172/jbb.1000330

9. Mukherjee PK, Maiti K, Mukherjee K, Houghton PJ: Leads from Indian medicinal plants with hypoglycemic potentials. *J Ethnopharmacol*, 106 (1): 1-28, 2006. DOI: 10.1016/j.jep.2006.03.021

10. Yeh GY, Eisenberg DM, Kaptchuk TJ, Phillips RS: Systematic review of herbs and dietary sublements for glycemic control in diabetes. *Diabetes Care,* 26 (4):1277-1294, 2003. DOI: 10.2337/diacare.26.4.1277

11. Nazarian-Samani Z, Sewell RDE, Lorigooini Z, Rafieian-Kopaei M: Medicinal plants with multiple effects on diabetes mellitus and its complications: A Systematic review. *Curr Diab Rep,* 18 (10): 72, 2018. DOI: 10.1007/s11892-018-1042-0

12. Suanarunsawa T, Anantasomboon G, Piewbang C: Anti-diabetic and anti-oxidative activity of fixed oil extracted from *Ocimum sanctum* L. leaves in diabetic rats. *Exp Ther Med*, 11 (3): 832-840, 2016. DOI: 10.3892/etm.2016.2991

13. Pattanayak P, Behera P, Das D, Panda SK: *Ocimum sanctum* Linn. A reservoir plant for therapeutic applications: An overview. *Pharmacogn Rev***,** 4 (7): 95-105, 2010. DOI: 10.4103/0973-7847.65323

14. Kanitkar M, Bhonde R: Existence of islet regenerating factors within the pancreas. *Rev Diabet Stud*, 1 (4): 185-192, 2004. DOI: 10.1900/RDS.2004.1.185

15. Luna LG: Manual of Histologic Staining Methods of the Armed Forces Institute of Pathology. 3rd ed., 72-100, Mc Graw-Hill Book Comp, 1968.

16. Zhu QY: Analysis of blood vessel invasion by cells of thyroid follicular carcinoma using image processing combined with immunohistochemistry. *Zhonghua Yi Xue Za Zhi,* 69 (10): 573-575, 1989.

17. Seidal T, Balaton AJ, Battifora H: İnterpretation and quantification of immunostains. *Am J Surg Pathol*, 25 (9): 1204-1207, 2001. DOI: 10.1097/00000478-200109000-00013

18. Bakir B, Karadag Sari E, Elis Yildiz S, Asker H: Effects of thymoquinone supplementation on somatostatin secretion in pancreas tissue of rats. *Kafkas Univ Vet Fak Derg*. 23 (3): 409-413, 2017, DOI: 10.9775/kvfd.2016.16893

19. Ramzan T, Aslam B, Muhammad F, Faisal MN, Hussain A: Influence of *Ocimum sanctum* (L.) extract on the activity of gliclazide in alloxan-induced diabetes in rats. *Rev Chim,* 71 (10): 101-110, 2020. DOI: 10.37358/RC.20.11.8379

20. Suanarunsawat T, Devakul Na Ayutthaya W, Thirawarapan S, Poungshompoo S: Anti-oxidative, anti-hyperglycemic and lipid-lowering effects of aqueous extracts of *Ocimum sanctum* L. leaves in diabetic rats. *Food Nutr Sci,* 5 (9), 801-811, 2014. DOI: 10.4236/fns.2014.59090

21. Antora RA, Salleh RM: Antihyperglycemic effect of Ocimum plants: A short review. *Asian Pac J Trop Biomed,* 7 (8): 755-759, 2017. DOI: 10.1016/j.apjtb.2017.07.010

22. Pandiri I, Moni A: Ocimum herb species: A potential treatment strategy for diabetic kidney disease. *J Adv Biotechnol Exp Ther*, 1 (3), 88-91, 2018. DOI: 10.5455/jabet.2018.d16

23. Narendhirakannan RT, Subramanian S, Kandaswamy M: Biochemical

evaluation of antidiabetogenic properties of some commonly used Indian plants on streptozotocin induced diabetes in experimental rats. *Clin Exp Pharmacol Physiol,* 33 (12): 1150–1157, 2006. DOI: 10.1111/j.1440-1681.2006.04507.x

24. Hannan JMA, Marenah L, Ali L, Rokeya B, Flatt PR, Abdel-Wahab YHA: *Ocimum sanctum* leaf extracts stimulate insulin secretion from perfused pancreas, isolated islets and clonal pancreatic beta-cells. *J Endocrinol,* 189 (1): 127-136, 2006. DOI: 10.1677/joe.1.06615

25. Lee EY, Lee MY, Hong SW, Chung CH, Yong Hong SY: Blockade of oxidative stres by vitamin C ameliorates albuminuria and renal sclerosis in experimental diabetic rats. *Yonsei Med J,* 48 (5): 847-855, 2007. DOI: 10.3349/ymj.2007.48.5.847

26. Singh LP, Crook ED: Hexosamine regulation of glucose-mediated laminin synthesis in mesangial cells involves proetin kinases A and C. *Am J Physiol Renal Physiol,* 279 (4): F646-F654, 2000. DOI: 10.1152/ajprenal.2000.279.4.F646

27. Reeves WB Andreoli TE: Transforming growth factor β contributes to progressive diabetic nephropathy. *Proc Natl Acad Sci USA,* 97 (14): 7667-7669, 2000. DOI: 10.1073/pnas.97.14.7667

28. Swaroop JJ, Rajarajeswari D, Naidu JN: Association of TNF-α with insulin resistance in type 2 diabetes mellitus. *Indian J Med Res*, 135 (1): 127-130, 2012. DOI: 10.4103/0971-5916.93435

29. Rochlani Y, Pothineni NV, Kovelamudi S, Mehta JL: Metabolic syndrome: Pathophysiology, management, and modulation by natural compounds. *Ther Adv Cardiovasc Dis,* 11 (8): 215-225, 2017. DOI: 10.1177/1753944717711379

30. Xu X, Qi X, Shao Y, Li Y, Fu X, Feng S, Wu Y: Blockade of TGF-β-activated kinase revents advanced glycation end products-induced inflammatory response in macrophages. *Cytokine*, 78, 62-68, 2016. DOI: 10.1016/j.cyto.2015.11.023

31. Ma L, Ni H, Zou X, Yuan Y, Luo C, Liu B, Wang F, Xi Y, Chu Y, Xu P, Qiu X, Li S, Bu S: *Mori cortex* prevents kidney damage through inhibiting expression of inflammatory factors in the glomerulus in streptozocin-induced diabetic rats. *Iran J Basic Med Sci,* 20 (6): 715-721, 2017. DOI: 10.22038/IJBMS.2017.8842

32. Senatorski G, Paczec L, Kropiewnicka E, Bartłomiejczyk I: Cytokines in non invasive diagnostics of diabetic nephropathy progression. *Pol Merkur Lekarski*, 13 (Suppl. 1): 28-32, 2002.

33. Hameed I, Masoodi SR, Malik PA, Mir SA, Ghazanfar K, Ganai BA: Genetic variations in key inflammatory cytokines exacerbates the risk of diabetic nephropathy by influencing the gene expression. *Gene,* 661, 51-59, 2018. DOI: 10.1016/j.gene.2018.03.095

34. Kumar Jayant S, Srivastava N: Effect of *Ocimum sanctum* against alloxan induced diabetes and biochemical alterations in rats. *Integr Obesity Diabetes,* 2 (5): 1-4. 2016. DOI: 10.15761/IOD.1000162

35. Utsav, Kumar B, Kumar A: Diabetes mellitus and its control by *Ocimum sanctum* extract in mice diabetic Model. *Int J Curr Microbiol App Sci*, 5 (11): 795-810, 2016. DOI: 10.20546/ijcmas.2016.511.091

Kafkas Universitesi Veterinar Fakultesi Dergisi
ISSN: 1300-6045 e-ISSN: 1309-2251
Journal Home-Page: http://vetdergikafkas.org

Kafkas Univ Vet Fak Derg
27 (3): 323-329, 2021
DOI: 10.9775/kvfd.2021.25370

RESEARCH ARTICLE

Detection of Methicillin Resistant *Staphylococcus aureus* Strains and Typing of Staphylococcal Cassette Chromosome *mec* from Various Foods Originated Different Region from Turkey [1]

Ghassan ISSA [1,a (*)] Ali AYDIN [2,b]

[1] *This study was supported from Technological Research Council of Turkey (TÜBİTAK-2216)*

[1] Medical Laboratory Techniques Program, Avrupa Vocational School, Kocaeli Health and Technology University, TR-34020 Zeytinburnu, İstanbul - TURKEY
[2] Department of Food Hygiene and Technology, Faculty of Veterinary Medicine, İstanbul University-Cerrahpaşa, TR-34320 Avcılar, İstanbul - TURKEY
ORCIDs: [a] 0000-0002-0229-7632; [b] 0000-0002-4931-9843

Article ID: KVFD-2021-25370 Received: 03.01.2021 Accepted: 08.04.2021 Published Online: 09.04.2021

Abstract

Staphylococcus aureus is a microorganism that is highly resistant to environmental conditions and is widely found in environmental sources. It can cause a large number of infections in both humans and animals. Resistance to methicillin in *S. aureus* strains occurs due to the production of low affinity penicillin binding proteins (PBP2a). PBP2a is encoded by the *mec*A gene. The *mec*A gene is located on a mobile, large genetic element called the staphylococcal cassette chromosome mec (SCC*mec*). Until now, 13 SCC*mec* (I-XIII) types have been identified in *S. aureus* strains. In this study, in different 7 regions (Marmara, Aegean, Central Anatolia, the Black Sea, the Mediterranean, Eastern and Southeastern Anatolia) of Turkey obtained from a variety of points of 700 food items in the [(dairy products (n:560), bakery products (n:89), ready meal (n:40), meat product (n:11)], after the isolation of cultural *S. aureus* and verification by PCR, MRSA detection and SCC*mec* typing were aimed. 67 (9.57%) *S. aureus* strains were isolated from 700 food samples analyzed within the scope of the study. Only 1 (0.14%) of the 67 *S. aureus* strains isolated, both phenotypically and genotypically, was found to be MRSA and when SCC*mec* was typed, it was found to be Type IV. Community-acquired MRSA strains can cause clinical cases ranging from skin infections to fatal pneumonia and sepsis, as well as foodborne diseases. As a result, it is considered that MRSA strains can be an important source of contamination for humans with the consumption of food of animal origin.

Keywords: *Staphylococcus aureus, Antibiotic Resistance, mecA, SCCmec, Food, Turkey*

Türkiye'nin Farklı Bölgeleri Kaynaklı Toplanan Çeşitli Gıda Maddelerinden Metisilin Dirençli *Staphylococcus aureus* Suşlarının Tespiti ve Stafilokokkal Kaset Kromozom *mec* Tiplendirilmesi

Öz

Staphylococcus aureus hem insanlarda, hem de hayvanlarda çok sayıda enfeksiyona neden olabilen, ortam şartlarına oldukça dayanıklı ve çevresel kaynaklarda yaygın olarak bulunan bir mikroorganizmadır. *S. aureus* suşlarında metisiline direnç, düşük afiniteli penisilin bağlayan proteinlerin (PBP2a) üretimine bağlı olarak meydana gelmektedir. PBP2a, *mec*A geni tarafından kodlanmaktadır. *mec*A geni ise stafilokokkal kaset kromozom mec (SCC*mec*) adı verilen hareketli, büyük genetik eleman üzerinde bulunmaktadır. *S. aureus* suşlarında şu ana kadar 13 SCC*mec* (I-XIII) tipi tespit edilmiştir. Bu çalışmada, Türkiye'nin 7 farklı bölgesindeki (Marmara, Ege, İç Anadolu, Karadeniz, Akdeniz, Doğu Anadolu ve Güneydoğu Anadolu) çeşitli noktalardan temin edilen 700 adet gıda maddesinde [(süt ürünü (n:560), unlu mamuller (n:89), hazır yemek (n:40), et ürünü (n:11)] kültürel *S. aureus* izolasyonu ve PCR ile doğrulaması yapıldıktan sonra MRSA tespiti ve SCC*mec* tiplendirilmesi amaçlanmıştır. Araştırma kapsamında analiz edilen 700 adet gıda numunesinden 67 (%9.57) adet *S. aureus* suşu izole edilmiştir. İzole edilen 67 *S. aureus* suşundan hem fenotipik, hem de genotipik olarak sadece 1 (%0.14) adedinin MRSA suşu olduğu saptanmış ve SCC*mec* tiplendirilmesi yapıldığında, Tip IV olduğu tespit edilmiştir. Toplumsal kökenli MRSA suşları, gıda kaynaklı hastalıkların yanı sıra deri enfeksiyonlarından ölümcül pnömoni ve sepsise varan klinik tablolara da neden olabilmektedir. Sonuç olarak hayvansal kökenli gıdaların tüketimi ile MRSA suşlarının insanlar için önemli bir bulaşma kaynağı olabileceği değerlendirilmektedir.

Anahtar sözcükler: *Staphylococcus aureus, Antibiyotik direnci, mecA, SCCmec, Gıda, Türkiye*

How to cite this article?

Issa G, Aydin A: Detection of methicillin resistant *Staphylococcus aureus* strains and typing of staphylococcal cassette chromosome *mec* from various foods originated different region from Turkey. *Kafkas Univ Vet Fak Derg,* 27 (3): 323-329, 2021.
DOI: 10.9775/kvfd.2021.25370

(*) Corresponding Author

Tel: +90 850 450 2828; Fax: +90 212 547 0068
E-mail: ghassan.issa@kocaelisaglik.edu.tr (G. İssa)

Introduction

Staphylococcus aureus is a microorganism that is highly resistant to environmental conditions and *S. aureus* widely found in environmental sources and can cause a large number of infections in both humans and animals. In addition, *S. aureus* is also widely found in food and food facilities, staff involved in food production, hospital staff and hospital settings. Personnel who carry and prepare food with their hands, especially in the food sector, are considered to be an important source of staphylococcal intoxications due to the risk of possible contamination [1-6].

Methicillin resistance in *S. aureus* strains occurs due to the production of low affinity penicillin binding proteins. Responsible for resistance to all beta-lactam antibiotics, PBP2a is encoded by the *mec*A gene. The *mec*A gene is located on a mobile, large genetic element called the staphylococcal cassette chromosome *mec*. The SCC*mec* structure of *S. aureus* consists of three elements: *mec* gene complex *(mec*A gene and its regulators *mec*I and *mec*R1), cassette chromosome recombinase *(ccr)* gene complex, and J (junkyard). SCC*mec*; they are divided into types according to *mec* and *ccr* gene complexes and subtypes according to differences in J regions. 13 SCC*mec* (I-XIII) types have been identified in *S. aureus* strains so far. Type I, II, III and VIII hospital-acquired methicillin-resistant *S. aureus* (HA-MRSA), types IV, V, VI and VII are CA-MRSA. While Type II and III cause multiple antibiotic resistance other than beta-lactam, Type I, IV and V do not carry multiple antibiotic resistance genes other than beta-lactam [7-15].

Turkey is located in the transition zone of the position as Asia, Europe and Africa. It has a very important geopolitical location. It is possible not only for humans or animals but also for microorganisms to pass between regions. This study was carried out in order to reveal the regional incidence of MRSA strains in Turkey, which is currently on the world agenda and draw attention in terms of public health for our country, and to make SCC*mec* typing in food-borne MRSA strains.

Material and Methods

Sampling

In this study, 560 dairy products (cheese), 89 bakery products (turkish raw flatbread [n:49], turkish handmade noodles [n:40]), 40 Ready To Eat Foods (raw meatballs [n:21], entrees [n:19]) and 11 meat products (sausages [n:6], salami [n:5]) to a total of 700 different food items in Turkey's seven regions (Black Sea region [n:100], Marmara region [n:100], Aegean region [n:100], Mediterranean region [n:100], Central Anatolia region [n:100], Southeastern Anatolia region [n:100], Eastern Anatolia region [n:100]) obtained from various points. Approximately 100 g of sample taken under aseptic conditions, depending on the type of sample, was brought to the laboratory under cold storage conditions (4°C) and microbiological analysis was performed as soon as possible.

Isolation and Identification of S. aureus from Food Samples

Food samples brought to the laboratory were weighed 10 g each in sterile stomacher bag and 90 mL peptone salt water (Maximum Recovery Diluent) solution (Oxoid CM 0733) was added and homogenized in stomacher (Seward 400, England) for about 2 min. From the obtained homogenization and dilutions, they were planted with the spreading technique on Baird Parker Agar (Oxoid, CM 0275) plates with tellurite added egg yolk (Oxoid SR 0054) and incubated for 24-48 h at 37°C. *S. aureus* colonies which ocur due to the lecithinase activity on BP agar with a diameter of 2-3 mm 'gray-black' zones around were considered suspicious. *S. aureus* isolates growing on BP agar were inoculated into Mannitol Salt Agar (Oxoid CM 0085) to evaluate mannitol fermentation at a later stage. Then, biochemical confirmation was performed on *S. aureus* strains by Gram staining, catalase test, DN*ase* test (Oxoid CM 321) and latex agglutination test (Oxoid, DR 100M) [16-20].

Determination of Methicillin Resistant S. aureus Strains by Phenotypic Methods

Kirby-Bauer disc diffusion method was carried out in accordance with the recommendations of CLSI (2009) in determining the methicillin resistance of the strains defined as *S. aureus*. Conventionally, cefoxitin disk diffusion (FOX 30 µg, Oxoid CT0119B), oxacillin disk diffusion (OX 1 µg, Oxoid CT0159B) and oxacillin resistance screening agar (ORSAB, Oxoid CM 1008) tests were used to determine methicillin resistant *S. aureus* strains [21-24].

Verification of S. aureus strains by Molecular Methods

DNA extraction of *S. aureus* strains was performed according to the instruction of Genomic DNA Isolation from Bacteria kit (RTA, 09005100). For PCR mix 30 µL Sterile dH_2O, 5 µL $(NH_4)_2SO_4$ containing 10x buffer (Fermentas, EP0402), 3 µL $MgCl_2$ (25Mm, Fermentas, EP0402), 1 µL Forward primer (10 mM), 1 µL Revers primer (10 mM), 5 µL dNTP mix (2 mM each, Fermentas, R0241), 0.24 µL *Taq* DNA polymerase (500 U, Fermentas, EP0402) and 5 µL Genomic DNA template after preparation to 50 µL containing PCR tubes were placed in the Thermal cycler (Biorad, Italy).

Following the amplification process, PCR products were analyzed by horizontal agarose gel electrophoresis. While protein A *(spa)*, thermonuclease *(nuc)* and coagulase *(coa)* genes were examined for molecular confirmation of strains, the presence of *mec*A gene was investigated for the determination of methicillin resistance. Primers and thermal cycling conditions used for the verification of *S. aureus* strains and detection of *mec*A are given in *Table 1* [25-27].

Table 1. *Primers and thermal cycling conditions used for the verification of S. aureus isolates and detection of mecA*

Target	Amplicon Size (bp)	Primer; Oligonucleotide Ssequence (5'-3')	Thermal Cycling Conditions
spa	100-450	1113F; TAAAGACGATCCTTCGGTGAGC 1514R; CAGCAGTAGTGCCGTTTGCTT	Initial Denaturation 80°C 5 min **Denaturation 94°C 45 s** **Annealing 60°C 45 s = 35 Cycles** **Extension 72°C 90 s** Final Extension 72°C 10 min
nuc	416	F; GGCAATTGTTTCAATATTAC R; TTTTATTTGCATTTTCTACC	Initial Denaturation 80°C 5 min **Denaturation 94°C 45 s** **Annealing 60°C 45 s = 35 Cycles** **Extension 72°C 90 s** Final Extension 72°C 10 min
coa	500-650	F; ATAGAGATGCTGGTACAGG R; GCTTCCGATTGTTCGATGC	Initial Denaturation 80°C 5 min **Denaturation 94°C 45 s** **Annealing 60°C 45 s = 35 Cycles** **Extension 72°C 90 s** Final Extension 72°C 10 min
mecA	162	*mec*A P4; TCCAGATTACAACTTCACCAGG *mec*A P7; CCACTTCATATCTTGTAACG	Initial Denaturation 80°C 5 min **Denaturation 94°C 45 s** **Annealing 60°C 45 s = 35 Cycles** **Extension 72°C 90 s** Final Extension 72°C 10 min

Table 2. *Primers and thermal cycling conditions used in SCCmec typing*

Primer	Oligonucleotide Sequence (5'-3')	Amplicon Size (bp)	Specificity (SCC*mec* type)	Thermal Cycling Conditions
CIF2F2 CIF2R2	TTCGAGTTGCTGATGAAGAAGG ATTTACCACAAGGACTACCAGC	495	I	Initial Denaturation 94°C 4 min **Denaturation 94°C 30 s** **Annealing 53°C 30 s = 30 Cycles** **Extension 72°C 1min** Final Extension 72°C 4 min
KDPF1 KDPR1	AATCATCTGCCATTGGTGATGC CGAATGAAGTGAAAGAAAGTGG	284	II	
MECIP2 MECIP3	ATCAAGACTTGCATTCAGGC GCGGTTTCAATTCACTTGTC	209	II, III	
DCSF2 DCSR1	CATCCTATGATAGCTTGGTC CTAAATCATAGCCATGACCG	342	I, II, IV	
RIF4F3 RIF4R9	GTGATTGTTCGAGATATGTGG CGCTTTATCTGTATCTATCGC	243	III	
RIF5F10 RIF5R13	TTCTTAAGTACACGCTGAATCG GTCACAGTAATTCCATCAATGC	414	III	

Mutiplex PCR was performed using primer sequences and protocol suggested by Oliveira and Lencastre [26] for SCC*mec* typing in *mec*A positive samples. Primers and thermal cycling conditions used in SCC*mec* typing are given in *Table 2*.

Results

The distribution of the sample types provided in our research by product groups and regions is given in *Table 3*. A total of 67 (9.57%) *S. aureus* strains were isolated from 700 food samples analyzed within the scope of the project. Of the 67 *S. aureus* strains; 50 (74.62%) were obtained from dairy products, 16 (23.88%) from bakery products, and 1 (1.50%) from RTE food samples. On the other hand, *S. aureus* was not found in any meat product samples. Accordingly, the distribution and percentages of *S. aureus* strains by product groups and regions are shown in *Table 4*. *spa*, *nuc* and *coa* genes were verified by PCR in 67 *S. aureus* strains isolated by cultural methods. The gel image of the detected genes *spa* (100-450 bp) is shown in *Fig. 1-A*, *nuc* (416 bp) in *Fig. 1-B* and *coa* (500-600 bp) in *Fig. 1-C*. Only 1 (0.14%) of 67 *S. aureus* strains isolated was identified as both phenotypically and genotypically MRSA. The detected MRSA strain was isolated from a cheese (dairy product) collected from the Marmara region. While the growth image of the MRSA positive strain in ORSAB medium is given in *Fig. 1-D*, the disk diffusion test image of oxacillin (1 µg) and cefoxitin (30 µg) is given in *Fig. 1-E*. *mec*A gene responsible for methicillin resistance was also detected by genotypic (PCR) methods in *S. aureus* strain isolated as MRSA by phenotypic methods. SCC*mec* typing of dairy derived MRSA strain detected by both phenotypic and genotypic methods and SCC*mec* Type IV (community-acquired) was found in our study. The detected *mec*A (162 bp) and SCC*mec* Type IV (342 bp) gel image is shown in *Fig. 1-F*.

Table 3. *The distribution of the sample types provided by product groups and regions*

Product Groups	n	Marmara Region n (%)	Aegean Region n (%)	Black Sea Region n (%)	Central Anatolia Region n (%)	Eastern Anatolia Region n (%)	Southeastern Anatolia Region n (%)	Mediterranean Region n (%)
Meat Products	11	11 (100)	-	-	-	-	-	-
Dairy Products	560	58 (10.35)	92 (16.45)	82 (14,64)	67 (11.96)	95 (16,96)	88 (15.71)	78 (13.93)
Bakery Products	89	15 (16.85)	2 (2.25)	17 (19.11)	18 (20.22)	3 (3.37)	12 (13.48)	22 (24.72)
Ready Meals	40	16 (40)	6 (15)	1 (2.5)	15 (37.5)	2 (5)	-	-
Total (%)	700	100 (14.29)	100 (14.29)	100 (14.29)	100 (14.29)	100 (14.29)	100 (14.29)	100 (14.29)

Table 4. *The distribution and percentages of S. aureus isolates by product groups and regions*

Product Groups	S. aureus n (%)	Marmara Region n (%)	Aegean Region n (%)	Black Sea Region n (%)	Central Anatolia Region n (%)	Eastern Anatolia Region n (%)	Southeastern Anatolia Region n (%)	Mediterranean Region n (%)
Meat Products	-	-	-	-	-	-	-	-
Dairy Products	50 (74.62)	5 (10)	7 (14)	4 (8)	7 (14)	7 (14)	11 (22)	9 (18)
Bakery Products	16 (23.88)	2 (12.5)	-	8 (50)	3 (18.75)	-	-	3 (18.75)
Ready Meals	1 (1.49)	1	-	-	-	-	-	-
Total (%)	67 (100)	8 (11.94)	7 (10.45)	12 (17.91)	10 (14.93)	7 (10.45)	11 (16.41)	12 (17.91)

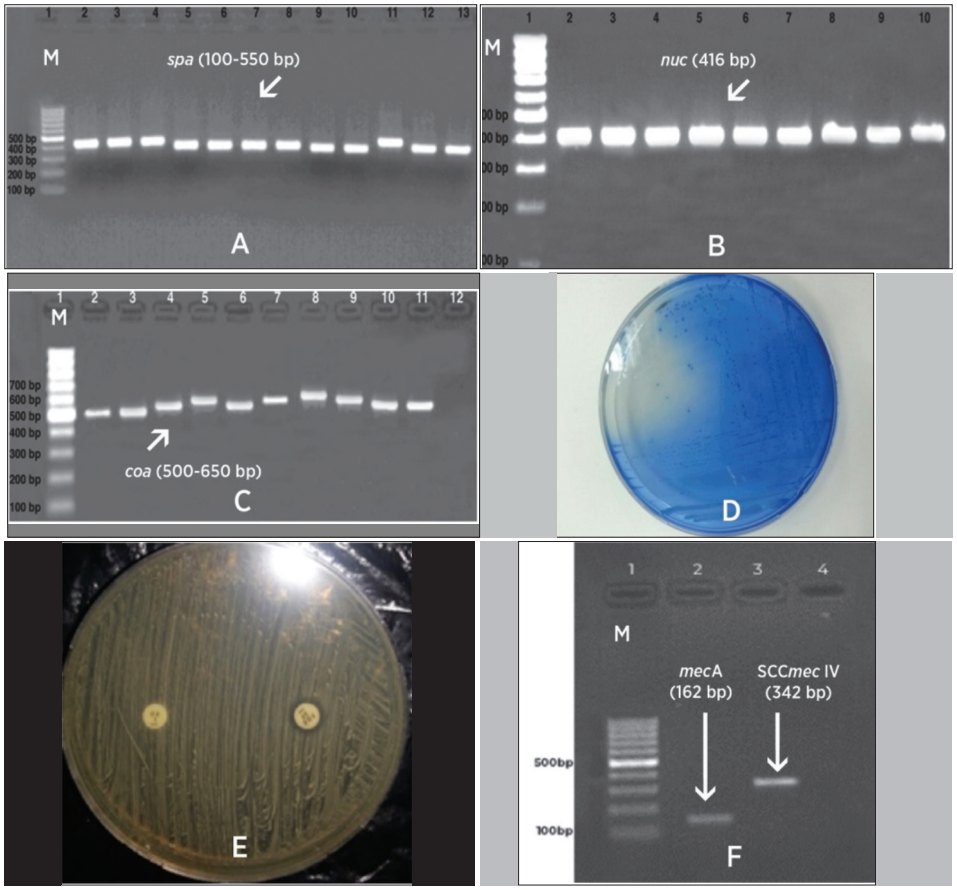

Fig 1. A- *spa* gene positive gel image (lane 1: DNA ladder [100 bp], lanes 2-13: *spa* gene positive samples); **B-** *nuc* gene positive gel image (lane 1: DNA ladder [100 bp], lanes 2-10: *nuc* gene positive samples); **C-** *coa* gene positive gel image (lane 1: DNA ladder [100 bp], lanes 2-11: positive samples of the *coa* gene, lane 12: negative control)**; D-** MRSA development on ORSAB agar**; E-** Disk diffusion test of oxacillin (1 µg) and cefoxitin (30 µg) in MHA; **F-** *mec*A gene positive and SCC*mec* Type IV gel image (lane 1: DNA ladder [100 bp], lane 2: *mec*A gene positive sample, lane 3: SCC*mec* Type IV positive sample, lane 4: negative control)

Discussion

Staphylococcus aureus causes significant infections in animals and humans. It is a source of nosocomial infection in humans. One of the most important hospital and community-acquired factors that lead to unsuccessful treatment and deaths is MRSA [28]. In addition, the increase in the frequency of MRSA strains in recent years has revealed the need to develop effective strategies to control staphylococcal infections and the development of resistance in microorganisms against antibiotics. Therefore, it is of great importance to know the epidemiology, pathogenesis and population genetics of *S. aureus*. Misuse and abuse of antibiotics emerges as an important factor that increases MRSA colonization. In our country, misuse of antibiotics and related resistance problems are frequently encountered in both veterinary and human medicine. CA-MRSA infections can be transmitted by direct contact as well as by consumption of animal-based foods. Poor personal hygiene increases the potential for contamination. In addition to the use of antibiotics in our country, there are also important problems in ensuring food hygiene and personal hygiene. Normanno et al.[29], isolated 160 (9.80%) *S. aureus* strains from 1634 animal origin food they collected, and reported that only 6 (3.75%) of the strains were MRSA. Meemken et al.[30], examined 687 swab samples taken from pig nose for MRSA and reported that 85 (12.37%) were positive. De Neeling et al.[31], reported that 209 (38.70%) of the 540 pig samples taken from the slaughterhouse were MRSA positive. Qudduomi et al.[32] evaluated 6 (0.84%) out of 717 meat samples as MRSA positive. Kwon et al.[11] detected the presence of *S. aureus* in 292 (31.40%) of the 930 food samples (cattle, chicken and pig) they collected from slaughterhouses and markets. They reported that 766 *S. aureus* strains isolated from these 292 foodstuffs, 4 of the isolated strains carried *mec*A and phenotypically only 3 were MRSA. They stated that 3 MRSA strains from 2 (0.22%) chicken samples detected and all 3 were SCC*mec* Type III. On the other hand, similar to our study, Uçan and Aslan [33] detected methicillin resistance in only 1 (1.33%) of 75 *S. aureus* strains. In the study conducted by İssa and Aksu [2], 119 (29.31%) *S. aureus* strains were detected from 406 raw milk samples, and only 1 (0.84%) of these 119 strains was reported to be MRSA. In another study, Kwon et al.[34], found that 14 (0.018%) of the 75335 milk samples they examined in Korea were MRSA. SCC*mec* typing of 14 isolated MRSA strains was made and it was revealed that all strains were Type IV. A total 67 (9.57%) strains of *S. aureus* were isolated from 700 food samples analyzed in our study, and it was found that only 1 (0.14%) strain was MRSA, and SCC*mec* Type IV (community acquired) were found.

Several studies [2,4,35-38] reported that the prevalence of *S. aureus* is relatively high in milk and dairy products. These reports are consistent with our results. Normanno et al.[37] examined the swabs taken from 11384 foodstuffs and food contact surfaces they bought from the markets in Italy and isolated 1971 (17.3%) coagulase positive *S. aureus*. At the same study, coagulase positive *S. aureus* was detected from 1245 (23.1%) samples of 5369 meat products and 168 (38.4%) of 437 raw milk samples. Juhasz-Kaszanyitzky et al.[38] examined 595 milk samples taken from cows with subclinical mastitis and isolated 375 (63.02%) of *S. aureus*. Of these 375 *S. aureus* strains, only 27 (7.20%) were found to be MRSA. Argudin et al.[4] found in a study they conducted that 2 (3.12%) of the 64 *S. aureus* strains they isolated from food and food processors were MRSA and when SCC*mec* was typed, and both were Type IV. Stastkova et al.[39], reported that they isolated 34 (22.22%) *S. aureus* strains out of 153 goat milk samples, 5 (3.26%) of the isolates were MRSA and these 5 strains were Type IV as a result of SCC*mec* typing. Similarly, Vanderhaeghen et al.[40] stated that 11 (9.30%) of 118 *S. aureus* strains isolated from mastitis cows were MRSA, 5 of them were SCC*mec* IV, 5 were SCC*mec* V and the other 1 strain could not be typed. Huber et al.[36] isolated 142 *S. aureus* strains from mastitis milk and stated that only 2 (1.40%) of the strains were MRSA and these 2 strains belonged to Type V as a result of SCC*mec* typing. In another study, Gülbandılar [17] took samples from the nasal mucosa of 3048 people from food processors (cooks, bakers, pastry makers, etc.) and tradesmen (barbers, hairdressers, etc.) who had direct contact with the public, and isolated a total 217 (7.12%) *S. aureus* strains. Gülbandılar [17] reported that only 12 (5.30%) of the 217 *S. aureus* strains they isolated were MRSA strains. Similarly, in a study conducted by Lee [22], they isolated 421 (22%) *S. aureus* from 1913 samples taken from cattle, pigs and chickens, and 28 (6.65%) of these 421 *S. aureus* strains were phenotypically MRSA. However, they found that only 15 (3.56%) of them were MRSA in genotypic evaluation.

Yang et al.[10], isolated 69 (12.54%) *S. aureus* strains out of 550 RTE food samples from the markets in their study between 2011-2014, and only 6 (1.09%) of these strains were MRSA, as a result of SCC*mec* typing. They found that 2 of them MRSA were evaluated as Type IV and 2 of them MRSA were evaluated as Type V, but the other 2 MRSA strains could not be typed. Wang et al.[9], isolated 455 (23%) *S. aureus* strains in a study they conducted with 1979 food samples collected from the markets between 2008-2012, only 17 (0.90%) of these strains were MRSA, and confirmed that as a result of SCC*mec* typing; 4 of them MRSA were Type II and 9 MRSA were Type IV, 2 of them MRSA strains were evaluated as Type V and the remaining strains could not be typed. The fact that both *S. aureus* and methicillin resistant *S. aureus* strains have been reported at different rates in studies conducted in our country and in the world may be caused by the differences in geographical regions, the difference of the samples from which the strains were isolated and the increase in resistant strains over time. Depending on the season, different rates of agent isolation may be in question. In this context, Stastkova et al.[39] reported that the rates of *S. aureus* and MRSA isolated from milk samples can be different according to the seasons.

CA-MRSA strains can cause clinical cases ranging from skin infections to fatal pneumonia and sepsis, as well as food-borne diseases. Several virulent genes have been identified, such as Panton-Valentin Leukocidin (PVL), which cause degradation of leukocytes and tissue necrosis in CA-MRSA strains and are not found in hospital-acquired MRSA strains [41-44]. The problem of antimicrobial resistance, which has reached serious level in recent years, causes adverse effects such as increased mortality rates, prolonged treatment periods, loss of work force due to prolonged hospital stay, and the necessity to use newly developed expensive antibiotics as a result of nosocomial and community-acquired bacterial infections in developed and developing countries.

As a result, consumption of animal origin foods is an important source of contamination of MRSA strains for humans. There is need for studies to determine the source of antibiotic resistant bacteria by using molecular methods. Based on these researches, it should be a correct policy regarding the use of antibiotics in human infections, veterinary medicine and animal husbandry. It is considered that generalizing the studies on antibiotic resistance and determining the types of MRSA will be beneficial for the protection of public health in our country.

Acknowledgement

This study was supported from Technological Research Council of Turkey (TUBITAK-2216).

Conflict of Interest

The authors declare that they have no conflict of interest.

Author Contributions

Gİ planned and designed the research, carried out experiments. Gİ and AA discussed the results. All authors contributed to writing of the final manuscript.

References

1. Wang W, Baloch Z, Jiang T, Zhang C, Peng Z, Li F, Fanning S, Ma A, Xu J: Enterotoxigenicity and antimicrobial resistance of *Staphylococcus aureus* isolated from retail food in China. *Front Microbiol*, 8:2256, 2017. DOI: 10.3389/fmicb.2017.02256

2. İssa G, Aksu H: Detection of methicillin-resistant *Staphylococcus aureus* in milk by PCR-based phenotyping and genotyping. *Acta Vet Eurasia*, 46, 120-124, 2020. DOI: 10.5152/actavet.2020.20011

3. Erol İ: Gıda Hijyeni ve Mikrobiyolojisi. 135-144, Pozitif Matbaacılık, Ankara, 2007.

4. Argudin MA, Mendoza MC, Gonzalez-Hevia MA, Bances M, Guerra B, Rodicio MR: Genotypes, exotoxin gene content, and antimicrobial resistance of *Staphylococcus aureus* strains recovered from foods and food handlers. *Appl Environ Microbiol*, 78 (8): 2930-2935, 2012. DOI: 10.1128/AEM.07487-11

5. Vural H, Öztan A: Effects of starter culteres on growth of *Staphylococcus aureus* in fermented meat products. *Gıda*, 18 (4): 259-263, 1993.

6. Sergelidis D, Angelidis AS: Methicillin-resistant *Staphylococcus aureus*: A controversial food-borne pathogen. *Lett Appl Microbiol*, 64, 409-418, 2017. DOI: 10.1111/lam.12735

7. Singh-Moodley A, Strasheim W, MogokotlengR, Ismail H, Perovic O: Unconventional SCC*mec* types and low prevalence of the Panton-Valentine Leukocidin exotoxin in South African blood culture *Staphylococcus aureus* surveillance isolates, 2013-2016. *PLoS ONE*, 14 (11): e0225726, 2019. DOI: 10.1371/journal.pone.0225726

8. Chen L, Mediavilla JR, Oliveira DC, Willey BM, Lencastre HD, Kreiswirth BN: Multiplex real-time PCR for rapid staphylococcal casette chromosome *mec* typing. *J Clin Microbiol*, 47, 3692-3706, 2009. DOI: 10.1128/JCM.00766-09

9. Wang X, Li G, Xia X, Yang B, Xi M, Meng J: Antimicrobial susceptibility and molecular typing of methicillin-resistant *Staphylococcus aureus* in retail foods in Shaanxi, China. *Foodborne Pathog Dis*, 11 (4): 281-286, 2014. DOI: 10.1089/fpd.2013.1643

10. Yang X, Zhang J, Yu S, Wu Q, Guo W, Huang J, Cai S: Prevalence of *Staphylococcus aureus* and methicillin-resistant *Staphylococcus aureus* in retail ready-to-eat foods in China. *Front Microbiol*, 7:816, 2016. DOI: 10.3389/fmicb.2016.00816

11. Kwon NH, Park KT, Jung WK, Youn HY, Lee Y, Kim SH, Bae W Lim JY, Kim JY, Hong SK, Park YH: Chracteristics of methicillin resistant *S. aureus* isolated from chicken meat and hospitalized dogs in Korea and their epidemiological relatedness. *Vet Microbiol*, 117, 304-312, 2006. DOI: 10.1016/j.vetmic.2006.05.006

12. Saber H, Jasni AS, Jamaluddin TZMT, Ibrahim R: A review of staphylococcal cassette chromosome *mec* (SCC*mec)* types in coagulase-negative staphylococci (CoNS) species. *Malays J Med Sci*, 24 (5): 7-18, 2017. DOI: 10.21315/mjms2017.24.5.2

13. Reichmann NT, Pinho MG: Role of SCC*mec* type in resistance to the synergistic activity of oxacillin and cefoxitin in MRSA. *Sci Rep*, 7:6154, 2017. DOI: 10.1038/s41598-017-06329-2

14. Afshari SG, Sepahi AA, Goudarzi H, Tabrizi MS, Goudarzi M, Hajikhani B, Heidary M, Azimi H: Distribution of SCC*mec* types in methicillin-resistant *Staphylococcus aureus* isolated from burn patients. *Arch Clin Infect Dis*, 12 (2): e62760, 2017. DOI: 10.5812/archcid.62760

15. Ghanbari F, Saberianpour S, Zarkesh-Esfahani FS, Ghanbari N, Taraghian A, Khademi F: Staphylococcal cassette chromosome *mec* (SCC*mec*) typing of methicillin-resistant *Staphylococcus aureus* strains isolated from community- and hospital-acquired infections. *Avicenna J Clin Microbiol Infect*, 4 (2): 42244, 2017. DOI: 10.5812/ajcmi.42244

16. ISO 6888-1: 1999/A1: 2003, Microbiology of food and animal feeding stuffs - Horizontal method for the enumeration of coagulase-positive staphylococci *(Staphylococcus aureus* and other species) - Part 1: Technique using Baird-Parker Agar medium (includes amendment A1: 2003).

17. Gülbandilar A: Investigation of *Staphylococcus aureus* carriage and antibiotic sensitivity in nose mucous membrane in Kütahya Province. *DPÜ Fen Bil Enst Derg*, 18, 1-6, 2009.

18. Amirkhiz MF, Rezaee MA, Hasani A, Aghazadeh M, Naghili B: SCC*mec* typing of methicillin-resistant *Staphylococcus aureus*: An eight year experience. *Arch Pediatr Infect Dis*, 3 (4): e30632, 2015. DOI: 10.5812/pedinfect.30632

19. APHA (American Publich Health Association): Compendium methods for the microbiological examination of foods. 4, 387-404, Washington DC, 2001.

20. Oxoid Manual: 8, Oxoid Ltd., Basingstok, UK, 1998.

21. Wikler MA, Cockerill FR, Craig WA, Dudley MN: Performance standards for antimicrobial susceptibility. Clinical and Laboratory Standards Institute. 17th ed., Informational Supplement, 27, 44-51, 2007.

22. Lee JH: Methicillin (oxacillin)-resistant *Staphylococcus aureus* strains isolated from maor food animals and their potential transmission to humans. *Appl Environ Microbiol*, 69 (11): 6489-6494, 2003. DOI: 10.1128/AEM.69.11.6489-6494.2003

23. Clinical and Laboratory Standards Institute (CLSI): Performance standards for antimicrobial susceptibility testing. 23rd Informational Supplement. CLSI document M100-S23, 33 (1): USA, 2013.

24. Nahimana I, Francioli P, Blanc DS: Evaluation of three chromogenic

media (MRSA-ID, MRSA-Select and CHROMagar MRSA) and ORSAB for surveillance cultures of methicillin-resistant *Staphylococcus aureus*. *Clin Microbiol Infect*, 12, 1168-1174, 2006. DOI: 10.1111/j.1469-0691.2006.01534.x

25. Hashemizadeh Z, Hadi N, Mohebi S, Kalantar-Neyestanaki D, Bazargani A: Characterization of SCC*mec, spa* types and multi drug resistant of methicillin-resistant *Staphylococcus aureus* isolates among inpatients and outpatients in a referral hospital in Shiraz, Iran. *BMC Res Notes*, 12:614, 2019. DOI: 10.1186/s13104-019-4627-z

26. Oliveira DC, De Lencastre H: Multiplex PCR strategy for rapid identification of structural types and variants of the *mec* element in methicillin resistant *Staphylococcus aureus*. *Antimicrob Agents Chemother*, 46 (7): 2155-2161, 2002. DOI: 10.1128/AAC.46.7.2155-2161.2002

27. Sudagidan M, Aydin A: Screening virulence properties of staphylococci isolated from meat and meat products. *Wien Tieraerztl Mschr*, 95, 128-134, 2008.

28. Bahrami N, Motamedi H, Tofighi SER, Akhoond MR: SCC*mec* typing and Panton-Valentine leukocidin occurrence in methicillin resistant *Staphylococcus aureus* isolates from clinical samples of Ahvaz, southwest of Iran. *Microbiol Medica*, 34:8050, 2019. DOI: 10.4081/mm.2019.8050

29. Normanno G, Corrente M, La Salandra G, Dambrosio A, Quaglia NC, Parisi A, Greco G, Bellacicco AL, Virgilio S, Celano GV: Methicillin-resistant *Staphylococcus aureus* (MRSA) in foods of animal origin product in Italy. *Int J Food Microbiol*, 117, 219-222, 2007. DOI: 10.1016/j.ijfoodmicro.2007.04.006

30. Meemken D, Cuny C, Witte W, Blaha T: Occurrence of MRSA in pıgs in the northwest of Germany. *Proceedings of the International Pig Veterinary Society Congress,* Durban, South Africa, 22-26, June-2008.

31. De Neeling AJ, Van Den Broek MJM, Spalburg EC, Van Santen-Verheuvel MG, Dam-Deisz WDC, Boshuizen HC, Van De Giessen AW, Van Duijkeren E, Huijsdens XW: High percentage of methicillin-resistant *Staphylococcus aureus* in pigs. *Vet Microbiol*, 122, 366-372, 2007. DOI: 10.1016/j.vetmic.2007.01.027

32. Qudduomi SS, Bdour SM, Mahasneh SM: Isolation and characterisation of methicillin-resistant *Staphylococcus aureus* from livestock and poultry meat. *Ann Microbiol*, 56, 155-161, 2006.

33. Uçan US, Aslan E: İnek mastitisislerinden izole edilen koagülaz pozitif stafilokok suşlarının penisilin direnci ve bazı antibiyotiklere duyarlılıkları. *Vet Bil Derg*, 18, 19-22, 2002.

34. Kwon NH, Park KT, Moon JS, Jung WK, Kim SH, Kim JM, Hong SK, Koo HC, Joo YS, Park YH: Staphylococcal casette chromosome *mec* (SCC*mec*) characterization and molecular analysis for methicillin-resistant *Staphylococcus aureus* and novel SCC*mec* subtype IVg isolated from bovine milk in Korea. *J Antimicrob Chemother*, 56, 624-632, 2005. DOI: 10.1093/jac/dki306

35. Aydin A, Sudagidan M, Muratoglu K: Prevalence of staphylococcal enterotoxins, toxin genes and genetic-relatedness of foodborne *Staphylococcus aureus* strains isolated in the Marmara Region of Turkey. *Int J Food Microbiol*, 148, 99-106, 2011. DOI: 10.1016/j.ijfoodmicro.2011.05.007

36. Huber H, Koller S, Giezendanner N, Stephan R, Zweifel L: Prevalence and characteristics of methicillin-resistant *Staphylococcus aureus* in human in contact with farm animals, in livestock, and in food of animal origin, Switzerland, 2009. *Euro Surveill*, 15 (16): pii=19542. 2010.

37. Normanno G, Firinu A, Virgilio S, Mula G, Dambrosio A, Poggiu A, Decastelli L, Mioni R, Scuota S, Bolzoni G, Di Giannatale E, Salinetti AP, La Salandra G, Bartoli M, Zuccon F, Pirino T, Sias S, Parisi A, Quaglia NC, Celano GV: Coagulase-positive *Staphylococci* and *Staphylococcus aureus* in food products marketed in Italy. *Int J Food Microbiol*, 98, 73-79, 2005. DOI: 10.1016/j.ijfoodmicro.2004.05.008

38. Juhasz-Kaszanyitzky E, Janosi S, Somogyi P, Dan A, Van Der Graaf-Von Bloois L, Van Duijkeren E, Wagenaar JA: MRSA transmission between cows and humans. *Emerg Infect Dis*, 13 (4): 630-632, 2007.

39. Stastkova Z, Karpiskova S, Karpiskova R: Occurrence of methicillin-resistant strains of *Staphylococcus aureus* at a goat breeding farm. *Vet Med*, 54 (9): 419-426, 2009. DOI: 10.17221/88/2009-VETMED

40. Vanderhaeghen W, Cerpentier T, Adriaensen C, Vicca J, Hermans K, Butaye P: Methicillin-resistant *Staphylococcus aureus* (MRSA) ST398 associated with clinical and subclinical mastitis in Belgian cows. *Vet Microbiol*, 144 (1-2): 166-171, 2010. DOI: 10.1016/j.vetmic.2009.12.044

41. Funaki T, Yasuhara T, Kugawa S, Yamazaki Y, Sugano E, Nagakura Y, Yoshida K, Fukuchi K: SCC*mec* typing of PVL positive community-acquired *Staphylococcus aureus* (CAMRSA) at a Japanese hospital. *Heliyon 5*:e01415, 2019. DOI: 10.1016/j.heliyon.2019.e01415

42. Ul Bashir Y, Bali N, Sharma S, Jahan T, Shafi H: SCC*mec* Type IV and V methicillin resistant *Staphylococcus aureus* intrusion in healthcare settings. *Am J Clin Microbiol Antimicrobial*, 2 (1): 1032, 2019.

43. Abdurahman MA, Tosun İ, Durukan İ, Khorshidtalab M, Kılıç AO: Four temperate bacteriophages from methicillin-resistant *Staphylococcus aureus* show broad bactericidal and biofilm removal activities. *Kafkas Univ Vet Fak Derg*, 27 (1): 29-36, 2021. DOI: 10.9775/kvfd.2020.24680

44. Tsilochristou O, Toit G, Sayre PH, MD, Roberts G, Lawson K, Sever ML, Bahnson HT, Radulovic S, Basting M, Plaut M, Lack G: Association of *Staphylococcus aureus* colonization with food allergy occurs independently of eczema severity. *J Allergy Clin Immunol*, 144 (2): 494-503, 2019. DOI: 10.1016/j.jaci.2019.04.025

Kafkas Universitesi Veteriner Fakultesi Dergisi
ISSN: 1300-6045 e-ISSN: 1309-2251
Journal Home-Page: http://vetdergikafkas.org

Kafkas Univ Vet Fak Derg
27 (3): 331-337, 2021
DOI: 10.9775/kvfd.2021.25375

RESEARCH ARTICLE

Evaluation of Feline-Specific Serum Sulphated Glycosaminoglycan and Dermatan Sulphate Levels in Cats with Non-Obstructive Lower Urinary Tract Dysfunction [1]

Didem PEKMEZCI [1,a (*)] Gulay CIFTCI [2,b] Umit OZCAN [1,c] Yucel MERAL [1,d] Duygu DALGIN [1,e]

[1] *This study was funded by The Scientific Research Council of Ondokuz Mayis University in Samsun, Turkey (Project number PYO.VET.1901.17.002)*

[1] Ondokuz Mayis University, Faculty of Veterinary Medicine, Internal Medicine Department, TR-55200 Samsun - TURKEY
[2] Ondokuz Mayis University, Faculty of Veterinary Medicine, Biochemistry Department, TR-55200 Samsun - TURKEY
ORCIDs: [a] 0000-0003-2072-8165; [b] 0000-0001-5384-2381; [c] 0000-0002-0868-6399; [d] 0000-0001-9099-5061; [e] 0000-0001-5253-5232

Article ID: KVFD-2021-25375 Received: 05.01.2021 Accepted: 19.05.2021 Published Online: 19.05.2021

Abstract

Lower urinary tract dysfunction (LUTD) is a commonly seen problem in cats. This chronic condition with no specific underlying cause remains a challenge for achieving effective treatment. Glycosaminoglycans (GAGs) are linear polysaccharides possessing characteristic repeated disaccharide sequences, thought to be involved in the pathogenesis of feline LUTD. The aim of the present study is to evaluate feline-specific serum sulphated glycosaminoglycan (S-GAG) and serum dermatan sulphate (DS) levels in cats with non-obstructive LUTD versus healthy controls. Eighteen client-owned cats suffering non-obstructive LUTD and 16 client-owned healthy cats were enrolled in this case-control study. Pre-treatment serum samples from cats in both the study (non-obstructive LUTD cats) and control (healthy cats) groups were analysed with "Quantitative Sandwich ELISA method" using feline-specific S-GAG and DS kits. The mean serum S-GAG and DS levels of the study group were measured against the control group. Measurements for study males were compared to the control males, and the neutered cats in the study group were compared to the intact ones in control group. Cats in study group had lower serum S-GAG concentrations (3.52±0.26 ng/mL) than the control ones (3.93±0.27 ng/mL). Cats in study group had higher serum DS levels (27.20±6.62 ng/mL) than control cats (16.79±5.21 ng/mL). This study reports serum S-GAG and DS data in cats with non-obstructed LUTD and in healthy cats for the first time.

Keywords: *Biomarker, Cat, Dermatan sulphate, Lower urinary tract dysfunction, Sulphated glycosaminoglycan*

Tıkanıklık Olmayan Aşağı Üriner Sistem Disfonksiyonu Olan Kedilerde Felin Spesifik Serum Sulfürlü Glikozaminoglikan ve Dermatan Sülfat Seviyelerinin Değerlendirilmesi

Öz

Alt üriner sistem disfonksiyonu (AÜSD) kedilerde yaygın olarak görülen bir sorundur. Altta yatan belirli bir nedeni olmayan bu kronik durum, etkili tedaviye ulaşmak için bir zorluk olmaya devam etmektedir. Glikozaminoglikanlar (GAG'lar), AÜSD'nun patogenezinde rol oynadığı düşünülen karakteristik tekrarlanan disakkarit sekanslarına sahip doğrusal polisakkaritlerdir. Bu çalışmanın amacını, tıkanıklık olmayan AÜSD gösteren kedilerde, kedilere özgü serum sülfatlanmış glikozaminoglikan (S-GAG) ve dermatan sülfat (DS) düzeylerinin sağlıklı kontrollere göre karşılaştırılması oluşturmuştur. Bu vaka kontrol çalışmasında, tıkanıklık olmayan AÜSD'dan mustarip, sahipli on sekiz kedi ile sahipli 16 adet sağlıklı kedi yer almıştır. Hem çalışma (tıkanıklık olmayan AÜSD kediler) hem de kontrol (sağlıklı kediler) grubundaki kedilerden alınan tedavi öncesi serum örnekleri, kedilere özgü S-GAG ve DS kitleri kullanılarak "Kantitatif Sandviç ELISA yöntemi" ile analiz edilmiştir. Çalışma ve kontrol gruplarına ait tüm kediler ile, çalışma ve kontrol grubundaki erkek kediler ve her iki gruptaki sterilize edilmiş kedilerin ortalama serum S-GAG ve DS seviyeleri karşılaştırılmıştır. Çalışma grubunun serum S-GAG konsantrasyonları (3.52±0.26 ng/mL) kontrol grubuna kıyasla daha düşük (3.93±0.27 ng/mL) bulunmuştur. Tersine çalışma grubu serum DS seviyeleri ise (27.20±6.62 ng/mL) kontrol grubuna (16.79±5.21 ng/mL) oranla yüksek bulunmuştur. Bu çalışma, tıkanma olmayan AÜSD'si kedilerde ve sağlıklı kedilerde ilk kez serum S-GAG ve DS verilerini bildirmektedir.

Anahtar sözcükler: *Alt üriner sistem disfonksiyonu, Biyobelirteç, Kedi, Dermatan sülfat, Sülfürlenmiş glikozaminoglikan*

How to cite this article?

Pekmezci D, Ciftci G, Ozcan U, Meral Y, Dalgin D: Evaluation of feline-specific serum sulphated glycosaminoglycan and dermatan sulphate levels in cats with non-obstructive lower urinary tract dysfunction. *Kafkas Univ Vet Fak Derg,* 27 (3): 331-337, 2021.
DOI: 10.9775/kvfd.2021.25375

(*) Corresponding Author

Tel: +90 362 312 1919, Cellular phone: +90 505 477 9524
E-mail: dkazanci@omu.edu.tr (D. Pekmezci)

Introduction

Feline lower urinary tract dysfunction (FLUTD) with a subset of problems, such as haematuria, periuria, pollakiuria, and stranguria, is a commonly seen problem in cats. It may occur as acute or chronic and can result from various abnormalities within the lumen of the lower urinary tract (local, external abnormalities) or other organ systems (internal abnormalities) that lead to dysfunction [1]. Various known aetiologies for FLUTD include bladder stones, bacterial and viral infections, urethral plugs, and neoplasia. However, bacterial infections associated with urinary system rarely seen in cats [2]. Urethral plugs associated with mucous-based sludge within the bladder are commonly seen as causative agents [3,4].

The terms "feline interstitial cystitis" or "feline idiopathic cystitis (FIC)" have been described for referring to the chronic conditions with no specific underlying cause of FLUTD as a naturally occurring model of interstitial cystitis (IC) in women [5,6]. Recently, the term "Pandora syndrome" proposed for describing chronic, recurrent FLUTD signs in the presence of comorbid disorders, such as behavioural, dermatological, endocrine, or gastrointestinal disorders, until a more biologically appropriate term is accepted [1]. Moreover, many treatment models for the aforementioned challenging situations in cats still seek understanding of their aetiologies and new treatment options [7-9].

To date, research has been focussed on creating a successful FIC or non-obstructive FLUTD treatment protocol, especially models of treatment protocols for IC in women, while cats, llamas, and dogs present similar signs of IC [10]. Urothelial ulceration with mural inflammation and fibrosis without bacterial cystitis in cats are accepted as the most similar findings to human IC [11]. Male, middle-aged (≈2-7 years), overweight cats are found to be at risk for having FIC [12]. FIC and IC share many similarities; the only major difference between the two seems to be the gender distribution. However, recent data shows that males suffering from some forms of chronic prostatitis could also have IC [13]. Findings in the last decade suggest that damage to the urothelial GAG layer might be played role in IC pathophysiology [14,15]. Moreover, it is now well-known that normal bladder urothelium in humans is lined with a specific GAG, defined as GP-51 [16], that inhibits bacterial adherence and protects the urothelium from noxious urine constituents. Alterations in urine GAGs have been reported in urolithiasis [17], renal injury [18], and IC [19]. However, decreased amounts of urine GAGs have also been reported in cats with FIC [10] and Feline Urologic Syndrome [20].

Glycosaminoglycans (GAGs) are linear polysaccharides possessing characteristic repeated disaccharide sequences, thought to be involved in several immune, cancer, inflammatory, and degenerative diseases [21,22]. Chondroitin sulphate (CH), DS, heparin (H), heparan sulphate (HS), keratan sulphate (KS), and hyaluronan are the most common GAG structures that are important biological response modifiers by acting as stabilisers, cofactors, or coreceptors for growth factors, cytokines, and chemokines [23].

New discoveries of the biological properties of GAGs-such as signalling molecules in response to cellular damage, including wounding, infection, and tumorigenesis-make these mucopolysaccharides have been the subject of more studies [23]. Semi-synthetic GAGs, such as *N*-acetyl glucosamine [24-26] and Pentosan polysulfide sodium [2,9], are the most commonly used agents in treating cats with FIC. It is still unknown whether GAG deficiency (when it occurs) is the primary reason for IC in people or whether it is secondary to other bladder processes, such as inflammation [27]. Another important issue to be clarified is how urine GAG levels reflect the state of the urothelium [27]. Pereira et al.[20] affirmed that cats with FUS might also have a decreased concentration of circulating GAGs.

Therefore, the main purpose of this study is to elucidate this unsolved issue by comparing serum feline S-GAG and DS levels in cats with non-obstructive LUTD to healthy cats.

Material and Methods

Ethical Statement

The present study was also approved by the Ondokuz Mayis University Animal Experiments Local Ethics Committee (Approval no: 2017/05).

Patients

Thirty-four client-owned cats between 5 months and 13 years of age, any breed and either sex, brought to the Veterinary Teaching Hospital between June and December 2017 were enrolled in the current case-control study. Eighteen cats diagnosed with non-obstructive LUTD formed the study group. None of the 16 healthy cats that formed the control group had any clinical signs of non-obstructive LUTD or other diseases prior to the sampling. Cats having urinary tract infections, azotaemia, diabetes mellitus, or hyperthyroidism with any recently administered GAG were excluded from the study. Client consent forms were provided to owners for all cats enrolled in this study. Appropriate treatments for the cats diagnosed with non-obstructive LUTD were performed, according to their clinical symptoms and the aetiologies of their LUTDs.

Procedures

All cats enrolled in the present study underwent a standard physical examination by the same veterinarian at their first visit. An FLUTD evaluation chart modified from Meyer and

Bečvářová [8] was completed for the study group. At the time of admission to the Veterinary Teaching Hospital, venous blood was taken from the cephalic vein of all searched cats, with 2 mL evacuated into a plain additive tube with K_3 EDTA (7.5% 0.040 mL) and 5 mL into a vacutainer without anticoagulant, for biochemical analysis. The 5 mL sample was centrifuged at 3000 g for 10 min at room temperature. The serum samples were separated and stored at -80ºC until analysis. Complete Blood Count analysis was performed by a BC-5000 Vet Auto Hematology Analyzer Mindray, and results were recorded. Ultrasonographic examinations of the extended urine bladders of the study group cats was performed with a micro convex high-frequency 3.5-7.0 MHz transducer (MyLab30; Esaote Pie Medical). The existence of a urolith was investigated by presenting the twinkling artefact (TA) during the colour Doppler ultrasonography examinations [28]. Urine samples were collected by voiding the midstream or catheterisation of the study group at the time of initial presentation. Cybow Urine reagent strips were used for analysis of pH, blood, leukocyte, nitrite, protein, ascorbic acid, ketone, glucose, and specific gravity levels. Microscopic examination of the urine sediment was also done, looking for existing RBC, WBC, casts, and crystals. While detection of nitrite in urine is routinely used for bacterial cystitis [29], any of the collected urine samples were submitted for quantitative urine culture because of their nitrite-negative status in the urine reagent strip analyses.

Serum S-GAG and DS Determination

The thirty-four stored serum samples from the cats in the present study were measured by the Quantitative Sandwich ELISA method using Cat S-GAG and Cat DS ELISA kits (MyBioSource©, San Diego, CA, USA, Cat. No.: MBS9348264, MBS077381), following the manufacturer's instructions. All samples were later measured on a spectrophotometer (Digital and Analog Systems S.R.L.).

Statistical Analysis

Feline serum-specific S-GAG and DS levels were the analysed parameters. The datasets were analysed for normality using the Kolmogorov-Smirnov test. The quantitative data on feline serum S-GAG and DS levels was found to be normally distributed. The differences between the means of feline serum S-GAG and DS levels in the study group versus the control group, between the two sexes, and between neutered cats versus non-neutered cats were compared using the Student-t test. The Mann-Whitney U test was used for the variables that did not show normality. The significance level of all comparisons was considered when P values <0.05. Sample size was calculated using an additional software (Gpower 3.0.10). The main outcome of the study sample size was the incidence of non-obstructed LUTD cases. Eighteen cats in the study group are required to demonstrate a difference with 95% statistical confidence and a power of 80%.

Results

Thirty-four cats were enrolled in this case-control study. Eighteen of these cats were clinically diagnosed with non-obstructed LUTD. Sixteen were clinically healthy controls. The mean ages of the non-obstructed LUTD and the clinically healthy cats were 5.3 and 4 years, respectively. The mean weight of the study and control cats were 3.9 and 3.3 kg, respectively. Ten of the 34 (29.4%) cats were domestic, short-haired cats. Eight (23.5%) were mackerel tabby, 7 (20.5%) were orange tabby, 5 (14.7%) were Persians, and there was one Chinchilla (2.9%), Van (2.9%), British short-haired (2.9%), and Scottish Fold (2.9%) cat. Sixteen (88.8%) cats in the study group were neutered, and four cats in the control group were neutered (25%). The CBC results of all the searched cats were within the reference ranges [30]. All cats in the study group demonstrated perianal grooming behaviour to varying degrees, at their clinical scoring. None of the study cats showed a TA during the colour Doppler ultrasonography examination. Urobilinogen, glucose, bilirubin, ketone, and nitrite were all negative in the urine dipsticks of the cats with non-obstructed LUTD. Most of the cats with non-obstructed LUTD had a urine specific gravity (SG) >1035. There were only four study cats that had a urine specific gravity <1035. However, their serum creatinine and urea concentrations were within the reference intervals. The urine pH of the study group cats measured 5.5-8.0. Seven of the study cats (38.8%) had a 2+ or 3+ dipstick protein reaction. Twelve (66.6%) of the cats with non-obstructed LUTD had more than three white blood cells in their microscopic urine sediment examination. Only four (22.2%) cats in the study group also had more than three red blood cells per high-power field. Struvite crystals (ST) were the most prevalent type crystals found in the urine sediment of the study cats (44.4%). However, four of the study cats (22.2%) had Ca oxalate monohydrate (CaOXM) crystals in their urine sediment. Two cats (11.1%) had both ST and CaOXM crystals in their urine sediment. Only two cats (11.1%) in the study group had more than three transitional epithels (TE) per high-power field in their urine sediment. Renal epithels (RE) were not seen in any of the study group cats *(Table 1)*.

The mean serum S-GAG level in cats with non-obstructed LUTD (3.52±0.26 ng/mL) was lower than the healthy cats' level (3.93±0.27 ng/mL) *(Table 2)*, however were not significantly different between the groups (P>0.05) *(Fig. 1)*. The cats with non-obstructed LUTD had higher serum DS (27.20±6.62 ng/mL) levels than the control group (16.79±5.21 ng/mL) *(Table 2)*. This difference was also not statistically significant (P>0.05) *(Fig. 1)*. The mean S-GAG levels in the male cats with non-obstructed LUTD (3.69±0.26 ng/mL) were not statistically different (P>0.05) *(Table 2)* from the healthy male cats' levels (3.98±0.45 ng/mL) *(Fig 2)*. The mean DS levels in the male cats with non-obstructed LUTD (28.67±7.79 ng/mL) were also not statistically different (P>0.05) *(Table 2)* from the healthy male cats' levels

Table 1. *Results of the urinalysis of the cats with non-obstructed LUTD*

Parameter	Value	Non-obstructed LUTD Cats		Parameter	Value	Non-obstructed LUTD Cats	
		n (18)	Percentage (%)			n (18)	Percentage (%)
Urine colour	Normal Concentrated Haematuria	13 1 4	72.2 5.5 22.2	Ascorbic acid	Negative + ++ +++	9 3 6 0	50 16.6 33.3 0
Urobilinogen	Negative	18	100	sWBC	0-3/Hpf >3/Hpf	6 12	33.3 66.6
Glucose	Negative	18	100	sRBC	0-3/Hpf >3/Hpf	16 4	88.8 22.2
Bilirubin	Negative	18	100	sTE	0-3/Hpf >3/Hpf	15 3	83.3 16.6
Ketone	Negative	18	100	sRE	Negative	18	100
SG	>1.035 <1.035	14 4	77.7 22.2	sST	Negative + ++ +++	10 4 3 1	55.5 22.2 16.6 5.5
Blood	Negative + ++ +++	11 3 1 3	61.1 16.6 5.5 16.6	sCaOXM	Negative + ++ +++	14 3 0 1	77.7 16.6 0 5.5
pH	5.0-6.0 6.0-7.0 7.0-8.0	3 12 3	16.6 66.6 16.6	TA	Negative Positive	18 0	100 0
Protein	Negative + ++ +++	11 0 4 3	61.1 0 22.2 16.6	Bladder Uroliths	Negative	18	100
Leukocyte	Negative + ++ +++	0 5 2 11	0 27.7 11.1 61.1	Perianal Grooming	Negative + ++ +++	0 12 4 2	0 66.6 22.2 11.1
Nitrite	Negative	18	100				

sWBC: *White Blood Cells in the high-power field,* ***sRBC:*** *Red Blood Cells in the high-power field,* ***sTE:*** *Transitional epithels in the high-power field,* ***sRE:*** *Renal epithels in the high-power field,* ***sST:*** *Struvite crystals in the high-power field,* ***sCaOXM:*** *Ca oxalate monohydrate crystals in the high-power field*

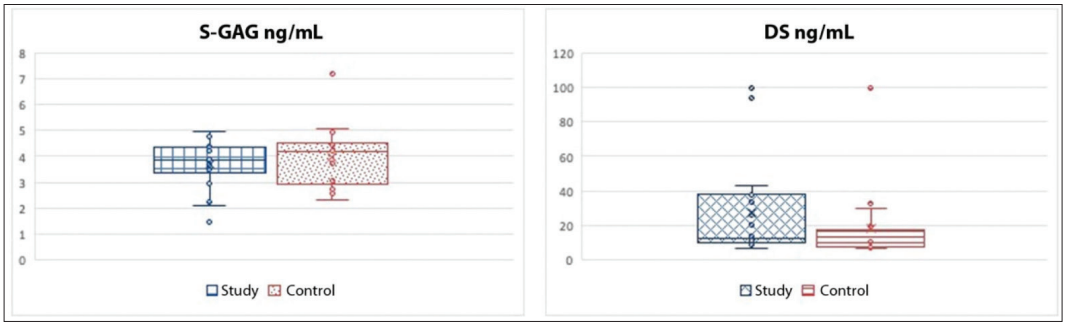

Fig 1. Box-and-whiskers plot of serum S-GAG and DS values in study (blue boxes) or control (red boxes) groups. The box incorporates the middle 50% of observation; the bottom of the box is the first quartile (25th percentile) and the top of the box is the third quartile (75th percentile). The horizontal line in the middle of the box is the median (50th percentile). The cross within each box represents the mean value. The whiskers extend to the smallest and largest observations that are 1.5 times removed from the interquartile range are plotted separately as dots

(23.14±9.07 ng/mL) *(Fig. 2)*. The mean serum S-GAG levels in neutered cats with non-obstructed LUTD (3.56±0.28 ng/mL) and in neutered control cats (3.53±0.23 ng/mL) *(Table 2)* were not significantly different (P>0.05) *(Fig. 3)*. Neutered cats with non-obstructed LUTD had higher serum DS levels (23.66±5.65 ng/mL) than the neutered control group (13.29±2.63 ng/mL) *(Table 2)*. However, this difference was not statistically significant (P>0.05) *(Fig. 3)*.

Discussion

The pioneer study conducted by Pereira et al.[20] provided the inspiration for the study. Pereira et al.[20] hypothesised that cats with low GAG levels in urologic syndrome might have damaged bladder surfaces and might also have a decreased concentration of circulating GAGs. We aimed to investigate Pereira et al.'s [20] results by comparing serum

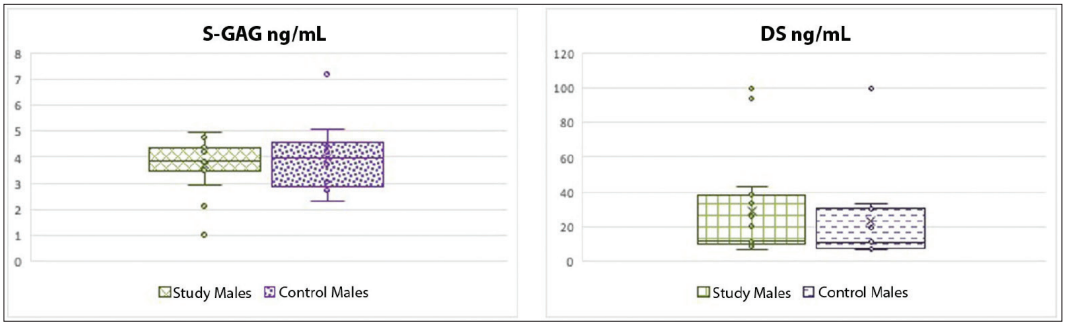

Fig 2. Box-and-whiskers plot of serum S-GAG and DS values in study male cats (green) or control male cats (purple). The box incorporates the middle 50% of observation; the bottom of the box is the first quartile (25th percentile) and the top of the box is the third quartile (75th percentile). The horizontal line in the middle of the box is the median (50th percentile). The cross within each box represents the mean value. The whiskers extend to the smallest and largest observations that are 1.5 times removed from the interquartile range are plotted separately as dots

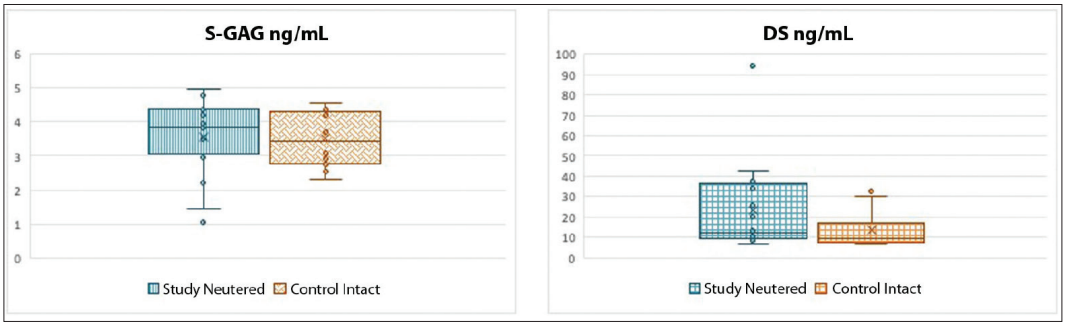

Fig 3. Box-and-whiskers plot of serum S-GAG and DS values in neutered cats in study group (turquoise) or intact control cats (orange). The box incorporates the middle 50% of observation; the bottom of the box is the first quartile (25th percentile) and the top of the box is the third quartile (75th percentile). The horizontal line in the middle of the box is the median (50th percentile). The cross within each box represents the mean value. The whiskers extend to the smallest and largest observations that are 1.5 times removed from the interquartile range are plotted separately as dots

Table 2. *Mean S-GAG and DS levels (ng/mL) of the Study and Control cats*

Parameters	Groups		P Value
	Study Cats	Control Cats	
Mean±S.E. S-GAG levels (ng/mL)	3.52±0.26	3.93±0.27	0.293
Mean ± S.E. DS levels (ng/mL)	27.20±6.62	16.79±5.21	0.226
	Study Male Cats	**Control Male Cats**	
Mean ± S.E. S-GAG levels (ng/mL)	3.69±0.26	3.98±0.45	0.554
Mean ± S.E. DS levels (ng/mL)	28.67±7.79	23.14±9.07	0.652
	Study Neutered Cats	**Control Neutered Cats**	
Mean ± S.E. S-GAG levels (ng/mL)	3.56±0.28	3.53±0.23	0.930
Mean ± S.E. DS levels (ng/mL)	23.66±5.65	13.29±2.63	0.148

feline S-GAGs and DS levels in cats with non-obstructive LUTD against healthy controls.

Interestingly, the main finding of the study presented here was an unexpected result. Contrary to the results found by Pereira et al.[20] our results showed that feline pre-treatment serum S-GAG and DS levels in cats with non-obstructed LUTD versus did not differ from the levels in the healthy controls. Research about FIC treatments showed that these cats have decreased levels of urine GAGs [20,31],

and treatment options are mainly aimed at replacing this deficiency by using semi-synthetic GAGs with various routes [2,7,9,24,26]. However, all these study results were not able to show the beneficial result of decreasing the recurrence rate, with amelioration of the clinical signs, by using semi-synthetic GAGs in FIC patients. Therefore, circulating GAG levels in FIC, both in cats with LUTD and their relations among the disease processes, has to be investigated, to determine an accurate treatment protocol.

To our knowledge after Pereira et al.[20], there was only one study that presents plasma GAG concentrations in FIC patients [25].

In the study presented here, we used feline-specific ELISA kits, rather than human kits. Therefore, our results first demonstrate the pre-treatment serum S-GAGs and DS levels in cats with non-obstructed LUTD against healthy controls. Our mean serum S-GAG level (3.52±0.26 ng/mL) in cats with non-obstructed LUTD was found to be lower than in healthy controls (3.93±0.27 ng/mL), but a statistically significant difference between groups was not found (P>0.05).

The DS level was the other investigated parameter in our study. Pereira et al.[20] showed that the main GAGs found in a cat's kidney and urinary tract was HS and DS. They also found that, in contrast to other GAGs, CS was the only GAG detected in the plasma of cats having urologic syndrome. Contrary to Pereira et al.[20], DS was measured in the cats' serum in the present study. Moreover, in the present study, cats with non-obstructed LUTD had higher serum DS levels (27.20±6.62 ng/mL) than the control group (16.79±5.21 ng/mL), but again this difference was not found to be statistically significant (P>0.05).

The trend of increased mean DS levels in the study group may be explained by the relationship between DS, chemokines, and cytokines. Recently, Parys et al.[32] investigated serum cytokine profiling in cats with acute FIC and found that serum concentrations of the pro-inflammatory cytokines and chemokines CXCL12, IL-12, IL-18, and Flt3L were increased in FIC-affected cats. Moreover, Brooks et al.[33] showed that Interferon gamma also binds to DS. IL-8, MIP-1α, and β (macrophage inflammatory peptides), and monocyte chemoattractant protein-1 (MCP-1) are the proteins that are able to bind to GAGs [23].

Therefore, pro-inflammatory processes in cats with non-obstructed LUTD may also increase some cytokines and chemokines, which later may have led to an increase in circulating DS in our non-obstructed LUTD cats.

The mean S-GAG levels in the male cats with non-obstructed LUTD were not statistically different from the healthy male cats' levels (3.69±0.26 ng/mL and 3.98±0.45 ng/mL, respectively). In the same vein, mean DS levels in the male cats with non-obstructed LUTD (28.67±7.79 ng/mL) were also not statistically differentiated (P>0.05), when compared to healthy male cats' levels (23.14±9.07 ng/mL). Also, no difference was found when comparing mean S-GAGs and DS levels between the neutered cats in both groups. However, the trend of increasing mean DS levels remained in the neutered cats with non-obstructed LUTD.

The studies investigating the relationship between GAGs in FIC and LUTD in cats mainly reported decreased urine or plasma GAGs. Therefore, one could expect a decreased concentration of circulating GAGs in this study's cats. In one study that evaluates the changes in total serum GAG levels in patients undergoing renal transplantation showed that measuring total serum GAG levels is more credible than measuring urinary GAG levels, since urine output may be compromised and does not accurately reflect the concentration of circulating GAGs, especially in patients with graft rejection [22]. This scenario may be valid for cats with FIC and LUTD.

However, our results showed that there were no differences of serum GAG levels between cats with non-obstructed LUTD and healthy cats. The main reason for this could be the duration of the disease. The cats in this study had their first LUTD diagnosis during their visits to the Veterinary Teaching Hospital. Contrary FIC the span of the inflammation could be the most important cause that may affect the circulating GAGs levels in non-obstructed LUTD in cats. Hence, a main limitation of the present study is that it was missing FIC patients. Further studies to confirm the suspected role of GAGs and their individual circulating levels in FIC and FLUTD are needed.

In conclusion, this study reports serum S-GAGs and DS levels in cats with non-obstructed LUTD against healthy cats. We believe that our findings may help develop a better understanding of the pathophysiology of FLUTD and FIC and the development of new treatment strategies.

Acknowledgements

The authors are especially thankful to Prof. Dr. Filiz Akdag for performing the statistical analyses of this study. We are appreciated to our clients for their special effort and thank to all of them for allowing their lovely cats to the present study.

Conflict of Interest

The authors declared no potential conflicts of interest with respect to the research, authorship, and/or publication of this article.

Author Contributions

DP coordinated the study and drafted the manuscript. DP also participated in the collection and preparation of samples and participated in the design of the study. GC

carried out the out the immunoassays and participated in the design of the study. UO, YM and DD participated in the collection and preparation samples and all participated in the design of the study. All authors also approved the final version of the article.

References

1. Westropp JL, Delgado M, Buffington CAT: Chronic lower urinary tract signs in cats: Current understanding of pathophysiology and management. *Vet Clin North Am Small Anim Pract,* 49 (2): 187-209, 2019. DOI: 10.1016/j.cvsm.2018.11.001

2. Wallius BM, Tidholm AE: Use of pentosan polysulphate in cats with idiopathic, non-obstructive lower urinary tract disease: A double-blind, randomised, placebo-controlled trial. *J Feline Med Surg*, 11 (6): 409-412, 2009. DOI: 10.1016/j.jfms.2008.09.003

3. Labato MA, Acierno MJ: Urology, An Issue of Veterinary Clinics of North America: Small Animal Practice. Volume 49-2, 125-324, Elsevier, USA, 2019.

4. Nivy R, Segev G, Rimer D, Bruchim Y, Aroch I, Mazaki-Tovi M: A prospective randomized study of efficacy of 2 treatment protocols in preventing recurrence of clinical signs in 51 male cats with obstructive idiopathic cystitis. *J Vet Intern Med*, 33 (5): 2117-2123, 2019. DOI: 10.1111/jvim.15594

5. Buffington CAT, Chew DJ, Woodworth BE: Feline interstitial cystitis. *J Am Vet Med Assoc*, 215 (5): 682-687, 1999.

6. Naarden B, Corbee RJ: The effect of a therapeutic urinary stress diet on the short-term recurrence of feline idiopathic cystitis. *Vet Med Sci*, 6 (1): 32-38, 2020. DOI: 10.1002/vms3.197

7. Bradley AM, Lappin MR: Intravesical glycosaminoglycans for obstructive feline idiopathic cystitis: A pilot study. *J Feline Med Surg*, 16 (6): 504-506, 2014. DOI: 10.1177/1098612X13510918

8. Meyer HP, Bečvářová I: Effects of a urinary food supplemented with milk protein hydrolysate and L-tryptophan on feline idiopathic cystitis – Results of a case series in 10 cats. *Intern J Appl Res Vet Med*, 14 (1): 59-65, 2016.

9. Delille M, Frohlich L, Muller RS, Hartman K, Dorsch R: Efficacy of intravesical pentosan polysulfate sodium in cats with obstructive feline idiopathic cystitis. *J Feline Med Surg*, 18 (6): 492-500, 2016. DOI: 10.1177/1098612X15588934

10. Buffington CAT, Blaisdell JL, Binns SP, Woodworth BE: Decreased urine glycosaminoglycan excretion in cats with interstitial cystitis. *J Urol*, 155 (5): 1801-1804, 1996. DOI: 10.1016/S0022-5347(01)66201-3

11. Lavelle JP, Meyers SA, Ruiz WG, Buffington CAT, Zeidel ML, Apodaca G: Urothelial pathophysiological changes in feline interstitial cystitis: A human model. *Am J Physiol Renal Physiol*, 278 (4): F540-F553, 2000. DOI: 10.1152/ajprenal.2000.278.4.F540

12. Sparkes A: Understanding feline idiopathic cystitis. *In Practice*, 40 (3): 95-101, 2018. DOI: 10.1136/inp.k435

13. Berger RE, Miller JE, Rothman I, Rothman I, Krieger JN, Muller CH: Bladder petechiae after cystoscopy and hydrodistension in men diagnosed with prostate pain. *J Urol*, 159 (1): 83-85, 1998. DOI: 10.1016/S0022-5347(01)64018-7

14. Morales A, Emerson L, Nickel JC, Lundie M: Intravesical hyaluronic acid in the treatment of refractory interstitial cystitis. *J Urol*, 156 (1): 45-48, 1996. DOI: 10.1016/S0022-5347(01)65933-0

15. Parsons CL: Epithelial coating techniques in the treatment of interstitial cystitis. *Urology*, 49 (5): 100-104, 1997. DOI: 10.1016/S0090-4295(97)00180-5

16. Shupp-Byrne DE, Sedor JF, Soroush M, McCue PA, Mulholland SG: Interaction of bladder glycoprotein GP51 with uropathogenic bacteria. *J Urol*, 165 (4): 1342-1346, 2001. DOI: 10.1016/S0022-5347(01)69896-3

17. Dissayabutra T, Kalpongnukul N, Chindaphan K, Srisa-Art M, Ungjaroenwathana W, Kaewwongse M, Lampenkhae K, Tosukhowong P: Urinary sulfated glycosaminoglycan insufficiency and chondroitin sulfate supplement in urolithiasis. *PloS One*, 14 (3): e0213180, 2019. DOI: 10.1371/journal.pone.0213180

18. Schmidt EP, Yang Y, Janssen WJ, Gandjeva A, Perez MJ, Barthel L, Zemans RL, Bowman JC, Koyanagi DE, Yunt ZX, Smith LP, Cheng SS, Overdier KH, Thompson KR, Geraci MW, Douglas IS, Pearse DB, Tuder RM: The pulmonary endothelial glycocalyx regulates neutrophil adhesion and lung injury during experimental sepsis. *Nat Med,* 18, 1217–1223, 2012. DOI: 10.1038/nm.2843

19. Lucon M, Martins JR, Leite KRM, Soler R, Nader HB, Srougi M, Bruschini H: Evaluation of the metabolism of glycosaminoglycans in patients with interstitial cystis. *Int Braz J Urol*, 40 (1): 72-79, 2014. DOI: 10.1590/S1677-5538.IBJU.2014.01.11

20. Pereira DA, Aguiar JAK, Hagiwara MK, Michelacci YM: Changes in cat urinary glycosaminoglycans with age and in feline urologic syndrome. *Biochim Biophys Acta Gen Subj*, 1672 (1): 1-11, 2004. DOI: 10.1016/j.bbagen.2004.02.002

21. Laurent TC, Laurent UBG, Fraser JER: Serum hyaluronan as a disease marker. *Ann Med*, 28 (3): 241-253, 1996. DOI: 10.3109/07853899609033126

22. Papaioannou EG, Magkou C, Kostakis A, Staikou C, Mitsoula P, Kyriakides S, Sitaras NM: Changes in total serum glycosaminoglycan levels in patients undergoing renal transplantation: Preliminary data. *Surg Today*, 34, 668-672, 2004. DOI: 10.1007/s00595-004-2795-4

23. Trowbridge JM, Gallo RL: Dermatan sulfate: New functions from an old glycosaminoglycan. *Glycobiology*, 12 (9): 117R-125R, 2002. DOI: 10.1093/glycob/cwf066

24. Gunn-Moore DA, Shenoy CM: Oral glucosamine and the management of feline idiopathic cystitis. *J Feline Med Surg*, 6 (4): 219-225, 2004. DOI: 10.1016/j.jfms.2003.09.007

25. Panchaphanpong J, Asawakarn T, Pusoonthornthum R: Effects of oral administration of *N*- acetyl-D-glucosamine on plasma and urine concentrations of glycosaminoglycans in cats with idiopathic cystitis. *Am J Vet Res*, 72 (6): 843-850, 2011. DOI: 10.2460/ajvr.72.6.843

26. Veir JK, Webb CB, Lappin MR: Systemic effects of a commercial preparation of chondroitin sulfate, hyaluronic acid and N acetyl-D-glucosamine when administered parenterally to healthy cats. *Intern J Appl Res Vet Med*, 11 (2): 91-95, 2013.

27. Wilkinson DR, Erickson DR: Urinary and serologic markers for interstitial cystitis: An update. *Curr Urol Rep*, 7 (5): 414-422, 2006.

28. Griffin S: Feline abdominal ultrasonography: what's normal? what's abnormal? The kidneys and perinephric space. *J Feline Med Surg*, 22 (5): 409-427, 2020. DOI: 10.1177/1098612X20917598

29. Lundberg JON, Carlsson S, Engstrand L, Morcos E, Wiklund NP, Weitzberg E: Urinary nitrite: More than a marker of infection. *Urology*, 50 (2): 189-191, 1997. DOI: 10.1016/S0090-4295(97)00257-4

30. Norsworthy GD, Restine LM, Romeo A: Normal Laboratory Values. **In,** Norsworthy GD (Ed): The Feline Patient. 5th ed., John Wiley & Sons, 2018.

31. Buffington CAT, Chew DJ, DiBartola SP: Interstitial cystitis in cats. *Vet Clin North Am Small Anim Pract*, 26 (2): 317-326, 1996. DOI: 10.1016/S0195-5616(96)50212-3

32. Parys M, Yuzbasiyan-Gurkan V, Kruger JM: Serum cytokine profiling in cats with acute idiopathic cystitis. *J Vet Intern Med*, 32 (1): 274-279, 2018. DOI: 10.1111/jvim.15032

33. Brooks B, Briggs DM, Eastmond NC, Fernig DG, Coleman JW: Presentation of IFN-gamma to nitric oxide-producing cells: A novel function for mast cells. *J Immunol*, 164 (2): 573-579, 2000. DOI: 10.4049/jimmunol.164.2.573

Kafkas Universitesi Veteriner Fakultesi Dergisi
ISSN: 1300-6045 e-ISSN: 1309-2251
Journal Home-Page: http://vetdergikafkas.org

Kafkas Univ Vet Fak Derg
27 (3): 339-346, 2021
DOI: 10.9775/kvfd.2021.25439

RESEARCH ARTICLE

Does Umbelliferone Protect Primary Cortical Neuron Cells Against Glutamate Excitotoxicity? [1]

Alper Kürşat DEMİRKAYA [1,a] Gülşah GÜNDOĞDU [2,b (*)] Songül KARAKAYA [3,c]
Şeymanur YILMAZ TAŞCI [4,d] Kemal Alp NALCI [5,e] Ahmet HACIMÜFTÜOĞLU [6,f]

[1] *This study was presented as poster presentation at "Turkish Society of Physiological Sciences 45th National Physiology Congress 31 October-03 November 2019 Kuşadası, Aydın, Turkey" and, it was published as a meeting abstract at the Acta Physiol, 227:722, 70, 2019.*

[1] Bilecik Seyh Edebali University, Vocational School, Food Processing Department, TR-11230 Bilecik - TURKEY
[2] Pamukkale University, Faculty of Medicine, Department of Physiology, TR-20070 Denizli - TURKEY
[3] Ataturk University, Faculty of Pharmacy, Department of Pharmacognosy, TR-25240 Erzurum - TURKEY
[4] Ataturk University, Faculty of Medicine, Department of Physiology, TR-25240 Erzurum - TURKEY
[5] Yuzuncu Yıl University, Faculty of Pharmacy, Department of Pharmacy, TR-65090 Van - TURKEY
[6] Ataturk University, Faculty of Medicine, Department of Medical Pharmacy, TR-25240 Erzurum - TURKEY
ORCIDs: [a] 0000-0002-7994-7832; [b] 0000-0002-9924-5176; [c] 0000-0002-3268-721X; [d] 0000-0003-2510-743X; [e] 0000-0003-3786-5246
[f] 0000-0002-9658-3313

Article ID: KVFD-2021-25439 Received: 21.01.2021 Accepted: 11.05.2021 Published Online: 17.05.2021

Abstract

Glutamate is the major excitatory neurotransmitter in the central nervous system. Excessive glutamate is known to cause excitotoxicity. Umbelliferone is a coumarin derivative compound and has antioxidant, anti-inflammatory, and neuroprotective effects. Also, umbelliferone can show neuroprotective effect by crossing the blood-brain barrier. In our study, it was aimed to investigate the neuroprotective effect of umbelliferone on primary cortical neuron (PCN) culture. Umbelliferone was isolated from the roots of *Ferulago cassia* dichloromethane sub-extract. The cerebral cortex of newborn Sprague Dawley rats was used to obtain PCNs. To stimulate glutamate excitotoxicity, cells were exposed to $6x10^{-5}$M glutamate. Then different concentrations (10-1000 µM) of umbelliferone were added into the medium and allowed to incubate for 24 and 72 h. MTT assay was used to measure cell viability. Total Antioxidant Status (TAS) and Total Oxidant Status (TOS) analyzes were used to evaluate reactive oxygen species. MTT results showed that cell viability was decreased with glutamate application. 25-250 µM umbelliferone had a significant protective effect against glutamate excitotoxicity at 72 h ($P<0.05$). Consistent with MTT results, TAS analysis results showed 50-250 µM umbelliferone increase the level of antioxidants in cells, which can help protect neurons against glutamate-induced excitotoxicity. In this study, umbelliferone showed a neuroprotective effect in PCN against glutamate excitotoxicity. These results suggest that umbelliferone may be used as therapeutic agent against glutamate excitotoxicity.

Keywords: *Glutamate, Ferulago, Primary cortical neuron culture, Umbelliferone*

Umbelliferon, Glutamat Eksitotoksisitesine Karşı Primer Kortikal Nöron Hücrelerini Korur mu?

Öz

Glutamat merkezi sinir sisteminin ana uyarıcı nörotransmitteridir. Aşırı glutamatın, glutamat reseptörlerinin uzun süreli aktivasyonu nedeniyle eksitotoksisiteye neden olduğu bilinmektedir. Umbelliferon, antioksidan, antiinflamatuar ve nöroprotektif etkilere sahip kumarin türevi bir bileşiktir. Ayrıca, umbelliferon kan beyin bariyerini geçerek nöronal hücreleri ölümden koruyabilmektedir. Bu çalışmada glutamat eksitotoksisitesine maruz bırakılan primer kortikal nöron (PCN) kültürlerinde umbelliferonun nöroprotektif etkisinin araştırılması amaçlanmaktadır. Umbelliferon, *Ferulago cassia* diklorometan alt ekstraktının köklerinden izole edildi. PCN'ler yenidoğan Sprague Dawley cinsi sıçanların serebral korteklerinden elde edilmiştir. Glutamat eksitotoksistesi oluşturmak için hücreler $6x10^{-5}$ M glutamata maruz bırakıldı. Daha sonra hücrelere farklı konsantrasyonlarda (10-1000 µM) umbelliferon uygulanarak 24 ve 72 saat inkübasyona bırakıldı. Hücre canlılık oranı MTT yöntemi ile belirlendi. Hücrelerde oluşan reaktif oksijen türleri Total oxidant status (TOS) ve Total antioxidant status (TAS) yöntemleri ile değerlendirildi. MTT analiz sonuçlarına göre, glutamat uygulaması ile hücre canlılığının azaldığı görüldü. 72. saatte 25-250 µM umbelliferonun glutamat eksitotoksisitesine karşı nöronlarda anlamlı düzeyde koruyucu etkiye sahip olduğu tespit edildi ($P<0.05$). MTT sonuçlarıyla tutarlı olarak TAS analizi sonuçları, 50-250 umbelliferonun hücrelerdeki antioksidan düzeyini artırdığını ve bu da nöronların glutamata bağlı eksitotoksisiteye karşı korunmasına yardımcı olabileceğini gösterdi. Bu çalışmada umbelliferon, PCN hücrelerinde glutamat eksitotoksisitesine karşı nöroprotektif bir etki göstermiştir. Bu sonuçlar ile umbelliferonun glutamat eksitotoksisitesine karşı terapötik bir ajan olarak kullanılabileceği sonucuna varıldı.

Anahtar sözcükler: *Glutamat, Ferulago, Primer kortikal nöron kültürü, Umbelliferon*

How to cite this article?

Demirkaya AK, Gündoğdu G, Karakaya S, Yılmaz Taşcı Ş, Nalcı KA, Hacimüftüoğlu A: Does umbelliferone protect primary cortical neuron cells against glutamate excitotoxicity? *Kafkas Univ Vet Fak Derg,* 27 (3): 339-346, 2021.
DOI: 10.9775/kvfd.2021.25439

(*) **Corresponding Author**

Tel: +90 258 296 1699
E-mail: gdemirkaya81@gmail.com (G. Gündoğdu)

Introduction

Glutamate, is a major excitatory neurotransmitter in the central nervous system. It is important in various physiological processes such as learning, memory, synaptic plasticity, and other cognitive functions [1,2]. Most excitatory neurons in the central nervous system are glutamatergic, more than 50% use glutamate as a neurotransmitter [3,4]. Glutamate shows its effect on the postsynaptic cell surface by stimulating its ionotropic and metabotropic receptors. Thus, it is resulted with action potential by depolarizing the cell membrane [5]. Glutamate is present in millimolar concentrations in the mammalian central nervous system [6]. Glutamate can not cross the blood-brain barrier, as it is all the glutamate present in the central nervous system (CNS) are produced here. Glutamate is synthesized from glutamine by glutaminase in presynaptic neurons or α-ketoglutarate by glutamate dehydrogenase enzyme. The synthesized glutamate is taken into vesicles by the vesicular transporter. After then, they are lead to an increase in glutamate concentration by excreting their contents into the synapse cavity by exocytosis in response to presynaptic depolarization [7,8]. Glutamate concentration in the synaptic cleft is increased by synaptic activity, but extracellular glutamate concentration is protected by glutamate uptake by glutamate transporter [9,10]. Hence, unused glutamate during synaptic transmission must be cleared from the extracellular space, rapidly. Glutamate clearance is achieved by astrocytes and is mediated by glutamate uptake transporters [11]. Although glutamate plays an important role in brain functions, its high concentration in CNS causes the neurotoxic effect [12]. The excessive increase of glutamate leads to prolonged activation of glutamate receptors and leads to excito-toxicity due to intracellular overload of Ca^{2+}. This state plays an important role in neurodegeneration, protease activation, mitochondrial dysfunction. Moreover, the reactive oxygen species (ROS) are increased with excessive intracellular Ca^{2+} concentration and, neuronal cell death occurs [13]. Glutamate-induced toxicity plays an important role in the pathogenesis of various neurodegenerative diseases such as amyotrophic lateral sclerosis, Alzheimer's Disease (AD), Huntington's Disease, Parkinson's Disease [14,15]. One of the important factors that cause neuronal cell death in neuropathological processes is oxidative stress [12,16]. AD arises from the accumulation of α and β plaques and tau protein hyperphosphorylation in neurons plays role in pathogenesis. The most important reason is thought of as the development of oxidative stress due to the generation of ROS [17]. The excessive glutamate concentration causes oxidative stress by inhibiting glutathione synthesis and leading to increased ROS production [12,16]. Therefore, therapeutic approach for neurodegenerative diseases may be protection of neuronal cells against glutamate-induced excitotoxicity [12]. Treatment with plants is a traditional process for the improvement of modern medicine from ancient times [18,19]. The use of herbal medicines is increasing worldwide, and although they have some negative effects, consumers believe that traditional herbal medicines are safe [20]. Since it is thought that plant origin compounds are effective in the treatment of many diseases and in reducing the prognosis, effective compounds obtained from plants by various methods have gained importance today. However, these compounds can be used as active substances in the preparation of drugs, and preclinical studies should be done initially.

Umbelliferone, a member of coumarin derivatives, is found in fruits, vegetables, and herbs such as citrus fruits and golden apples. It is a compound with antioxidant and free radical scavenging properties [21]. Umbelliferone is widely consumed by humans as a medicine and dietary supplement [22]. It has been shown that it can be used safely and effectively in the diet and is not toxic at low doses [23]. It has also been shown to have a neuroprotective effect in the study conducted with the experimental Parkinson's Disease model [24]. Also, an important property of umbelliferone is that it can cross the blood-brain barrier [25]. In recent years, because coumarins have an anti-neurodegenerative disease potential, the search for medicinal plants that can be used in the isolation of coumarins has become the focus of researchers as they are natural sources of coumarins [26]. Therefore, it can be considered that umbelliferone has a protective potential in neurodegenerative diseases. The various studies showed that umbelliferone, is a plant-derived coumarin derivative, has anticancer, antitumoral, anti-inflammatory, neuroprotective, and antioxidant effects [27-29]. However, the neuroprotective effect of umbelliferone against glutamate excitotoxicity is unknown. Therefore, in our study, we aimed to investigate the neuroprotective effect of umbelliferone isolated from *Ferulago cassia Boiss* (Apiaceae) dichloromethane sub-extract in PCN cultures exposed to glutamate excitotoxicity.

Material and Methods

Ethical Statement

This study was approved by Atatürk University Local Animal Experiments Ethics Committee with the work permit dated 28.03.2019 and numbered (93722986-000-E.1900094667) and was carried out in the cell culture laboratory of the Medical Pharmacology Department in the Atatürk University Faculty of Medicine.

Reagents

In this study, Neurobasal medium (NBM), fetal bovine serum (FBS) (Gibco, USA), B-27, Penicillin/Streptomycin-Amphotericin B (Thermo Fisher, Germany), dimethylsulfoxide (DMSO) (Roche) (Santa Cruz), sterile culture dishes (Petri), 96-well cell culture plate (Greiner), MTT kits (Cayman

Chemical, Ann Arbor, MI, USA) ve Hanks'Balanced Salt solution (HBSS), Trypsin-Ethylenediaminetetraacetic acid (EDTA) (Sigma Aldrich®, ABD) were used. Umbelliferone was isolated from the roots of *Ferulago cassia* dichloromethane sub-extract.

Plant Material, Extraction, and Purification of Umbelliferone

Plant material of *Ferulago cassia* extraction and purification of umbelliferone were obtained using the method described via Karakaya et al.[30] 200 g dried powdered root was used and 12.32 g dichloromethane sub-extract was obtained. Eluting with Hexane: Ethyl acetate over silica gel column gave known compound umbelliferone (215 mg).

Preparation of Primary Cortical Neuron Culture

In this study, the cortex neurons, which were obtained from a newborn Sprague-Dawley rat that did not complete 24 h, were used. Twenty rat cubs were quickly decapitated and, their brain cortexes were removed. The extracted brain cortexes were transferred to 5 mL of Hanks' Balanced Salt Solution (HBSS) and macro-fragments were performed in a petri dish with the help of a double scalpel. The crushed cortices were taken into DMEM solution. Then, ¼ ratio trypsin-ethylenediaminetetraacetic acid (EDTA) (0.25% trypsin-0.02% EDTA) was added and micro-fragmented. The cells were centrifuged 3 times at 1200 rpm for 5 min and the upper medium was changed each time. Culture medium containing 88% NBM, 10% FBS, 2% B-27 and 0.1% antibiotics (penicillin-streptomycin-amphotericin B) was added on the precipitated pure neuronal cells. And then, cells were added to 96-well polylysine coated plates at a concentration of 1×10^5 per well. The cells were incubated for 10 days (37°C and 5% CO_2) by changing the medium for 3 days intervals for branching.

Exposure of Glutamate Excitotoxicity and Treatment with Various Concentration of Umbelliferone

$6x10^{-5}$ M concentration of glutamate was applied to the culture medium to induce glutamate excitotoxicity. Then, various concentrations of umbelliferone (10-1000 µM) were applied to the medium and allowed to incubate for 24 and 72 h. After the incubation period, 3- (4,5-dimethylthiazol-2-yl)-2,5-diphenyltetrazolium bromide, cell viability (cytotoxicity status) was evaluated by yellow tetrazole (MTT) assay.

MTT Analysis

The MTT analysis method is used for determination of cytotoxic and proliferative effects of substances, which is one of the enzymatic test methods commonly used in the determination of cytotoxicity. The proliferation-inducing effect on cell viability of umbelliferone on PCN cells with glutamate toxicity was determined by using MTT assay (Sigma, USA) concerning manufacturers' protocols (Cayman Chemical, Ann Arbor, MI, USA). Briefly, PCN cells were treated with various concentrations of umbelliferone as mentioned earlier and incubated for 24 and 72 h (37°C and 5% CO_2). The stock MTT solution prepared in sterile PBS was added to 96 well-plates at a concentration of 10%. After incubation for 4 h (37°C and 5% CO_2), it was provided that the formazan crystals were dissolved by adding 100 mL DMSO. Formazan crystal formation was evaluated by spectrophotometric method at 570 nm (reference wavelength 630 nm) using a microplate reader.

Measurements of Total Oxidant Status (TOS)

Total oxidant status of umbelliferone was determined with a method based on color change developed by Erel [31]. For this purpose, 10-1000 µM concentration range umbelliferone with PCN cells for 24 and 72 h were incubated and cell culture mediums were removed, and supernatants were analyzed to determine the TOS. Each group was repeated three times. If there are oxidants in the sample, it oxidizes the ferrous ion-o-dianisidine complex to the ferric ion. This reaction is increased with abundant glycerol molecules. In an acidic medium, the ferric ion formed a colored complex with xylenol orange. The intensity of the color formed, related to the total oxidant molecules amount in the sample, was measured by the spectrophotometric method. The method was calibrated with H_2O_2 and the obtained results were given as µmol H_2O_2 equiv./L. The precision of the method was lower than 2%.

Measurements of Total Antioxidant Status (TAS)

Total antioxidant status of umbelliferone was determined with a method based on color change developed by Erel [32]. For this purpose, 10-1000 µM concentration range umbelliferone with PCN cells for 24 and 72 h were incubated and cell culture mediums were removed, and supernatants were analyzed to determine the TAS. Each group was repeated three times. The novel automated method is based on the production of OH^- radicals by Fenton reaction and its reaction with the colorless substrate O-dianisidine to produce dianisyl radical, which has a bright yellowish-brown color. When adding a sample of cell culture medium, the oxidative reactions initiated by the OH^- radicals present in the reaction are suppressed by the antioxidants in samples, preventing the color change and thereby producing an effective way to determine the TAS levels. The obtained results were given as mmol Trolox Eq/L.

Statistical Analysis

All results were performed using SPSS 20 software for statistical analysis. The results were calculated as mean±standard error. Results were analyzed using the One-way ANOVA with Duncan's Posthoc test. P values <0.05 were taken in consideration to indicate statistical significance.

Results

MTT Analysis Results

The proliferative effect of umbelliferone on PCN was determined using MTT analysis. Various concentrations of umbelliferone (final concentration in each well; 10-1000 µM) were used to determine its proliferative effects on PCN culture with glutamate toxicity, with results shown in *Fig. 1* and *Fig. 2*. At the end of 24 and 72 h of incubations, it was determined that following the application of $6x10^{-5}$ M glutamate, cell viability decreased to 62.87% and 42.88%, respectively. It was shown that cell viability increase in PCN with glutamate toxicity following administration of low concentrations of umbelliferone. An increase in cell viability was observed in PCN with glutamate toxicity following administration of low concentrations of umbelliferone. Especially after 72 h of incubation, it was found that 25-250 µM concentration of umbelliferone have a statistically significant protective effect on cell viability compared to glutamate control (P<0.05) *(Fig. 1-A,B)*.

TAS and TOS Analysis Results

Following the application of umbelliferone at various concentrations (10-1000 µM) for 24 and 72 h in PCN culture against glutamate excitotoxicity, the cell culture medium was taken and total antioxidant and oxidant capacities were measured with a commercial kit. TAS results showed that cells treated with 50-250 µM umbelliferone statistically significantly increased the antioxidant capacity compared to glutamate control (P<0.05). Low antioxidant capacity was found in cells treated with a high dose (500-1000 µM) umbelliferone. It was also found that TAS results were in line with MTT results and that 50-250 µM umbelliferone had the highest effect on both cell viability and antioxidant capacity *(Fig. 2-A,B)*.

Total oxidant status results showed the level of oxidant and free radical in the cell culture medium. The obtained results showed that the cells treated with 500-1000 µM umbelliferone had high oxidant capacity, which in turn induced toxicity and increased cell death by intracellular stress factor. Consistent with the TAS results, a statistically significant decrease in TOS levels was detected in the cells

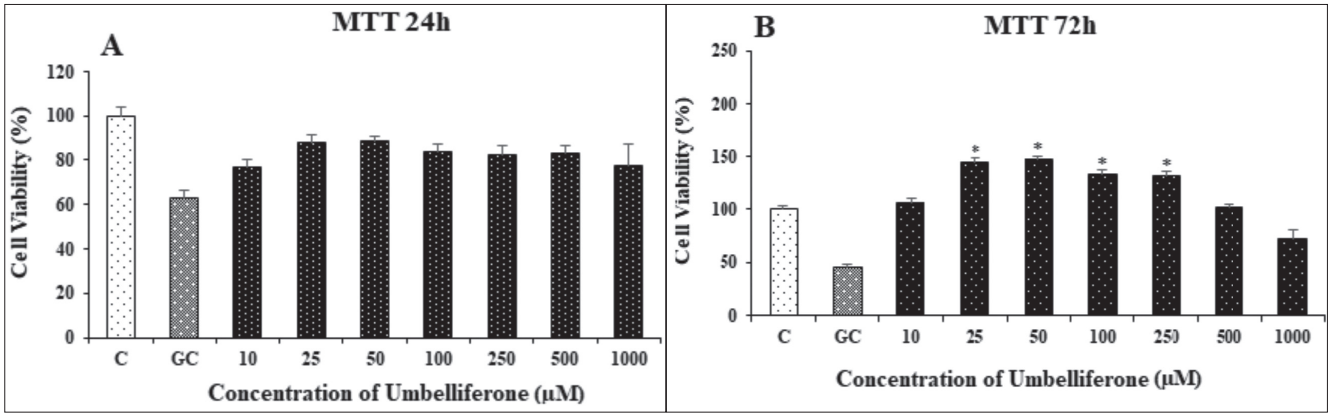

Fig 1. The proliferative effects of umbelliferone on the viability of primary cortical neuron cells with glutamate toxicity. **A:** in 24 h incubation, **B:** in 72 h incubation [results are given as mean ± SE, n = 8, * statistically significant in comparison with glutamate control, P<0.05, C: Control (untreated cells), GC: Glutamate control (Cells treated with $6x10^{-5}$ M glutamate)]

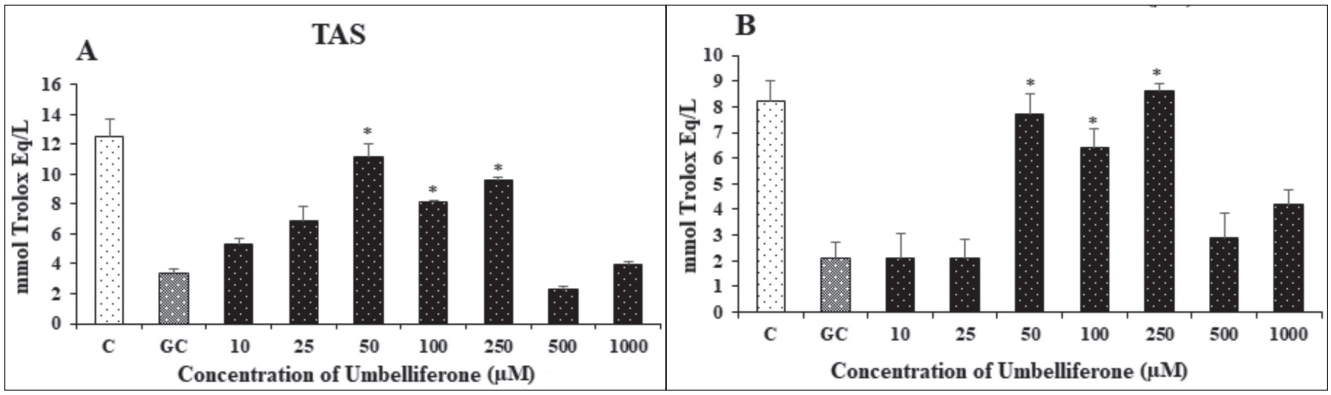

Fig 2. The determined TAS analysis for various concentrations of umbelliferone in primer cortical neuron culture against glutamate excitotoxicity. **A:** in 24 h incubation, **B:** in 72 h incubation [results are given as mean ± SE, * P<0.05 statistically significant compared to glutamate control; C: Control (nontreated cells), GC: Glutamate control ($6x10^{-5}$ M glutamate exposed cell)]

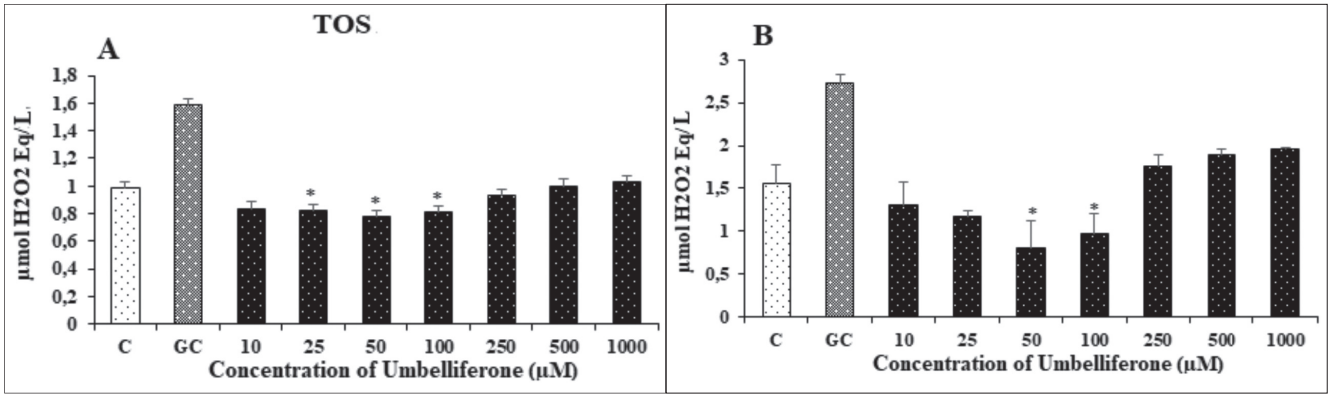

Fig 3. The determined TOS analysis for various concentrations of umbelliferone in primer cortical neuron culture against glutamate excitotoxicity. **A:** in 24 h incubation, **B:** in 72 h incubation [results are given as mean ± SE, * P<0.05 statistically significant compared to glutamate control; C: control (nontreated cells), GC: Glutamate control (6x10^{-5} M glutamate exposed cell)]

treated with 50-100 µM umbelliferone compared to the glutamate control (P<0.05). However, it was found that the oxidant level (stress factor level) was the lowest following the application of 50-100 µM umbelliferone, inconsistent with both our MTT and TAS results *(Fig. 3-A,B)*.

Discussion

The central nervous system has excitatory and inhibitory neurotransmitters that cause excitation and inhibition. One of the excitatory neurotransmitters is glutamate that can pass through the blood-brain barrier at presynaptic neuron terminals and is synthesized from glutamine [3,33]. Excessive glutamate, because of changes in glutamate metabolism trigger various pathological events, is known to cause excitotoxicity [34,35]. Glutamate excitotoxicity also accelerates neuronal cell death by causing oxidative stress [36,37]. Also, glutamate excitotoxicity has a role in the pathogenesis of various neurodegenerative diseases such as Alzheimer's and Parkinson's [38,39].

Umbelliferone is a 7-hydroxycoumarin derivative compound, which is a pharmacologically active agent. Studies have been shown that umbelliferone exhibit pharmacological activities in degenerative diseases caused by cancer cells, pro-oxidants, and ROS [40]. Given the role of oxidative stress in glutamate excitotoxicity, we assumed that the antioxidant activity of umbelliferone contributed significantly to its protective role against glutamate excitotoxicity. This study demonstrated the proliferative and antioxidant effects of umbelliferone against glutamate excitotoxicity in PCN cells. MTT, which is a colorimetric analysis, is a method that determines the amount of cell viability in proliferative and cytotoxic studies. Since MTT is a fast, useful, and low-cost technique, it has become a very popular method for determining the amount of cell viability in cell culture studies [41]. In the study, we used MTT assay and a significant decrease in cell viability was detected in PCN cells with glutamate toxicity. As a result of our study, following 50-250 µM concentration of umbelliferone application, an increase in cell viability on PCN cells against glutamate excitotoxicity was detected.

Oxidative stress is an indicator of tissue damage due to increased ROS. The oxidant effect created by ROS is blocked by the antioxidant defense system. Disruption of the balance between free radicals and the antioxidant defense system causes oxidative stress and oxidative damage [42,43].

SOD activity and TAC are generally suppressed, redox balance cannot be maintained and oxidative stress occurs in the organism.

As a result of glutamate-induced excitotoxicity, an uncontrolled increase in ROS and intracellular Ca^{+2} concentration is observed due to excessive activation of glutamate receptors. At the same time, glutamate causes neuronal degeneration by causing partial depolarization in the mitochondrial membrane and triggering an increase in intracellular ROS concentration and oxidation [44]. Organisms protect the intracellular environment from the effects of ROS by activating their antioxidant systems to protect the cell from damage caused by free radicals [45].

Coumarins are known to have antioxidant and neuro-protective effects [46] Therefore, natural plants that can be used in the isolation of coumarins have become the focus of researchers [47]. Umbelliferone is one of the most widespread coumarin compounds found in the Apiaceae family and it has many biological effects like anti-inflammatory, anti-lipid peroxidation, antimicrobial, antidiabetic, anticancer, and antioxidant potential [48]. The antioxidant potential of umbelliferone has been previously reported in some studies. Umbelliferone has been shown to stop the cell cycle in the G0/G1 phase by increasing oxidative stress and induce apoptosis in human oral carcinoma cells through oxidative DNA damage [49]. Germoush et al.[50] showed umbelliferone modulates the glutamate-NO-cGMP pathway and prevents oxidative

damage in the brain of hyperammonemic rats. And also, in that study it was shown that umbelliferone suppressed oxidative stress, glutamine synthesis in the cerebrum and reduced the expression and activity of cerebral Na^+/K^+-ATPase. Hindam et al.[51] showed that umbelliferone or xanthotoxin treatments significantly mitigated the oxidative stress via decreased MDA levels in STZ-treated rats. Also, umbelliferone was reported to possess anti-oxidant properties in various tissues [50]. Karakaya et al.[52] showed that extracts of *Zosima absinthfolia* containing umbelliferone have a high anti-oxidant capacity.

In the current study, TAS-TOS analysis was used to evaluate its effect on oxidative damage. Umbelliferone was isolated from *Ferulago cassia*. The obtained results showed that the cells treated with 500-1000 µM umbelliferone had high oxidant and low antioxidant capacity, which in turn induced toxicity and increased cell death by intracellular stress factor. It was found that the antioxidant level was the highest following the application of 50-100 µM umbelliferone, consistent with both our MTT and TOS results. Similarly, in the literature, the antioxidant effect of umbelliferone was also shown on PCN against glutamate excitotoxicity.

In conclusion, umbelliferone, is a coumarin derivative compound, has a neuroprotective effect in PCN culture against glutamate toxicity. It is thought that umbelliferone shows this effect by increasing antioxidant properties in cells while decreasing oxidant capacity. In this study, we showed that umbelliferone can be a concentration-dependent agent that can be used as a protective and therapeutic agent against glutamate excitotoxicity. To better understand the effect of umbelliferone on glutamate toxicity, different comprehensive studies are needed both *in vitro* and *in vivo*.

Acknowledgements

The authors thank Prof. Dr. Hayri Duman for identification of Ferulago cassia also thank Prof. Dr. Ceyda Sibel Kılıç for collecting of plant with Songül Karakaya.

Financial Support

None.

Conflict of Interest

The authors' declares that they have no confict of interest.

Author Contributions

Concept: AKD, GG; Isolation of Umbelliferone: SK; Experimental of Cell Culture: GG, SYT, KAN, AH; Statistical analysis and Calculation: AKD, GG, SK, AH; All authors contributed on article writing and approved the final article.

References

1. Albright TD, Jessell TM, Kandel ER, Posner MI: Neural science: A century of progress and the mysteries that remain. *Neuron,* 25, S1-S55, 2000. DOI: 10.1016/s0896-6273(00)80912-5

2. Wen SY, Li AM, Mi KQ, Wang RZ, Li H, Liu HX, Xing Y: *In vitro* neuroprotective effects of ciliary neurotrophic factor on dorsal root ganglion neurons with glutamate-induced neurotoxicity. *Neural Regen Res,* 12 (10): 1716-1723, 2017. DOI: 10.4103/1673-5374.217352

3. Howes O, McCutcheon R, Stone J: Glutamate and dopamine in schizophrenia: An update for the 21st century. *J Psychopharmacol,* 29 (2): 97-115, 2015. DOI: 10.1177/0269881114563634

4. Krebs HA: Metabolism of amino-acids: IV. The synthesis of glutamine from glutamic acid and ammonia, and the enzymic hydrolysis of glutamine in animal tissues. *Biochem J,* 29 (8): 1951-1969, 1935. DOI: 10.1042/bj0291951

5. Rueda CB, Llorente-Folch I, Traba J, Amigo I, Gonzalez-Sanchez P, Contreras L, Juaristi I, Martinez-Valero P, Pardo B, Del Arco A, Satrustegui J: Glutamate excitotoxicity and Ca^{2+}-regulation of respiration: Role of the Ca^{2+} activated mitochondrial transporters (CaMCs). *Biochim Biophys Acta,* 1857 (8): 1158-1166, 2016. DOI: 10.1016/j.bbabio.2016.04.003

6. Hacimuftuoglu A, Tatar A, Cetin D, Taspinar N, Saruhan F, Okkay U, Turkez H, Unal D, Stephens RL, Suleyman H: Astrocyte/neuron ratio and its importance on glutamate toxicity: An *in vitro* voltammetric study. *Cytotechnology,* 68 (4): 1425-1433, 2016. DOI: 10.1007/s10616-015-9902-9

7. Schousboe A, Scafidi S, Bak LK, Waagepetersen HS, McKenna MC: Glutamate metabolism in the brain focusing on astrocytes. **In,** Parpura V, Schousboe A, Verkhratsky A (Eds): Glutamate and ATP at the Interface of Metabolism and Signaling in the Brain.13-30, Springer, Cham, Switzerland, 2014. DOI: 10.1007/978-3-319-08894-5_2

8. Olsen GM, Sonnewald U: Glutamate: Where does it come from and where does it go? *Neurochem Int*, 88, 47-52, 2015. DOI: 10.1016/j.neuint.2014.11.006

9. Kanamori K: *In vivo* N-15 MRS study of glutamate metabolism in the rat brain. *Anal Biochem*, 529, 179-192, 2017. DOI: 10.1016/j.ab.2016.08.025

10. Zhao J, Verwer RWH, Van Wamelen DJ, Qi XR, Gao SF, Lucassen PJ, Swaab DF: Prefrontal changes in the glutamate-glutamine cycle and neuronal/glial glutamate transporters in depression with and without suicide. *J Psychiatr Res,* 82, 8-15, 2016. DOI: 10.1016/j.jpsychires.2016.06.017

11. Mahmoud S, Gharagozloo M, Simard C, Gris D: Astrocytes maintain glutamate homeostasis in the CNS by controlling the balance between glutamate uptake and release. *Cells,* 8 (2): 184, 2019. DOI: 10.3390/cells8020184

12. Song JH, Kang KS, Choi YK: Protective effect of casuarinin against glutamate-induced apoptosis in HT22 cells through inhibition of oxidative stress-mediated MAPK phosphorylation. *Bioorg Med Chem Lett,* 27 (23): 5109-5113, 2017. DOI: 10.1016/j.bmcl.2017.10.075

13. Zhao H, Ji ZH, Liu C, Yu XY: Neuroprotective mechanisms of 9-hydroxy epinootkatol against glutamate-induced neuronal apoptosis in primary neuron culture. *J Mol Neurosci,* 56 (4): 808-814, 2015. DOI: 10.1007/s12031-015-0511-z

14. Jia N, Sun Q, Su Q, Chen G: SIRT1-mediated deacetylation of PGC1α attributes to the protection of curcumin against glutamate excitotoxicity in cortical neurons. *Biochem Biophys Res Commun,* 478 (3): 1376-1381, 2016. DOI: 10.1016/j.bbrc.2016.08.132

15. Mehta A, Prabhakar M, Kumar P, Deshmukh R, Sharma PL: Excitotoxicity: Bridge to various triggers in neurodegenerative disorders. *Eur J Pharmacol,* 698 (1-3): 6-18, 2013. DOI: 10.1016/j.ejphar.2012.10.032

16. Floyd RA, Hensley K: Oxidative stress in brain aging: Implications for therapeutics of neurodegenerative diseases. *Neurobiol Aging,* 23 (5): 795-807, 2002. DOI: 10.1016/s0197-4580(02)00019-2

17. Anand P, Singh B, Singh N: A review on coumarins as acetylcholinesterase inhibitors for Alzheimer's disease. *Bioorg Med Chem,* 20 (3): 1175-1180, 2012. DOI: 10.1016/j.bmc.2011.12.042

18. Adsersen A, Gauguin B, Gudiksen L, Jäger AK: Screening of

plants used in Danish folk medicine to treat memory dysfunction for acetylcholinesterase inhibitory activity. *J Ethnopharmacol,* 104 (3): 418-422, 2006. DOI: 10.1016/j.jep.2005.09.032

19. Tavakoli S, Vatandoost H, Zeidabadinezhad R, Hajiaghaee R, Hadjiakhoondi A, Abai MR, Yassa N: Gas chromatography, GC/Mass analysis and bioactivity of essential oil from aerial parts of *Ferulago trifida:* Antimicrobial, antioxidant, AChE inhibitory, general toxicity, MTT assay and larvicidal activities. *J Arthropod-Borne Dis,* 11 (3): 414-426, 2017.

20. Abotsi WK, Ainooson GK, Gyasi EB, Abotsi WKM: Acute and sub-acute toxicity studies of the ethanolic extract of the aerial parts of *Hilleria latifolia* (Lam.) H. Walt.(Phytolaccaceae) in rodents. *West Afr J Pharm,* 22 (1): 27-35, 2011.

21. Vasconcelos JF, Teixeira MM, Barbosa-Filho JM, Agra MF, Nunes XP, Giulietti AM, Ribeiro-Dos-Santos R, Soares MBP: Effects of umbelliferone in a murine model of allergic airway inflammation. *Eur J Pharmacol,* 609 (1-3): 126-131, 2009. DOI: 10.1016/j.ejphar.2009.03.027

22. Kumar V, Bhatt PC, Rahman M, Al-Abbasi FA, Anwar F, Verma A: Umbelliferon-α-d-glucopyranosyl-($2^{I}\rightarrow1^{II}$)-α-Dglucopyranoside ameliorates Diethylnitrosamine induced precancerous lesion development in liver via regulation of inflammation, hyperproliferation and antioxidant at pre-clinical stage. *Biomed Pharmacother,* 94, 834-842, 2017. DOI: 10.1016/j.biopha.2017.07.047

23. Barber SC, Higginbottom A, Mead RJ, Barber S, Shaw PJ: An *in vitro* screening cascade to identify neuroprotective antioxidants in ALS. *Free Radic Biol Med,* 46 (8): 1127-1138, 2009. DOI: 10.1016/j.freeradbiomed.2009.01.019

24. Subramaniam SR, Ellis EM: Neuroprotective effects of umbelliferone and esculetin in a mouse model of Parkinson's disease. *J Neurosci Res,* 91 (3): 453-461, 2013. DOI: 10.1002/jnr.23164

25. Sundt TM, Anderson RE: Umbelliferone as an Intracellular pH-sensitive fluorescent indicator and blood-brain barrier probe: Instrumentation, calibration, and analysis. *J Neurophysiol,* 44 (1): 60-75, 1980. DOI: 10.1152/jn.1980.44.1.60

26. Ali MY, Jannat S, Jung HA, Choi RJ, Roy A, Choi JS: Anti-Alzheimer's disease potential of coumarins from *Angelica decursiva* and *Artemisia capillaris* and structure-activity analysis. *Asian Pac J Trop Med,* 9 (2): 103-111, 2016. DOI: 10.1016/j.apjtm.2016.01.014

27. Jayakumar S, Bhilwade H, Chaubey R: Umbelliferone suppresses radiation induced DNA damage and apoptosis in hematopoietic cells of mice. **In,** *Proceedings of the International Conference on Emerging Frontiers and Challenges in Radiation Biology.* 24-25 Jan, India, 2012.

28. Vijayalakshmi A, Sindhu G: Data on efficacy of umbelliferone on glycoconjugates and immunological marker in 7, 12-dimethylbenz (a) anthracene induced oral carcinogenesis. *Data Brief,* 15, 216-221, 2017. DOI: 10.1016/j.dib.2017.09.035

29. Finn GJ, Creaven B, Egan DA: Study of the in vitro cytotoxic potential of natural and synthetic coumarin derivatives using human normal and neoplastic skin cell lines. *Melanoma Res,* 11 (5): 461-467, 2001. DOI: 10.1097/00008390-200110000-00004

30. Karakaya S, Koca M, Sytar O, Dursunoglu B, Ozbek H, Duman H, Guvenalp Z, Kilic CS: Antioxidant and anticholinesterase potential of *Ferulago cassia* with farther bio-guided isolation of active coumarin constituents. *S Afr J Bot,* 121, 536-542, 2019. DOI: 10.1016/j.sajb.2019.01.020

31. Erel O: A new automated colorimetric method for measuring total oxidant status. *Clin Biochem,* 38 (12): 1103-1111, 2005. DOI: 10.1016/j.clinbiochem.2005.08.008

32. Erel O: A novel automated method to measure total antioxidant response against potent free radical reactions. *Clin Biochem,* 37 (2): 112-119, 2004. DOI: 10.1016/j.clinbiochem.2003.10.014

33. Dwivedi Y, Pandey GN: Glutamatergic neurotransmission abnormalities and schizophrenia. **In,** Ritsner M (Ed): Handbook of Schizophrenia Spectrum Disorders. 287-304, Springer, Dordrecht, 2011. DOI: 10.1007/978-94-007-0837-2_13

34. Michaels RL, Rothman SM: Glutamate neurotoxicity *in vitro:* Antagonist pharmacology and intracellular calcium concentrations. *J Neurosci,* 10 (1): 283-292, 1990. DOI: 10.1523/JNEUROSCI.10-01-00283.1990

35. Sasaki-Hamada S, Suzuki A, Sanai E, Matsumoto K, Oka JI: Neuroprotection by chotosan, a Kampo formula, against glutamate excitotoxicity involves the inhibition of GluN2B-, but not GluN2A-containing NMDA receptor-mediated responses in primary cultured cortical neurons. *J Pharmacol Sci,* 135 (3): 134-137, 2017. DOI: 10.1016/j.jphs.2017.10.009

36. Coyle JT, Puttfarcken P: Oxidative stress, glutamate, and neurodegenerative disorders. *Science,* 262 (5134): 689-695, 1993. DOI: 10.1126/science.7901908

37. Depp C, Bas-Orth C, Schroeder L, Hellwig A, Bading H: Synaptic activity protects neurons against calcium-mediated oxidation and contraction of mitochondria during excitotoxicity. *Antioxid Redox Signal,* 29 (12): 1109-1124, 2018. DOI: 10.1089/ars.2017.7092

38. Kortagere S, Mortensen OV, Xia J, Lester W, Fang Y, Srikanth Y, Salvino JM, Fontana ACK: Identification of novel allosteric modulators of glutamate transporter EAAT2. *ACS Chem Neurosci,* 9 (3): 522-534, 2018. DOI: 10.1021/acschemneuro.7b00308

39. Lipton SA, Rosenberg PA: Excitatory amino acids as a final common pathway for neurologic disorders. *N Engl J Med,* 330 (9): 613-622, 1994. DOI: 10.1056/nejm199403033300907

40. Mazimba O: Umbelliferone: Sources, chemistry and bioactivities review. *Bull Fac Pharm Cairo Univ,* 55 (2): 223-232, 2017. DOI: 10.1016/j.bfopcu.2017.05.001

41. Sylvester PW: Optimization of the tetrazolium dye (MTT) colorimetric assay for cellular growth and viability. **In,** Satyanarayanajois S (Ed): Drug Design and Discovery. 157-168, Humana Press, 2011. DOI: 10.1007/978-1-61779-012-6_9

42. Shen C, Cai GQ, Peng JP, Chen XD: Autophagy protects chondrocytes from glucocorticoids-induced apoptosis via ROS/Akt/FOXO3 signaling. *Osteoarthritis Cartilage,* 23 (12): 2279-2287, 2015. DOI: 10.1016/j.joca.2015.06.020

43. Çenesiz S: The role of oxidant and antioxidant parameters in the infectious diseases: A systematic literature review. *Kafkas Univ Vet Fak Derg,* 26 (6): 849-858, 2020. DOI: 10.9775/kvfd.2020.24618

44. Ghezzi F, Monni L, Corsini S, Rauti R, Nistri A: Propofol protects rat hypoglossal motoneurons in an *in vitro* model of excitotoxicity by boosting GABAergic inhibition and reducing oxidative stress. *Neuroscience,* 367, 15-33, 2017. DOI: 10.1016/j.neuroscience.2017.10.019

45. Hara Y, McKeehan N, Dacks PA, Fillit HM: Evaluation of the neuroprotective potential of N-acetylcysteine for prevention and treatment of cognitive aging and dementia. *J Prev Alz Dis,* 4 (3): 201-206, 2017. DOI: 10.14283/jpad.2017.22

46. Karakaya S, Gözcü S, Güvenalp Z, Özbek H, Yuca H, Dursunoğlu B, Kazaz C, Kılıç CS: The α-amylase and α-glucosidase inhibitory activities of the dichloromethane extracts and constituents of *Ferulago bracteata* roots. *Pharm Biol,* 56 (1): 18-24, 2018. DOI: 10.1080/13880209.2017.1414857

47. Fylaktakidou KC, Hadjipavlou-Litina DJ, Litinas KE, Nicolaides DN: Natural and synthetic coumarin derivatives with anti-inflammatory/antioxidant activities. *Curr Pharm Des,* 10 (30): 3813-3833, 2004. DOI: 10.2174/1381612043382710

48. Kutlu Z, Celik M, Bilen A, Halıcı Z, Yıldırım S, Karabulut S, Karakaya S, Bostanlık DF, Aydın P: Effects of umbelliferone isolated from the *Ferulago pauciradiata* Boiss. & Heldr. Plant on cecal ligation and puncture-induced sepsis model in rats. *Biomed Pharmacother,* 127:110206, 2020. DOI: 10.1016/j.biopha.2020.110206

49. Vijayalakshmi A, Sindhu G: Umbelliferone arrest cell cycle at G0/G1 phase and induces apoptosis in human oral carcinoma (KB) cells possibly via oxidative DNA damage. *Biomed Pharmacother,* 92, 661-671, 2017. DOI: 10.1016/j.biopha.2017.05.128

50. Germoush MO, Othman SI, Al-Qaraawi MA, Al-Harbi HM, Hussein OE, Al-Basher G, Alotaibi MF, Elgebaly HA, Sandhu MA, Allam AA, Mahmoud AM: Umbelliferone prevents oxidative stress, inflammation and hematological alterations, and modulates glutamate-nitric oxide-cGMP signaling in hyperammonemic rats. *Biomed Pharmacother,* 102, 392-402, 2018. DOI: 10.1016/j.biopha.2018.03.104

51. Hindam MO, Sayed RH, Skalicka-Woźniak K, Budzyńska B, El Sayed NS: Xanthotoxin and umbelliferone attenuate cognitive dysfunction in a streptozotocin-induced rat model of sporadic Alzheimer's disease: The role of JAK2/STAT3 and Nrf2/HO-1 signalling pathway modulation. *Phytother Res,* 34 (9): 2351-2365, 2020. DOI: 10.1002/ptr.6686

52. Karakaya S, Koca M, Yılmaz SV, Yıldırım K, Pınar NM, Demirci B, Brestic M, Sytar O: Molecular docking studies of coumarins isolated from extracts and essential oils of zosima absinthifolia link as potential inhibitors for Alzheimer's disease. *Molecules,* 24 (4):722, 2019. DOI: 10.3390/molecules24040722

Kafkas Universitesi Veteriner Fakultesi Dergisi
ISSN: 1300-6045 e-ISSN: 1309-2251
Journal Home-Page: http://vetdergikafkas.org

Kafkas Univ Vet Fak Derg
27 (3): 347-353, 2021
DOI: 10.9775/kvfd.2021.25486

RESEARCH ARTICLE

Determining the Location of Tibial Fracture of Dog and Cat Using Hybridized Mask R-CNN Architecture

Berker BAYDAN [1,a (*)] Necaattin BARIŞÇI [2,b] Halil Murat ÜNVER [1,c]

[1] Kırıkkale University, Faculty of Engineering, Department of Computer Engineering, TR-71451 Kırıkkale - TÜRKİYE
[2] Gazi University, Faculty of Technology, Department of Computer Engineering, TR-06560 Ankara - TÜRKİYE
ORCIDs: a 0000-0003-2806-368X; b 0000-0002-8762-5091; c 0000-0001-9959-8425

Article ID: KVFD-2021-25486 Received: 01.02.2021 Accepted: 01.05.2021 Published Online: 01.05.2021

Abstract

The aim of this study is to hybridize the original backbone structure used in the Mask R-CNN framework, and to detect fracture location in dog and cat tibia fractures faster and with higher performance. With the hybrid study, it will be ensured that veterinarians help diagnose fractures on the tibia with higher accuracy by using a computerized system. In this study, a total of 518 dog and cat fracture tibia images that obtained from universities and institutions were used. F1 score value of this study on total dataset was found to be 85.8%. F1 score value of this study on dog dataset was found to be 87.8%. F1 score value of this study on cat dataset was found to be 77.7%. With the developed hybrid system, it was determined that the localization of the fracture in an average tibia image took 2.88 seconds. The results of the study showed that the hybrid system developed would be beneficial in terms of protecting animal health by making more successful and faster detections than the original Mask R-CNN architecture.

Keywords: *Cat, Dog, Fracture, Hybrid, Mask R-CNN, Tibia*

Hibrit Mask R-CNN Mimarisi Kullanılarak Köpek ve Kedi Tibia Kırık Yerinin Belirlenmesi

Öz

Bu çalışmanın amacı Mask R-CNN çatısında kullanılan orjinal omurga yapısını hibrit hale getirerek köpek ve kedi tibia kırıklarındaki kırık bölgelerinin tespitini daha hızlı ve daha yüksek performans ile sağlamaktır. Yapılan hibrit çalışma ile bigisayarlaştırılmış sistem kullanılarak daha yüksek doğruluk oranıyla veteriner hekimlerin tibia üzerindeki kırık teşhislerine yardımcı olması sağlanacaktır. Bu çalışmada üniversitelerden ve kurumlardan elde edilen toplam 518 adet köpek ve kedi kırık tibia kemiği görüntüsü kullanıldı. Bu çalışmanın F1 skor değeri toplam veri seti üzerinde %85.8 olarak bulundu. Çalışmanın köpek veri seti üzerindeki F1 skor değeri %87.8 olarak bulundu. Çalışmanın kedi veri seti üzerindeki F1 skor değeri %77.7 olarak bulundu. Geliştirilen hibrit sistem ile ortalama bir kırık tibia görüntüsündeki kırık yerinin lokalizasyonu 2.88 saniye sürdüğü tespit edildi. Çalışmanın sonuçları, geliştirilen hibrit sistemin orjinal Mask R-CNN mimarisine göre daha başarılı ve hızlı tespitler yaparak hayvan sağlığının korunması açısından faydalı olacağını gösterdi.

Anahtar sözcükler: *Hibrit, Kedi, Kırık, Köpek, Mask R-CNN, Tibia*

INTRODUCTION

Artificial Intelligence (AI) is a term that developed by John McCarthy in 1956 and was briefly defined as "the science and engineering of making smart machines". AI is a system that can deal with complexity and uncertainty, including learning from past experiences, decision-making logic, power of inference and rapid response [1]. AI includes neural networks, deep learning, statistics, machine learning, which are successfully used in many areas such as security, research, robotics, voice recognition, and transportation [2].

Artificial neural networks and deep learning (DL) under AI form the basis of most applications [3]. DL is a complex computational model that uses multiple layers of computing algorithms [4]. The deep learning algorithm extracts the features of the data from the lower layer to the higher layer [5,6]. Deep learning modeling of big data is a machine

How to cite this article?

Baydan B, Barışçı N, Ünver HM: Determining the location of tibial fracture of dog and cat using hybridized mask R-CNN architecture. *Kafkas Univ Vet Fak Derg,* 27 (3): 347-353, 2021.
DOI: 10.9775/kvfd.2021.25486

(*) Corresponding Author

Tel: +90 533 139 7579
E-mail: baydanberker@gmail.com (B. Baydan)

learning technique that has been successfully used in different areas from self-driving cars to medical decisions [4,7]. Diagnosis of cases such as eye problems, malignant melanoma and tuberculosis in medicine with the help of DL has been successfully performed comparable to humans [4,8]. In recent years, there are some studies in the field of orthopedics and traumatology where DL is also used to detect fractures radiographically [5]. Medical images obtained by examinations such as X-Ray, computed tomography (CT), magnetic resonance imaging (MRI), gamma scan (scintigraphy), and ultrasound examinations in the health field are important data for research and clinical applications. These data help automatically detect diseases by minimizing human errors, establishment of study protocols, reduction ofradiation dose by improving image quality, decreasing MRI scanner time, optimize personnel and scanner use, and finally diminish costs [7]. In the field of veterinary medicine, the application of deep learning algorithm is too limited compared to human medicine [9]. In recent years, important legal steps have been taken on animal health and welfare worldwide. In this context, modern techniques are used for more accurate and rapid diagnosis and treatment clinically in animals [9,10]. Tibia fracture is observed frequently in cats and dogs. To diagnose fracture in veterinary medicine, X-ray image is routine and this procedure is always hazardness for operaters [11]. In addition, the increasing demand for radiology services today causes significant pressure on the workforce, and sometimes it can be a difficult and time-consuming process to evaluate medical images. AI helps in solving these problems [5,12]. But there are very few studies in this field. Although there is a study on pig bones using deep learning technology, this study is not about fracture detection, but on classification [13]. The first retrospective study of bone fractures using deep learning technology in animals was conducted on dog tibia [14].

Current approaches regarding object recognition make great use of machine learning methods. Since the object recognition function is quite complex, the used model must have a lot of data. Convolutional Neural Networks (CNNs) constitute a class of models that are easy to train because they contain fewer connections and parameters [15] The name CNN comes from the mathematical linear operation between matrices called convolution. Generally, CNN is divided into input layer, hidden layer (also known as feature extraction layers) and output layers. Hidden layers consist of multiple layers such as convolutional layer, nonlinear layer, pooling layer and fully connected layer. The number of layers differs for different CNNs [16,17]. CNN is a branch of deep learning technology. Deep learning modeling of big data is a machine learning technique that has been used successfully in a variety of fields, from web search to financial technology banking, from self-driving cars to facial recognition and medical decision support, and has a huge impact on modern society [7]. Mask Regional Convolutional Neural Network (Mask R-CNN) is the one of the most important deep learning object detection methods that detect objects in an image by segmentation with masking method [18].

Most of the hybrid studies are aim to concatenate state of art CNN models instead of using single-handed [19]. The main goal of the scientist in computer science is to solve and improve complex problems by replacing existing algorithms with algorithms that make less computation. This development ensure to solve current problem effectively [20]. In recent years, hybrid models have been applied in different areas to increase performance in deep learning algorithms [6,21,22].

In this study, it was aimed to increase the performance of localization of the fracture of tibia using a new developed hybrid deep learning method.

Material and Methods

Ethical Statement

This study was approved by the Kırıkkale University Animal Experiments Local Ethics Committee (Approval no: 60821397-010.99)

Dataset

The dataset was gathered from tibial fracture of dog and cat. Tibia fracture was obtained from veterinary faculities and Ankara municipality. To have these images, were consulted with Surgery Department of Veterinary Faculties of Ankara, Kırıkkale, Selçuk Universities and Ankara Metropolitan Municipality Sincan Temporary Animal Care Home Rehabilitation Center. 518 fracture of tibial fracture (441 dogs and 77 cats) were used for this research. These radiograph images were taken as Digital Imaging and Communication in Medicine (DICOM) format.

Labeling Fracture Location of Fracture Tibia

LabelImg [23] graphical image annotation software tool was used to annotate 518 fracture tibia images. Fractures oftibia were annotated by veterinarian. Fractures oftibia images were taken into bounding box by using LabelImg. To utilize DICOM images in the computerized system, they were converted to JPEG format. For this process, the Angora Viewer software which works on the institution's computer, was used.

System Architecture of Proposed Framework

In order to localize and detect fracture location of tibia, a new hybrid CNN model was developed on Mask R-CNN. Mask R-CNN [18] is the one of the most robust object detection framework. Original Mask R-CNN framework consists of three part [24]. First part is backbone (ResNet-101, FPN-Feature Pyramid Network). Second part is RPN (Regional Proposal Network). Third part is three branches (Category,

Coordinates and Mask). Backbone can be described as the most critic part for Mask R-CNN framework. Because feature extraction process is performed in the backbone section. Whether good or bad of feature extraction results depend on good training of this process. For this reason, it has been thought that hybridization in the backbone will further increase the performance. ResNet model, one of the important CNN models, was used in the backbone part of the original Mask R-CNN framework. ResNet uses skip-connections and identity functions to jump the non-linear transmissions. So, it passes from back layers to front layers via gradient identity function. Nevertheless, it may have a lot of parameters, can block the flow information in the network and have gradient problem disappearing. This can slow down the flow of information and reduce performance due to long training [24]. Since ResNet has been seen to give very successful results in terms of feature extraction [18], instead of removing ResNet completely and using another CNN model alone, the section that may cause slowness in ResNet was improved by using hybrid CNN. Instead of the section that may cause slowness in the network, the "dense block" which contain a narrower network layer and used in DenseNet [24] and "ResNet" turned into a hybrid structure *(Table 1)*. ResNet architecture consists of 5 phases *(Table 1)*. Considering that the 4th phase of the ResNet architecture may cause slowness due to the convulution structure of 23 blocks, it was modified by reducing one block to 22 blocks *(Table 1)*. In the 5th phase, it was aimed to increase the learning performance of the model by accelerating the flow of information in the network by removing a block from the network containing 3 block convolution and adding one dense block, which is also used in DenseNet, instead *(Table 1)*.

Dataset of tibial fracture of dog and cat was trained by using hybridized backbone (Modified ResNet 101 + Dense Block-from DenseNet) Mask R-CNN framework for detection and localization fracture location of tibial fracture. The dataset was divided into two parts as training and testing. This dataset was re-trained with new developed hybrid Mask R-CNN model for the detection and localization of fracture location of fracture tibia. The weights of Mask_RCNN_COCO model were used for training. The configuration values of hybrid Mask R-CNN model were determined as follows: Batch size: 2, learning rate: 0.001, learning momentum: 0.9, weight decay: 0.0001, epoch: 4000. To use different size of images, image was scaled (image_min_dim: 800 and image_max_dim: 1024 pixel). Keras API was used for developing this application. The development system was implemented on 30.5 GB NVIDIA Tesla M60 GPU and Ubuntu 18.04 operating system.

Qualifications of Metrics

Performance metrics are required to qualify the performance of detection and localization of fracture location of tibial fracture. One of the most frequently used metric is Intersection of Union (IoU) to qualify performance of application. In this research, IoU refers that coincide between the ground truth and the bounding box on the fracture tibia image. According IoU threshold value, the result can be whether True Positive or False Positive. In this research IoU was specified as 0.4. False Positive was called when threshold value was less than 0.4. If not, it was called as True Positive. "True Positive-TP" was described as matching up with labelled fracture and detected fracture location by the application. Otherwise, it was described as "False Positive-FP". "False Negative-FN" was described

Table 1. *Architecture comparison of modified ResNet 101 + Dense Block (from DenseNet) and ResNet 101*

Layers	**Modified ResNet 101 + Dense Block (DenseNet)**	**ResNet101** [24]
Convolution	7 x 7 conversion, Stride 2	7 x 7 conversion, Stride 2
Pooling	3 x 3 max pool, Stride 2	3 x 3 max pool, Stride 2
Conv2_X	1x1 conv 3x3 conv x 3 1x1 conv	1x1 conv 3x3 conv x 3 1x1 conv
Conv3_X	1x1 conv 3x3 conv x 4 1x1 conv	1x1 conv 3x3 conv x 4 1x1 conv
Conv4_X	1x1 conv 3x3 conv x 22 **(Modified part of ResNet 101)** 1x1 conv	1x1 conv 3x3 conv x 23 1x1 conv
Conv5_X	1x1 conv 3x3 conv x 2 1x1 conv + **Hybrid CNNs**	1x1 conv 3x3 conv x 3 1x1 conv
Dense Block	1x1 conv 3x3 conv x 1	-
Convolution Layer	3 x 3 conv	3 x 3 conv

as nothing to detect any fracture on image by system but if there was a fracture on image. Confidence score which is another valuable metric for evaluation this application performance, is the possibility of localization and detection fracture on fracture tibia [11]. In order to get overall system performance, F-Score [25] was calculated.

Results

In this research, fractures of fracture tibia were detected using hybridized backbone (Modified ResNet 101 + Dense Block-from DenseNet) Mask R-CNN framework. 518 fracture dataset were split into 415 training (360 dog and 55 cat) and 103 test (81 dog and 22 cat). IoU rate was specified as greater than 0.4. The F1 score of hybrid model on the total dataset were 85.8%. Only 18 images out of 103 could not make a prediction for the detection of fracture on the fracture tibia. The F1 score of hybrid model on the dog dataset were 87.8%. Only 12 images out of 81 could not make a prediction for the detection of fracture of tibia. The F1 score of hybrid model on the cat dataset were 77.7%. Only 6 images out of 22 could not make a prediction for the detection of fracture of tibia. The detected fracture locations of tibia were shown in *Fig. 1* and *Fig. 2*. Fracture location of tibia in 103 test data were detected and localized within 296.64 seconds. It took an average of 2.88 seconds for an image. Fracture location of tibia in 81 dog test data were detected and localized within 233.28 seconds. Fracture location of tibia in 22 cat test data were detected and localized within 63.36 seconds. The metrics of these studies were given in *Table 2*.

Discussion

According to the 2018 data of the World Health Organization (WHO), approximately 34% of human deaths on a global scale may result from misinterpretation of medical data. Therefore, it is important to improve all stages of clinical diagnosis [26]. Recent developments, especially in the field of deep learning, have enabled better perception of images and better interpretation of complex data by machines [5,27]. Convolutional neural network (CNN) is a class of deep neural networks where in deep learning most commonly used to analyze images and video processing [6]. There are several learning methods that have advantages and disadvantages.

Many hybrid machine learning methods have been developed to minimize the disadvantages of being used alone and to combine the useful aspects of each [28]. The adaptive neuro-fuzzy inference system (ANFIS) is combined with five different evolutionary algorithms to estimate the diffusion coefficient of carbon dioxide. ANFIS-PSO's hybrid machine learning model outperforms other models (R2: 0.9978) [29]. A hybrid approach based on a new combination of independent component analysis (ICA) and adaptivenoise cancellation (ANC) has been devoleped for Removal of ocular artifacts (OA) in real-time in electroencephalography (EEG) based brain computer interface (BCI) applications. It has been observed that the performance of the hybrid method is better than other compared methods in terms of removal of OA and recovery of the underlying EEG [30]. A new hybrid method which combined VGG Data STN with CNN (VDSNet) have been developed for diagnosis lung disease. VDSNet had been exhibited higher a validation accuracy (73%) than the other methots (vanilla gray, 67.8%; vanilla RGB, 69%; hybrid CNN, 69.5%; VGG, 63.8%) [31]. Brain monitoring combined with automatic analysis of EEGs important for clinicians. However, clinicians had been stated that the sensitivity and specificity of the method should be 95% and below 5%, respectively, for clinical acceptance [32]. Golmohammadi et al.[32] stated that the hybrid structure

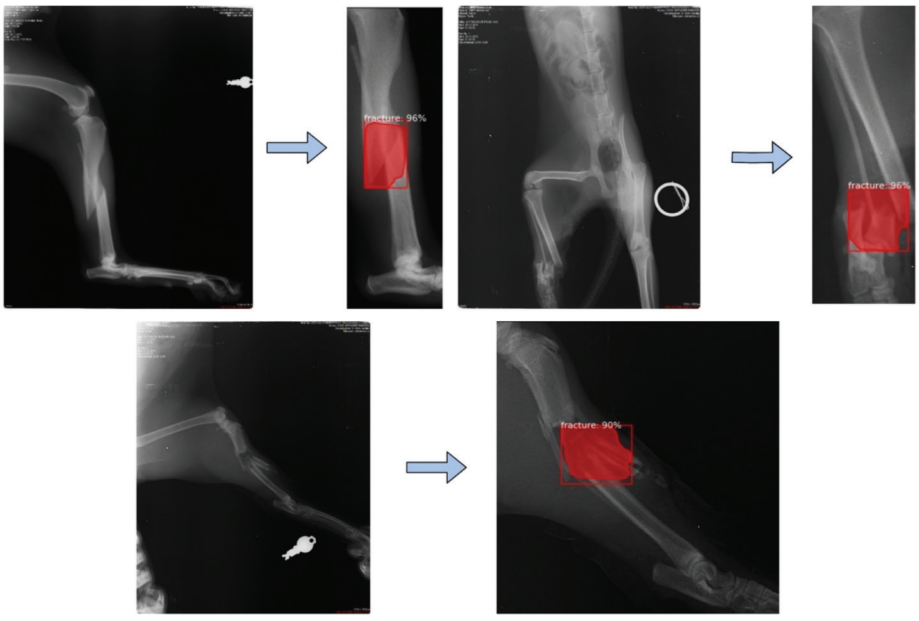

Fig 1. The detected and localized fracture locations on fracture tibia of cats by using Hybridized Backbone Mask R-CNN

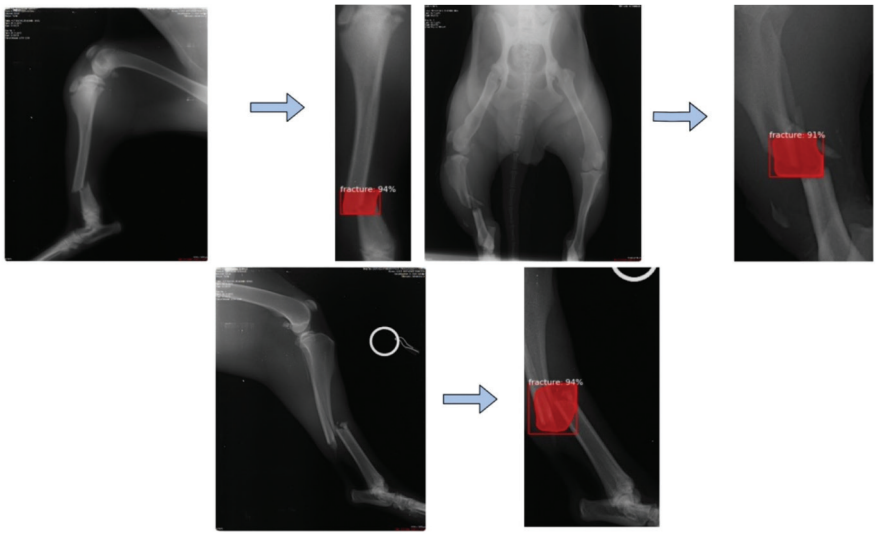

Fig 2. The detected and localized fracture locations on fracture tibia of dogs by using Hybridized Backbone Mask R-CNN

Table 2. *The performance results of detection and localization of cat and dog tiba bone fracture using original mask r-cnn and hybridized backbone Mask R-CNN*

Methods	Dog				Cat				Total			
	P (%)	R (%)	F1 (%)	ART (sec)	P (%)	R (%)	F1 (%)	ART (sec)	P (%)	R (%)	F1 (%)	ART (sec)
Original Mask R-CNN [11]	83.1	91.4	87.1	3.6	65	86.6	74.3	3.6	79.3	90.5	84.5	3.6
Hybridized backbone Mask R-CNN	91.5	84.4	87.8	2.88	87.5	70	77.7	2.88	90.8	81.4	85.8	2.88

P: *Precision,* ***R:*** *Recall,* ***F1:*** *F1 Score,* ***ART:*** *Average Response Time*

based on hidden Markov models and deep learning can approach clinically acceptable performance levels. Although hybrid applications have been made in different fields of medicine, there is no application developed on fracture detection in both medicine and veterinary medicine in fracture diagnosis. Therefore, in this research, it is aimed to develop a hybrid method in the field of AI for better detection of canine and cat tibia fractures.

In the literature searches, retrospective research was not found on bones in which the deep learning method was used for clinical diagnosis in animals. The study of segmentation and classification of spine and limb bones using Computed Tomography (CT) scanned images in pigs is one of several studies of deep learning technology experiments on animal bones. In the study, 3470 CT images were used for spine segmentation, 2000 for spine classification and limb segmentation, and additionally 1428 CT images in the second stage. As a result, according to sagital and coronal, the highest values in the spine classification are cranium (100%) and sacrum + coccyx (100%) for sagittal; the highest value for coronal was found for cranium (99.8%), cervical vertebrae (99.8%) and sacrum + coccyx (99.8%). The highest values in limb segmentation were found for sternum as 84.9% according to sagittal and for right forelimb as 98.2% according to coronal. In limb classification, the highest values were found for scapula as 98.4% according to sagittal and for femur as 95% according to coronal [13]. There are some studies on the detection of bone fractures with CNN in humans compared to animals. 1052 X-ray images were used to test the system in another study performed to detect bone fractures in humans using the two-stage Crack Sensitive CNN system (526 fractures, the remainder without fractures). In the first stage, 20 different bone types were determined from X-ray images using Faster R-CNN. In the second stage, the location of the fracture in the fracture area was determined with CrackNet. As a result, the performance of the two-phase system (F-score) was found as 90.14% [33]. Nine hundered eighty X-ray images were used in the fracture detection of child tibia bones. In this study, Xception-V3 method which is under CNN roof, was applied and the accuracy performance of this method was found as 95.9% [34]. The reason for the low performance of this hybrid study (F-score: 85.8%) in dogs and cats compared to previous studies suggests that the bones belong to different species and the method used is different. However, the result of the fracture detection performance of hybrid study was quite successful compared to the method performed with SSD (68%) in dog tibia fractures [14]. In the study performed with another deep learning algorithm (VGG 16) the performance of fracture detection of Wrist, Hand, ankle (83%) [35] was also lower than this hybrid operation performance (85.8%).

In conclusion, when the original Mask R-CNN framework was compared with hybridized backbone (Modified ResNet 101 + Dense Block - from DenseNet) Mask R-CNN

framework for the detection and localization of fractures of tibia, it was observed that the hybridized model (85.8%) gave more successful results than the classical model (84.5%) [11]. Besides, the response time of detection and localization of fractures of dogs and cats tibia using hybridized backbone Mask R-CNN (2.88 seconds) was quicker than original Mask R-CNN (3.6 seconds) [11]. When the performance and response time results of detection and localization of fractures on dogs and cats were examined separately, hybridized model improved results better than the classical model. Briefly, the proposed system showed that the results were promising in terms of detection and localization of fracture tibia in dogs and cats.

Financial Support

This research received no grant from any funding agency/ sector.

Conflict of Interest

The authors declared that there is no conflict of interest.

Author Contributions

B. Baydan collected data, implemented and developed a new hybrid model. B. Baydan wrote the manuscript. N. Barışçı and H. M. Ünver evaluated the results of study, read and approved final version of manuscript.

References

1. Singh G, Mishra A, Sagar D: An overview of artificial intelligence. *SBIT J Sci Technol*, 2 (1): 1-4, 2013. DOI: 10.13140/RG.2.2.20660.19840

2. Dhankar M, Walia N: An introduction to artificial intelligence. **In,** Kumar M, Choudhary R, Pandey SK (Eds): Emerging Trends in Big Data, IoT and Cyber Security. First Impression, 105-108, Maharaja Surajmal Institute. Excellent Publishing Services, New Delhi, 2020.

3. Haenlein M, Kaplan A: A brief history of artificial intelligence: On the past, present, and future of artificial intelligence. *Calif Manag Rev*, 61 (4): 5-14, 2019. DOI: 10.1177/0008125619864925

4. Yi PH, Hui FK, Ting DSW: Artificial intelligence and radiology: Collaboration is key. *J Am Coll Radiol*, 15 (5): 781-783, 2018. DOI: 10.1016/j.jacr.2017.12.037

5. Kalmet PHS, Sanduleanu S, Prımakov S, Wu G, Jochems A, Refaee T, Ibrahim A, Hulst LV, Lambin P, Poeze M: Deep learning in fracture detection: A narrative review. *Acta Orthop*, 91 (2): 215-220, 2020. DOI: 10.1080/17453674.2019.1711323

6. Pak U, Kim C, Ryu U, Sok K, Pak S: A hybrid model based on convolutional neural networks and long short-term memory for ozone concentration prediction. *Air Qual Atmos Health*, 11 (3): 883-895, 2018. DOI: 10.1007/s11869-018-0585-1

7. Pesapane F, Volonte C, Codari M, Sardanelli F: Artificial intelligence as a medical device in radiology: Ethical and regulatory issues in Europe and the United States. *Insights Imaging*, 9 (5): 745-753, 2018. DOI: 10.1007/s13244-018-0645-y

8. Ting DSW, Wu WC, Toth C: Deep learning for retinopathy of prematurity screening. *Br J Ophthalmol*, 103 (5): 577-579, 2019. DOI: 10.1136/bjophthalmol-2018-313290

9. Cihan P, Gökçe E, Kalıpsız O: A review of machine learning applications in veterinary field. *Kafkas Univ Vet Fak Derg*, 23 (4): 673-680, 2017. DOI: 10.9775/kvfd.2016.17281

10. Cihan P, Gökçe E, Atakişi O, Kırmızıgül AH, Erdoğan HM: Prediction of immunoglobulin G in lambs with artificial intelligence methods. *Kafkas Univ Vet Fak Derg*, 27 (1): 21-27, 2021. DOI: 10.9775/kvfd.2020.24642

11. Baydan B, Ünver HM: Detection of tibial fracture in cats and dogs with deep learning. *Ankara Univ Vet Fak Derg*, 2021 *(Article in press)*. DOI: 10.33988/auvfd.772685

12. Kim DH, MacKinnon T: Artificial intelligence in fracture detection: Transfer learning from deep convolutional neural networks. *Clin Radiol*, 73 (5): 439-445, 2018. DOI: 10.1016/j.crad.2017.11.015

13. Kvam J, Gangsei LE, Kongsro J, Schistad Solberg AH: The use of deep learning to automate the segmentation of the skeleton from CT volumes of pigs. *Transl Anim Sci*, 2 (3): 324-335, 2018. DOI: 10.1093/tas/txy060

14. Baydan B, Ünver HM: Dataset creation and SSD mobilenet V2 performance evaluation for dog tibia fracture detection. **In,** *II. International Ankara Congress of Scientific Research*, Ankara, Turkey, 6-8 March, 2020.

15. Krizhevsky A, Sutskever I, Hinton GE: ImageNet classification with deep convolutional neural networks. *Commun ACM*, 60 (6): 84-90, 2017. DOI: 10.1145/3065386

16. Albawi S, Mohammed TA, Al-Zawi S: Understanding of a convolutional neural network. **In,** *International Conference on Engineering and Technology (ICET)*. Antalya, Turkey, 21-23 August, 2017, DOI: 10.1109/icengtechnol.2017.8308186

17. Ting DSW, Peng L, Varadarajan AV, Keane PA, Burlina PM, Chiang MF, Schmettere L, Pasquale LR, Bressler NM, Webster DR, Abramorff M, Wong TY: Deep learning in ophthalmology: The technical and clinical considerations. *Prog Retin Eye Res*, 72:100759, 2019. DOI: 10.1016/j.preteyeres.2019.04.003

18. He K, Gkioxari G, Dollar P, Girshick R: Mask R-CNN. **In,** *IEEE International Conference on Computer Vision (ICCV)*. Venice, Italy, 22-29 October 2017. DOI: 10.1109/ICCV.2017.322

19. Gavrishchaka V, Yang Z, Miao R, Senyukova O: Advantages of hybrid deep learning frameworks in applications with limited data. *Int J Mach Learn Comput*, 8 (6): 549-558, 2018. DOI: 10.18178/ijmlc.2018.8.6.744

20. Villagra A, Alba E, Leguizamon G: A methodology for the hybridization based in active components: The case of cGA and scatter search. *Comput Intell Neurosci*, 2016:8289237, 2016. DOI: 10.1155/2016/8289237

21. Ding P, Li J, Wang L, Wen M, Guan Y: HYBRID-CNN: An efficient scheme for abnormal flow detection in the SDN-Based Smart Grid. *Secur Commun Netw*, 2020 (4): 1-20, 2020. DOI: 10.1155/2020/8850550

22. Gülgün OD, Erol H: Medical image classification with hybrid convolutional neural network models. *J Comput Sci Technol*, 1 (1): 28-41, 2020.

23. Tzutalin: LabelImg. Git code. https://github.com/tzutalin/labelImg; *Accessed:* 27 February 2020.

24. Chen Q, Gan X, Huang W, Feng J, Shim H: Road damage detection and classification using Mask R-CNN with DenseNet Backbone. *Comput Mater Contin*, 65 (3): 2201-2215, 2020. DOI: 10.32604/cmc.2020.011191

25. Tychsen-Smith L, Petersson L: Improving object localization with fitness nms and bounded IOU loss. **In,** *Proceedings of the IEEE Conference on Computer Vision and Pattern Recognition*. 2018. https://arxiv.org/pdf/1711.00164.pdf; *Accessed:* 21 July 2020.

26. Battula BP, Balaganesh D: Medical image data classification using deep learning based hybrid model with CNN and Encoder. *RIA*, 34 (5): 645-652, 2020. DOI: 10.18280/ria.340516

27. Hosny A, Parmar C, Quackenbush J, Schwartz LH, Aerts HJWL: Artificial intelligence in radiology. *Nat Rev Cancer*, 18 (8): 500-510, 2018. DOI: 10.1038/s41568-018-0016-5

28. Miskovic V: Machıne learning of hybrid classification models for decision support. **In,** Sinteza 2014. Impact of Internet on Business Activities in Serbia and Worldwide, Belgrade, Singidunum University, Serbia, 318-323, 2014. DOI: 10.15308/SINTEZA-2014-318-323

29. Bemani A, Baghban A, Mosavi A, Shahab S: Estimating CO2-Brine diffusivity using hybrid models of ANFIS and evolutionary algorithms.

Eng Appl Comput Fluid Mech, 14 (1): 818-834, 2020. DOI: 10.1080/19942060.2020.1774422

30. Jafarifarmand A, Badamchizadeh MA, Khanmohammadi S, Nazari MA, Tazehkand BM: Real-time ocular artifacts removal of EEG data using a hybrid ICA-ANCapproach. *Biomed Signal Process Control*, 31, 199-210, 2017. DOI: 10.1016/j.bspc.2016.08.006

31. Bharati S, Podder P, Mondal MRH: Hybrid deep learning for detecting lung diseases from X-ray images. *Inform Med Unlocked*, 20:100391, 2020. DOI: 10.1016/j.imu.2020.100391

32. Golmohammadi M, Torbati AHHN, Diego SL, Obeid I, Picone J: Automatic analysis of EEGs using big data and hybrid deep learning architectures. *Front Hum Neurosci*, 13:76, 2019. DOI: 10.3389/fnhum.2019.00076

33. Ma Y, Luo Y: Bone fracture detection through the two-stage system of Crack-Sensitive Convolutional Neural Network, *Inform Med Unlocked*, 22:100452, 2021. DOI: 10.1016/j.imu.2020.100452

34. Starosolski ZA, Herman Kan J, Annapragada A: CNN-based detection of distal tibial fractures in radiographic images in the setting of open growth plates. **In,** *Medical Imaging 2020: Computer-Aided Diagnosis*. Houston, United States, 16-19 February, 2020. DOI: 10.1117/12.2549297

35. Olczak J, Fahlberg N, Maki A, Razavian AS, Jilert A, Stark A, Sköldenberg O, Gordon M: Artificial intelligence for analysing orthopaedic trauma radiographs. *Acta Orthop*, 88 (6): 581-586, 2017. DOI: 10.1080/17453674.2017.1344459

Kafkas Universitesi Veteriner Fakultesi Dergisi
ISSN: 1300-6045 e-ISSN: 1309-2251
Journal Home-Page: http://vetdergikafkas.org

Kafkas Univ Vet Fak Derg
27 (3): 355-361, 2021
DOI: 10.9775/kvfd.2021.25525

RESEARCH ARTICLE

The Effect of Synovial Fluid as a Natural Source of Hyaluronic Acid on Limberg Flap and Elliptical Rotation Flap Healing: A Comparative Study of Full-Thickness Excisional Dermal Wounds in Mice

Hasan ÇANTAY [1,a (*)] Uğur AYDIN [2,b] Turgut ANUK [1,c]
Emin KARAKURT [3,d] Uğur YILDIZ [2,e] Hilmi NUHOĞLU [3,f]

[1] Kafkas University, Faculty of Medicine, Department of General Surgery, TR-36100 Kars - TURKEY
[2] Kafkas University, Faculty of Veterinary Medicine, Department of Surgery, TR-36100 Kars - TURKEY
[3] Kafkas University, Faculty of Veterinary Medicine, Department of Pathology, TR-36100 Kars - TURKEY
ORCIDs: [a] 0000-0003-3309-8879; [b] ORCID: 0000-0001-5756-4841; [c] ORCID: 0000-0002-8903-9993; [d] ORCID: 0000-0003-2019-3690
[e] ORCID: 0000-0002-4782-1012; [f] ORCID: 0000-0003-2530-2542

Article ID: KVFD-2021-25525 Received: 06.02.2021 Accepted: 20.05.2021 Published Online: 24.05.2021

Abstract

The purpose of this study was to investigate the efficacy of synovial fluid (SF) as a source of hyaluronic acid (HA) on Limberg and Elliptical rotation flap healing. In this study conducted on 24 male Mus musculus mice, the animals were divided into 2 main groups. Group 1 (n = 12): Limbergflap group; Group 2 (n = 12) Elliptical rotation flap group. Six of the animals in Group 1 and Group 2 were assigned as the Flap (Control) Group, and 6 as the Flap + SF Group. In SF subgroups of animals in each group, 1 mL SF was injected into the operation area in addition to the flap surgical procedure. The groups were compared in terms of epithelialization, angiogenesis, neutrophil leukocyte infiltration and fibroblast activity, and the effect of SF on the inflammation and wound healing was evaluated. It was observed that epithelization was completed in all animals in the groups which were administered compared to the other groups, and there was a statistically significant difference ($P<0.05$). In addition, no necrosis or abscess was found in the groups which were administered SF. There was no statistical difference in the paired comparisons of neutrophil-leukocyte infiltration and fibroblast activity parameters. Although the Limberg flap technique is more commonly used today, it can be said that elliptical rotation flap is a method that can be used in routine practice due to a lower complication rate. However, SF increases epithelization and plays a regulatory role on angiogenesis. Therefore, it is concluded that the use of SF as a source of HA in combination with elliptical rotation flap in wounds with material tissue loss will contribute to clinical practice.

Keywords: *Elliptical rotation flap, Hyaluronic acid, Limberg flap, Synovial fluid, Experimental study, Wound healing*

Doğal Bir Hyaluronik Asit Kaynağı Olarak Sinovyal Sıvının Limberg Flep ve Eliptik Rotasyon Flep İyileşmesi Üzerine Etkisi: Farelerde Tam Katmanlı Eksizyonel Dermal Yaralarda Karşılaştırmalı Bir Çalışma

Öz

Bu çalışmada, doğal bir hyaluronik asit (HA) kaynağı olarak sinovyal sıvının (SS) Limberg ve Eliptik rotasyon flep iyileşmesi üzerine etkinliğinin araştırılması amaçlandı. Yirmi dört adet erkek Mus musculus cinsi fare üzerinde yapılan bu çalışmada hayvanlar 2 ana gruba ayrıldı. Grup 1 (n=12): Limberg flep grubu; Grup 2 (n=12) Eliptik rotasyon flep grubu. Grup 1 ve Grup 2'deki hayvanların 6'sı Flep (Kontrol) Grubu, 6'sı ise Flep + SS Grubu olarak ayrıldı. Her bir gruptaki hayvanların SS alt gruplarında flep cerrahi prosedürüne ek olarak operasyon bölgesine 1 mL SS enjekte edildi. Epitelizasyon, anjiyogenezis, nötrofil lökosit infiltrasyonu ve fibroblast aktivitesi yönünden gruplar karşılaştırılarak SS'nın flep viabilitesi ve yara iyileşmesine olan etkisi değerlendirildi. SS uygulanan gruplarda hayvanların tamamında, diğer gruplara göre epitelizasyonun tamamlandığı ve istatistiksel olarak anlamlı farklılık olduğu görüldü ($P<0.05$). Ayrıca, SS verilen gruplarda nekroz ve apseye rastlanmadı. Nötrofil-lökosit infiltrasyonu ve fibroblast aktivitesi parametrelerindeki ikili karşılaştırılmalarda ise istatistiksel fark saptanmadı. Limberg flep tekniği günümüzde daha çok uygulanıyor olsa da eliptik rotasyon flebinde komplikasyonun daha az olması nedeniyle rutinde uygulanabilecek bir yöntem olduğu söylenebilir. Bununla birlikte SS, epitelizasyonu arttırmakta ve angiogenezis üzerinde düzenleyici rol üstlenmektedir. Bu sebeplerle, bir HA kaynağı olarak SS'nın, maddi doku kayıplı yaralarda eliptik rotasyon flebi ile birlikte kullanımının klinik pratiğe katkı sağlayacağı belirlenmiştir.

Anahtar sözcükler: *Eliptik rotasyon flebi, Hyaluronik asit, Limberg flep, Sinovyal sıvı, Deneysel çalışma, Yara iyileşmesi*

How to cite this article?

Çantay H, Aydın U, Anuk T, Karakurt E, Yıldız U, Nuhoğlu H: The effect of synovial fluid as a natural source of hyaluronic acid on limberg flap and elliptical rotation flap healing: A comparative study of full-thickness excisional dermal wounds in mice. *Kafkas Univ Vet Fak Derg,* 27 (3): 355-361, 2021. DOI: 10.9775/kvfd.2021.25525

(*) Corresponding Author

Tel: +90 533 623 5576
E-mail: hasan_cantay@hotmail.com (H. Çantay)

Introduction

Wound is defined as the disruption of the anatomical and functional continuity of living tissue. Wound healing occurs as a result of a series of events consisting of hemostasis and inflammation, proliferation (proliferation of cells) and restructuring and maturation phases in order to restore the integrity and functional capacity of the tissue. Prolonged duration or interruption of any of these phases causes delay in wound healing or the wound to become chronic [1,2]. In addition to biochemical markers such as nitric oxide (NO), histamine and polypeptide growth factors, nutrition, diabetes, chemotherapy, radiotherapy, genetic and immunological disorders and infection are among the factors affecting wound healing [3].

In traumatic situations with severe tissue loss, flap surgery is a method frequently used to repair defects. For this purpose, many local flap techniques such as elliptical rotation, Limberg, V-Y advancement flaps and Z-plasty are used. Despite advances in surgical techniques, ischemia and necrosis of flaps remain a critical problem. Furthermore, excessive fibrosis and generalized adhesions are also an important problem in tissue healing [4,5].

Hyaluronic acid (HA), a glycosaminoglycan first discovered by Meyer and Palmer in 1934, is known to be involved in the regulation of TGF β-1 (carrier growth factor) and wound healing by providing fibroblast and myofibroblastic proliferation [4-6]. It is commonly used as a viscoelastic material, especially in eye, nerve and muscle surgery, to contribute to the primary healing of injured tissues by preventing adhesion [7-10].

The purpose of this study was to compare the effects of Limberg and Elliptical rotation flap techniques on tissue viability and to investigate the efficacy of SF as a source of HA in preventing excessive fibrosis, which is an important problem in tissue healing.

Material and Methods

Ethical Approval

The study was conducted with the approval of the Ethics Committee of Kafkas University Animal Experiments Local Ethics Committee with the research code (Approval no: KAU -HADYEK/2020-157).

Animals

A total of 24 male *Mus musculus* mice, 8-12 weeks old and weighing 40-45 g, were included in the study. Mice were housed in separate cages under standard laboratory conditions (12 h dark/12 h daylight, 45%-55% humidity, and room temperature 20-22°C). Animals were fed *ad libitum* with a standard feed and water.

Study Groups

Animals were divided into two main groups (n=12).

Group 1: Limberg Flap Group

Group 1-A (n = 6): Limberg Flap (Control) Group

Group 1-B (n = 6): Limberg Flap + Synovial Fluid Group

Group 2: Elliptical Rotation Flap Group

Group 2-A (n = 6): Elliptical Rotation Flap (Control) Group

Group 2-B (n = 6): Elliptical Rotation Flap + Synovial Fluid Group

In addition to the flap technique used in SF subgroups in Group 1 and Group 2, 1 mL volume of SF was administered to the wound area (subcutaneous and intradermal). Synovial fluid was collected from both tarsal joints of a healthy bovine after the asepsis of the area, by arthrocentesis and used after centrifugation using a Rotina 380 R device for 10 min at 3500 rpm. The cow whose synovial fluid was taken was a healthy animal raised at the university, and the synovial fluid taken was used without waiting.

Anesthesia

The study was conducted under general anesthesia induced by intraperitoneal injection of 10 mg/kg xlazine HCl (Rompun, 2%, Bayer®) and 100 mg/kg ketamine HCl (Ketas, 50 mg/mL, Pfizer®) mixture.

Surgery

After shaving and disinfection of the dorsal area (povidone iodine + 70% ethanol, ISOLABÒ) in each of the animals included in the experiment, a skin excision with a diameter of 2.5x3.0 cm containing all layers which can not be closed without flap was made, and tissue loss wound was created *(Fig. 1-a, Fig. 2-a)*.

The excisional wound created in Group 1-A was closed using the Limberg flap technique *(Fig. 1)* and in Group 2-A using the Elliptical Rotation Flap technique *(Fig. 2)*; no other procedure was performed. These subgroups were evaluated as the control group of each flap technique. In the animals in Group 1-B and Group 2-B, SF (1 mL) was administered subcutaneously and intradermally to the wound area, following the closure of the wound with suture in accordance with the flap technique in their groups *(Fig. 3-a,b)*.

Wound closure in all groups 4/0 polyglactin 910 (VicrylÒ, ETHICONÒ) was performed with a simple separate suture technique using absorbable suture material.

Postoperative Care

All mice were housed individually in standard cages under

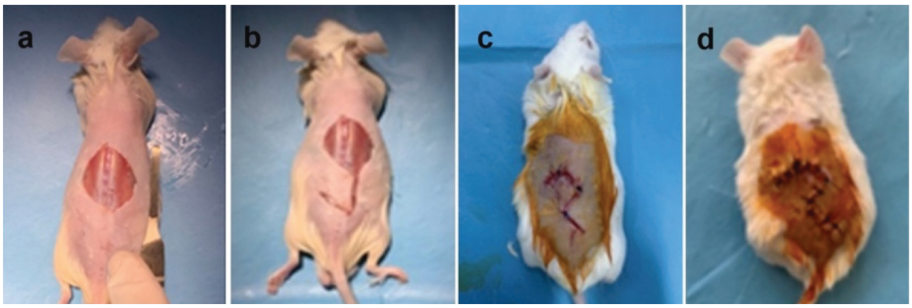

Fig 1. View of Limberg Flap Technique (Group 1-A) application; **a)** Full-thickness excisional wound, **b)** Limberg flap incision, **c-d)** Closure of the incision

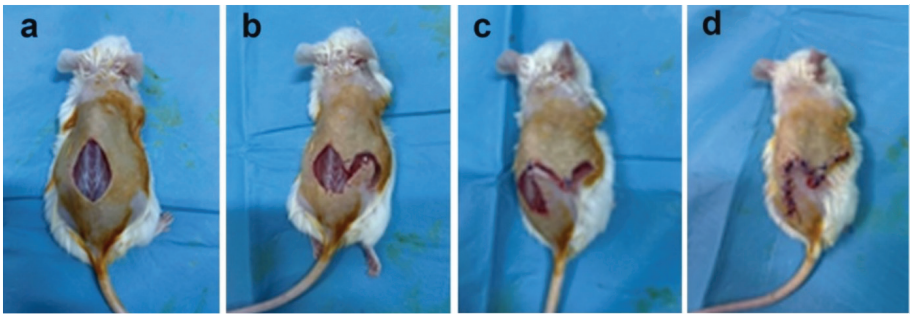

Fig 2. Elliptical Rotation Flap Technique (Group 2-A) application; **a)** Full-thickness excisional wound, **b)** Elliptical rotation flap incision, **c-d)** Closure of the incision

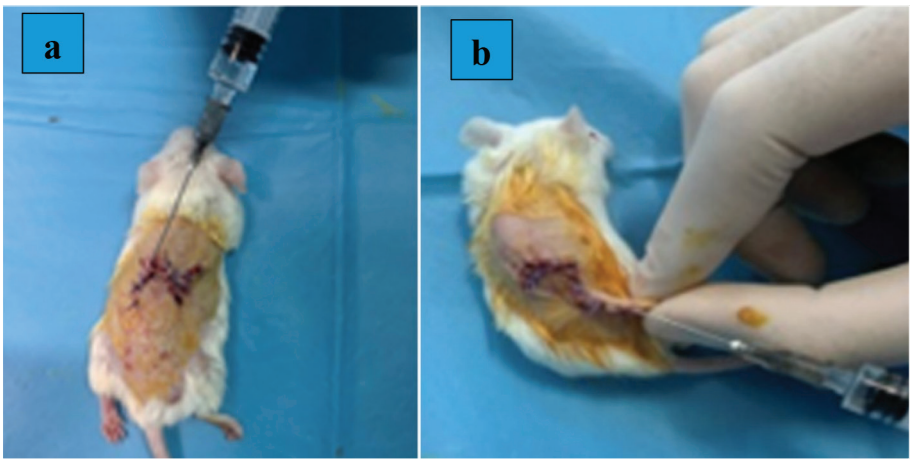

Fig 3. Synovial fluid injection to the wound area. **a)** Limberg Flap Technique (Group 1-B), **b)** Elliptical Rotation Flap Technique (Group 2-B)

standard laboratory conditions, and feed and water were provided to the mice regularly for 7 days.

Macroscopic Examination

On the 7th day of the study, a high dose of pentobarbital sodium was administered by IP route followed by euthanasia. Following euthanasia, the wound site was evaluated and photographed macroscopically. The skin and subcutaneous tissues were excised in full layers, including the entire flap, and submitted to the pathology laboratory for evaluation in 10% formaldehyde solution.

Histopathological Examination

After performing routine tissue follow-up procedures, 4-5 micron thick sections were collected from the prepared paraffin blocks on the microtome device, and Hematoxylin & Eosin (H&E) and Masson's Trichrome staining (Facepath Commercial Kit) were performed to evaluate histopathological changes. Sections were examined under a light microscope (Olympus Bx53) and photographed by the Cell ^P Program (OlympusSoftImaging Solutions GmbH, 3,4).

The sections with H&E and Masson's Trichrome staining were examined and evaluated for epithelization, angiogenesis, neutrophil leukocyte infiltration and fibroblast activity. In the examinations, the suture line in the flap shifted for epithelization was examined; the cases in which epithelization started in the epidermis layer but there was little progress were scored as 1 (+), the cases in which epithelization started but did not close the epidermis scar line were scored as 2 (++), and the cases in which epithelization was completed were scored as 3 (+++). For neutrophil leukocyte infiltration and fibroblast activation, all flap areas in the sections were evaluated and scored as mild (1), moderate (2) and severe (3) based on their severity. For angiogenesis, neocapillary vessels in the regions where angiogenesis was most intense (HighScore method) were counted at 200x magnification.

Statistical Analysis

The normal distribution of the intragroup data was determined by the Shapiro-Wilk test. Mann-Whitney U test was used for comparison of the groups. P<0.05 was considered statistically significant.

Results

Clinical Observations

During the study, all the animals continued their normal lives, and there were no adverse conditions related to the animals or the wound area. It was macroscopically observed that wound healing occurred in all groups on the postoperative day 7 *(Fig. 4)*.

Macroscopic Results

In all groups, when the skin and subcutaneous tissues were excised in full layers, including the entire flap, no macroscopic evidence of infection or necrosis was observed.

Histopathological Results

Group 1-A (Limberg Flap Control Group): Two animals had necrosis and abscess. While epithelization was well formed but not completed in most animals, epithelization was completed in one animal. It was seen that angiogenesis was well formed, and the average of neocapillary vessels counted at 200x magnification was 44.33. It was found that the fibroblast activity was severe in half of the group, and moderate in the other half. It was shown that the fibroblast activity was also moderate in the animal with abscess *(Fig. 5-a,e)*.

Group 1-B (Limberg Flap + Synovial Fluid Group): No signs of necrosis or infection were found. It was found that epithelization was completed in all animals. On the other hand, it was observed that angiogenesis was less than that of the Limberg group and the group mean was 31.33. In all animals except one animal, it was noted that fibroblast activity was severe, but in one animal the fibroblast activity was moderate *(Fig. 5-b,f)*.

Group 2-A (Elliptical Rotation Flap Control Group): One animal had bleeding, necrosis and infection. It was observed that epithelization was good, including the animal with necrosis and infection, but epithelization was not completed except only in one animal. The group average of neocapillary vessel formation was 35.66. Fibroblast activity was moderate, but mild in an animal with necrosis *(Fig. 5-c,h)*.

Group 2-B (Elliptical Rotation Flap + Synovial Fluid Group): No signs of necrosis or infection were found. It was found that epithelization was completed in all animals. The group average of neocapillary vessel formation was 36.00. In all animals except one, it was observed that the fibroblast activity was severe, and this parameter was moderate in one animal *(Fig. 5-d,g)*.

There was no difference in neutrophil leukocyte infiltrates between the groups.

In the statistical comparison, there was a significant difference in epithelization formation between Group 1-A and Group 1-B and Group 2-A and Group 2-B (P<0.05). There was also a statistical difference in terms of angiogenesis in the comparison of Group 1-A and Group 2-A (P<0.05). On the other hand, there was no significant difference in angiogenesis between Group 2-A and Group 2-B, and there was no statistical difference in paired comparisons of neutrophil-leukocyte infiltration and fibroblast activity parameters (P>0.05). In addition, there was no statistical difference in all parameters between Group 1-A and Group 2-A and Group 1-B and Group 2-B (P>0.05) *(Table 1)*.

Discussion

As a natural source of HA, SF contains enzymes such as matrix metallopeptidase-1 (MMP-1), elastase and plasmin, as well as hyaluronan and DN-acetyl glucosamine, which are involved in tissue remodeling in varying concentrations [11]. As is known, HA and viscoelastic materials are antiadhesive agents due to their viscoelastic properties rather than their anti-inflammatory effects [7,8]. In our study, we aimed to

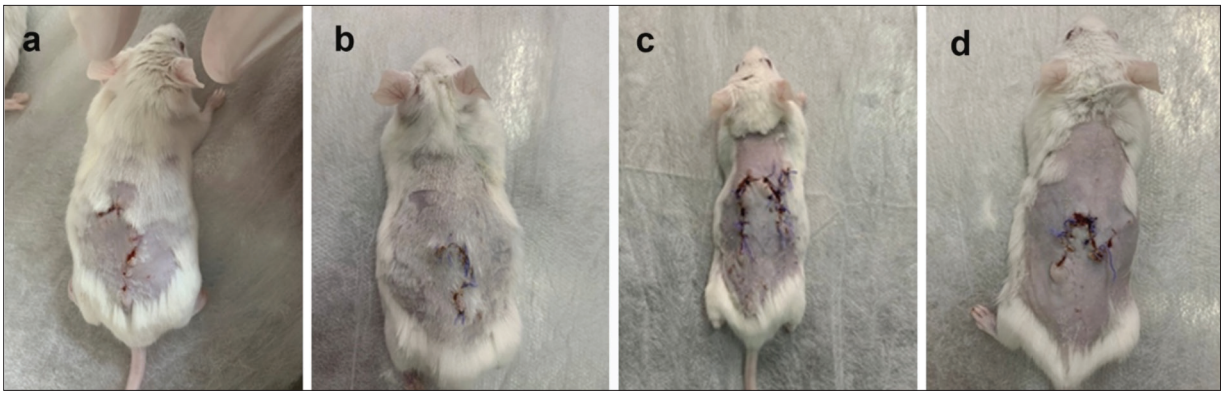

Fig 4. Postoperative 7th day view of all groups; **a)** Group 1-A, **b)** Group 1-B, **c)** Group 2-A, **d)** Group 2-B

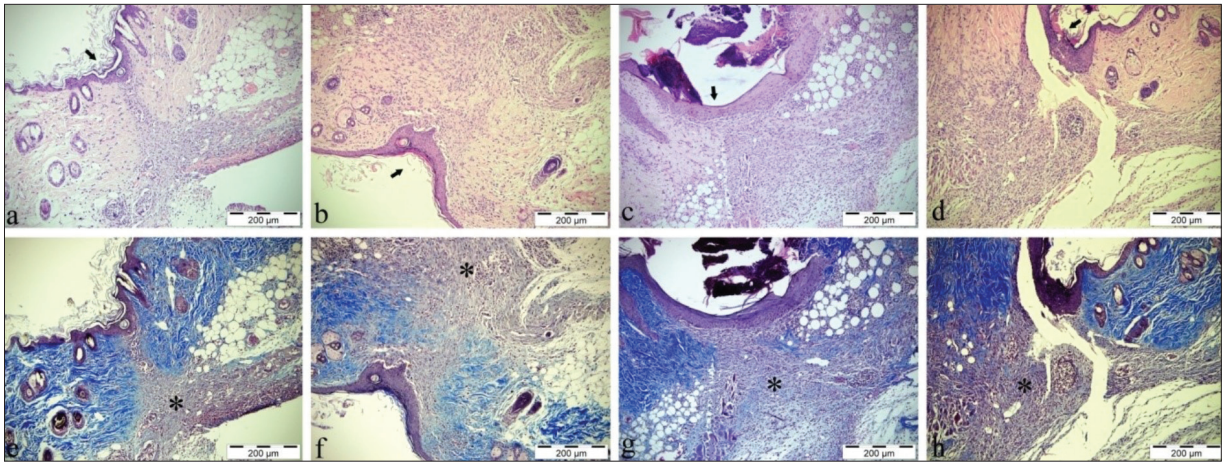

Fig 5. Microscopic images. **a)** Limberg group, H&E, Bar = 200 µm, **b)** Limberg + SF group, H&E, Bar = 200 µm, **c)** Elliptical Group, H&E, Bar = 200 µm, **d)** Elliptical + SF group, H&E, Bar = 200 µm, **e)** Limberg group, MassonTrichrom, Bar = 200 µm, **f)** Limberg + SF group, MassonTrichrom, Bar = 200 µm, **g)** Elliptical + SF group, MassonTrichrom, Bar = 200 µm, **h)** Elliptical group, MassonTrichrom, Bar = 200 µm (Arrows: areas of epithelization, stars: fibroblast activity)

Table 1. *Statistical comparison of the groups in terms of epithelization, angiogenesis, neutrophil-leukocyte infiltration and fibroblast activity*

Groups	Epithelization* (X±SE)	Angiogenesis (X±SE)	Neutrophil Leukocyte Infiltration (X±SE)	Fibroblast Activity (X±SE)
Group 1-A (Limberg Flap)	2.17±0.167 [a]	44.33±2.963 [a]	2.17±0.307 [a]	2.50±0.224 [a]
Group 1-B (Limberg Flap + SF)	3.00 [b]	31.33±2.789 [b]	2.17±0.307 [a]	2.83±0.167 [a]
Group 2-A (Elliptical Rotation Flap)	2.17±0.167 [1]	35.67±6.119 [1]	2.50±0.224 [1]	2.17±0.307 [1]
Group 2-B (Elliptical Rotation Flap + SF)	3.00 [2]	36.00±4.163 [1]	2.33±0.211 [1]	2.83±0.167 [1]

** Due to the lack of variation in the data in the Limberg and Elliptical Rotation Flap + SF groups, only value was given; a,b and 1,2; There is a statistical difference between the groups with different letters and numbers in the same column (P<0.05).* ***SF:*** *Synovial fluid*

investigate the effect of SF on tissue viability, which is one of the most common problems in flap surgery and affects healing, and its effectiveness in preventing excessive fibrosis.

Flap techniques are frequently used in surgery, especially in sacrococcygeal pilonidal sinus disease. Various flap techniques have been described in the treatment of pilonidal sinus disease. These include Z-plasty, W-plasty, VY advancement flap, Limberg Flap, gluteus maximus myocutaneous flap, and fasciocutaneous rotation flap [12]. Limberg flap technique is a method preferred more than other flap techniques due to its satisfactory results [13-15]. The most common complications in flap methods are tissue ischemia, dehiscence, and infection [16]. Furthermore, there are studies showing that maceration, dehiscence and infection are less common in the elliptical rotation flap technique compared to Limberg flap method due to the absence of acute angled end points (corner points) [17–19]. In this study, Limberg and Elliptical rotation flap methods were compared on mice with tissue loss, and it was observed that two mice developed necrosis and abscess in the Limberg group, and one animal developed necrosis and infection in the elliptical rotation group. Although elliptical rotation flap is used less frequently, it can be said that it has a lower rate of complications and can be applied routinely.

It is known that HA, which is a glycosaminoglycan and has regulatory roles in the immune system, mitosis, migration and inflammation, is generally derived from umbilical cord, cockscomb, skin, joint fluid and spinal cord, bacteria and marine animals [9,20]. It has been proven that HA can be used as a potential material to prevent bacterial contamination in dressings for wounds [21]. It is known that HA acts as an antioxidant by retaining free radicals and has a protective effect by removing tissue-destroying enzymes from the environment in inflammation [22,23]. The viscous structure of HA helps delay the viral and bacterial passage in the pericellular region rich in hyaluronic acid [24-26]. In our study, SF obtained from bovine joints was used as the source of HA. No mice developed necrosis and abscess in mice administered intradermal and subcutaneous SF in Group 1-B and Group 2-B, and a total of three mice developed necrosis and abscess in Group 1-A and Group 2-A without SF injection. These results suggest that SF creates a barrier

in the wound area due to its viscous structure, preventing the infection and thus the development of necrosis and abscess.

The role of HA in the wound healing process is fundamental to the wound healing process in many of the HA-mediated biological processes. Wound healing after injury consists of tightly regulated successive processes. These are inflammation, granulation tissue formation, reepithelization and remodeling. HA has a versatile role in these cellular and matrix related events. It is known that HA makes wound matrix more permeable for fibroblast migration and accelerates wound healing [4,22,23]. When evaluated in terms of epithelization, in our study, it was observed that epithelization was completed in all mice in the groups that received SF compared to the groups that did not receive SF.

Hyaluronic acid has a role in the control of angiogenesis. High molecular weight HA in the extracellular matrix has been shown to inhibit angiogenesis. In contrast, various experimental models have shown that low molecular weight HA oligosaccharides stimulate angiogenesis and increase collagen production by endothelial cells [22,23]. HA also reduces platelet adhesion and thrombosis. However, sulfated HA derivatives exhibit heparin-like properties, preventing blood coagulation [27]. In terms of angiogenesis, there was a statistically significant difference only between Group 1-A and Group 1-B in the comparison of the groups. Angiogenesis was lower in the Limberg group administered SF compared to the group without SF. The probable reason for this may be explained by both the stimulating and the inhibitory effect of SF during the angiogenesis process.

It is known that HA makes the wound matrix more permeable in terms of fibroblast migration and accelerates wound healing [4,23]. In our study, histopathologically, there was no statistically significant difference in fibroblastic activity between the groups, and it was observed that SF did not increase the fibroblastic activity.

In the healing process which begins immediately after wound formation, neutrophils and macrophages migrate from the circulation to the wound area due to the effect of mediators secreted in the first stage of inflammation, and wound healing occurs as a result of collagen synthesis and contraction with the contribution of other cells [28]. In a study conducted on mice, HA was found to be effective in the restoration of wound matrix and rapid migration of leukocytes [29]. In our study, it was observed that SF did not affect neutrophil leukocyte infiltration.

In conclusion, although the Limberg flap technique is commonly used as a flap method today, it can be said that elliptical rotation flapis a method that can be used in routine practice due to a lower complication rate. However, SF, a source of HA, which has a role in almost every stage of wound healing, increases epithelization and plays a regulatory role in angiogenesis. For these reasons, it is concluded that the use of SF as a source of HA in combination with the elliptical rotation flap technique in wounds with material tissue loss will contribute to clinical practice.

Study Limitations

Since the number of subjects in the study is limited, it is necessary to be careful in generalizing the results to the population.

Financial Support

This research did not receive any specific grant from funding.

Conflict of Interest

The authors declared no conflict of interest.

Author Contributions

HÇ - Study design, data collections, data analysis, writing. UA, TA, EK, UY, HN - Study design, Data collections

References

1. Anuk T, Öztürk S, Özaydin İ, Kahramanca Ş, Yayla S, Aksoy Ö, Okumuş Z, Aydin U, Bilgin BÇ, Demirkan İ: Comparison of three fixation methods for the prevention of wound contractions in diabetic and non-diabetic mice with full-thickness skin excision. *Kafkas Univ Vet Fak Derg*, 22 (5): 647-651, 2016. DOI: 10.9775/kvfd.2015.14837

2. Özaydin İ, Aksoy Ö, Yayla S, Kurt B, Kılıç E, Bingöl SA, Can İ, Deprem T: Clinical, histopatological and immunohistochemical evaluation of the effects of topical NPH-insulin on full-thickness open wounds: An *in-vivo* study in diabetic and non-diabetic mice. *Ankara Univ Vet Fak Derg,* 65, 219-228, 2018. DOI: 10.1501/Vetfak_0000002850

3. Kurt B, Bilge N, Sözmen M, Aydın U, Önyay T, Özaydın İ: Effects of *Plantago lanceolata* L. extract on full thickness excisional wound healing in a mouse model. *Biotech Histochem,* 93 (4): 249-257, 2018. DOI: 10.1080/10520295.2017.1421773

4. Özer K, Karabağlı M, Uğurlu K: A new flap model in the treatment of non-healing elbow wounds in dogs: The island arterial composite flap comprising the skin originating from the thoracodorsal artery, the cutaneous trunci muscle and fascia of the latissimus dorsi muscle. *Kafkas Univ Vet Fak Derg*, 22 (6): 829-835, 2016. DOI: 10.9775/kvfd.2016.15425

5. Lee MS, Ahmad T, Lee J, Awada HK, Wang Y, Kim K, Shin H, Yang HS: Dual delivery of growth factors with coacervate-coated poly(lactic-co-glycolicacid) nanofiber improves neovascularization in a Mouse skin flap model. *Biomaterials*, 124, 65-77, 2017. DOI: 10.1016/j.biomaterials.2017.01.036

6. Dehdashtian A, Afshari K, Jazaeri SZ, Haddadi NS, Sheikhi M, Abbaszadeh-Kasbi A, Tavangar SM, Jazaeri F, Amirlak B, Dehpour AR: Sumatriptan increase skin flap survival through activation of 5HT 1b/1d receptors in rats: the mediating role of nitric oxide pathway. *Plast Reconstr Surg*, 144 (1): 70e-77e, 2019. DOI: 10.1097/PRS.0000000000005740

7. Çolak A, Özaydın İ, Okumuş Z, Özcan K, Oral H: Koyunlarda deneysel meme başı lezyonlarının viskoşirurjikal sağaltımı. *Kafkas Univ Vet Fak Derg*, 1 (1-2): 36-41, 1995.

8. Cihan M: Viskoşirurji. *Kafkas Univ Vet Fak Derg*, 4 (1-2): 119-122, 1998.

9. Ermutlu CŞ, Kılıç E, Aksoy Ö, Yayla S, Baran V, Dağ S, Ulkay MB, Aydın U, Demirtaş B: Effect of bovine corpus vitreum on full-thickness dermal wound healing: An experimental study in rats. *Kafkas Univ Vet Fak*

Derg, 24 (1): 33-38, 2018. DOI: 10.9775/kvfd.2017.18189

10. Özaydın İ, Ünsaldı E, Aksoy Ö, Yayla S, Kaya M, Ulkay Tunalı MB, Aktaş A, Taşdemiroğlu E, Cihan M, Kurt B, Yıldırım HC, Şengöz A, Erdoğan H: The effect of silicone tube and silicone tube + hyaluronic acid application on adhesion formation in experimental peri- and epi-neurorrhaphy in a rat model. *Kafkas Univ Vet Fak Derg*, 20 (4): 591-597, 2014. DOI: 10.9775/kvfd.2014.10583

11. Palmer M, Stanford E, Murray MM: The effect of synovial fluid enzymes on the biodegradability of collagen and fibrin clots. *Materials*, 4, 1469-1482, 2011. DOI: 10.3390/ma4081469

12. Sarı R, Akbaba S, Gündoğdu RH, Yazıcıoğlu MÖ: Comparison of the V-Y flap and limberg flap operations in pilonidal sinus surgery. *Turk J Colorectal Dis*, 29, 69-74, 2019. DOI: 10.4274/tjcd.galenos.2018.10437

13. Lee PJ, Raniga S, Biyani DK, Watson AJM, Faragher IG, Frizelle FA: Sacrococcygeal pilonidal disease. *Colorectal Dis*, 10, 639-650, 2008. DOI: 10.1111/j.1463-1318.2008.01509.x

14. Sevinc B, Damburacı N, Karahan Ö: Longterm results of minimaly invasive treatment of pilonidal disease by platelet rich plasma. *J Visc Surg*, 157, 33-35, 2020. DOI: 10.1016/j.jviscsurg.2019.07.004

15. Isik A, Idiz O, Firat D: Novel approaches in pilonidal sinus treatment. *Prague Med Rep*, 117, 145-152, 2016. DOI: 10.14712/23362936.2016.15

16. Sit M, Aktas G, Yilmaz EE: Comparison of three surgical flap techniques in pilonidal sinus surgery. *Am Surg*, 79, 1263-1268, 2013. DOI: 10.1177/000313481307901217

17. Dizen H, Yoldas O, Yıldız M, Cilekar M, Dilektaslı E: Modified elliptical rotation flap for sacrococcygeal pilonidal sinus disease. *ANZ J Surg*, 84, 769-771, 2014. DOI: 10.1111/ans.12818

18. Yoldas O, Dizen H , Cilekar M, Yildiz M , Dilektasli E : Comparison of modified limberg flap and modified elliptical rotation flap for pilonidal sinus surgery: a retrospective cohort study. *Int J Surg*, 16, 74-77, 2015. DOI: 10.1016/j.ijsu.2015.02.024

19. Gundogdu E: Fasciocutaneous elliptical rotation flap for pilonidal sinus disease and its outcomes. *Turk J Surg*, 36 (3): 310-316, 2020. DOI: 10.47717/turkjsurg.2020.4917

20. Giji S, Arumugam M: Isolation and characterization of hyaluronic acid from marine organisms. *Adv Food Nutr Res*, 72, 61-77, 2014. DOI: 10.1016/B978-0-12-800269-8.00004-X

21. Lequeux I, Ducasse E, Jouenne T, Thebault P: Addition of antimicrobial properties to hyaluronic acid by grafting of antimicrobial peptide. *Eur Polym J*, 51, 182-190, 2014. DOI: 10.1016/j.eurpolymj.2013.11.012

22. Chen WYJ, Abatangelo G: Functions of hyaluronan in wound repair. *Wound Repair Regen*, 7, 79-89, 1999. DOI: 10.1046/j.1524-475x.1999.00079.x

23. Jiang D, Liang J, Noble PW: Hyaluronan in tissue injury and repair. *Annu Rev Cell Dev Biol*, 23, 435-461, 2007. DOI: 10.1146/annurev.cellbio.23.090506.123337

24. Almond A: Hyaluronan. *Cell Mol Life Sci*, 64 (13): 1591-1596, 2007. DOI: 10.1007/s00018-007-7032-z

25. Girish KS, Kemparaju K: The magic glue hyaluronan and its eraser hyaluronidase: A biological overview. *Life Sci*, 80 (21): 1921-1943, 2007. DOI: 10.1016/j.lfs.2007.02.037

26. Price RD, Berry MG, Navsaria HA: Hyaluronic acid: The scientific and clinical evidence. *J Plast Reconstr Aesthet Surg,* 60, 1110-1119, 2007. DOI: 10.1016/j.bjps.2007.03.005

27. Barbucci R, Magnani A, Casolaro M,Marchettini N, Rosi C, Bosco M: Modification of hyaluronic acid by insertion of sulfate groups to obtain a heparin like molecule. Part I. Characterization and behavior in aqueous solution towards H+ and Cu2+ ions. *Gazz Chim Ital,* 125, 169-180, 1995.

28. Özler M, Şimşek K, Topal T, Öter Ş, Korkmaz A: Pinealektomili ratlarda yara iyileşmesi. *Gulhane Med J*, 52, 181-184, 2010.

29. Mack JA, Feldman RJ, Itano N, Kimata K, Lauer M, Hascall VC, Maytin EV: Enhanced inflammation and accelerated wound closure following tetraphorbol ester application or full-thickness wounding in mice lacking hyaluronan synthases *Has1* and *Has3*. *J Invest Dermatol*, 132 (1): 198-207, 2012. DOI: 10.1038/jid.2011.248

Kafkas Universitesi Veteriner Fakultesi Dergisi
ISSN: 1300-6045 e-ISSN: 1309-2251
Journal Home-Page: http://vetdergikafkas.org

Kafkas Univ Vet Fak Derg
27 (3): 363-370, 2021
DOI: 10.9775/kvfd.2021.25633

RESEARCH ARTICLE

In vitro Antileishmanial Effect of the Plant Extracts from *Aloe vera* (L.) Burm.f. and *Hypericum perforatum* L. Leaves [1]

Mahmut ÜLGER [1,a] Seda TEZCAN ÜLGER [2,b (*)] Efdal OKTAY GÜLTEKİN [2,c] Erdal YABALAK [3,d]
Harun GÜLBUDAK [2,e] Nuran DELİALİOĞLU [2,f] Ahmet Murat GİZİR [3,g] Gönül ASLAN [2,h]

[1] *This study was supported by grants from the Mersin University Research Foundation, Mersin, Turkey [Project no. 2019-1-AP4-3489]*

[1] Mersin University, Faculty of Pharmacy, Department of Pharmaceutical Microbiology, TR-33169 Mersin - TURKEY
[2] Mersin University, Faculty of Medicine, Department of Medical Microbiology, TR-33343 Mersin - TURKEY
[3] Mersin University, Faculty of Arts and Science, Department of Chemistry, TR-33343 Mersin - TURKEY
ORCIDs: [a] 0000-0001-6649-4195; [b] 0000-0002-0823-3680; [c] 0000-0002-0962-152X; [d] 0000-0002-4009-4174; [e] 0000-0003-3199-3132
[f] 0000-0001-8535-3291; [g] 0000-0002-9781-446X; [h] 0000-0002-1221-7907

Article ID: KVFD-2021-25633 Received: 17.02.2021 Accepted: 25.05.2021 Published Online: 26.05.2021

Abstract

The activity of currently available antiparasitic drugs has been threatened by the occurrence of drug-resistant parasite populations, toxic effects, and high cost. Therefore, the discovery of more potent antiparasitic drugs coming from medicinal plants is seen as a significant approach to overcome the problem. This study aimed to evaluate the *in vitro* efficiency of plant extracts of *Aloe vera* (L.) Burm.f. and *Hypericum perforatum* L. leaves against promastigote forms of *Leishmania tropica*. The antileishmanial activity of the plant extracts was determined using *in vitro* microdilution method. Decreasing concentrations (25 to 0.01 mg/mL) of extracts were tested on *Leishmania* promastigotes. The effect of plant extracts on the viability of promastigotes of *L. tropica* was evaluated by counting viable or motile forms in a Neubauer hemocytometer. The data assessed as % growth in comparison to the controls. The 50% inhibitory concentration (IC_{50}) values of the plant extracts were determined using The Quest Graph™ IC_{50} Calculator by logistic regression analysis. *A. vera* (L.) Burm.f. showed leishmanicidal activity at high concentrations of 25, 12.5, and 6.25 mg/ml with 100% growth inhibition of *L. tropica* promastigotes, while *H. perforatum* L. was found to be effective at the concentration range of 25 to 1.56 mg/mL. The IC_{50} of *H. perforatum* L. was determined as 0.23 mg/mL, and IC_{50} of *A. vera* (L.) Burm.f was determined as 1.91 mg/mL. Our study showed that *A. vera* (L.) Burm.f. and *H. perforatum* L. leaves can be a potential medicinal alternatives for the treatment of Leishmaniasis. The antiparasitic efficiency of these plant extracts can be considered a significant improvement in the specification of antileishmanial agents and should be supported by further *in vivo* studies.

Keywords: *In vitro antileishmanial effect, Aloe vera (L.) Burm.f., Hypericum perforatum L.*

Aloe vera (L.) Burm.f. ve *Hypericum perforatum* L. Yapraklarından Elde Edilen Bitki Ekstraktlarının *İn vitro* Antileishmanial Etkisi

Öz

Günümüzde mevcut antiparazitik ilaçların etkinliği, ilaca dirençli parazit popülasyonlarının ortaya çıkması, toksik etkiler ve yüksek maliyet nedeniyle tehdit altındadır. Bu nedenle, tedavi edici bitkilerden parazitlere karşı daha etkili ilaçların ortaya çıkarılması, bu sorunun üstesinden gelmek için önemli bir yaklaşım olarak görülmektedir. Çalışmada, *Aloe vera* (L.) Burm.f. and *Hypericum perforatum* L. bitki ekstraktlarının *Leishmania tropica*'nın promastigot formlarına karşı *in vitro* etkinliğinin değerlendirilmesi amaçlandı. Bitki ekstraktlarının *in vitro* antileishmanial aktivitesi mikrodilüsyon yöntemi kullanılarak belirlendi. Ekstraktların azalan konsantrasyonları (25 ila 0.01 mg/mL) *Leishmania* promastigotları üzerinde test edildi. Bitki ekstraktlarının *L. tropica* promastigotlarının canlılığı üzerindeki etkisi, Neubauer hemositometrede canlı veya hareketli formlar sayılarak değerlendirildi ve veriler kontrollere kıyasla % büyüme olarak değerlendirildi. Her ekstrakt için %50 inhibitör konsantrasyon (IC_{50}) değerleri, Quest Graph™ IC_{50} Hesaplayıcı kullanılarak lojistik regresyon analizi ile belirlendi. *A. vera* (L.) Burm.f., *L. tropica* promastigotları üzerinde %100 büyüme inhibisyonu ile 25, 12.5 ve 6.25 mg/mL'lik yüksek konsantrasyonlarda *Leishmania* parazitlerini öldürücü aktivite gösterirken, *H. perforatum* L.'un 25 ila 1.56 mg/mL konsantrasyon aralığında etkili olduğu bulundu. *H. perforatum* L.'nin IC_{50}'si 0.23 mg/mL ve *A. vera* (L.) Burm.f'nin IC_{50}'si 1.91 mg/mL olarak belirlendi. Çalışmamız, *A. vera* (L.) Burm.f. ve *H. perforatum* L. yapraklarının, leishmaniasis tedavisi için potansiyel tıbbi alternatif olabileceğini gösterdi. Bu bitki ekstraktlarının antiparazitik etkinliği, antileishmanial ajanlarının belirlenmesinde büyük bir gelişme olarak düşünülebilir ve daha ileri *in vivo* çalışmalarla desteklenmelidir.

Anahtar sözcükler: *İn vitro antileishmanial etki, Aloe vera (L.) Burm.f., Hypericum perforatum L.*

How to cite this article?

Ülger M, Tezcan Ülger S, Oktay Gültekin E, Yabalak E, Gülbudak H, Delialioğlu N, Gizir AM, Aslan G: *In vitro* antileishmanial effect of the plant extracts from *Aloe vera* (L.) Burm.f. and *Hypericum perforatum* L. leaves. *Kafkas Univ Vet Fak Derg,* 27 (3): 363-370, 2021.
DOI: 10.9775/kvfd.2021.25633

(*) Corresponding Author

Tel: +90 324 341 2815-1576 Cellular phone: +90 532 761 0723 Fax: +90 324 341 2312
E-mail: tezcanseda@yahoo.com, tezcanseda@mersin.edu.tr (S. Tezcan Ülger)

Introduction

Leishmaniasis is a vector-borne tropical/subtropical disease caused by the *Leishmania* genus obligate intracellular parasite and is still one of the globally major health problems, particularly in developing countries [1]. The transmission of *Leishmania* to humans occurs through the bite of the *Phlebotomus* genus sandfly or the *Lutzomyia* species in the Old World and the New World, respectively [1,2]. *L. major*, *L. tropica*, *L. infantum*, *L. donovani,* and *L. aethiopica* are Old World leishmaniasis agents [3]. The disease has three clinical manifestations called Visceral, Mucocutaneous and Cutaneous Leishmaniasis (CL). The visceral form is the severest caused mostly by *L. donovani* and *L. infantum* and manifested by an infection of the liver and spleen. The predominantly CL agents are *L. tropica*, *L. major,* and *L. aethiopica*, and CL skin lesions, in most cases, heal on their own and leave permanent scars. Mucocutaneous Leishmaniasis which is caused by *L. braziliensis* and *L. amazonensis* is characterized by destruction and/or obstruction of the nose, pharynx, larynx, and generation of painful mucosal lesions [4].

The treatment of Leishmaniasis is very difficult because the amastigotes, one of the developmental forms of the parasite, are reside in the macrophages of the host [5]. The drug-resistance developed by parasites is the main determinant of treatment failure, although other factors also lead to this event, including immune-deficiency in patients and malnourishment prevent from elimination of the parasites by a natural defense mechanism [5,6]. The pentavalent antimonials have been the first-choice drugs for the treatment of Leishmaniasis, but high cardiotoxicity and development of resistance are the main reasons for treatment failure [7]. Amphotericin B and its lipid formulations, paromomycin, pentamidine, and miltefosine have been alternative drugs for antileishmanial chemotherapy, however, they have restricted use owing to their severe side effects, high cost, or high potential for resistance [6,8]. The toxic effects of the drugs used in the treatment of Leishmaniasis, the expensive treatment, and the resistance of the parasite to the drug have led to the research of alternative treatment methods [9,10].

In search of a better and cheaper leishmanicidal agent, plant extracts and plant-derived bioactive compounds are probably to be a new source of medicinal agents [11]. Moreover, the results obtained from a search about natural products with antileishmanial activity raise the interest in synthetic compounds as potential therapeutic candidates [2,12]. According to the World Health Organization (WHO), up to 80% of developing country populations rely on traditional medicine because of cultural customs or no other choice [13]. Due to the urgent need for alternative treatments in the treatment of Leishmaniasis, it has led researchers screen the activities of natural products for potential use.

A. vera (L.) Burm.f. is a widely used multifunctional medicinal plant belonging to the *Liliaceae* family and has been recognized as an excellent source of home remedies in Asia and the world [14]. The different fractions of *A. vera* leaf are well documented for their different potential activities, including cytotoxic, antimicrobial, anti-leishmanial, antioxidant, and wound healing [14-16]. These features are mainly related to the found of more than 200 different biologically active substances in the inner gel of the leaves [17].

H. perforatum L., belongs to the *Hypericaceae* family, and the olive oil macerate of the flowering plants is a popular home-remedy especially used for quick recovery of cuts and burns in Turkish folk medicine [18]. Moreover, therapeutic effects of this plant have been confirmed for numerous medicinal purposes such as wound healing, treatment of myalgia, antioxidant, anti-inflammatory, anti-cancer, antimicrobial effects, and the antidepressant in different parts of the world [19-21].

The current problems with anti-leishmania drugs have led to the growing need for new drug alternatives. The plants such as *A. vera* (L.) Burm.f. and *H. perforatum* L., which have the potential to be used for drug development against *Leishmania* parasites, may lead to the development of new medicinal substances with more study. The present study was intended to evaluate the *in vitro* efficiency of plant extracts of the *A. vera* (L.) Burm.f. and *H. perforatum* L. leaves obtained by Soxhlet and ultrasonic-assisted extraction (UAE) methods against *L. tropica* promastigotes.

Material and Methods

Preparation of Plant Extract

The *A. vera* (L.) Burm.f. and *H. perforatum* L. leaves were obtained from local people during summer 2018 in the Mersin Province of Southern Turkey.

Soxhlet apparatus was used for Soxhlet extraction, and Bandelin Sonopuls HD 3200 (Berlin, Germany) ultrasonic apparatus (20 kHz, 200 W) with a probe (KE-76) were used for sonication in the UAE method. Ethanol was supplied from JT Baker. Rotary evaporator (Hei-VAP, Heidolph Instruments) was used to concentrate the plant extracts.

Soxhlet Extraction Method

In this study, the most commonly used soxhlet extraction method was used in plant extraction, and ethanol was used as a solvent. 10 g of air-dried and grounded *H. perforatum* L. and *A. vera* (L.) Burm.f. samples were extracted with 300 mL of ethanol for 3.5 h under reflux in each experiment. The densities of the obtained extracts of *H. perforatum* L. and *A. vera* (L.) Burm.f. after concentrating by rotary evaporator were found as 0.068 g/mL and 0.0424 g/mL, respectively.

Ultrasonic Assisted Extraction Method

Ultrasonic-assisted extraction is the other method used in the extraction of *A. vera* (L.) Burm.f. and *H. perforatum* L. samples. 8.3 g of air-dried and grounded samples were placed into a glass beaker following by the addition of 250 mL of ethanol in each experiment. After immersing the probe of the ultrasonic system into the beaker, the UAE process was initialized at 36% amplitude value. The process was carried out under atmospheric pressure for an hour at a fixed temperature of 333 K of temperature. The densities of the concentrated extracts of *A. vera* (L.) Burm.f. and *H. perforatum* L. were found as 0.0295 g/mL and 0.0439 g/mL, respectively.

Preparation of the Dilution of Plant Extracts

The concentrations of *A. vera* (L.) Burm.f. and *H. perforatum* L. plants extract obtained by Soxhlet and UAE methods were adjusted to 25 mg/mL with diluted RPMI 1640 medium (Sigma-Aldrich). The stock solutions were sterilized by filtration through a 0.22 µm pore diameter membrane filter in a laminar cabinet. The extract was utilized fresh and also prepared at different concentrations to evaluate its antileishmanial activity.

Parasite Cultures

L. tropica patient isolate was kindly provided by Professor Gulnaz Culha (Mustafa Kemal University, Faculty of Medicine, Parasitology Department). *L. tropica* promastigotes were cultured in Novy-MacNal-Nicol (NNN) medium overlaid with consolidation fluid, supplemented with 20% heat-inactivated fetal bovine serum (FBS, Biological Industries, USA), 100 IU/mL penicillin-G/0.1 mg/mL streptomycin (Pen Strep, Gibco Thermo Fisher Scientific, USA). Mid-log phase promastigotes were maintained in T25 sterile disposable culture flasks (25 cm^2) by weekly passages at 26°C in RPMI-1640 medium with L-glutamine at pH 6.9 supplemented with 10% FBS, and 100 IU/mL penicillin/0.1 mg/mL streptomycin. The culture is observed daily for parasitic density by using light inverted microscopy and Neubauer haemocytometer. Promastigotes were kept at densities ranging between 1-5x10^5 promastigotes/mL growth.

Promastigote counts: The appearance and motility of promastigotes were monitored microscopic examinations and evaluated by counting the parasites on a Neubauer hemocytometer. Parasite culture samples mixed with vortex were mixed with an equal volume of 0.01 M phosphate-buffered saline (PBS), pH 7.2 containing 2% formaldehyde (Riedel-de Hain, Germany) for immobilization of promastigotes. The promastigote concentration was determined after counting fixed parasites in a Neubauer hemocytometer (Marienfeld SuperiorTM, Germany) at 400x magnification, followed by sufficient dilution in PBS. Parasites were adjusted at densities 5x10^5 promastigotes/mL growth.

In vitro Antileishmanial Activity Assay

In this study, the antileishmanial activity of plant extracts obtained by two different methods was investigated in 96-well microplates by the microdilution method. Promastigotes of *L. tropica* (5x10^5 on growth concentration) were subjected to decreasing concentrations (25 to 0.01 mg/mL) of plant extracts in RPMI-1640 medium supplemented with 20% heat-inactivated FBS on 96 well microtiter plates at 26°C. As a control antileishmanial drug, Amphotericin B (Biological Industries, USA) was used at 4 µg/mL concentration (100% of mortality). After 4 days of cultivation at 26°C, parasites viability was evaluated by counting viable or motile forms in a Neubauer hemocytometer to determine the number of live parasites per well. All experiments were performed in duplicate; after calculating the means, the parasites counted in each dilution well were evaluated as % growth compared to controls [22].

Statistical Analysis

The statistical analysis was determined by Mann Whitney U test and statistical differences were considered significant at p-values less than 0.05. The 50% inhibitory concentration (IC_{50}) values of the plant extracts were determined using The Quest Graph™ IC_{50} Calculator by logistic regression analysis [23]. Drug concentration-parasite inhibition curves were was determined by graphical extrapolation.

Results

After 4 days of incubation at +26°C, the antileishmanial activity of *A. vera* (L.) Burm.f. and *H. perforatum* L. extracts (25 to 0.01 mg/mL) with both of Soxhlet and UAE method resulted in dose-dependent parasite killing by microdilution method. The results were shown as % growth inhibition calculated after counting motile or viable promastigotes for all dilutions of both plant extracts.

A. vera (L.) Burm.f. extracts obtained by Soxhlet extraction method at concentrations of 25, 12.5, and 6.25 mg/mL showed 100% growth inhibition of *L. tropica* promastigotes and showed high to moderate leishmanicidal activity at the concentration range of 3.12 to 0.01 mg/mL by reducing the parasite viability in the range of 95% to 3.4%. *H. perforatum* L. extracts obtained by Soxhlet extraction method at the concentration range of 25 to 1.56 mg/mL showed 100% growth inhibition of promastigotes and showed high to moderate leishmanicidal activity at the concentration range of 0.78 to 0.01 mg/mL by reducing the parasite viability in the range of 96.2% to 3.8% *(Table 1; Fig. 1)*.

At the end of incubation, IC_{50} of the *A. vera* (L.) Burm.f. against *L. tropica* promastigotes was determined as 1.91 mg/mL and IC_{50} of *H. perforatum* L. as 0.23 mg/mL with Soxhlet extraction method.

A. vera (L.) Burm.f. extracts obtained by UAE at concentrations of 25, 12.5, and 6.25 mg/mL showed 100% growth inhibition

Table 1. *Antileishmanial activity of A. vera (L.) Burm.f. and H. perforatum L. plant extracts obtained by Soxhlet extraction method*

Concentration (mg/mL)	*A. vera* (L.) Burm.f.		*H. perforatum* L.	
	Growth Rate (%)	Inhibition Rate (%)	Growth Rate (%)	Inhibition Rate (%)
25	0	100	0	100
12.5	0	100	0	100
6.25	0	100	0	100
3.12	5	95	0	100
1.56	71.8	28.2	0	100
0.78	86.8	13.2	3.8	96.2
0.39	92.3	7.7	11.1	88.9
0.19	94	6	67.2	32.8
0.09	95.2	4.8	87.4	12.6
0.04	96	4	93.6	6.4
0.02	96.2	3.8	95.1	4.9
0.01	96.6	3.4	96.2	3.8

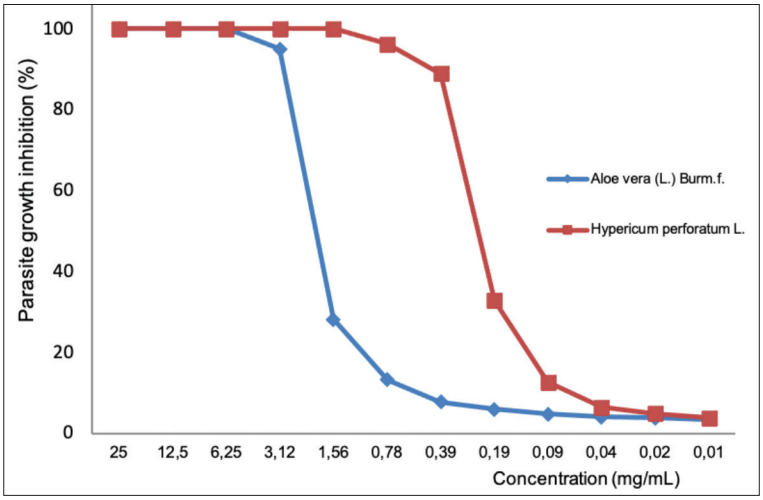

Fig 1. Inhibition of *L. tropica* promastigote growth by *A. vera* (L.) Burm.f. (diamonds) and *H. perforatum* L. (squares) extracts by Soxhlet extraction method

and showed high to moderate leishmanicidal activity at the concentration range of 3.12 to 0.01 mg/mL by reducing the parasite viability in the range of 95.3 to 2.8%. *H. perforatum* L. extracts obtained by UAE at the concentration range of 25 to 1.56 mg/mL showed 100% growth inhibition and showed high to moderate leishmanicidal activity at the concentration range of 0.78 to 0.01 mg/mL by reducing the parasite viability in the range of 98.6% to 3.9% *(Table 2; Fig. 2)*.

There was no statistically significant difference between the effects of extracts of *A. vera* and *H. perforatum* L. plants obtained by Soxhlet extraction method and UAE method on Leishmania promastigotes (P= 0.887).

The IC_{50} of the *A. vera* (L.) Burm.f. against *L. tropica* promastigotes was determined as 2.08 mg/mL and IC_{50} of *H. perforatum* L. as 0.23 mg/mL with UAE method. Amphotericin B was found 100% active at 4 µg/mL against *L. tropica* promastigotes.

Discussion

Leishmaniasis is recognized as a major public health problem by the WHO. It is reported that approximately 350 million people worldwide are at risk of becoming infected with Leishmaniasis, and approximately 0.7-1.2 million of CL and 0.2-0.4 million of Visceral Leishmaniasis cases occur annually [3]. The most common clinical form of Leishmaniasis is CL, and it generally affects poor and developing countries such as the Mediterranean Basin, Asia, the Middle East, Africa, and South America [2,3]. CL is endemic, particularly in the Southeastern and Mediterranean Regions in Turkey [24]. Because of the civil war in Syria, the southern or the southeastern part of Turkey have received great migration, and this is the cause of the complicated epidemiological status of Leishmaniasis [25]. In Turkey, *L. tropica* is responsible for the CL cases, and meglumine antimonate is widely used in the treatment of patients with CL. It has been experimentally shown that

Table 2. *Antileishmanial activity of A. vera (L.) Burm.f. and H. perforatum L. plant extracts obtained by UAE method*

Concentration (mg/mL)	*A. vera* (L.) Burm.f.		*H. perforatum* L.	
	Growth Rate (%)	Inhibition Rate (%)	Growth Rate (%)	Inhibition Rate (%)
25	0	100	0	100
12.5	0	100	0	100
6.25	0	100	0	100
3.12	4.7	95.3	0	100
1.56	83.8	16.2	0	100
0.78	89.1	10.9	1.4	98.6
0.39	92.1	7.9	3.6	96.4
0.19	93.2	6.8	74	26
0.09	94.4	5.6	91.1	8.9
0.04	94.7	5.3	93.1	6.9
0.02	96.1	3.9	94.4	5.6
0.01	97.2	2.8	96.1	3.9

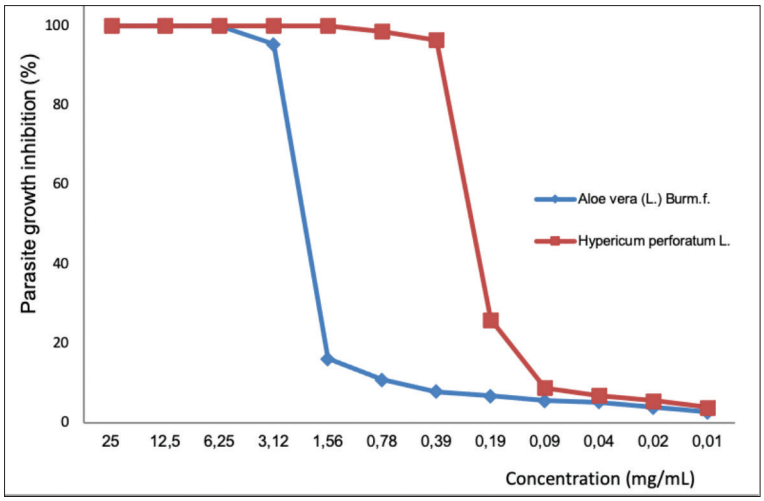

Fig 2. Inhibition of *L. tropica* promastigote growth by *A.vera* (L.) Burm.f. (diamonds) and *H. perforatum* L. (squares) extracts by UAE method

L. tropica isolates acquire resistance against meglumine antimoniate in a very short time in our country and stated that in case of inadequate and incomplete treatment of CL patients, the number of resistant cases might increase rapidly, and resistant leishmaniasis foci might occur [26].

Due to the drug resistance, toxic effects, and high cost of the available drugs for the current treatment of Leishmaniasis [12], various studies have focused on *in vitro/vivo* efficiency of various plant extracts against *Leishmania* species to detect a new antileishmanial component. A range of plant extracts have been shown to exhibit *in vitro* antileishmanial activity and have been approved for use in folk medicine [27].

This is the first study reporting the leishmanicidal activity for locally grown *A. vera* (L.) Burm.f. and *H. perforatum* (L.) species on *L. tropica* in our region, Mersin Province of Southern Turkey. Here, it was shown that, the ethanolic extracts of *A. vera* (L.) Burm.f. and *H. perforatum* (L.) were able to kill promastigote forms of *L. tropica* with the dose-dependent manner.

A. vera (L.) Burm.f. has widespread use in health products, and studies can be performed on the whole herbs, inner gel, and leaf exudate. In several studies, it was identified that the *Aloe* plant extracts had a direct leishmanicidal activity on promastigotes. In a study aimed at evaluating the *in vitro* efficiency of *A. vera* leaf exudate (AVL) against Leishmaniasis, promastigotes were found as susceptible to AVL, and their IC_{50} ranged from 100 to 180 µg/mL [28]. The efficiency of *A. nyeriensis* extracts used in the treatment of parasitic diseases by rural indigenous communities against *L. major* promastigotes was shown to exhibit 68.4±6.30% mortality at 1000 g/mL [9]. In a study by De Queiroz et al.[29] for the first time to confirm the ethno-pharmacological use of traditional medicinal plants including *A. vera* from the Brazilian flora for the treatment of Leishmaniasis, it has been shown that an extract of the *A. vera* plant exhibits direct activity against promastigote

forms at 100 µg/mL and inhibits growth by 82.9%. The IC_{50} values of methanol fraction of *A. vera*, on promastigotes of *L. infantum* were reported as 1.54 µg/mL. The inhibitory effect was determined in *L. infantum* promastigotes, but the low efficiency on amastigote forms and high cytotoxicity in the *in vivo* tests were attributed to secondary metabolites belonging to the quinone group abundant in this plant [30]. However, we found a relatively low efficiency at higher concentrations. In our study, it was observed that ethanolic extracts of *A. vera* (L.) Burm.f. totally inhibited the *in vitro* growth of promastigote forms of *L. tropica* at concentrations of 25, 12.5, and 6.25 mg/mL, by both Soxhlet and UAE methods. The IC_{50} of the *A. vera* (L.) Burm.f. against *L. tropica* promastigotes was determined as 1.91 mg/mL with Soxhlet extraction method and 2.08 mg/mL with UAE method. The low effect of this plant can be attributed to the different distribution or amounts of active substances that mediate the antileishmanial effect.

It has been reported that different extracts of *Aloe* genus plants show activity against protozoa such as *Toxoplasma gondii*, *Plasmodium falciparum*, *Babesia* sp. [31-33], confirming this potential. Therefore, we think that with more studies to be conducted, *A. vera* (L.) Burm.f. may have the potential to develop drugs against *Leishmania* parasites.

Based on our research, although biological activity has been discovered from *H. perforatum*, we did not attain sufficient regional studies on antileishmanial activity. Several reports have confirmed the therapeutical potential of the *Hypericum* genus plants for many medicinal purposes, but there is still insufficient evidence on the efficiency of *H. perforatum* L. against the *Leishmania* parasites. Promising results have been reported showing that lipophilic extracts of *Hypericum* plants are contain useful bioactive compounds for treating leishmaniasis. It was shown that *H. carinatum*, *H. polyanthemum* and *H. linoides* could kill the *Leishmania* parasites depending on the dose, and *H. polyanthemum* exhibited significant IC_{50} leishmanicidal activity at concentration of 36.1 µg/mL [34]. Here we demonstrate antileishmanial activity obtained from extracts of *H. perforatum* L. against promastigote forms of the *L. tropica* parasite. It was observed that ethanolic extracts of *H. perforatum* L. totally inhibited the *in vitro* growth of promastigote forms of *L. tropica* at concentrations of 25 to 1.56 mg/mL, by both of Soxhlet and UAE methods in our study. The IC_{50} of the *H. perforatum* L. against *L. tropica* promastigotes was determined as 0.23 mg/mL with both of Soxhlet and UAE methods.

Studies have shown that plant extracts or isolated compounds belonging to the *Hypericum* genus exhibit antiprotozoal activity against *Trichomonas vaginalis*, *P. falciparum*, *T. gondii*, and inhibition on *Entamoeba* encystation [35-38]. In one study, it was reported that *H. perforatum* olive oil macerate showed mild inhibitory activity against *Trypanosoma brucei rhodesiense* (IC_{50} of 15.9-64.5 µg/mL) [39]. These results demonstrated that *Hypericum* species is a candidate to treat other parasitic diseases, the antiparasitic properties of *H. perforatum* should be revealed by further *in vitro* and *in vivo* studies.

The applied extraction method and the solvent used are among the most important factors in the extraction process from various matrices [40,41]. In our study, for the extraction of antileishmanial agents from plants preferred to use the Soxhlet extraction method and UAE methods using ethanol as a solvent. The methods based on ultrasonic irradiation are new and effective as well as they are environmentally friendly [42]. Nowadays, ultrasonic irradiation-based methods are used in many processes such as oxidation, extraction, etc. [42,43]. UAE method has advantages over conventional methods such as high extraction yield, short extraction time and low energy consumption [44]. At the end of our study, it was determined that there was no difference in the antileishmanial activities of the plant extracts obtained by both methods.

In conclusion, the results of the present study showed that both Soxhlet and ultrasonic-assisted extracts of *A. vera* (L.) Burm.f. and H. *perforatum* L. leaves exhibited antileishmanial activity against *L. tropica* promastigotes *in vitro*, which seems to be promising their use in folk medicine. The antiparasitic efficiency of these plant extracts can be considered as a major improvement in the specification of antileishmanial agents and should be supported by further *in vivo* studies.

Acknowledgments

This study was supported by grants from the Mersin University Research Foundation, Mersin, Turkey [Project no. 2019-1-AP4-3489]. We wish to thank Damla Hazal Sucu from the Department of Biostatistics and Medical Informatics, Mersin University Medical Faculty, for assistance in statistical analysis.

Conflict of Interests

The authors declare that there is no conflict of interest.

Author Contributions

MÜ, STÜ, and GA designed the project. EY, EOG, and AMG performed the extraction of plants. MÜ, STÜ, and EOG performed the experiment and analyzed the data. HG and ND maintained of parasite culture. MÜ and STÜ wrote the manuscript. All authors reviewed and approved the final manuscript.

References

1. Sheikh SS, Amir AA, Amir BA, Amir AA: Leishmaniasis. **In**, Pacheco GAB, Kamboh AA (Eds): Parasitology and Microbiology Research. IntechOpen, 2020. DOI: 10.5772/intechopen.90680

2. Torres Suarez E, Granados-Falla DS, Robledo SM, Murillo J, Upegui Y, Delgado G: Antileishmanial activity of synthetic analogs of the naturally occurring quinolone alkaloid N-methyl-8-methoxyflindersin.

PLoS One, 15 (12): e0243392, 2020. DOI: 10.1371/journal.pone.0243392

3. Alvar J, Vélez ID, Bern C, Herrero M, Desjeux P, Cano J, Jannin J, den Boer M; WHO Leishmaniasis Control Team: Leishmaniasis worldwide and global estimates of its incidence. *PLoS One*, 7 (5): e35671, 2012. DOI: 10.1371/journal.pone.0035671

4. Hong A, Zampieri RA, Shaw JJ, Floeter-Winter LM, Laranjeira-Silva MF: One health approach to leishmaniases: Understanding the disease dynamics through diagnostic tools. *Pathogens,* 9 (10): 809, 2020. DOI: 10.3390/pathogens9100809

5. Ponte-Sucre A, Gamarro F, Dujardin JC, Barrett MP, López-Vélez R, García-Hernández R, Pountain AW, Mwenechanya R, Papadopoulou B: Drug resistance and treatment failure in leishmaniasis: A 21st century challenge. *PLoS Negl Trop Dis,* 11 (12): e0006052, 2017. DOI: 10.1371/journal.pntd.0006052

6. Monge-Maillo B, López-Vélez R: Therapeutic options for visceral leishmaniasis. *Drugs,* 73 (17): 1863-1888, 2013.

7. Ghorbani M, Farhoudi R: Leishmaniasis in humans: Drug or vaccine therapy? *Drug Des Devel Ther,* 12, 25-40, 2017. DOI: 10.2147/DDDT.S146521

8. Moore EM, Lockwood DN: Treatment of visceral leishmaniasis. *J Glob Infect Dis,* 2 (2): 151-158, 2010.

9. Kigondu EVM, Rukunga GM, Keriko JM, Tonui WK, Gathirwa JW, Kirira PG, Irungu B, Ingonga JM, Ndiege IO: Anti-parasitic activity and cytotoxicity of selected medicinal plants from Kenya. *J Ethnopharmacol,* 123 (3): 504-509, 2009. DOI: 10.1016/j.jep.2009.02.008

10. Riezk A, Raynes JG, Yardley V, Murdan S, Croft SL: Activity of chitosan and its derivatives against *Leishmania major* and *Leishmania mexicana in vitro*. *Antimicrob Agents Chemother,* 64 (3): e01772-19, 2020.

11. Andima M, Ndakala A, Derese S, Biswajyoti S, Hussain A, Yang LJ, Akoth OE, Coghi P, Pal C, Heydenreich M, Wong VK, Yenesew A: Antileishmanial and cytotoxic activity of secondary metabolites from *Taberneamontana ventricosa* and two *aloe* species. *Nat Prod Res,* 1-5, 2021. DOI: 10.1080/14786419.2021.1871906

12. Ullah N, Nadhman A, Siddiq S, Mehwish S, Islam A, Jafri L, Hamayun M: Plants as antileishmanial agents: Current scenario. *Phytother Res,* 30 (12): 1905-1925, 2016. DOI: 10.1002/ptr.5710

13. World Health Organization: New WHO guidelines to promote proper use of alternative medicines, *2004, Geneva.* https://www.who.int/mediacentre/news/releases/2004/pr44/en/; *Accessed:* 05.10.2021

14. Tariq H, Zia M, Ihsan-Ul-Haq, Muhammad SA, Khan SA, Fatima N, Mannan A, Abbasi AM, Zhang M: Antioxidant, antimicrobial, cytotoxic, and protein kinase inhibition potential in *Aloe vera* L. *Biomed Res Int,* 2019:6478187, 2019. DOI: 10.1155/2019/6478187

15. Le TB, Beaufay C, Nghiem DT, Mingeot-Leclercq MP, Quetin-Leclercq J: *In vitro* anti-leishmanial activity of essential oils extracted from vietnamese plants. *Molecules,* 22 (7): 1071, 2017. DOI: 10.3390/molecules22071071

16. Soliman AM, Teoh SL, Ghafar NA, Das S: Molecular concept of diabetic wound healing: Effective role of herbal remedies. *Mini Rev Med Chem,* 19 (5): 381-394, 2019. DOI: 10.2174/1389557518666181025155204

17. Radha MH, Laxmipriya NP: Evaluation of biological properties and clinical effectiveness of Aloe vera: A systematic review. *J Tradit Complement Med,* 5 (1): 21-26, 2015. DOI: 10.1016/j.jtcme.2014.10.006

18. Yeşilada E, Honda G, Sezik E, Tabata M, Fujita T, Tanaka T, Takeda Y, Takaishi Y: Traditional medicine in Turkey. V. Folk medicine in the inner Taurus Mountains. *J Ethnopharmacol,* 46 (3): 133-152, 1995. DOI: 10.1016/0378-8741(95)01241-5

19. Barnes J, Anderson LA, Phillipson JD: St John's wort (*Hypericum perforatum L.*): A review of its chemistry, pharmacology and clinical properties. *J Pharm Pharmacol,* 53 (5): 583-600, 2001. DOI: 10.1211/0022357011775910

20. Wölfle U, Seelinger G, Schempp CM: Topical application of St. John's wort (*Hypericum perforatum*). *Planta Med,* 80 (2-3): 109-120, 2014. DOI: 10.1055/s-0033-1351019

21. Zirak N, Shafiee M, Soltani G, Mirzaei M, Sahebkar A: *Hypericum perforatum* in the treatment of psychiatric and neurodegenerative disorders: Current evidence and potential mechanisms of action. *J Cell Physiol,* 234 (6): 8496-8508, 2019. DOI: 10.1002/jcp.27781

22. Delorenzi JC, Attias M, Gattass CR, Andrade M, Rezende C, da Cunha Pinto A, Henriques AT, Bou-Habib DC, Saraiva EM: Antileishmanial activity of an indole alkaloid from *Peschiera australis*. *Antimicrob Agents Chemother,* 45 (5): 1349-1354, 2001. DOI: 10.1128/AAC.45.5.1349-1354.2001

23. AAT Bioquest, Inc: *"Quest Graph™ IC_{50} Calculator"*. https://www.aatbio.com/tools/ic50-calculator; *Accessed:* 04.02.2021.

24. Ok UZ, Balcioğlu IC, Taylan Ozkan A, Ozensoy S, Ozbel Y: Leishmaniasis in Turkey. *Acta Trop*, 84 (1): 43-48, 2002. DOI: 10.1016/s0001-706x(02)00134-1

25. Karakuş M, Çizmeci Z, Karabela ŞN, Erdoğan B, Güleç N: The impact of refugees on leishmaniasis in Turkey: A new Syrian/Turkish *Leishmania tropica* population structure described by multilocus microsatellite typing (MLMT). *Parasitol Res,* 118 (9): 2679-2687, 2019. DOI: 10.1007/s00436-019-06392-w

26. Özbilgin A, Zeyrek FY, Güray MZ, Çulha G, Akyar I, Harman M, Özbel Y, Ertabaklar H, Çavuş İ, Gündüz C: Türkiye'de kutanöz leyşmanyazis etkeni *Leishmania tropica*'da antimon direnç mekanizmasının belirlenmesi. *Mikrobiyol Bul,* 54 (3): 444-462, 2020. DOI: 10.5578/mb.69702

27. Rocha LG, Almeida JRGS, Macêdo RO, Barbosa-Filho JM: A review of natural products with antileishmanial activity. *Phytomedicine,* 12 (6-7): 514-535, 2005. DOI: 10.1016/j.phymed.2003.10.006

28. Dutta A, Mandal G, Mandal C, Chatterjee M: *In vitro* antileishmanial activity of *Aloe vera* leaf exudate: A potential herbal therapy in leishmaniasis. *Glycoconj J*, 24 (1): 81-86, 2007. DOI: 10.1007/s10719-006-9014-z

29. De Queiroz AC, Dias Tde LMF, Da Matta CBB, Cavalcante Silva LHA, de Araújo-Júnior JX, de Araújo GB, Moura Fde BP, Alexandre-Moreira MS: Antileishmanial activity of medicinal plants used in endemic areas in northeastern Brazil. *Evid Based Complement Alternat Med,* 2014:478290, 2014. DOI: 10.1155/2014/478290

30. Rondon FCM, Bevilaqua CML, Accioly MP, Morais SM, Andrade-Junior HF, Machado LKA, Cardoso RPA, Almeida CA, Queiroz-Junior EM, Rodrigues ACM: *In vitro* effect of *Aloe vera*, *Coriandrum sativum* and *Ricinus communis* fractions on *Leishmania infantum* and on murine monocytic cells. *Vet Parasitol,* 178 (3-4): 235-240, 2011. DOI: 10.1016/j.vetpar.2011.01.007

31. Mirzaalizadeh B, Sharif M, Daryani A, Ebrahimzadeh MA, Zargari M, Sarvi S, Mehrzadi S, Rahimi MT, Mirabediny Z, Golpour M, Montazeri M: Effects of *Aloe vera* and *Eucalyptus* methanolic extracts on experimental toxoplasmosis *in vitro* and *in vivo*. *Exp Parasitol,* 192, 6-11, 2018. DOI: 10.1016/j.exppara.2018.07.010

32. Amoah LE, Kakaney C, Kwansa-Bentum B, Kusi KA: Activity of herbal medicines on *Plasmodium falciparum* gametocytes: Implications for malaria transmission in Ghana. *PLoS One,* 10 (11): e0142587, 2015. DOI: 10.1371/journal.pone.0142587

33. Naidoo V, Zweygarth E, Eloff JN, Swan GE: Identification of anti-babesial activity for four ethnoveterinary plants *in vitro*. *Vet Parasitol,* 130 (1-2): 9-13, 2005. DOI: 10.1016/j.vetpar.2005.03.001

34. Dagnino AP, de Barros FMC, Ccana-Ccapatinta GV, Prophiro JS, von Poser GL, Romão PR: Leishmanicidal activity of lipophilic extracts of some *Hypericum* species. *Phytomedicine*, 22 (1): 71-76, 2015. DOI: 10.1016/j.phymed.2014.10.004

35. Menezes CB, Rigo GV, Bridi H, Trentin DDS, Macedo AJ, von Poser GL, Tasca T: The anti-*Trichomonas vaginalis* phloroglucinol derivative isoaustrobrasilol B modulates extracellular nucleotide hydrolysis. *Chem Biol Drug Des,* 90 (5): 811-819, 2017. DOI: 10.1002/ptr.3104

36. Moon HI: Antiplasmodial and cytotoxic activity of phloroglucinol derivatives from *Hypericum erectum* thunb. *Phytother Res,* 24 (6): 941-944, 2010. DOI: 10.1002/ptr.3104

37. Shinjyo N, Nakayama H, Ishimaru K, Hikosaka K, Mi-Ichi F, Norose K, Yoshida H: *Hypericum erectum* alcoholic extract inhibits *Toxoplasma* growth and *Entamoeba* encystation: An exploratory study on the anti-protozoan potential. *J Nat Med,* 74 (1): 294-305, 2020. DOI: 10.1007/

s11418-019-01369-6

38. Shinjyo N, Nakayama H, Li L, Ishimaru K, Hikosaka K, Suzuki N, Yoshida H, Norose K: *Hypericum perforatum* extract and hyperforin inhibit the growth of neurotropic parasite *Toxoplasma gondii* and infection-induced inflammatory responses of glial cells *in vitro*. *J Ethnopharmacol,* 267:113525, 2021. DOI: 10.1016/j.jep.2020.113525

39. Orhan IE, Kartal M, Gülpinar AR, Cos P, Matheeussen A, Maes L, Tasdemir D: Assessment of antimicrobial and antiprotozoal activity of the olive oil macerate samples of *Hypericum perforatum* and their LC-DAD-MS analyses. *Food Chem,* 138 (2-3): 870-875, 2013. DOI: 10.1016/j.foodchem.2012.11.053

40. Yabalak E: Radical scavenging activity and chemical composition of methanolic extract from *Arum dioscoridis* SM. var. *dioscoridis* and determination of its mineral and trace elements. *JOTCSA,* 5 (1): 205-218, 2018. DOI: 10.18596/jotcsa.350370

41. Yabalak E, Emire Z, Adıgüzel AO, Könen Adıgüzel S, Gizir AM: Wide-scale evaluation of *Origanum munzurense* Kit Tan & Sorger using different extraction techniques: Antioxidant capacity, chemical compounds, trace element content, total phenolic content, antibacterial activity and genotoxic effect. *Flavour Fragr J,* 35 (4): 394-410, 2020. DOI: 10.1002/ffj.3574

42. Yabalak E, Külekçi B, Gizir AM: Application of ultrasound-assisted and subcritical water oxidation methods in the mineralisation of Procion Crimson H-EXL using response surface methodology and artificial neural network. *J Environ Sci Health A Tox Hazard Subst Environ Eng,* 54 (14): 1412-1422, 2019. DOI: 10.1080/10934529.2019.1647749

43. Hadidi M, Ibarz A, Pagan J: Optimisation and kinetic study of the ultrasonic-assisted extraction of total saponins from alfalfa (*Medicago sativa*) and its bioaccessibility using the response surface methodology. *Food Chem*, 309:125786, 2020. DOI: 10.1016/j.foodchem.2019.125786

44. Wang Y, Liu J, Liu X, Zhang X, Xu Y, Leng F, Avwenagbiku MO: Kinetic modeling of the ultrasonic-assisted extraction of polysaccharide from Nostoc commune and physicochemical properties analysis. *Int J Biol Macromol,* 128, 421-428, 2019. DOI: 10.1016/j.ijbiomac.2018.12.247

Kafkas Universitesi Veteriner Fakultesi Dergisi
ISSN: 1300-6045 e-ISSN: 1309-2251
Journal Home-Page: http://vetdergikafkas.org

Kafkas Univ Vet Fak Derg
27 (3): 371-379, 2021
DOI: 10.9775/kvfd.2021.25653

RESEARCH ARTICLE

Functional Variables of Bull Sperm Associated with Cryotolerance

Alicia GILMORE [1,a] Mustafa HITIT [1,2,b] Muhammet Rasit UGUR [1,c] Thu Tran Nhat DINH [1,d] Wei TAN [3,e] Dean JOUSAN [1,f] Molly NICODEMUS [1,g] Einko TOPPER [4] Abdullah KAYA [5,h] Erdogan MEMILI [1,i (*)]

[1] Department of Animal and Dairy Sciences, Mississippi State University, Mississippi State, MS, USA
[2] Department of Animal Genetics, School of Veterinary Medicine, Kastamonu University, TR-37150 Kastamonu - TURKEY
[3] Department of Basic Sciences, Mississippi State University, Mississippi State, MS USA
[4] Alta Genetics, Inc. Watertown, WI, USA
[5] Department of Artificial Insemination and Reproduction, School of Veterinary Medicine, Selcuk University, TR-42130 Konya - TURKEY
ORCIDs: [a] 0000-0002-0385-9369; [b] 0000-0001-5636-061X; [c] 0000-0003-1234-6693; [d] 0000-0001-5416-4949; [e] 0000-0002-0340-9739
[f] 0000-0002-2006-0612: [g] 0000-0001-8646-994X; [h] 0000-0002-8022-3743; [i] 0000-0002-8335-5645

Article ID: KVFD-2021-25653 Received: 19.02.2021 Accepted: 01.06.2021 Published Online: 01.06.2021

Abstract

The objective of this study was to ascertain sperm population and cellular characteristics as well as total antioxidant capacity in spermatozoa from Holstein bulls with Good (11 bulls) and Poor (5 bulls) cryotolerance. Post-thaw sperm kinetics were evaluated using CASA, membrane integrity was assessed via HOS test, and DNA fragmentation was measured using the HaloSperm kit. Data were analyzed using principal component analysis. The spermatozoa from Good bulls had a higher number of cells with intact membranes (P=0.029), non-fragmented DNA (P=0.018), and post-thaw viability (P<0.001) compared to sperm cells from Poor cryotolerance bulls. Sperm cells from Good bulls also had a faster average path velocity (P=0.017) and straight-line velocity (P=0.036), along with a greater distance average path (P=0.006) and distance straight line (P=0.011). However, total antioxidant capacity, number of live cells, and other kinetic parameters between spermatozoa from Good and Poor groups were not different. There is no one specific sperm function variable alone that can accurately predict cryotolerance of bull spermatozoa, and thus, a combination of sperm cell attributes and kinematics needs to be utilized by the AI industry in differentiating between freezability of spermatozoa between bulls.

Keywords: *Sperm cryotolerance, Sperm freezability, Sperm parameters*

Boğa Sperminin Kriyotolerans İle İlişkili Fonksiyonel Değişkenleri

Öz

Bu çalışmanın amacı, iyi (11 boğa) ve zayıf (5 boğa) kriyotoleransa sahip Holstein boğalardan sperm popülasyonun ve hücresel özelliklerinin yanı sıra toplam antioksidan kapasitesini belirlemektir. Dondurma çözdürme sonrası sperm kinetiği CASA kullanılarak değerlendirildi, membran bütünlüğü HOS testi ile değerlendirildi ve DNA fragmantasyonu HaloSperm kiti kullanılarak ölçüldü. Veriler, temel bileşen analizi kullanılarak değerlendirildi (PCA). İyi kriyotoleransa sahip boğalardan elde edilen spermatozoa, zayıf kriyotoleranslı boğalardan alınan sperme kıyasla daha fazla sayıda intakt membran (P=0.029), fragmente olmamış DNA'ya (P=0.018) ve dondurma çözdürme sonrası canlılığa (P<0.001) sahip hücre bulunmaktadır. İyi kriyotoleransa sahip boğa sperm hücreleri daha fazla ortalama yol (P=0.017) ve ileri doğru doğrusal hareket hızına sahiptir (P=0.036), bunula birlikte daha büyük bir ortalama mesafe hızı (P=0.006) ve ileri doğru doğrusal mesafe hızına (P=0.011) sahiptir. Ancak, toplam antioksidan kapasitesi, canlı hücre sayısı ve kinetik parametreler iyi ve zayıf kriyotoleransa sahip spermatozoa grupları arasında farklı değildir. Boğa spermatozoanın kriyotoleransını doğru bir şekilde tahmin edebilecek tek bir spesifik sperm fonksiyon değişkeni yoktur ve bu nedenle, sperm hücresi özelliklerinin ve kinematiklerin bir kombinasyonunun, boğalar arasındaki spermlerin dondurulabilirliğini ayırt etmede suni tohumlama endüstrisi tarafından kullanılması önerilmektedir.

Anahtar sözcükler: *Sperm kriyotolerans, Sperm dondurulabilirliği, Sperm parametreleri*

INTRODUCTION

The spermatozoon is composed of several membrane-bound sections, consisting of the plasma membrane, acrosome membrane, and mitochondrial membrane, that must be intact to ensure the viability of the spermatozoa to fertilize

How to cite this article?

Gilmore A, Hitit M, Ugur MR, Dinh TTN, Tan W, Jousan FD, Nicodemus M, Kaya A, Memili E: Functional variables of bull sperm associated with cryotolerance. *Kafkas Univ Vet Fak Derg,* 27 (3): 371-379, 2021.
DOI: 10.9775/kvfd.2021.25653

(*) **Corresponding Author**

Tel: +1 (662) 325-2937
E-mail: em149@msstate.edu (E. Memili)

an oocyte. Any damage incurred by these membranes is detrimental to the sperm cell health, freezability, and fertilizing ability [1,2]. Over the years, numerous studies have shown that any abnormalities to the structure of the sperm cell will assist with predicating infertility in males [3-5].

Sperm motility and morphology are intricately linked because any anatomical abnormalities will cause sperm to swim slower and less effectively [6,7]. Motility is crucial for sperm transportation in the female reproductive tract and penetration of the oocyte. The numbers of spermatozoa that show forward progressive motility and navigate the barriers of the female reproductive tract is positively associated with fertility and freezability [8,9]. Using computer assisted sperm analyses (CASA), it was revealed that sperm cells with the highest velocity and progressive motion were positively correlated with their resilience post-cryopreservation [10], indicating the importance of motility to determining fertility.

The process of cryopreservation involves extension, temperature reduction, addition of cryoprotectants, and freezing and thawing of sperm cells [11]. The rapid change in temperature alters the physical characteristics of the sperm plasma membrane [12] by forming water crystals within the cell, which causes physical damage and the loss of the acrosomal cap [13,14]. Spermatozoa are not designed to withstand rapid changes in temperature and experience cold shock during freezing. This causes disruption and rearrangement of membrane constituents, resulting in loss of plasma membrane integrity [15]. The thawing process requires the sperm cell to rapidly recover, rehydrate, and expand back into its normal shape in a brief timeframe, resulting in alteration of membrane function [1,16].

One way that sperm cells can become damaged and negatively influence the fertility of a bull is through oxidative stress [17,18], which is defined as imbalance between higher levels of reactive oxygen species (ROS) production and low antioxidant activity in sperm that leads to DNA damage by base oxidation, chromatic dispersion and DNA protamine complex, and apoptosis, all of which then impair sperm viability [19,20]. Integrity of DNA is critical during freezing in several species, such as humans, stallions, and bulls, as cryopreservation alters mitochondrial membrane that induce the generation of ROS, which may consequently undergo oxidation of DNA, generating double and single-strand DNA breaks [21-23].

While research has improved cryopreservation over the years, today's beef producers are commonly facing post-thaw viability of less than 50% [24]. The goal of this study was to ascertain sperm population and cellular characteristics as well as total antioxidant capacity of bull sperm associated with cryotolerance to better understand and improve the post-thaw viability.

Material and Methods

Determination of Sperm Freezability and Sample Processing

Cryopreserved sperm samples and bull fertility data from 16 mature Holstein bulls that had satisfactory semen quality were provided by Alta Genetics (Watertown, WI, USA). Thus, experiments performed in our laboratories did not involve any live animals for this study. All bulls were housed and fed identically during the collection period. Bulls had contrasting freezability phenotypes based upon post-thaw viability with 11 bulls categorized as having good freezability (average postthaw viability 62.16%; Good) and 5 bulls with poor freezability (average post-thaw viability 52.59%; Poor). Bull semen freezability was determined using methods as previously described [25]. Briefly, sperm collection was done using an artificial vagina after false mounting of a teaser animal. Semen was extended with a commercial egg-yolk-tris-based extender and frozen at Alta Genetics as described methods [26]. Frozen sperm were packaged into 250 µL straws and stored in liquid nitrogen. Post-thaw viability of sperm was evaluated using flow-cytometry (CyFlow SL, Partec, Germany). The proportion of the live and dead sperm were quantified through the dual staining with SYBR-14 and propidium iodide (PI) (SYBR-14/PI, Live/Dead Sperm Viability Kit L-7011, Thermo Fisher Scientific) [27]. The percentage of live sperm (stained green) were considered as the freezability parameter for Good and Poor bulls.

The post-thaw viability database used in this study included 100.448 ejaculates from 860 Holstein bulls that were collected at least 20 different times over a 3-month period. The average of population post-thaw viability was the threshold value to determine freezability phenotype. Bulls with greater post-thaw viability than population average considered as good freezability (Good), and those lower than population average considered as poor freezability (Poor) *Table 1*.

Computer Assisted Sperm Analyses (CASA)

CASA was used to evaluate sperm cell motility and kinetic parameters. Cryopreserved sperm cells were thawed in a 37°C water bath for 30 sec. Five µL of each sample was loaded into a prewarmed chamber slide and 400 spermatozoa were evaluated per chamber immediately. A total of 12 parameters were assessed [28]. These parameters included the following: total motility (TM), progressive motility (PM), linearity (LN), straightness (ST), wobble (WB), curvilinear velocity (VCL), straight line velocity (VSL), beat cross frequency (BCF), average path velocity (VAP), amplitude of lateral head displacement (ALH), distance average path (DAP), distance straight line (DSL), and distance curved line (DCL).

Hypoosmotic Swelling (HOS) Test

The HOS test was used to analyze the membrane integrity

Table 1. *Average sperm population characteristic values of bulls with varying cryotolerance*

Variable	Phenotype		Standard Error	P-value
	Good	Poor		
Intact membranes	27.95[a]	19.00[b]	3.059	0.02
Live cells	43.63[a]	37.95[a]	4.85	0.34
Non-fragmented DNA	63.45[a]	43.26[b]	6.27	0.01
Total Motility	44.95[a]	45.56[a]	4.73	0.91
Progressive motility	29.48[a]	29.24[a]	3.40	0.95
Linearity	58.37[a]	56.70[a]	1.63	0.41
Straightness	88.16[a]	86.34[a]	1.05	0.17
Wobble	64.95[a]	64.26[a]	1.19	0.63
Post-thaw viability	62.16[a]	52.15[b]	1.13	<.0001

[a,b] *Means within a row with different superscripts differ (P≤0.05)*

of the sperm cells as reported [29]. The sperm pellet was resuspended in 250 µL of PBS. Fifty µL of the sperm sample was transferred into 450 µL of HOS test solution (150 mOsm/kg pre-equilibrated at 37ºC for 1 h) and gently mixed by hand. The mixture was then incubated in a 37ºC water bath for 30 min upon when 10 µL of sample were transferred onto a clean glass slide. Each slide was evaluated for HOS-positive (presence of coiled tail) or HOS-negative (absence of coiled tail) sperm by counting a total of 200 spermatozoa/sample using 40 x objective of a phase-contrast microscope.

Eosin-Nigrosine Staining

Eosin-Nigrosin staining was used to assess the viability of sperm cells according to the method as reported [30]. This assessment of sperm vitality is used to distinguish between immotile dead sperm and immotile live sperm. Frozen sperm cells were thawed in a 37ºC water bath for 30 sec, transferred to a 1.5 mL tube that contained 1 mL of PBS, and centrifuged at 3700 rpm for 10 min. The supernatant was aspirated, and this process was repeated 3 times. One mL of pre-equilibrated PBS was added to the tube and gently agitated by hand. 10 µL of sperm suspension and 10 µL of eosin-nigrosin solution (0.67 g eosin Y and 0.9 g of sodium chloride in 100 mL of distilled water) was transferred into another tube and gently mixed together by hand. 10 µL of this solution was smeared on a glass slide using a coverslip and air dried for evaluation of 200 sperm cells per slide via light microcopy. The underlying principle of this assay is that spermatozoa with structurally intact cell membranes (live spermatozoa) are not stained, while dead spermatozoa with disintegrating cell membranes take up the eosin stain.

HaloSperm Experiment

The Halosperm G2 test kit (Halotech DNA, SL San Diego, CA) is an *in vitro* diagnostic kit that measures DNA fragmentation in sperm cells. The experiment was carried out according to the manufacturer's instructions. An agarose screw tube (ACS) was melted using a 100ºC water bath for 5 min. One hundred µL of the melted agarose was transferred into a 1.5 mL tube. Sperm cells were thawed in a 37ºC water bath for 30 sec, transferred to a 1.5 mL tube that contained 1 mL of PBS, and centrifuged at 3700 rpm for 10 min. The supernatant was removed, and 1 mL of pre-equilibrated PBS was added to the tube and mixed gently by hand. Fifty mL of the sperm sample was transferred to an Eppendorf tube containing 100 µL of the agarose and mixed with a micropipette. Eight µL of the cell suspension was placed in the center of a sample well and covered with a coverslip. Next, slides were placed on a plate precooled to 4ºC, and then, put into the fridge for 5 min. to solidify the agarose. Slides were kept in a horizontal position throughout the entire process. Solution 2 (LS) was applied until the sample well was fully immersed and incubated for 20 min, and then, washed with distilled water. The slides were dehydrated by flooding slides with 70% ethanol and incubating for 2 min. The 70% ethanol was drained off and 100% ethanol was applied for 2 min. Excess ethanol was drained off slides and slides were allowed to air dry horizontally on filter paper. Slides were then transferred into a petri dish and Solution 3 (SSA) was applied until sample well was completely immersed, incubated for 7 min. and then, the excess stain was drained off. Solution 4 (SSB) was then applied until sample wells were fully immersed, incubated for another 7 min, and then, the excess stain was drained off. Slides were dried at room temperature, and then, evaluated under bright field microscopy, counting 300 cells per slide.

Trolox Equivalent Antioxidant Capacity (TEAC)

The TEAC experiment was conducted according to the method as reported [31] to measure the total antioxidant capacity of sperm cells utilizing the Total Antioxidant Capacity (TAC) Colorimetric Assay kit (Cat # 709001; Cayman Chemical, Ann Arbor, Michigan). Frozen sperm cells were thawed in a 37ºC water bath for 30 sec, transferred to a 1.5 mL tube containing 1 mL of PBS, and centrifuged at 3700

rpm for 10 min. The supernatant was aspirated, and this was repeated 3 times. One mL of pre-equilibrated PBS was added to the tube and gently agitated. 0, 4, 8, 12, 16, 20 µL of the Trolox standard were added to individual wells of the plate. Fifty µL of samples were added to individual wells. 100 µL of Cu^{2+} working solution was added to all wells on the plate. The plate was then covered and incubated at room temperature for 90 min. Following the incubation, the absorbance was read at 750 nm using a microplate reader.

Statistical Analysis

Sixteen Holstein bulls (n=11 Good, n=5 Poor) were used for statistical analysis. Principal component analysis (PCA) performed by the FACTOR procedure of SAS 9.4 was used to reduce sperm population variables (POP). The number of live cells, cells with intact membranes, cells without fragmented DNA, total motility, progressive motility, linearity (LIN), straightness (STR), wobble (WOB), and post-thaw viability (PTV) were reduced to 2 principal components (POP1 and POP2), while preserving total variance in the data. The correlation coefficients of POP variables with POP1 and POP2 were used to map these variables in a biplot. The principal component analysis was also used to reduce sperm cell characteristic variables (CELL), including curvilinear velocity (VCL µm/s), straight line velocity (VSL µm/s), beat cross frequency (BCF Hz), average path velocity (VAP µm/s), amplitude of lateral head (ALH µm), distance average path (DAP µm), distance straight line (DSL µm), and distance curved line (DCL µm) to two principal components CELL1 and CELL2, while preserving the total variance within the data. The correlation coefficients of CELL variables with CELL1 and CELL2 were used to map these variables in another biplot. The scores of bulls calculated from the POP and CELL variables were also used to map the bulls in both biplots. Additionally, correlation coefficients of total antioxidant capacity (TAC) with the scores were determined by the CORR procedure (SAS version 9.4; SAS Inst. Inc., Cary, NC) and were used to map TAC variable on both biplots. The CORR procedure was also used to determine Spearman's correlation coefficients between the POP and CELL variables. Univariate analysis of variance was performed by the GLIMMIX procedure of SAS 9.4 with freezability phenotype being the fixed effect in a generalized linear mixed model. The degree of freedom was estimated by the Kenward-Roger approximation method and means were separated by a protected *t-test*. Actual probability values were reported with statistical comparisons (α≤0.05).

Results

Sperm Population Dynamics

Principal component analysis designated that the total variance of sperm population characteristics was largely explained by two principal components, POP1 (60.6% of total variance) and POP2 (39.4% of total variance; *Fig. 1*). Factor pattern analysis indicated a strong correlation between POP1 and the number of live cells (LC; r = 0.70; P=0.002), LIN (r = 0.91; P<0.001), STR (r = 0.87; P<0.001), and WOB (r = 0.87; P<0.001); whereas POP2 was correlated with cells with non-fragmented DNA (NF; *r* = -0.57; P=0.020), total motility (TM; *r* = 0.91; P<0.001), progressive motility

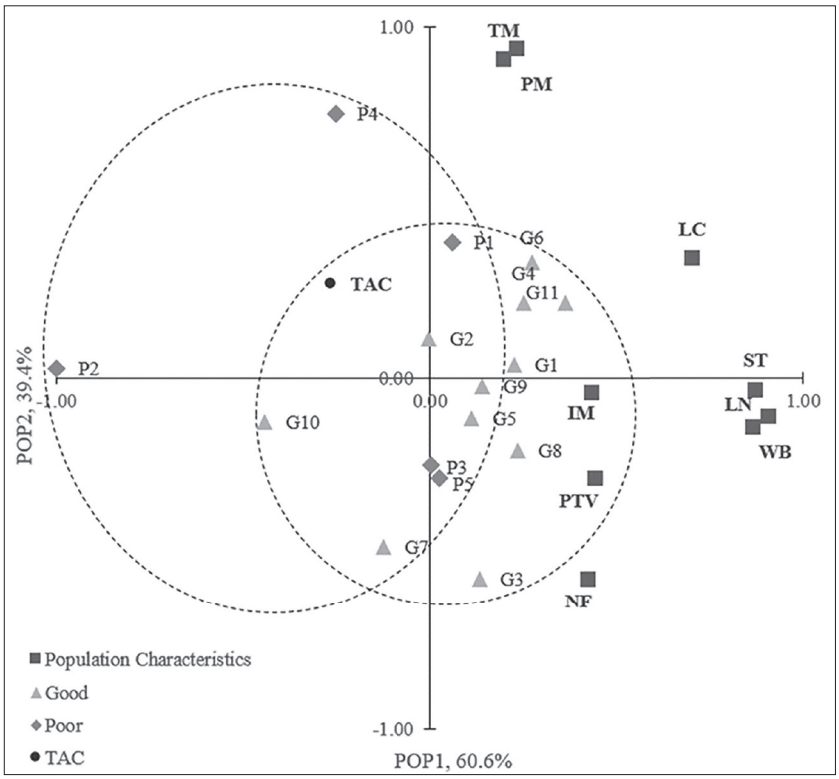

Fig 1. Sperm Population Variables PCA. Principal component analysis of sperm population variables (POP) of bulls with good and poor cryotolerance: percentage of total motility (TM), percentage of progressive motility (PM), percentage of live sperm (LC), percentage of sperm that travel straight (ST), percentage of sperm with linear movement (LN), percentage of deviation of the sperm head from the path of progression (WB), percentage of sperm with intact membranes (IM), post-thaw viability (PTV), percentage of sperm with non-fragmented DNA, and total antioxidant capacity (TAC). The coordinates are correlation coefficients of POP with principal component 1 (POP1; explaining 60.6% of variance) and principal component 2 (POP2; 39.4% of variance) and scores of individual bulls

Table 2. *Average sperm cellular characteristic values of bulls with varying cryotolerance*

Variable	Phenotype		Standard Error	P-value
	Good	Poor		
Curvilinear velocity (VCL; µm/s)	118.25[a]	108.40[a]	4.70	0.10
Straight line velocity (VSL; µm/s)	67.54[a]	59.38[b]	2.50	0.01
Beat cross frequency (BCF; Hz)	30.98[a]	28.80[a]	1.19	0.15
Average path velocity (VAP; µm/s)	75.14[a]	67.82[b]	2.61	0.03
Amplitude of lateral head (ALH; µm)	4.92[a]	4.84[a]	0.26	0.79
Distance average path (DAP; µm)	31.52[a]	27.32[b]	1.07	<.01
Distance straight line (DSL; µm)	29.19[a]	23.90[b]	1.50	0.01
Distance curved line (DCL; µm)	47.78[a]	43.84[a]	2.66	0.24

[a,b] *Means within a row with different superscripts differ (P≤0.05)*

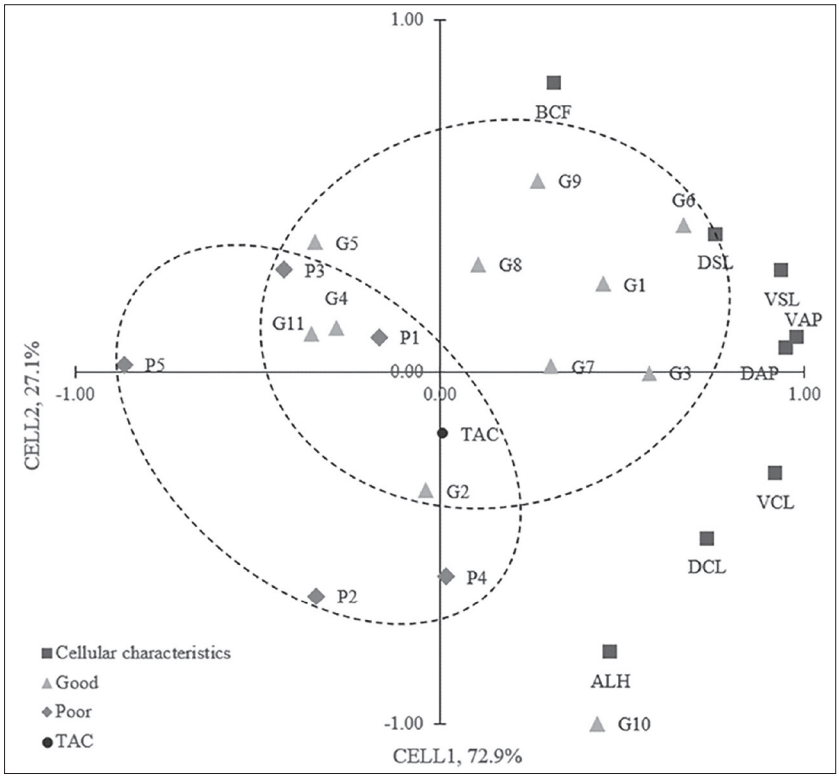

Fig 2. Sperm Cellular Characteristic Variable PCA. Principal component analysis of sperm cellular characteristic variables (CELL) of bulls with good and poor cryotolerance: curvilinear velocity (VCL; µm/s), straight line velocity (VSL; µm/s), beat cross frequency (BCF; Hz), average path velocity (VAP; µm/s), amplitude of lateral head (ALH; µm), distance average path (DAP; µm), distance straight line (DSL; µm), distance curved line (DCL; µm), and total antioxidant capacity (TAC). The coordinates are correlation coefficients of CELL with principal component 1 (CELL1; explaining 72.9% of variance) and principal component 2 (CELL2; 27.1% of variance) and scores of individual bulls

(PM; $r = 0.94$; P<0.001; *Table 1*). The PCA scores of individual bulls on the population characteristic biplot *(Fig. 1)* showed that there was slight separation between Good and Poor groups; however, there was an overlap between the two populations. The Good bulls clustered within the proximity of the center of the biplot in quadrant II and III with two bulls in quadrant IV. The Poor bulls did not cluster well, locating in quadrant I and II. The Good bulls were in the close proximity of IM, NF, and PTV and scored positively by POP1 variables (ST, LN, and WB); whereas the Poor bulls were in the close proximity of TM, PM, and PTV. One Poor bull was scored negatively by POP1 variables. Univariate analysis revealed that the Good bulls had 9% greater IM (P=0.029), 20% greater NF (P=0.018), and 10% greater PTV (P<0.001).

Sperm Cellular Characteristics

The total variance of sperm cellular characteristics was also explained by two principal components, CELL1 (72.9%) and CELL2 (27.1%; *Fig. 2*). Factor loadings on the biplot revealed a strong correlation between CELL1 and VCL (r = 0.92; P<0.0001), VSL (r = 0.94; P<0.0001), VAP (r = 0.98; P<0.0001), DAP (r = 0.95; P<0.0001), DSL (r = 0.76; P=0.001), and DCL (r = 0.73; P=0.001); whereas, CELL2 was correlated with BCF (r = 0.82; P<0.001) and ALH (r = -0.80; P<0.001; *Table 2*). The PCA scores of each bull on the cellular characteristic biplot displayed a slight partition between the Good and Poor groups, although there was an overlap among the two groups. The Good bulls clustered into quadrants I, II, and III *(Fig. 2)*. The Poor bulls did not cluster very well,

localizing into quadrants I and IV. The majority of the Good bulls were in close proximity and scored positively with CELL1 variables (DSL, VSL, VAP, and DAP); whereas the Poor bulls were not in close proximity to any of the sperm cellular characteristic variables. Four of five Poor bulls were negatively scored by the CELL1 variables. The univariate analysis showed that spermatozoa from Good bulls was faster for VSL (8.17 µm/s; P=0.017) and VAP (7.33 µm/s; P=0.036) compared to spermatozoa from Poor bulls. In addition, spermatozoa from Good bulls traveled 4.21 µm further as measured by DAP (P=0.006) and 5.29 µm further as measured by DSL (P=0.011) compared to spermatozoa from Poor bulls.

Total Antioxidant Capacity

The TAC was in close proximity to the origin of both POP and CELL biplots *(Fig. 1, Fig. 2)*, but not in close proximity to any sperm population or cellular characteristics. This indicated that TAC is not correlated with POP1 and POP2 or CELL1 and CELL2. Univariate analysis of variance indicated that TAC was similar between Good (0.182 nm) and Poor (0.260 nm) groups.

Discussion

We hypothesized that a combination of sperm cell attributes and kinematics of bull sperm are associated with cryotolerance. To test our hypothesis, we carried out a study evaluating sperm kinematics, viability, plasma membrane and DNA integrity, and TAC. In this study, we used the bull model which is directly relevant to human reproductive mechanisms to examine a fundamental issue of predicting sperm freezability. In addition, significant similarities exist between the bovine and the other mammals including humans both in genetics and reproductive physiology. Rather than relying on anecdotal records, for the bulls, there is a wealth of valuable reliable fertility data for the discovery of biomarkers. Through an existing partnership with the beef industry, semen samples from bulls with well-documented sperm freezability phenotypes were used for this project. These results have exceptional importance because the findings shed light onto population and cellular underpinnings of sperm cryopreservation, ultimately mammalian reproduction and development.

Among the CELL parameters measured, membrane motility is one of the most crucial sperm characteristics linked to the fertility of spermatozoa, signifying its importance in sperm viability and membrane integrity. Motility is essential for successful sperm transport and fertilization *in vivo* and *in vitro*. Apart from motility analysis, our study as well as others have validated that the velocity parameters, such as VSL and VAP, are linked with the fertilizing capacity of frozen-thawed sperm [32,33]. Therefore, velocity of VSL and VAP rather than post thaw total and progressive motility was used to predict cryotolerance of human and bull sperm [34,35]. Our results were found to be in accordance with that the higher velocity can in part be attributed to the higher number of cells with intact plasma membranes in the Good bulls [36,37], which ensures the viability of the cell. In our study, of the CELL parameters analyzed, the VSL and VAP were significantly faster in the Good bulls versus the Poor bulls, showing that the speed in which a spermatozoon travels aids in its post-thaw viability. It was also in line with our study that VSL could be better utilized as a determining component of sperm which help distinguish quality of frozen bull semen [38]. Accordingly, the velocity parameters could be the outcome of intact plasma membranes that maintain sperm cell viability [39] which, in our study, VSL and VAP had strong correlation with cellular characteristics of Good bull sperm from differing cryotolerance. In addition, VSL and VAP had proximity and scored positively with CELL1 variables, allowing that velocity parameters may be used to narrow down cryotolerance parameters. In addition to VSL and VAP, there was also an increase in the DAP and the DSL for spermatozoa from Good bulls compared to Poor bulls *(Table 2)*. These results confirm that bulls with good freezability have a higher number of spermatozoa that traveled longer distances and at higher speeds in comparison to the sperm from Poor freezability bulls.

Among the POP parameters measured, membrane and DNA integrity, along with post-thaw viability, differed among the bulls with different cryotolerance and showed a significant relationship with sperm cryo-survival *(Table 1)*. Although sperm quality is generally assessed based on sperm motility characteristics, other parameters can be considered, such as viability and sperm membrane integrity post-thaw [40]. When sperm cells are cryopreserved, they undergo thermal stress, which results in protein denaturation, shrinkage, and collapse of the plasma membrane, gravely damaging the viability of the spermatozoon [15,41]. This is consistent with reports that the spermatozoa from Good bulls had a higher number of cells with post-thaw viability in comparison to those of the Poor cryotolerance bulls. Because the sperm membrane is known to be the primary site of cryodamage during cryopreservation [42], it has been proposed to be linked with alterations in membrane dynamics including cholesterol content and phospholipid compound, as well as membrane permeability. As such, procedures of cryopreservation cause dramatic changes in the cell which cause injuries to the sperm membrane, thereby reducing sperm quality [14,43]. In our study, spermatozoa from Good cryotolerance bulls have higher percentage of cells with intact plasma membrane and non-fragmented DNA. Therefore, the Good bulls were in the close proximity of IM, NF, and PTV and scored positively by POP1 variables which may highlight the clear associations of cryotolerance.

Sperm nuclear changes can be affected by the critical

procedure of freezing and thawing because distinct mechanisms lead to DNA damage owing to high levels of ROS production [44]. Accordingly, OS stress gives rise to impaired sperm function by causing DNA damage, thus remaining an important factor for male fertility and potential embryonic loss [45,46]. On the other hand, morphological abnormalities were attributed to poor DNA quality [47]. It has also been demonstrated that sperm with abnormal morphology are more vulnerable to DNA damage during cryopreservation [20]. Therefore, sperm DNA fragmentation was indicative of low AI success in bulls [48] and was the mostly affected marker of sperm cryopreservation [39,49]. In our study, DNA fragmentation was significantly higher in the Poor bull group in our study, and thus, we propose that assessment of sperm DNA, in addition to conventional semen analysis, may offer additional insight into identifying poor cryotolerance bulls. Our conclusions are supported by multiple studies where DNA fragmentation is much higher in cryopreserved bull sperm that non-fragmented DNA is greater in Good freezability than Poor freezability bull, thus seems to be related to those variables of which sperm intact membranes and post-thaw viability were explained by components of POP1.

Both spermatozoa and seminal plasma contain antioxidants to protect against oxidative stress [50], but due to the small size of spermatozoa, their antioxidant capacity is limited. The previous reports on TAC of semen are contradictory. Studies revealed that infertile men demonstrated a lower TAC than fertile men and lower levels of individual antioxidants [51,52]. It was shown that the TAC did not differ among fertile and infertile men [53]. Similarly, the TAC levels in our study did not differ significantly among the Good and Poor bulls. During the cryopreservation process the naturally occurring antioxidants lose their strength. The relationship between TAC and cryotolerance is highly variable partly due to the varying number of antioxidants in commercial semen extenders used for cryopreservation [54]. Thus, these inconsistencies between studies show that TAC alone may not be used to predict freezability phenotype of bulls. Instead, prediction of freezability phenotype of bulls needs at least one other independent variable that is more correlated with POP1 and CELL1 to better predict freezability of bull spermatozoa along with TAC.

In conclusion, the comprehensive assessment of varying sperm functions and the subsequent analysis of these functions indicated that semen from bulls with Good cryotolerance differed in post-thaw viability, plasma membrane and DNA integrity, VSL, VAP, DAP, and DSL in comparison to the bulls with Poor cryotolerance. The PCA also indicated that spermatozoa from Good cryotolerance bulls was strongly correlated with a higher percentage of cells with intact plasma membrane and DNA, and post-thaw viability, along with higher levels of certain sperm kinematic parameters (VSL, VAP, DAP, and DSL) compared to spermatozoa from Poor bulls. There is no one specific sperm function variable alone that can accurately predict cryotolerance of bull spermatozoa, and thus, a combination of sperm cell attributes and kinematics needs to be utilized by the AI industry in differentiating between freezability of spermatozoa between bulls.

No study has shown that a single sperm parameter can be used to predict spermatic fertility or cryotolerance. The current study investigated sperm population and cellular dynamics as well as TAC levels in bull spermatozoa of Good and Poor cryotolerance. Sperm from Good cryotolerance bulls had more intact membranes and non-fragmented DNA with higher post-thaw viability and key kinematics, including VAP, VSL, DAP, and DSL, as compared to sperm from Poor cryotolerance bulls. However, there was no statistical difference in TAC levels between the groups. These results can be used to concentrate the focus on critical parameters that can be used to best predict cryotolerance of spermatozoa.

Author Contributions

Conceptualization: AG, MH, TTND, AK, EM; Data curation: AG, MH, TTND; Formal analysis: AG, MH, TTND; Investigation: AG, MH, MRU, TTND, WT, AK, EM; Methodology: AG, MH, MRU, TTND, WT, ET, AK, EM; Writing - original draft preparation: AG, MH, MRU, TTND, WT, DJ, MN, AK, EM; Writing - review and editing: AG, MH, MRU, TTND, WT, DJ, MN, AK, EM.

Conflict of Interest

The authors declare no potential conflicts of interest with respect to the research, authorship, and/or publication of this article.

References

1. Graham JK, Kunze E, Hammerstedt RH: Analysis of sperm cell viability, acrosomal integrity, and mitochondrial function using flow cytometry. *Biol. Reprod*, 43 (1): 55-64, 1990. DOI: 10.1095/biolreprod43.1.55

2. Ugur MR, Saber Abdelrahman A, Evans HC, Gilmore AA, Hitit M, Arifiantini RI, Purwantara B, Kaya A, Memili E: Advances in cryopreservation of bull sperm. *Front Vet Sci*, 6:268, 2019. DOI: 10.3389/fvets.2019.00268

3. Barth AD, Oko RJ: Abnormal morphology of bovine spermatozoa. (Iowa State University Press), 1989.

4. Kastelic JP, Thundathil JC: Breeding soundness evaluation and semen analysis for predicting bull fertility. *Reprod Domest Anim*, 43, 368-373, 2008. DOI: 10.1111/j.1439-0531.2008.01186.x

5. Nagata MPB, Egashira J, Katafuchi N, Endo K, Ogata K, Yamanaka K, Yamanouchi T, Matsuda H, Hashiyada Y, Yamashita K: Bovine sperm selection procedure prior to cryopreservation for improvement of post-thawed semen quality and fertility. *J Anim Sci Biotechnol*, 10:91, 2019. DOI: 10.1186/s40104-019-0395-9

6. Katz DF, Diel L, Overstreet JW: Differences in the movement of morphologically normal and abnormal human seminal spermatozoa. *Biol Reprod,* 26 (4): 566-570, 1982. DOI: 10.1095/biolreprod26.4.566

7. Li Y, Kalo D, Zeron Y, Roth Z: Progressive motility-a potential predictive parameter for semen fertilization capacity in bovines. *Zygote*, 24 (1): 70-82, 2016. DOI: 10.1017/s0967199414000720

8. Nadir S, Saacke RG, Bame J, Mullins J, Degelos S: Effect of freezing semen and dosage of sperm on number of accessory sperm, fertility, and embryo quality in artificially inseminated cattle. *J Anim Sci*, 71 (1): 199-204. 1993. DOI: 10.2527/1993.711199x

9. Pardede BP, Supriatna I, Yudi Y, Agil M: Decreased bull fertility: age-related changes in sperm motility and DNA fragmentation. *E3S Web Conf*, 151:01010, 2020. DOI: 10.1051/e3sconf/202015101010

10. Muiño R, Rivera MM, Rigau T, Rodriguez-Gil JE, Peña AI: Effect of different thawing rates on post-thaw sperm viability, kinematic parameters and motile sperm subpopulations structure of bull semen. *Anim Reprod Sci*, 109 (1-4): 50-64, 2008. DOI: 10.1016/j.anireprosci.2007.11.028

11. Medeiros CMO, Forell F, Oliveira ATD, Rodrigues JL: Current status of sperm cryopreservation: Why isn't it better? *Theriogenology,* 57, 327-344, 2002. DOI: 10.1016/S0093-691X(01)00674-4

12. Gunawan M, Kaiin EM, Mudita GS, Chaidir RRA: Soybean phospholipids-based extender as an alternative for bull sperm cryopreservation. *IOP Conf Ser Earth Environ Sci*, 478:012014, 2020. DOI: 10.1088/1755-1315/478/1/012014

13. Yoon SJ, Kwon WS, Rahman MS, Lee JS, Pang MG: A novel approach to identifying physical markers of cryo-damage in bull spermatozoa. *PLoS One,* 10 (5): e0126232, 2015. DOI: 10.1371/journal.pone.0126232

14. Peris-Frau P, Soler AJ, Iniesta-Cuerda M, Martín-Maestro A, Sánchez-Ajofrín I, Medina-Chávez DA, Fernández-Santos MR, García-álvarez O, Maroto-Morales A, Montoro V, Garde JJ: Sperm cryodamage in ruminants: Understanding the molecular changes induced by the cryopreservation process to optimize sperm quality. *Int J Mol Sci,* 21 (8): 2781, 2020. DOI: 10.3390/ijms21082781

15. Khalil WA, El-Harairy MA, Zeidan AE, Hassan MA, Mohey-Elsaeed O: Evaluation of bull spermatozoa during and after cryopreservation: Structural and ultrastructural insights. *Int J Vet Sci Med,* 6, S49-S56, 2018. DOI: 10.1016/j.ijvsm.2017.11.001

16. Grötter LG, Cattaneo L, Marini PE, Kjelland M, and Ferré LB: Recent advances in bovine sperm cryopreservation techniques with a focus on sperm post-thaw quality optimization. *Reprod Domest Anim,* 54 (4): 655-665, 2019. DOI: 10.1111/rda.13409

17. Aitken RJ, Mark AB, Brett Nixon: Are sperm capacitation and apoptosis the opposite ends of a continuum driven by oxidative stress? *Asian J Androl*, 17 (4): 633-639, 2015. DOI: 10.4103/1008-682X.153850

18. Diether N, Dyck MK: Male fertility evaluation using biomarkers in livestock. *JSM Biomar*, 3 (1): 1011, 2017.

19. Aitken RJ, De Iuliis GN: On the possible origins of DNA damage in human spermatozoa. *Mol Hum Reprod*, 16 (1): 3-13, 2010. DOI: 10.1093/molehr/gap059

20. Di Santo M, Tarozzi N, Nadalini M, Borini A: Human sperm cryopreservation: Update on techniques, effect on DNA integrity, and implications for ART. *Adv Urol*, 2012:854837, 2012.

21. Evenson DP, Larson KL, Jost LK: Sperm chromatin structure assay: its clinical use for detecting sperm DNA fragmentation in male infertility and comparisons with other techniques. *J Androl,* 23, 25-43, 2002. DOI: 10.1002/j.1939-4640.2002.tb02599.x

22. Said TM, Gaglani A, Agarwal A: Implication of apoptosis in sperm cryoinjury. *Reprod Biomed Online,* 21 (4): 456-462, 2010. DOI: 10.1016/j.rbmo.2010.05.011

23. Gürler H, Malama E, Heppelmann M, Calisici O, Leiding C, Kastelic JP, Bollwein H: Effects of cryopreservation on sperm viability, synthesis of reactive oxygen species, and DNA damage of bovine sperm. *Theriogenology*, 86, 562-571, 2016. DOI: 10.1016/j.theriogenology.2016.02.007

24. Ballester J, Johannisson A, Saravia F, Håård M, Gustafsson H, Bajramovic D, Rodriguez-Martinez H: Post-thaw viability of bull AI-doses with low-sperm numbers. *Theriogenology*, 68 (6): 934-943, 2007. DOI: 10.1016/j.theriogenology.2007.07.008

25. Ugur MR, Dinh T, Hitit M, Kaya A, Topper E, Didion B, Memili E: Amino acids of seminal plasma associated with freezability of bull sperm. *Front Cell Dev Biol*, 7:347, 2020. DOI: 10.3389/fcell.2019.00347

26. Pace MM, Sullivan JJ, Elliott FI, Graham EF, Coulter GH: Effects of thawing temperature, number of spermatozoa and spermatozoal quality on fertility of bovine spermatozoa packaged in. 5-ml French straws. *J Anim Sci,* 53, 693-701, 1981. DOI: 10.2527/jas1981.533693x

27. Garner DL, Johnson LA, Yue ST, Roth BL, Haugland RP: Dual DNA staining assessment of bovine sperm viability using sybr-14 and propidium iodide. *J Androl,* 15 (6): 620-629, 1994.

28. Ibănescu I, Leiding C, Ciornei ŞG, RoŞca P, Sfartz I, Drugociu D: Differences in CASA output according to the chamber type when analyzing frozen-thawed bull sperm. *Anim Reprod Sci*, 166, 72-79, 2016. DOI: 10.1016/j.anireprosci.2016.01.005

29. Gadkar S, Shah CA, Sachdeva G, Samant U, Puri CP: Progesterone receptor as an indicator of sperm function. *Biol Reprod*, 67 (4): 1327-1336, 2002. DOI: 10.1095/biolreprod67.4.1327

30. Dogan S, Mason MC, Govindaraju A, Belser L, Kaya A, Stokes J, Rowe D, Memili E: Interrelationships between apoptosis and fertility in bull sperm. *J Reprod Dev*, 59 (1): 18-26, 2013. DOI: 10.1262/jrd.2012-068

31. Roychoudhury S, Sharma R, Sikka S, Agarwal A: Diagnostic application of total antioxidant capacity in seminal plasma to assess oxidative stress in male factor infertility. *J Assist Reprod Genet,* 33 (5): 627-635, 2016. DOI: 10.1007/s10815-016-0677-5

32. Kumar D, Kumar PR, Singh PA, Yadav SP, Sarkar SK, Bharadwaj A, Yadav PS: Characteristics of frozen thawed semen in predicting the fertility of buffalo bulls. *Indian J Anim Sci*, 84, 389-392, 2014.

33. Karunakaran M, Devanathan TG: Evaluation of bull semen for fertility-associated protein, in vitro characters and fertility. *J Appl Anim Res,* 45 (1): 136-144, 2017. DOI: 10.1080/09712119.2015.1129343

34. Jiang XP, Zhou WM, Wang SQ, Wang W, Tang JY, Xu Z, Zhang ZX, Qin C, Wang ZJ, Zhang W: Multivariate model for predicting semen cryopreservation outcomes in a human sperm bank. *Asian J Androl,* 19 (4): 404-408, 2017. DOI: 10.4103/1008-682X.178488

35. Singh P, Kumar D, Kumar P, Singh I, Yadav PS: Cryopreservation and quality assessment of buffalo bull semen collected from farmer's doorstep. *Agric Res,* 2 (2): 148-152, 2013. DOI: 10.1007/s40003-013-0056-8

36. Nagy Á, Polichronopoulos T, Gáspárdy A, Solti L, Cseh S: Correlation between bull fertility and sperm cell velocity parameters generated by computer-assisted semen analysis. *Acta Vet Hung*, 63 (3): 370-381, 2015. DOI: 10.1556/004.2015.035

37. Bollwein H, Bittner L: Impacts of oxidative stress on bovine sperm function and subsequent in vitro embryo development. *Anim Reprod*, 15 (Suppl. 1): 703-710, 2018. DOI: 10.21451/1984-3143-AR2018-0041

38. Morrell JM, Valeanu AS, Lundeheim N, Johannisson A: Sperm quality in frozen beef and dairy bull semen. *Acta Vet Scand*, 60:41, 2018. DOI: 10.1186/s13028-018-0396-2

39. Ismail NH, Osman K, Mohd Yusof FZ, Syed Mohamad SF, Jaafar FHF, Ibrahim SF: Improvement of post-thaw sperm kinematics and dna integrity of cross-bred bovine sperm by incorporating dgc as selection method prior to cryopreservation. *J Agric Sci,* 9 (13): 24-31, 2017. DOI: 10.5539/jas.v9n13p24

40. Sieme H, Oldenhof H, Wolkers WF: Sperm membrane behaviour during cooling and cryopreservation. *Reprod Domest Anim,* 50, 20-26, 2015. DOI: 10.1111/rda.12594

41. Kasimanickam R, Kasimanickam V, Thatcher CD, Nebel RL, Cassell BG: Relationships among lipid peroxidation, glutathione peroxidase, superoxide dismutase, sperm parameters, and competitive index in dairy bulls. *Theriogenology*, 67 (5): 1004-1012, 2007. DOI: 10.1016/j.theriogenology.2006.11.013

42. Ryu DY, Song WH, Pang WK, Yoon SJ, Rahman MS, Pang MG: Freezability biomarkers in bull epididymal spermatozoa. *Sci Rep,* 9:12797, 2019. DOI: 10.1038/s41598-019-49378-5

43. Nijs M, Creemers E, Cox A, Janssen M, Vanheusden E, Castro-Sanchez Y, Thijs H, Ombelet W: Influence of freeze-thawing on hyaluronic acid binding of human spermatozoa. *Reprod Biomed,* 19, 202-206, 2009. DOI: 10.1016/S1472-6483(10)60073-9

44. Castro LS, Hamilton TRS, Mendes CM, Nichi M, Barnabe VH, Visintin JA, Assumpção MEOA: Sperm cryodamage occurs after rapid freezing phase: Flow cytometry approach and antioxidant enzymes

activity at different stages of cryopreservation. *J Anim Sci Biotechnol,* 7:17, 2016. DOI: 10.1186/s40104-016-0076-x

45. El-Regalaty H: Effects of cryopreservation of buffalo and bovine spermatozoa on sperm dna damage and early embryonic development. *J Anim Poult Prod*, 8 (7): 167-172, 2017. DOI: 10.21608/jappmu.2017.45843

46. Kumaresan A, Gupta MD, Datta TK, Morrell JM: Sperm DNA integrity and male fertility in farm animals: A review. *Front Vet Sci*, 7:321, 2020. DOI: 10.3389/fvets.2020.00321

47. Enciso M, Cisale H, Johnston SD, Sarasa J, Fernández JL, Gosálvez J: Major morphological sperm abnormalities in the bull are related to sperm DNA damage. *Theriogenology*, 76 (1): 23-32, 2011. DOI: 10.1016/j.theriogenology.2010.12.034

48. Karoui S, Díaz C, González-Marín C, Amenabar ME, Serrano M, Ugarte E, Gosálvez J, Roy R, López-Fernández C, Carabaño MJ: Is sperm DNA fragmentation a good marker for field AI bull fertility?. *J Anim Sci,* 90 (8): 2437-2449, 2012. DOI: 10.2527/jas.2011-4492

49. Li MW, Lloyd KCK: DNA fragmentation index (DFI) as a measure of sperm quality and fertility in mice. *Sci Rep*. 10:3833, 2020. DOI: 10.1038/s41598-020-60876-9

50. Hitit M, Ugur MR, Dihn TT, Sajeev D, Kaya A, Topper E, Tan W, Memili E: Cellular and functional physiopathology of bull sperm with altered sperm freezability. *Front Vet Sci*, 7:581137, 2020. DOI: 10.3389/fvets.2020.581137

51. Lewis SEM, Sterling ESL, Young IS, Thompson W: Comparison of individual antioxidants of sperm and seminal plasma in fertile and infertile men. *Fertil Steril*, 67 (1): 142-147, 1997. DOI: 10.1016/s0015-0282(97)81871-7

52. Smith R, Vantman D, Ponce J, Escobar J, Lissi E: Andrology: Total antioxidant capacity of human seminal plasma. *Hum Reprod*, 11 (8): 1655-1660, 1996. DOI: 10.1093/oxfordjournals.humrep.a019465

53. Siciliano L, Tarantino P, Longobardi F, Rago V, De Stefano C, Carpino A: Impaired seminal antioxidant capacity in human semen with hyperviscosity or oligoasthenozoospermia. *J Androl*, 22 (5): 798-803, 2001.

54. Bucak MN, Tuncer PB, Sarıözkan S, Baspınar N, Taspınar M, Çoyan K, Bilgili A, Peker Akalın P, Büyükleblebici S, Aydos S, Ilgaz S, Sunguroğlu A, Öztuna D: Effects of antioxidants on post-thawed bovine sperm and oxidative stress parameters: Antioxidants protect DNA integrity against cryodamage. *Cryobiology*, 61, 248-253, 2010. DOI: 10.1016/j.cryobiol.2010.09.001

Kafkas Universitesi Veteriner Fakultesi Dergisi
ISSN: 1300-6045 e-ISSN: 1309-2251
Journal Home-Page: http://vetdergikafkas.org

Kafkas Univ Vet Fak Derg
27 (3): 381-387, 2021
DOI: 10.9775/kvfd.2021.25656

RESEARCH ARTICLE

Assessment of *In-vitro* Antileishmanial Activities of *Cynara scolymus* Extracts Against *Leishmania tropica* [1]

Ahmet YILDIRIM [1,a (*)] Tülay AKSOY [1,b] Ş. Sahra CEYLAN [1,c]
Hüsniye KAYALAR [2,d] Eda TAYFUR [3,e] İ. Cüneyt BALCIOĞLU [1,f]

[1] *This study was funded and supported by the scientific research project commission of Manisa Celal Bayar University (Project No: BAP 2019-100)*

[1] University of Manisa Celal Bayar, Faculty of Medicine, Department of Medical Parasitology, TR-45030 Yunusemre, Manisa - TURKEY
[2] University of Ege, Faculty of Pharmacy, Department of Pharmacognosy, TR-35040 Bornova, İzmir - TURKEY
[3] University of Ege, Faculty of Medicine, Department of Medical Biyology, TR-35100 Bornova, İzmir - TURKEY
ORCIDs: [a] 0000-0003-4411-8185; [b] 0000-0003-3397-8411; [c] 0000-0002-1571-3711; [d] 0000-0001-7882-0517; [e] 0000-0002-0162-1322 [f] 0000-0002-4801-1855

Article ID: KVFD-2021-25656 Received: 24.02.2021 Accepted: 29.05.2021 Published Online: 31.05.2021

Abstract

It was aimed to investigate *in vitro* antileishmanial activities of the receptacle, bractea, and stem leaves extracts of *Cynara scolymus* (artichoke) against *Leishmania tropica*. The *Leishmania* isolate, isolated from a cutaneous leishmaniasis patient from Manisa province, Turkey and stored in liquid nitrogen, was identified as *L. tropica* (MHOM/TR/2012/CBCL-LT) by genotyping. *In vitro* antileishmanial activities of *C. scolymus* plant extracts were examined by CelltTiter-glo and hemocytometry, and cytotoxic activities by MTT. IC_{50} values of receptacle water (WRC), aqueous ethanol (ARC) and ethanol (ERC), bractea leaf water (WBC), aqueous ethanol (ABC) and ethanol (EBC), and stem leaf water (WSC), aqueous ethanol (ASC) and ethanol (ESC) extracts were determined as 2.45 mg/mL, 1.52 mg/mL, 1.66 mg/mL, 3.45 mg/mL, 1.46 mg/mL and 0.58 mg/mL, 0.24 mg/mL, 0.21 mg/mL and 0.08 mg/mL, respectively. When these results are compared with the drug-free control group, it was determined that stem leaf aqueous ethanol (SI: 7.98), ethanol (SI: 4.96) and water (SI: 2.71) extracts with the highest selectivity index (SI) values showed antileishmanial activity ($P<0.05$). Extracts of *C. scolymus* did not show cytotoxic activity except for WBC, WRC and ARC. In conclusion, the data presented in the current study indicated that *C. scolymus* stem leaf extracts (ESC, ASC and WSC) present effective antileishmanial activity. Future studies could focus on the identification and purification of the antileishmanial compounds within these extracts for analysis of their *in vivo* antileishmanial activity.

Keywords: *Antileishmanial activity, Artichoke, Cutaneous leishmaniasis, Cynara scolymus, Leishmania tropica*

Leishmania tropica'ya Karşı *Cynara scolymus* Ekstrelerinin *In-vitro* Antileishmanial Etkinliğinin Değerlendirilmesi

Öz

Çalışmamızda *Cynara scolymus* (enginar) bitkisinin reseptakulum, brakte ve gövde yaprağı kısımlarından hazırlanmış ekstrelerinin *Leishmania tropica*'ya karşı *in vitro* antileishmanial aktivitelerinin araştırılması amaçlanmıştır. Türkiye'nin Manisa ilinden kutanöz leishmaniasis hastasından izole edilen ve sıvı azotta saklanan bir *Leishmania* izolatı, yapılan tür tayini sonucunda *L. tropica* (MHOM/TR/2012/CBCL-LT) olarak saptanmıştır. *Cynara scolymus* bitki ekstrelerinin *in vitro* antileishmanial aktiviteleri CelltTiter-glo ve hemositometri yöntemleriyle, sitotoksik aktiviteleri ise MTT yöntemiyle incelenmiştir. Reseptakulum su, sulu etanol ve etanol, brakte yaprağı su, sulu etanol ve etanol ve gövde yaprağı su, sulu etanol ve etanol ekstrelerinin IC_{50} değerleri sırasıyla 2.45 mg/mL, 1.52 mg/mL, 1.66 mg/mL, 3.45 mg/mL, 1.46 mg/mL ve 0.58 mg/mL, 0.24 mg/mL, 0.21 mg/mL ve 0.08 mg/mL olarak saptanmıştır. Bu sonuçlar ilaçsız kontrol grubuyla karşılaştırıldığında; en yüksek seçicilik indeksi (SI) değerlerine sahip olan gövde yaprağı sulu etanol (SI: 7.98), etanol (SI: 4.96) ve su (SI: 2.71) ekstrelerinin antileishmanial etkinlik gösterdiği saptanmıştır ($P<0.05$). *Cynara scolymus* bitkisinin brakte yaprağı su, reseptakulum su ve reseptakulum sulu etanol ekstreleri dışındaki ekstreler sitotoksik aktivite göstermemiştir. Sonuç olarak elde edilen verilere göre *C. scolymus* gövde yaprağı sulu etanol, etanol ve su ekstrelerinin etkili antileishmanial aktivite gösterdiği saptanmıştır. İleriki çalışmalarda, bu ekstrelerin içeriğindeki antileishmanial aktiviteden sorumlu bileşiklerinin tanımlanması, saflaştırılması ve *in vivo* antileishmanial aktivitelerinin analizine çalışılacaktır.

Anahtar sözcükler: *Antileishmanial aktivite, Cynara scolymus, Enginar, Kutanöz leishmaniasis, Leishmania tropica*

How to cite this article?

Yıldırım A, Aksoy T, Ceylan ŞS, Kayalar H, Tayfur E, Balcıoğlu İC: Assessment of *in-vitro* antileishmanial activities of *Cynara scolymus* extracts against *Leishmania tropica*. *Kafkas Univ Vet Fak Derg,* 27 (3): 381-387, 2021.
DOI: 10.9775/kvfd.2021.25656

(*) Corresponding Author

Tel: +90 507 881 8920
E-mail: ahmet.yildirim@cbu.edu.tr (A. Yıldırım)

Introduction

Leishmaniasis is a zoonotic/anthroponotic parasitic infectious disease caused by obligate intracellular *Leishmania* protozoan parasites and transmitted by the sand fly vector *(Phlebotomus* spp.). Leishmaniasis, which ranks second among the neglected parasitic diseases in the world after malaria that causes the most common death, is seen in a wide geographical area including Turkey, especially in developing countries (Middle East, South America, Africa, Central Asia and Mediterranean Basin) [1]. According to the World Health Organization (WHO), more than 1 billion people in 92 countries and 83 regions, worldwide in 2018, were living at risk of infection in areas endemic for leishmaniasis, and an estimated 30.000 new cases of visceral leishmaniasis (VL) and more than 1 million new cases of cutaneous leishmaniasis (CL) are reported each year [2].

The clinical manifestation of the disease varies depending on the species of parasite and isoenzyme structure. Accordingly, in addition to the CL and VL forms of leishmaniasis, there are different clinical forms such as mucocutaneous leishmaniasis (MKL), post kala azar dermal leishmaniasis (PKDL) and diffuse cutaneous leishmaniasis (DCL). The cases usually recover spontaneously without treatment by leaving a scar in CL, which is the clinically mildest form of the disease. *Leishmania tropica*, *L. major*, *L. aethiopica* and *L. infantum* are causative agents of CL in the Old World include. The causative agents of CL in Turkey are *L. tropica* and *L. infantum*. However, recently, *L. major* and *L. donovani* were identified by molecular methods using clinical samples of patients with CL from Şanlıurfa and Adana provinces in the southern part of Turkey [3]. There is a decrease in the incidence of leishmaniasis due to malaria eradication studies that have been implemented in Turkey since the 1950s. However, since 1980, it has come up again as a public health problem in certain regions, especially in Cukurova and Southeast Anatolia. Because of the migration to Turkey from countries and regions, where leishmaniasis is endemic, the increasing number of cases has been confirmed in recent studies [4,5].

Pentavalent antimonial compounds are used as the first line treatment of leishmaniasis. In addition, drugs such as paramomycin, miltefosine, fluconazole and liposomal amphotericin b are beneficial as an alternative therapy. For reasons such as development of resistance to drugs in use, the toxic side effects of some drugs and their high cost, studies on alternative treatment methods and vaccine development carry on. Investigating the use of herbal products for medical purposes in the development of new drugs with low cost and few side effects take an important place in the development of alternative treatment methods [1].

In this study, it was aimed to investigate *in vitro* antileishmanial activity of *C. scolymus* (artichoke) plant extracts, prepared from the receptacle, bractea leaves and stem leaves, by using water, aqueous ethanol and ethanol solvents, against *L. tropica* in order to investigate new active substances and new drug candidates that can be used in the treatment of leishmaniasis.

Material and Methods

Ethical Statement

This study was approved by the Ethics Committee of Clinical Research at Medical School of Manisa Celal Bayar University (Approval no: 21/05/2019-E.42582).

Preparation of Cynara scolymus Plant Extracts

Cynara scolymus aerial parts were gathered from the region belonging to 38°25'24.0"N 26°35'05.0"E coordinates from İzmir province *(Fig. 1)*. The receptacle, bractea leaves and stem leaves of the gathered *C. scolymus* plant were separated and air dried under appropriate conditions and pulverized in the grinder. The water extracts were prepared by 2% infusion of plant materials. The ethanol and 50% aqueous ethanol extracts were prepared by maceration under stirring whereas the solvent/plant material ratio was 15/1. The water extract of bractea leaf (WBC), aqueous ethanol extract of bractea leaf (ABC), ethanol extract of bractea leaf (EBC), water extract of receptacle (WRC), aqueous ethanol extract of receptacle (ARC), ethanol extract of receptacle (ERC), water extract of stem leaf (WSC), aqueous ethanol extract of stem leaf (ASC), ethanol extract of stem leaf (ESC) of *C. scolymus*, nine extracts in total, were filtered through Whatman no. 1 filter paper and evaporated under reduced pressure to dryness. The dried residues were lyophylisied and stored in screw capped vials at -20°C until analysis [6,7].

In Vitro Culture of Leishmania spp. Isolate

The *Leishmania* isolate, obtained from Turkey and stored in liquid nitrogen at the Parasite Bank of Medical School of Manisa Celal Bayar University, was removed from the liquid nitrogen tank under proper conditions and cultured in NNN medium after viability control. The NNN medium

Fig 1. *Cynara scolymus* plant

was placed in an incubator at 26°C and incubated. The medium was checked for growth on consecutive days after inoculation. Promastigotes, obtained from NNN medium detected parasite growth, were inoculated into 5 mL RPMI-1640 medium (10% FCS) in cell culture flask on the fifth day of incubation. The flasks were then incubated in an incubator (Panasonic®, Japan) at 26°C. On consecutive days, the medium was controlled for promastigote growth. *Leishmania* promastigotes, grew logarithmically ($1x10^6$ promastigotes/mL), were used in the current study [8].

Genotyping of Leishmania spp. Isolate

Genetic material was obtained to determine the genotype of the *Leishmania* isolate and DNA isolation was performed in accordance with the High Pure PCR Template Preparation Kit (Qiagen®, Germany) procedure. Real-time PCR method was applied using probes specific to the internal transcribed spacer 1 (ITS1) gene region in the current study. Ribosomal ITS1 region, separating the genes encoded SSU rRNA and 5.8S rRNA of *Leishmania* parasites, was amplified using the specific primers, the QuantiTect Probe PCR Kit Master (Qiagen®, Germany) mix and the specific probes [9,10]. A total of 25 µL reaction mixture, prepared for real-time PCR analysis, contained 4.5 µL H_20, 1 µL forward primer, 1 µL reverse primer, 0.5 µL probe1, 0.5 µL probe 2, 12.5 µL QuantiTect Probe PCR Kit Master mix (Qiagen®, Germany) and 5 µL gDNA. The *Leishmania* isolate was genotyped with the results obtained by melting analysis in the Rotor-Gene.

Cytotoxic Activity (CC_{50})

L-929 fibroblast cell line was cultured to evaluate the cytotoxic activity of nine different extracts prepared from receptacle, bractea leaves and stem leaves samples of *C. scolymus*. The cell line was cultivated in cell culture flasks under appropriate conditions (37°C, 5% CO_2 and 95% humidity/incubator (Thermo Fisher Scientific® USA) using RPMI-1640 medium (10% FCS). By preparing different final concentrations from plant extracts, their cytotoxic activities were determined colorimetrically using the MTT (Biomatik®, Germany) method and the cytotoxic concentration (CC_{50}) values, killing 50% of the cells, were determined statistically [11].

In Vitro Antileishmanial Activity (IC_{50})

Concentrations of each plant extracts (WBC, ABC, EBC, WRC, ARC, ERC, WSC, ASC, ESC) (0.01 mg/mL - 125 mg/mL) were prepared for *in vitro* experiments. The extracts were dissolved and diluted in fresh RPMI-1640 medium containing 10% FCS. The final volume was adjusted to 200 µL with fresh RPMI-1640 medium for each well of a 96-well flat-bottom cell culture plate (Ratiolab®, Germany). Promastigotes were suspended to yield 1×10^6 promastigotes/mL in each well by haemocytometry. Cell culture plates were incubated at 26°C for 48 h. At the end of the incubation process, *in vitro* antileishmanial activities of *C. scolymus* plant extracts were evaluated by hemocytometry and CellTiter-Glo methods, and inhibitor concentration (IC_{50}) values, killed 50% of the cells, were determined. Otherwise, Giemsa-stained slides were prepared and examined under the light microscope to evaluate the changes in promastigote morphology due to the efficiency of *C. scolymus* plant extracts after 48 h of incubation. As a reference drug, amphotericin b was prepared in sterile DMSO. In all experiments, in order not to affect parasite growth rate, mobility or morphology, the final concentration of DMSO was not higher than 0.5% (v/v). Cell culture plates were then read in luminoscan ascent (Thermo Fisher Scientific®, USA), viability and the antileishmanial activity values (IC_{50}) were calculated according to the absorbance values obtained, and all the tests were carried out in triplicate in the current study [8,12].

Selectivity Index (SI)

The selectivity index (SI) is a comprehensive parameter used to express *in vitro* efficacy of an herbal compound in parasite proliferation inhibition and the ratio of the cytotoxic activity value (CC_{50}) to the antileishmanial activity value (IC_{50}). SI values were determined for each plant extract of *C. Scolymus* [11].

Statistical Analysis

Statistical analysis of the data, obtained by applying Sidak's multiple comparisons test with GraphPad Prism 8 software (GraphPad Software Inc., San Diego, CA), was performed.

Results

Genotyping the Leishmania Isolate

The *Leishmania* strain, isolated from CL patient in Turkey and stored in liquid nitrogen at Parasite Bank of Medical School of Manisa Celal Bayar University, was matched to *L. tropica* (MHOM/TR/2012/CBCL-LT) as a result of genotyping with the RT-PCR method.

Cytotoxic Activity (CC_{50})

Cytotoxic activities (CC_{50}) of *C. scolymus* plant extracts, water, aqueous ethanol and ethanol extracts prepared from the receptacle, bractea and stem leaves, were determined colorimetrically by MTT method and were statistically evaluated. While WBC, ARC and WRC plant extracts of *C. scolymus* exhibited cytotoxic activity and CC_{50} values were determined as 1.61 mg/mL, 0.58 mg/mL and 1.71 mg/mL, respectively, all other extracts didn't display cytotoxic activity.

Antileishmanial Activity (IC_{50})

Antileishmanial activity (IC_{50}) of different concentrations of *C. scolymus* plant extracts, water, aqueous ethanol and ethanol extracts prepared from the receptacle, bractea

leaves and stem leaves, on *L. tropica* promastigotes were evaluated by haemocytometry and CellTiter-glo® methods after 48 h of incubation. In the evaluation of antileishmanial activity, the IC_{50} value of AmB as a control drug was evaluated as 0.05 µM. When the antileishmanial effects of water, aqueous ethanol and ethanol extracts prepared from the receptacle, bractea leaves and stem leaves of *C. scolymus* were evaluated, IC_{50} values of ESC (0.08 mg/mL), ASC (0.21 mg/mL), WSC (0.24 mg/mL), EBC (0.58 mg/mL), ABC (1.46 mg/mL), ARC (1.52 mg/mL), ERC (1.66 mg/mL), BRC (2.45 mg/mL) and WBC (3.45 mg/mL) plant extracts were determined. When these results are compared with parasite control (drug-free) results; ESC (IC_{50}=0.08 mg/mL), ASC (IC_{50}=0.21 mg/mL), WSC (IC_{50}=0.24 mg/mL) and EBC (IC_{50}=0.58 mg/mL) extracts exhibited antileishmanial effect ($P<0.05$). However, other extracts did not display antileishmanial effect ($P>0.05$). It is seen that the ESC (IC_{50}=0.08 mg/mL) extract has the highest inhibition degree among the extracts with antileishmanial activity *(Fig. 2)*. In the wake of light microscopic examination of Giemsa-stained slides, prepared after 48 h of incubation, nuclear and cytoplasmic changes of promastigotes weren't detected in promastigotes at concentrations below the IC_{50} values of *C. scolymus* extracts in terms of promastigote morphology. On the other hand, significant pathological changes such as rounding, granulation, shortening or extinction of flagellum, and expansion of nucleus were observed at IC_{50} values and higher concentrations of *C. scolymus* plant extracts *(Fig. 3-A,B)*.

Selectivity Index (SI)

The selectivity index (SI) is the ratio of the cytotoxic activity value (CC_{50}) to the antileishmanial activity value (IC_{50}). Selectivity index values were determined for each plant extract of *C. scolymus*, ESC (4.96), ASC (7.98), WSC (2.71), EBC (1.65), ABC (1.10), WBC (0.46), ERC (1.64), ARC (0.38), WRC (0.69), and control drug (AmB) (277.2) *(Table 1)*.

Discussion

Meglumine antimoniate (Glucantime®) and sodium stibogluconate (Pentostam®) are used as the first preference in the treatment of CL. When long-term use of these drugs is required, many disadvantages such as toxicity, cost and drug resistance are encountered. In recent years, resistance development against these drugs has been reported, notably in the northern regions of India [13]. AmB is highly costly and preferred secondary option in the treatment of leishmaniasis, and has been reported to

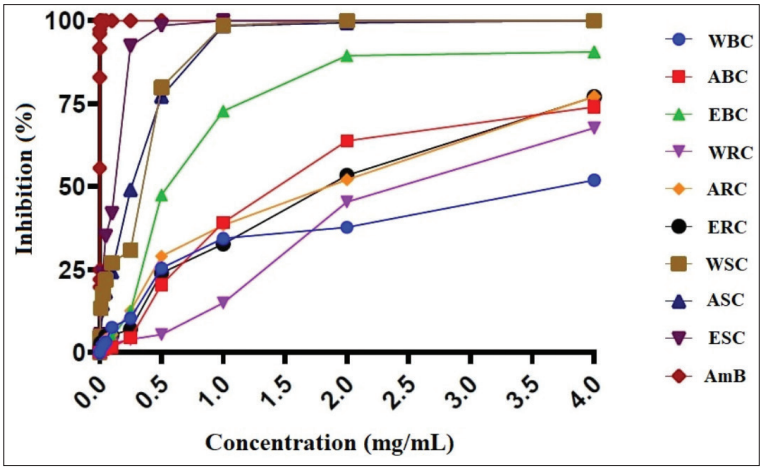

Fig 2. Antileishmanial activities of receptacle, bractea leaf and stem leaf extracts of *Cynara scolymus*. WRC: Water extract of receptacle, ARC: Aqueous ethanol extract of receptacle, ERC: Ethanol extract of receptacle, WBC: Water extract of bractea leaf, ABC: Aqueous ethanol extract of bractea leaf, EBC: Ethanol extract of bractea leaf, WSC: Water extract of stem leaf, ASC: Aqueous ethanol extract of stem leaf, ESC: Ethanol extract of stem leaf, AmB: Amphotericin B

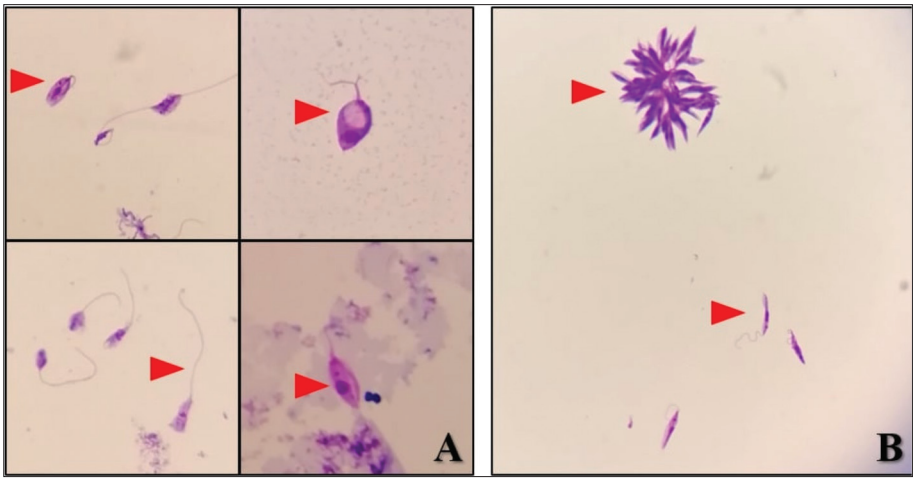

Fig 3. Morphological changes of *Leishmania tropica* promastigotes. A: Cytopathological changes due to *Cynara scolymus* stem leaf extracts on *Leishmania tropica* promastigotes, B: *Leishmania tropica* promastigotes with normal morphology (1.000× magnification)

have toxic effects on the kidneys. In addition, miltefosine, a new drug perorally used, has been reported to have teratogenic effects [14]. There is no vaccine currently in use for leishmaniasis prophylaxis. Thus, there is a need for safe, effective and cheap drugs. WHO encourages the search for new drugs and the use of natural products for the treatment of leishmaniasis due to the limitations of current treatment regimens [15]. It is believed that the plants used to treat tropical diseases can be obtained by establishing the new generation of antiparasitic drugs or the necessary infrastructure for their synthesis [16]. Therefore, new treatment options for leishmaniasis are being investigated. Especially, new drugs are defined on the basis of pharmacological concepts related to the activity of active molecules of medicinal plants or compounds with similar structures [17]. In order for chemical compounds obtained from natural sources or synthesized within the scope of pre-clinical evaluation to be used in clinical practice, toxicity and screening tests must be performed in the process of development and evaluation of new antileishmanial drugs. Although drug screening tests can mostly be performed in an *in vitro* experimental model, *in vivo* experimental models are suitable for studies investigating metabolic rates, biokinetic properties of the active substance and interaction between organs. The compounds, found effective as a result of drug screening tests, are subjected to toxicity tests in order to examine their histopathological, biochemical and functional toxic effects. It has been reported that phase I, phase II, phase III and phase IV steps should be implemented within the scope of clinical evaluation [18].

It is reported that natural plant extracts, which have the potential to be used in the treatment of leishmaniasis, can be used in the treatment by determining their biological activities with drug screening tests or by making synthetic forms of some natural compounds. In a study, conducted by Costa et al.[19] in 2021, which evaluated the antileishmanial activity of the synthetic Rip-E compound of riparin, which is an alkamide found in the immature fruits of *Aniba riparia*, $IC_{50}^{promastigote}$=4.7 µg/mL, $IC_{50}^{amastigote}$=1.3 µg/mL, CC_{50}=50.6 µg/mL and SI=38.9 values were attained and the synthetic Rip-E compound of riparin was found to show antileishmanial activity against *L. amazonensis*.

Table 1. *In vitro antileishmanial activity, cytotoxicity and selectivity index values of water, aqueous ethanol and ethanol extracts prepared from the receptacle, bractea leaf and stem leaf of Cynara scolymus*

Extracts	IC_{50} (mg/mL)	CC_{50} (mg/mL)	SI (CC_{50}/IC_{50})
ESC	0.08	0.40	4.96
ASC	0.21	1.68	7.98
WSC	0.24	0.65	2.71
EBC	0.58	0.96	1.65
ABC	1.46	1.61	1.10
WBC	3.45	1.61	0.46
ERC	1.66	2.73	1.64
ARC	1.52	0.58	0.38
WRC	2.45	1.71	0.69
AmB (Control drug)	0.0005	0.14	277.2

Cynara scolymus, researched in the current study in terms of antileishmanial activity, is a medicinal plant with a wide range of different study areas. Artichoke leaf extract (ALE) has been reported to show antioxidant, anti-inflammatory, antibacterial, antiviral, and anticancer activity. When the efficacy of C. scolymus plant extracts on parasites was researched, a limited number of references were found. The antiparasitic and hepato-protective properties of ALE on mice, experimentally infected with *Schistosoma mansoni,* were examined and compared with praziquantel in a study conducted by Sharaf EL-Deen et al.[20] in 2017. In order to evaluate the antischistosomial features of ALE, parasite burden, number of eggs, number and diameter of granuloma were measured. Although ALE did not have a significant effect on egg load and number of granulomas, it was ultimately observed that it caused a significant decrease in diameter of granuloma and improvement in liver functions and liver fibrosis [20]. In the current study, the antileishmanial effects of water, aqueous ethanol and ethanol extracts prepared from the receptacle, bracktea leaves and stem leaves of *C. scolymus* plant extracts were evaluated and compared with AmB, and it was observed that EBC, ESC, ASC and WSC extracts exhibited antileishmanial effect and were statistically significant.

Antifungal activities of chloroform, ethanol and ethyl acetate extracts of leaves, heads and stems of *C. scolymus* plant were investigated using agar-well diffusion technique in a study conducted by Zhu et al.[21] in 2005. All structures of the *C. scolymus* (leaf, head and stem) showed activity against the organisms tested. At the end of the study, it was concluded that leaf extracts and ethanol fractions were the most effective extracts against all organisms tested. It was reported that *C. scolymus* leaves could be a new potential agent in the treatment of fungal infections in the study [21]. Also, the antileishmanial activity of the receptacle, brachtea leaves and stem leaves of the *C. scolymus* plant extracts was investigated and it was concluded that the leaf extracts were superior to other extracts in the current study.

The effects of chloroform, ethyl acetate and n-butanol extracts of *C. scolymus* leaf extracts on seven bacteria, four yeast and four mold species were investigated by antimicrobial disc method in a study conducted by Zhu et al.[22] in 2004. Eight phenolic compounds were isolated from artichoke leaf n-butanol extracts and when examined for their antimicrobial activities, all of them were reported to be effective against the studied organisms. Among

these compounds, chlorogenic acid, cynarin, luteolin-7-rutinoside and sinoroside have been reported to show higher activity than other compounds, are more effective against fungi compared to bacteria, and the minimum inhibitory concentration (MIC) of these compounds is 50-200 µg/mL. Among these compounds, chlorogenic acid, cynarin, luteolin-7-rutinoside and sinoroside have been reported to show higher activity than other compounds and be more effective against fungi compared to bacteria, and the minimum inhibitory concentrations (MIC) of these compounds are 50-200 µg/mL [22].

When the cytotoxic concentrations (CC_{50}) of the water, aqueous ethanol and ethanol extracts, prepared from the receptacle, bractea leaves and stem leaves of the *C. scolymus*, were evaluated, ESC, ASC, WSC, EBC, ABC and ERC extracts did not show cytotoxic activity. However, EBC, ARC ve ERC extracts of *C. scolymus* showed cytotoxic activity.

When the efficacy of the water extract obtained from *Physalis angulata* roots against *Leishmania amazonensis* was evaluated, morphological changes, observed in promastigotes at concentrations of IC_{50} and above, were associated with antileishmanial activity by Da-Silva et al.[23] in 2015. Similarly, significant pathological changes such as rounding of promastigotes, granulation, shortening or disappearance of flagellum length, widening of the nucleus were also described at IC_{50} and higher concentrations following incubation with *C. scolymus* plant extracts in the current study.

The selectivity index (SI) is an important indicator of whether a plant compound is effective or not. The selectivity index is used in *in vitro* efficacy studies of herbal compounds that inhibit parasite reproduction and is widely accepted as an important parameter. The SI value is calculated by the ratio of the cytotoxic concentration (CC_{50}) value to the inhibitor concentration (IC_{50}) value [24]. Cytotoxic concentration (CC_{50}) values and SI values of water, aqueous ethanol and ethanol extracts, prepared from the receptacle, bracktea leaves and stem leaves of *C. scolymus*, are between 0.40-2.73 mg/mL and 0.38-7.98, respectively. Various criteria have been stated in the studies to define the selective antiparasitic activities of medicinal plant extracts. For instance; selective antiparasitic activity has been reported for medicinal plant extracts when the SI value is greater than 1 by Tempone et al.[25], greater than 2 by Arevalo-Lopez et al.[26], and greater than 3 by Joshi et al.[27]. In addition, researchers working on synthetic derivatives recommend SI>6 as a convenient criterion [28]. It was accepted that *C. scolymus* plant extracts with a SI value greater than 2 showed antileishmanial activity in the current study. Compared with AmB SI value (277.2), ESC, ASC and WSC extracts with the SI values of 4.96, 7.98 and 2.21, respectively, showed high antileishmanial activity against *L. tropica* promastigotes. Therefore, the antileishmanial activity of ESC, ASC and WSC extracts whose SI values are greater than two is considered to be an important and promising development in the detection of antileishmanial agents, which is the aim of the current study.

In conclusion, according to IC50, CC50 and SI data, the lack of cytotoxic activity of stem leaf extracts (ESC, ASC and WSC) of C. scolymus and the detection of antileishmanial activity on promastigotes of L. tropica, which is the predominant etiologic agent of CL in Turkey, is considered to be an important and promising development for screening antileishmanial agents, which is the aim of the project.

Acknowledgements

We would like to express our very great appreciation to Prof. Ahmet Özbilgin, PhD. İbrahim Çavuş, Bio and the Parasite Bank of Medical School of Manisa Celal Bayar University for providing the *Leishmania* strain of this research work.

Conflict of Interest

The authors declare no potential conflicts of interest with respect to the research, authorship, and/or publication of this article.

Author Contributions

ICB, AY and TA designed the project. HK obtained plant extracts. AY, TA, SSC and ET carried experiments. AY, TA and SSC performed statistical analysis of data. The manuscript was written by TA and AY.

References

1. Özbel Y, Töz SO: Leishmaniasis. **In,** Özcel MA, Özbel Y AM (Eds): Özcel'in Tıbbi Parazit Hastalıkları. 197-244, Türkiye Parazitoloji Derneği, İzmir, 2007.

2. WHO: Leishmaniasis. https://www.who.int/news-room/fact-sheets/detail/leishmaniasis; *Accessed:* 20.01.2021.

3. Özbilgin A, Çulha G, Uzun S, Harman M, Topal SG, Okudan F, Zeyrek F, Gündüz C, Östan İ, Karakuş M, Töz S, Kurt Ö, Akyar I, Erat A, Güngör D, Kayabaşı Ç, Çavuş İ, Bastien P, Pratlong F, Kocagöz T, Özbel Y: Leishmaniasis in Turkey: First clinical isolation of *Leishmania major* from 18 autochthonous cases of cutaneous leishmaniasis in four geographical regions. *Trop Med Int Health*, 21 (6): 783-791, 2016. DOI: 10.1111/tmi.12698

4. Ok UZ, Balcioglu IC, Taylan Ozkan A, Ozensoy S, Ozbel Y: Leishmaniasis in Turkey. *Acta Trop*, 84 (1): 43-48, 2002. DOI: 10.1016/S0001-706X(02)00134-1

5. Toz SO, Nasereddin A, Ozbel Y, Ertabaklar H, Culha G, Sevil N, Alkan MZ, Jaffe CL: Leishmaniasis in Turkey: Molecular characterization of *Leishmania* from human and canine clinical samples. *Trop Med Int Health,* 14 (11): 1401-1406, 2009. DOI: 10.1111/j.1365-3156.2009.02384.x

6. Ural IO, Kayalar H, Durmuskahya C, Cavus I, Özbilgin A: *In vivo* antimalarial activity of methanol and water extracts of *Eryngium thorifolium* Boiss (Apiaceae Family) against *P. berghei* in infected mice. *Trop J Pharm Res*, 13 (8): 1313-1317, 2014. DOI: 10.4314/tjpr.v13i8.16

7. Ozbilgin A, Durmuskahya C, Kayalar H, Ostan I: Assessment of *in vivo* antimalarial activities of some selected medicinal plants from Turkey. *Parasitol Res*, 113 (1): 165-173, 2014. DOI: 10.1007/s00436-013-3639-1

8. Ozbilgin A, Cavuş I, Yıldırım A, Kaya T, Ertabaklar H: Evaluation of

in vitro and *in vivo* drug efficacy over *Leishmania tropica*: A pilot study. *Turkiye Parazitol Derg*, 42 (1):11-19, 2018. DOI: 10.5152/tpd.2018.5554

9. Toz SO, Culha G, Zeyrek FY, Ertabaklar H, Alkan MZ, Vardarlı AT, Gunduz C, Ozbel Y: A real-time ITS1-PCR based method in the diagnosis and species identification of *Leishmania* parasite from human and dog clinical samples in Turkey. *PLoS Negl Trop Dis*, 7(5):e2205, 2013. DOI: 10.1371/journal.pntd.0002205

10. An I, Harman M, Cavus I, Ozbilgin A: The diagnostic value of lesional skin smears performed by experienced specialist in cutaneous leishmaniasis and routine microbiology laboratory. *Turk J Dermatol*, 13 (Suppl. 1): 1-5, 2019. DOI: 10.4274/tdd.galenos.2018.3812

11. Badirz adeh A, Heidari-Kharaji M, Fallah-Omrani V, Dabiri H, Araghi A, Salimi Chirani A: Antileishmanial activity of *Urtica dioica* extract against zoonotic cutaneous leishmaniasis. *PLoS Negl Trop Dis*, 14 (1): e0007843, 2020. DOI: 10.1371/journal.pntd.0007843

12. Ostan I, Saglam H, Limoncu ME, Ertabaklar H, Toz SO, Ozbel Y, Ozbilgin A: *In vitro* and *in vivo* activities of *Haplophyllum myrtifolium* against *Leishmania tropica*. *New Microbiol*, 30 (4): 439-445, 2007.

13. Croft SL, Yardley V: Chemotherapy of Leishmaniasis. *Curr Pharm Des*, 8 (4): 319-342, 2002. DOI: 10.2174/1381612023396258

14. Ponte-Sucre A, Gamarro F, Dujardin JC, Barrett MP, López-Vélez R, García-Hernández R, Pountain AW, Mwenechanya R, Papadopoulou B: Drug resistance and treatment failure in leishmaniasis: A 21st century challenge. *PLoS Negl Trop Dis*, 11 (12): e0006052, 2017. DOI: 10.1371/journal.pntd.0006052

15. WHO: Status of endemicity of cutaneous leishmaniasis: 2019. https://apps.who.int/neglected_diseases/ntddata/leishmaniasis/leishmaniasis.html; *Accessed:* 20.01.2021.

16. Newman DJ, Cragg GM: Natural products as sources of new drugs over the 30 years from 1981 to 2010. *J Nat Prod*, 75 (3): 311-335, 2012. DOI: 10.1021/np200906s

17. Araújo IAC, Paula RC, Alves CL, Faria KF, Oliveira MM, Mendes GG, Dias EMFA, Ribeiro RR, Oliveira AB, Silva SM: Efficacy of lapachol on treatment of cutaneous and visceral leishmaniasis. *Exp Parasitol*, 199, 67-73, 2019. DOI: 10.1016/j.exppara.2019.02.013

18. Kayaalp SO: Klinik öncesi değerlendirmesi. **In,** Klinik Farmakolojinin Esasları ve Temel Düzenlemeler. 4th ed., 29-46, Faryal Matbaacılık, Ankara, 2008.

19. Costa LM, Alves MMM, Brito LM, Abi-Chacra EA, Barbosa-Filho JM, Gutierrez SJC, Barreto HM, Carvalho FAA: *In vitro* antileishmanial and immunomodulatory activities of the synthetic analogue riparin E. *Chem Biol Interact*, 336:109389, 2021. DOI: 10.1016/j.cbi.2021.109389

20. Sharaf EL-Deen SA, Brakat RM, Mohamed ASED: Artichoke leaf extract protects liver of *Schistosoma mansoni* infected mice through modulation of hepatic stellate cells recruitment. *Exp Parasitol*, 178, 51-59, 2017. DOI: 10.1016/j.exppara.2017.05.005

21. Zhu XF, Zhang HX, Lo R: Antifungal activity of *Cynara scolymus* L. extracts. *Fitoterapia*, 76 (1): 108-111, 2005. DOI: 10.1016/j.fitote.2004.1 0.016

22. Zhu X, Zhang H, Lo R: Phenolic compounds from the leaf extract of artichoke (*Cynara scolymus* L.) and their antimicrobial activities. *J Agric Food Chem*, 52 (24): 7272-7278, 2004. DOI: 10.1021/jf0490192

23. Meira CS, Guimarães ET, Dos Santos JAF, Moreira DRM, Nogueira RC, Tomassini TCB, Ribeiro IM, Campos de Souza CV, Dos Santos RR, Soares MBP: *In vitro* and *in vivo* antiparasitic activity of *Physalis angulata* L. concentrated ethanolic extract against *Trypanosoma cruzi*. *Phytomedicine*, 22 (11): 969-974, 2015. DOI: 10.1016/j.phymed.2015.07.004

24. Badirzadeh A, Heidari-Kharaji M, Fallah-Omrani V, Dabiri H, Araghi A, Chirani AS: Antileishmanial activity of *Urtica dioica* extract against zoonotic cutaneous leishmaniasis. *PLoS Negl Trop Dis*, 14 (1): e0007843, 2020. DOI: 10.1371/journal.pntd.0007843

25. Tempone AG, Martins De Oliveira C, Berlinck RGS: Current approaches to discover marine antileishmanial natural products. *Planta Med*, 77 (6): 572-585, 2011. DOI: 10.1055/s-0030-1250663

26. Arévalo-Lopéz D, Nina N, Ticona JC, Limachi I, Salamanca E, Udaeta E, Paredes C, Espinoza B, Serato A, Garnica D, Limachi A, Coaquira D, Salazar S, Flores N, Sterner O, Giménez A: Leishmanicidal and cytotoxic activity from plants used in Tacana traditional medicine (Bolivia). *J Ethnopharmacol*, 216, 120-133, 2018. DOI: 10.1016/j.jep.2018.01.023

27. Joshi B, Hendrickx S, Magar LB, Parajuli N, Dorny P, Maes L: *In vitro* antileishmanial and antimalarial activity of selected plants of Nepal. *J Intercult Ethnopharmacol*, 5 (4): 383-389, 2016. DOI: 10.5455/jice.20160728031236

28. Leal SM, Amado DF, Kouznetsov VV, Escobar P: *In Vitro* antileishmanial, trypanocidal, and mammalian cell activities of diverse N,N′-dihetaryl substituted diamines and related compounds. *Sci Pharm*, 81 (1): 43-55, 2013. DOI: 10.3797/scipharm.1205-14

Kafkas Universitesi Veteriner Fakultesi Dergisi
ISSN: 1300-6045 e-ISSN: 1309-2251
Journal Home-Page: http://vetdergikafkas.org

Kafkas Univ Vet Fak Derg
27 (3): 389-395, 2021
DOI: 10.9775/kvfd.2021.25714

RESEARCH ARTICLE

The Effects of *MBL1* Gene Polymorphism on Subclinical Mastitis in Holstein Cows

Esma Gamze AKSEL [1,a] Aytaç AKÇAY [2,b (*)] Korhan ARSLAN [1,c]
Mahmodul Hasan SOHEL [1,d] Güven GÜNGÖR [3,e] Bilal AKYÜZ [1,f]

[1] Erciyes University, Faculty of Veterinary Medicine, Department of Genetics, TR-38039 Kayseri - TURKEY
[2] Ankara University, Faculty of Veterinary Medicine, Department of Biostatistics, TR-06110 Ankara - TURKEY
[3] Erciyes University, Faculty of Veterinary Medicine, Department of Biometrics, TR-38039 Kayseri - TURKEY
ORCIDs: [a] 0000-0002-0040-8933; [b] 0000-0001-6263-5181; [c] 0000-0002-2440-884X; [d] 0000-0003-2224-085X; [e] 0000-0003-3695-9443
[f] 0000-0001-7548-9830

Article ID: KVFD-2021-25714 Received: 03.03.2021 Accepted: 01.06.2021 Published Online: 01.06.2021

Abstract

This study aims to investigate the effects of three single nucleotide (SNPs) polymorphisms of the *MBL1* gene on subclinical mastitis for Holstein cows. For this study, a total of 151 Holstein cows were selected in their third lactation. The subclinical mastitis conditions were determined using the California Mastitis Test (CMT). Genotyping was carried out with the PCR-RFLP method. The results revealed that the wild-type allele frequencies were 0.72 (G allele), 0.40 (G allele), and 0.37 (T allele) for 1252 G>A, 2534 G>A, and 2569 T>C SNPs, respectively. Among the investigated SNPs, only the 1252 G>A SNP was not found in Hardy-Weinberg equilibrium. The effects of SNPs on subclinical mastitis were modeled using multiple logistic regression analysis. The established model can identify cows with subclinical mastitis with a separation efficiency of 62.3%. It was thought that 1252 G>A and 2534 G>A SNPs may affect subclinical mastitis rates.

Keywords: *Cow, MBL1, Multiple logistic regression analysis, SNP, Subclinical mastitis*

Holstein İneklerinde *MBL1* Geni Polimorfizminin Subklinik Mastitis Üzerine Etkileri

Öz

Bu çalışma, *MBL1* geninde bulunan üç tek nükleotid polimorfizminin (SNP) Holstein ineklerinde subklinik mastitis üzerine etkilerini incelemeyi amaçlamaktadır. Çalışma için üçüncü laktasyonlarında olduğu bildirilen toplam 151 Holstein inek seçilmiştir. Subklinik mastitis kondüsyonları California Mastitis Testi (CMT) kullanılarak belirlenmiştir. Genotipleme PCR-RFLP yöntemi kullanılarak gerçekleştirilmiştir. Sonuç olarak doğal tip allel frekanslarının 1252 G>A, 2534 G>A ve 2569 T>C SNP'leri için sırasıyla 0.72 (G allel), 0.40 (G allel) ve 0.37 (T allel) olduğu belirlenmiştir. İncelenen SNP'ler arasında sadece 1252 G>A SNP'sinin Hardy-Weinberg dengesinde olmadığı belirlenmiştir. SNP'lerin subklinik mastitis üzerindeki etkileri, çok değişkenli lojistik regresyon analizi kullanılarak modellenmiştir. Oluşturulan model, subklinik mastitisli inekleri %62.3 verimlilikle belirleyebilmektedir. 1252 G>A ve 2534 G>A SNP'lerin subklinik mastitis oranları için etkili faktörler olabileceği düşünülmüştür.

Anahtar sözcükler: *Çok değişkenli lojistik regresyon analizi, İnek, MBL1, SNP, Subklinik mastitis*

INTRODUCTION

Infectious diseases lead to significant economic losses in both the dairy and meat industry because of the cost of treatment, loss of productivity, and finally the death of infected animals [1]. Among the infectious diseases, mastitis leads to huge economic losses in the dairy cattle industry, however, the total cost of economic losses is tried to be determined using several simulation models [2]. Mastitis is an infection occurring in the udder lobes as a result of an infection by different types of bacteria such as *Escherichia coli*, *Klebsiella spp*., *Staphylococcus aureus, Streptococcus spp*. [3-5], and some species of yeast, fungi, and mycobacteria [6]. Mastitis is usually classified as clinical, subclinical, and chronic mastitis according to the symptoms of infected animals [6]. Clinical mastitis (CM) was characterized by swelling, pain, and redness of the mammary, it can cause decreased yield of milk, and altered appearance of milk [4].

How to cite this article?

Aksel EG, Akçay A, Arslan K, Sohel MH, Güngör G, Akyüz B: The effects of MBL1 gene polymorphism on subclinical mastitis in Holstein cows. *Kafkas Univ Vet Fak Derg,* 27 (3): 389-395, 2021.
DOI: 10.9775/kvfd.2021.25714

(*) Corresponding Author

Tel: +90 312 317 0315/4475 Cellular Phone: +90 505 502 5823 Fax: +90 312 316 4472
E-mail: aytacakcay@ankara.edu.tr (A. Akçay)

On the other hand, subclinical mastitis does not create any visible changes, neither in the udder physiology nor in the appearance of milk. Besides the reduction in milk production, subclinical mastitis could transform into clinical mastitis if it is diagnosed at a later stage. Moreover, this leads to the early culling of productive animals from the herd that ultimately resulted in serious economic losses for farms [7,8]. It has been reported that subclinical mastitis cases are more common than clinical mastitis in Turkey, and about 70-80% of the loss of milk production cases concerning mastitis are caused by sub-clinical mastitis [9]. The prevalence rate of subclinical mastitis per cow was reported to be 46.4% in Brazil [10], 43.1% in Rwanda in Africa [11], 42.5% in Iran [12], and 40% in Turkey [13].

Animal care, udder and milking hygiene, and herd management play a significant role in the prevention of mastitis [4]. Nevertheless, most of the studies have concentrated on establishing genetically resistant herds against diseases [14-16]. The MBL is a collagenous serum lectin that can bind to many pathogens including bacteria, fungi, viruses, and parasites. Moreover, it participates in the activation of the innate and adaptive immune systems of organisms [17,18]. By binding with the surface carbohydrates of pathogens, MBL activates the lectin pathway, which facilitates the recognition of immune cells and mediates their phagocytosis [19]. It was reported that a low level of serum MBL protein was significantly associated with susceptibility to bacterial and fungal infections [17]. Eleven collagenous lectin genes were identified in cattle, including genes encoding *MBL1* (A-type lectin) and *MBL2* (C-type lectin) in the MBL pathway [1]. It was reported that several SNPs in *MBL1* and *MBL2* genes were associated with mastitis resistance [1]. Furthermore, it is reported to be associated with a missense mutation (Val24Ile, rs109492835) in the exon 2 of the *MBL1* gene in cattle as well as with another mutation detected in the promoter region and the somatic cell score (SCS) in milk [14,15,20]. In another study was undertaken to identify whether the SNP rs109231409 (g.855G>A) of the *MBL1* gene was associated with mastitis tolerance or not which were analyzed with CMT and SCS [21]. Also on the *MBL1* gene, 1252 G>A, 2534 G>A, and 2569 T>C SNPs were examined to be associated with mastitis [14,15,20,22]. However, the association of these SNPs in the *MBL1* gene with subclinical mastitis has not been investigated yet.

In the present study, we have genotyped three SNPs including in intron 1 (1252 G>A) and exon 2 (2534 G>A and 2569 T>C) of the *MBL1* gene. This study was aimed to identify the separation efficiency of genotypes in positive and negative cases of subclinical mastitis at the end of genotyping by using a statistical model of Multiple Logistic Regression.

Material and Methods

Animals and Mastitis Test

A total of 151 Holstein dairy cows in their third lactation were randomly selected for this study. Blood samples of the cows used in the study were collected in accordance with the permission of Erciyes University Animal Experiments Local Ethics Committee, dated 14.06.2017 and numbered 17/056. The presence or absence of subclinical mastitis was determined by the CMT in farm conditions. According to CMT test results, the animals were categorized as positive (1) or negative (0).

Sample Collection and Processing

Blood samples were collected from the *vena jugularis* of cows. DNA was isolated from collected blood samples using the standard phenol:chloroform:isoamyl alcohol method [23]. DNA purity and concentrations were measured using a spectrophotometer (BioSpech-nano, SWEDEN).

PCR Primers and PCR Conditions

The sequences of primers [20] are presented in *Table 1*. The final volume of PCR reaction was found to be 20 µL consisting of 3 µL DNA (50 ng/µL), 1X buffer ($(NH_4)_2SO_4$ 500 mmol/L), 2.0 mmol/L $MgCl_2$, 0.25 mmol/l dNTP, and 0.5 U Taq DNA polymerase. The thermal cycles were as follows: 1 cycle at 95°C for 5 min after pre-denaturation, followed by 35 cycles at 95°C for 30 sec, at the annealing temperatures

Table 1. *Information on genotyped SNPs*

SNP	Forward and Reverse Primers	AL	TA	Genotype/bp	RE
1252 G>A	F: ACCTTGGGTCACCTGCAACAG R: GGTAGTTTAGGCAGCCCTAAAGC	*226 bp*	62.5°C	GG: 193,33 GA: 226, 193, 33 AA: 226	*Ava*II
2534 G>A	F: GTATCCTTCTCAAATACAAAAG**A**C R: CCCCTGTCTCTATGCTAGAC	*217 bp*	52.5°C	GG: 194, 23 GA: 217, 194, 23 AA: 217	*Mae*II
2569 T>C	F: GTGGTGGCAAATGTTGGCTAAAC R: TGGCTCTCCCTTTTCTCCCTT	*255 bp*	63.5°C	TT: 255 TC: 255, 178, 77 CC: 178, 77	*Hae*III

AL: *Amplicon Length;* ***bp:*** *base pair;* ***TA:*** *temperature of anneling;* ***RE:*** *Restriction enzyme*

for 30 sec *(Table 1)*, at 72°C for 30 sec, and finally, 1 cycle at 72°C for 7 min.

Genotyping of DNA

The resulting PCR products were digested using the restriction endonuclease enzymes (Thermo Scientific, USA) following the manufacturer's instructions. Briefly, enzymatic digestion was conducted in a 20 µL final volume containing 5 U of restriction enzyme *(Table 1)* and 10 µL of PCR products. The reaction mix was placed at various incubation temperatures as reported in the manufacturer's protocols for 4 h and inactivated at 80°C for 20 min. The digested products were visualized at 90 V and 300 mA on a 2% agarose gel dyed ethidium bromide for 40 min using an ultra-violet (UV) transilluminator. Expected restricted band sizes for each SNP after the restriction enzyme digestion are presented in *Table 1*.

Statistical Analysis

In the study, genotypic examinations were performed for the three SNPs in the intron 1 (1252 G> A) and exon 2 regions (2534 G> A, 2569 T> C) of the *MBL1* gene. The genotype, allele frequencies of the studied samples, and whether the population was in Hardy Weinberg equilibrium in terms of three SNPs were analyzed using the Chi-square goodness of fit test. Moreover, the effect of the presence of subclinical mastitis on their genotypes was identified using the multivariate logistic regression analysis. Univariate logistic regression analysis was conducted to examine the relationship between the candidate variables, which were not included in the logistic model, and mastitis.

In the multiple logistic regression model, the presence of mastitis was defined as the dependent variable (Y) while the genotypic frequencies of 1252 G>A, 2534 G>A, 2569 T>C SNPs were defined as independent variables. The backward elimination method was used in the logistic regression analysis. The statistical significance of the variables in the multiplee model was tested using the Wald test. The success of the model was determined using the deviation and Chi-square goodness of fit criteria. The coefficients of the logistics model were calculated using the maximum likelihood estimation method. The goodness of fit test of the final model was evaluated using the Hosmer-Lemeshow test value (Ĉg*). The classification accuracy of the model (the separation efficiency of the model to separate subclinical mastitis positive and negative cows using the predicted probabilities) was determined. The final model was evaluated by using odds ratios [OR, Exp(β)]. The statistical analyses were carried out using SPSS for Windows 14.01 (License No: 9869264) software package.

Results

The size of the PCR product of the 1252G> A SNP in the intron-1 region was found to be 226 bp. The results revealed that there were three genotypes *(Table 1)* for the 1252G>A SNP which were restricted with the *Ava*II enzyme *(Fig. 1)*. The size of the PCR product of the 2534 G>A SNP in the exon-2 region was found to be 217 bp. Three genotypes *(Table 1)* were determined after the digestion of the PCR products using the *Mae*II restriction enzyme *(Fig. 2)*. The size of the PCR product of the 2569 T>C SNP in the exon-2 region was found to be 255 bp. Three genotypes *(Table 1)* were observed after the digestion of the PCR products using the *Hae*III restriction enzyme *(Fig. 3)*.

The Chi-square test was conducted to investigate whether the genotypes of the 1252 G>A, 2534 G>A, 2569 T>C SNPs were in the Hardy-Weinberg (H-W) equilibrium. The results revealed that the analyzed samples of the 1252 G>A SNP were not in the H-W equilibrium (P<0.05), while the 2534 G>A and 2569 T>C SNPs were in the H-W equilibrium (P>0.05) *(Table 2)*. The genotype frequency of the 1252 G>A SNP was observed to be 11.9%, 31.8%. 56.3% for the AA, GA, and GG genotypes, respectively. On the other hand, the allele frequency was 0.28 and 0.72 for the A and

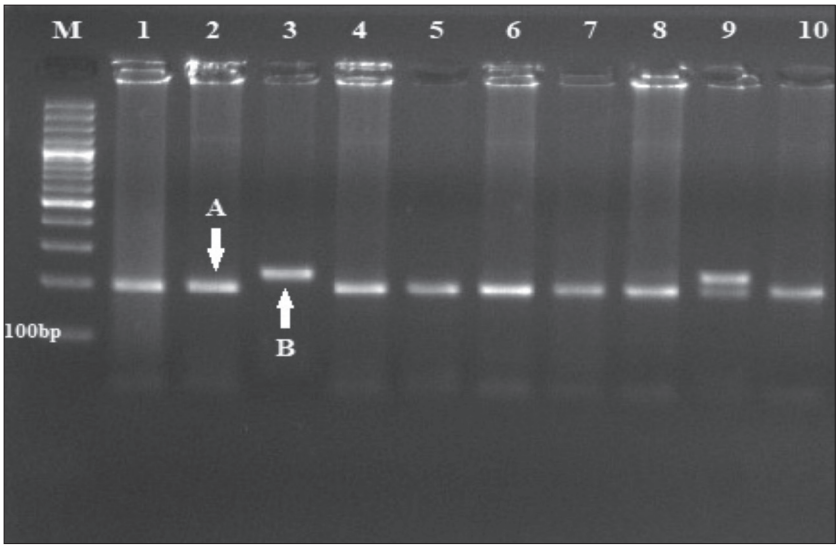

Fig 1. Gel-electrophoresis image of restricted PCR products for 1252 G>A SNP; M: Marker with 100 base pairs; A:193 bp ; B:226 bp; GG: 3; GA: 9; AA: 1, 2, 4, 5, 6, 7, 8, 10

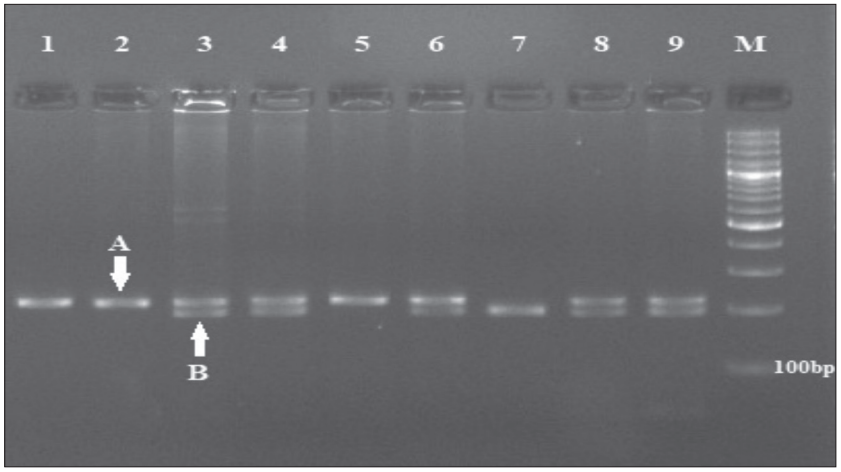

Fig 2. Gel-electrophoresis image of restricted PCR products for 2534 G>A; M: Marker with 100 base pairs. A: 217; B: 194; AA: 1, 2, 5; GA: 3, 4, 6, 8, 9; GG: 7

Fig 3. Gel-electrophoresis image of restricted PCR products for 2569 T>C; M: Marker with 100 base pairs. A: 255; B: 178; C: 77; TT: 5; TC: 1, 2, 4, 6, 7, 9; CC: 3, 8

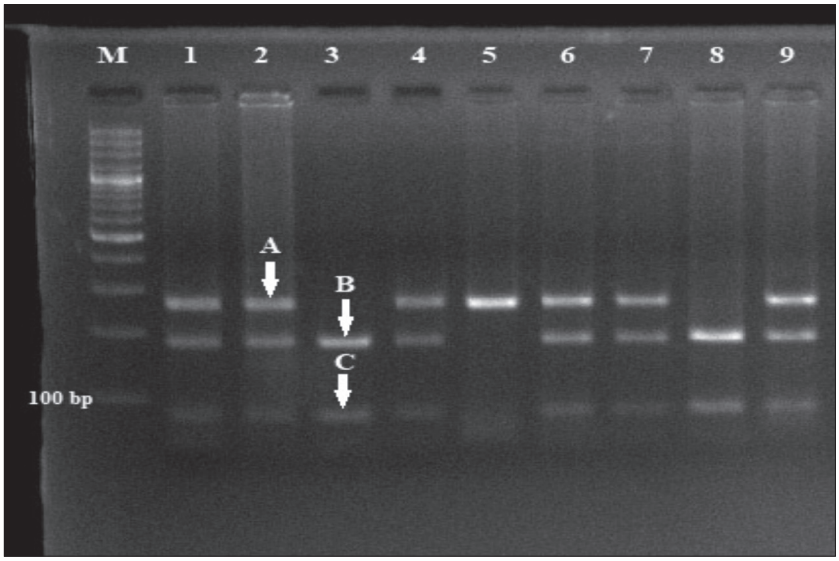

Table 2. *Goodness of fit test for Hardy-Weinberg Equilibrium*

SNP	Genotype Fraquency (Observed Valeu)			Allele Frequency		Chi-square Analysis (HW)
1252 G>A	AA: 11.9 (18)	GA: 31.8 (48)	GG: 56.3 (85)	A: 0.28	G: 0.72	$X^2 = 6.562^{*}$ P=0.038 (Df=1)
2534 G>A	AA: 39.7 (60)	GA: 41.1 (62)	GG: 19.2 (29)	A: 0.60	G: 0.40	$X^2 = 3.075^{NS}$ P= 0.215 (Df=1)
2569 T>C	TT: 17.2 (26)	TC: 40.4 (61)	CC: 42.4 (64)	T: 0.37	C: 0.63	$X^2 = 2.853^{NS}$ P=0.240 (Df=1)

Df: *Degree of freedom; * Statistically significant at 0.05 level; NS: Not significant*

G alleles, respectively *(Table 2)*. The details of the genotype and allele frequencies for all SNPs are presented in *Table 2*.

Genotype distribution of the 1252 G> A, 2534 G> A, and 2569 T> C SNPs in mastitis positive and negative cows in the study is presented in *Table 3*.

The effect sizes of the genotypes of the 1252 G>A, 2534 G>A, and 2569 T>C SNPs, which were thought to affect subclinical mastitis, were determined using the logistic regression analysis. Univariate logistic regression analysis was conducted to examine the relationship between the candidate variables, which were not included in the logistic model, with mastitis. According to the results, the 1252 G>A and 2534 G>A SNPs were found to be statistically significantly associated with subclinical mastitis (P<0.25) *(Table 4)*.

The backward elimination method was used in the multiple logistics model. Initially, all variables were taken into the model. Then those found to be statistically non-significant were deleted from the model at each step. The iteration was completed in 2 steps. The results of the backward elimination method are presented in *Table 5*.

At the end of the second step of the logistic regression

Table 3. *Genotype frequencies of cows subclinical mastitis status*

SNPs	Genotype	Subclinic Mastitis Negative		Subclinic Mastitis Positive	
		n	%	n	%
1252 G>A SNP	AA	13	18.8	5	6.1
	GA	21	30.4	27	32.9
	GG	35	50.7	50	61.0
2534 G>A SNP	AA	23	33.3	37	45.1
	GA	29	42.0	33	40.2
	GG	17	24.6	12	14.6
2569 T>C SNP	TT	11	15.9	15	18.3
	TC	30	43.5	31	37.8
	CC	28	40.6	36	43.9

Table 4. *Univariate logistic regression models of genotypes*

SNPs	Genotypes	β	SE (β)	Wald	P	OR	OR's 95% Confidence Interval	
							Min	Max
1252 G>A	AA			5.355	0.069			
	GA	1.207	0.601	4.028	0.045	3.343	1.029	10.863
	GG	1.312	0.571	5.290	0.021	3.714	1.214	11.363
	Constant	-0.956	0.526	3.297	0.069	0.385		
2534 G>A	AA			3.238	0.198			
	GA	0.824	0.461	3.191	0.074	2.279	0.923	5.627
	GG	0.478	0.455	1.102	0.294	1.612	0.661	3.932
	Constant	-0.348	0.377	0.853	0.356	0.706		
2569 T>C	TT			0.516	0.773			
	TC	0.059	0.470	0.016	0.900	1.061	0.422	2.665
	CC	-0.219	0.359	0.370	0.543	0.804	0.397	1.625
	Constant	0.251	0.252	0.995	0.319	1.286		

β: *Estimated slope coefficient;* ***SE (β):*** *Standard error of the estimated slope coefficient;* ***Wald:*** *Wald statistic, which tests whether the slope coefficients for the model are equal to zero;* ***P:*** *P value of Wald statistics;* ***OR:*** *Estimated odds ratio and 95% confidence interval values are given*

models, the level of correlations between the dependent variable and independent variables were evaluated using the Cox-Snell's R^2 and Nagelkerke's R^2 (Pseudo R^2) statistics. According to the results of this evaluation, the correlations between the dependent and independent variables in the second step were found to range between 8% and 12%.

The Hosmer-Lemeshow test value ($\hat{C}g^*$) is one of the goodness of fit test statistics calculating the success of the model to explain the dependent variable. The Hosmer-Lemeshow test ($\hat{C}g^*$) values ($\chi^2 = 0.063$, $P>0.05$) calculated for the second step showed that the independent variables (genotypes) in the logistic regression model sufficiently explained the dependent variable (mastitis ratio).

The variable coefficients were evaluated for each step using the backward elimination method, and the non-significant variables were removed from the model in the next step. That the constant term and the coefficients of the independent variables were different from zero in the model obtained in the second step was found to be statistically significant ($P<0.05$). According to the final model, the independent variables "1252 G>A, 2534 G>A" were found to affect the mastitis rate, and the obtained model could predict the probability of mastitis (P) by using the following equation:

$$\ln\left[\frac{p}{1-p}\right] = 0.120 + 4.220GA + 6.447GG + 3.839GA + 1.866GG$$

The classification rate of the model, i.e. the separation efficiency of the model in separating mastitis positive and mastitis negative cows using the predicted probabilities, was found to be 62.3%.

Discussion

The mannose-binding lectin pathway is one of three pathways that stimulate the complement system in the immune system [24]. This pathway binds to the mannose sugar of the pathogen, allowing early complement system members to be drawn into the pathogenic focus. Thereby, it plays a role in the activation of the complement system

Table 5. *Multivariate logistic regression model in the second step*

SNPs	Genotype	β	SE (β)	Wald	P	OR	OR's 95% Confidence Interval	
							Min	Max
1252 G>A	AA			8.787	**0.012**			
	GA	1.440	0.461	5.068	**0.024**	4.220	1.205	14.781
	GG	1.864	0.630	8.759	**0.003**	6.447	1.877	22.146
2534 G>A	AA			6.886	**0.032**			
	GA	1.345	0.530	6.435	**0.011**	3.839	1.358	10.852
	GG	0.624	0.496	1.584	**0.208**	1.866	0.706	4.931
Constant		-2.119	0.722	8.619	**0.003**	0.120		

β: *Estimated slope coefficient;* ***SE (β):*** *Standard error of the estimated slope coefficient;* ***Wald:*** *Wald statistic, which tests whether the slope coefficients for the model are equal to zero; P: P value of Wald statistics; OR: Estimated odds ratio and 95% confidence interval values are given.*

and thus in the pathogen phagocytosis of the natural immune cells [25]. Furthermore, the development of the membrane attack complex, and thus the direct lysis of the pathogen, is achieved through this pathway [25]. Mastitis is a disease leading to significant economic losses in the dairy cattle industry throughout the world since it is the most common disease caused by bacteria [5].

Molecular characterization of a gene and alleles are a useful tool to evaluate the effect of that gene on a certain character [26]. The present study investigates the relationship between the three SNPs in the *MBL1* gene and the subclinical mastitis at a molecular level. The frequency of the G allele in the 2534 G>A SNP was found to be 0.40. In a study on Holstein cattle in China, the G allele frequency in the g.2651G>A coded SNP in the *MBL1* gene (same as 2534 G>A coded SNP used in the present study) was reported to be 0.58 [15], while another study conducted in China reported that the frequency was 0.61 [14]. A recent study on the Zavot, Native Black, Eastern Anatolian Red, Turkish Grey Cattle, Southern Anatolian Red, Brown Swiss, and Simmental cattle breeds, it was revealed that Brown Swiss had the highest GG estimated genotype frequency (0.83) of the 1262G>A SNP, while the Eastern Anatolian Red had the lowest estimated genotype frequency (0.68); also, Southern Anatolian Red was found to have the highest GG estimated genotype frequency (0.74) of the 2534G>A SNP, while Simmental (0.23) had the lowest estimated genotype frequency [22]. A similar study reported that the GG estimated genotype frequency of the 1252 G>A SNP was the highest (0.50) in the Sahne breed, while the lowest frequency was observed in the Holstein breed (0.33). Also, the Holstein breed was found to have the highest GG estimated genotype frequency of the 2534 G>A SNP (0.44) while the Sahne breed was found to have the lowest frequency (0.29). On the other hand, the TT estimated genotype frequency of 2569 T>C SNP was found to be the highest (0.45) in the Holstein breed while the lowest frequency (0.37) was observed in the Sahne breed [17].

In the present study, the G allele frequencies of the 1252 G>A SNP and the 2534 G>A SNP were found to be 0.72 and 0.40, respectively. Also, the T allele frequency of the 2569 T>C SNP was found to be 0.37. The wild-type allele frequencies of the two SNPs (2534 G>A SNP and 2569 T>C SNP) other than 1252 G>A SNP reported by Yuan et al.[20] were observed to be higher than those found in the present study [17]. The differences in the results might be due to the difference between the sample sizes since a low number of animals were used in the present study. Notably, unlike the other two SNPs, the 1252 G>A SNP was not found to be in the Hardy-Weinberg equilibrium. Therefore, it was considered that the lack of equilibrium in the population of the present study caused this difference in the wild-type alleles frequency of the 1252 G>A SNP compared to the study conducted by Yuan et al.[20].

Yuan et al.[17] investigated the relationship between three SNPs in the *MBL1* gene and SCS in Holstein breed cattle in China, and they reported that the individuals with AA genotype in terms of 2534 G>A (g.2651G>A) have a higher SCS than individuals with GG and GA genotypes. The results of the correlation analysis between the genotypes of the SNPs that were utilized in the present study and the somatic cell score [17] revealed that there was a correlation particularly between the 2534 G>A SNP and the SCS in the Sahne, Holstein, and Simmental breed cattle, moreover, individuals with GG genotype had a lower somatic cell score than the individuals with GA and AA genotypes.

In the present study, the genotype frequency of the 2534 G>A coded SNP in the subclinical mastitis was found to be 45.1%, 40.2%, and 14.6% for AA, GA, and GG genotypes, respectively. These results are in accordance with the results found by Yuan et al.[20] and Wang et al.[15], where the authors reported that the individuals with GG genotype of 2534 G>A SNP may have a lower mastitis rate [15,17]. Moreover, we have investigated the association of subclinical mastitis with the genotype frequency in the Holstein breed cattle using multiple logistic regression analysis. According to the final model, the 1252 G>A, and the 2534 G>A coded SNPs were found to affect the subclinical mastitis, and the

separation efficiency of the model in separating cows with subclinical mastitis was determined as 62.3%.

It was concluded that the 1252 G>A SNPs in the intron region and the 2534 G>A SNPs in the exon region of the *MBL1* gene may had a functional role that affected subclinical mastitis. Based on the obtained results, it was interpreted that the probability of subclinical mastitis could be determined considering the allelic structure of the cows. But further studies are required with more sample and also subclinic mastitis values should were verified with SCS for CMT tests.

Financial Support

This research received no grant from any funding agency/ sector.

Conflict of Interest

The authors declare that they have no conflict of interest.

References

1. Fraser RS, Lumsden JS, Lillie BN: Identification of polymorphisms in the bovine collagenous lectins and their association with infectious diseases in cattle. *Immunogenetics,* 70 (8): 533-546, 2018. DOI: 10.1007/s00251-018-1061-7

2. Nolan, DT: The economics of milk quality management practices and milk pricing in simulated united states dairy herd. *PhD Thesis. University of Kentucky, College of Agriculture, Food and Environment, 2020.*

3. Fernández G, Barreal ML, Pombo MB, Ginzo-Villamayor MJ, González-Manteiga W, Prieto A, Lago N, González-Palencia J: Comparison of the epidemiological behavior of mastitis pathogens by applying time-series analysis in results of milk samples submitted for microbiological examination. *Vet Res Commun*, 37 (4): 259-267, 2013. DOI: 10.1007/s11259-013-9570-1

4. Kulkarni AG, Kaliwal BB: Bovine mastitis: A Review. *Int J Recent Sci Res*, 4 (5): 543-548, 2013.

5. Schabauer A, Pinior B, Gruber CM, Firth CL, Käsbohrer A, Wagner M, Rychli K, Obritzhauser W: The relationship between clinical signs and microbiological species, spa type, and antimicrobial resistance in bovine mastitis cases in Austria. *Vet Microbiol*, 227, 52-60, 2018. DOI: 10.1016/j.vetmic.2018.10.024

6. Shoukat S, Wani H, Ali U, Ali M, Ahmad PP, Singh C, Ganguly S: Recent research trends in veterinary sciences and animal husbandry. **In,** Editor Ganguly S, Shoukat S (Eds): Mastitis and Its Diagnosis: A Review. 1st ed., 69-86, Akinik Publications, Rohini, Delhi, India, 2018.

7. Halasa T, Huijps K, Osteras O, Hogeveen H: Economic effects of bovine mastitis and mastitis management: A review. *Vet Q*, 29, 18-31, 2007. DOI: 10.1080/01652176.2007.9695224

8. Narayana SG, Miglior F, Naqvi SA, Malchiodi F, Martin P, Barkema H: Genetic analysis of subclinical mastitis in early lactation of heifers using both linear and threshold models. *J Dairy Sci*, 101 (12): 11120-11131, 2018. DOI: 10.3168/jds.2018-15126

9. Gürbulak K, Canooğlu E, Abay M, Atabay Ö, Bekyürek T: Determination of subclinical mastitis in dairy cows by different methods. *Kafkas Univ Vet Fak Derg*, 15, 765-770, 2009. DOI: 10.9775/kvfd.2009.105-A

10. Busanello M, Rossi RS, Cassoli LD, Pantoja JCF, Machado PF: Estimation of prevalence and incidence of subclinical mastitis in a large population of Brazilian dairy herds. *J Dairy Sci*, 100 (8): 6545-6553, 2017. DOI: 10.3168/jds.2016-12042

11. Ndahetuye JB, Persson Y, Nyman AK, Tukei M, Ongol MP, Båge R: Aetiology and prevalence of subclinical mastitis in dairy herds in peri-urban areas of Kigali in Rwanda. *Trop Anim Health Prod*, 51 (7): 2037-2044, 2019. DOI: 10.1007/s11250-019-01905-2

12. Hashemi M, Kafi M, Safdarian M: The prevalence of clinical and subclinical mastitis in dairy cows in the central region of Fars province, south of Iran. *Iran J Vet Res*, 12 (3): 236-241, 2011. DOI: 10.22099/IJVR.2011.71

13. Akçay A, Abay M, Çelik E: Meta-analysis of prevalence of subclinical mastitis in dairy cattle in turkey. **In,** *8th National & 2nd International Congress of Turkish Society of Veterinary Gynaecology*, October, Antalya, Turkey, 2019.

14. Liu J, Ju Z, Li Q, Huang J, Li R, Li J, Ma L, Zhong J, Wang C: Mannose-binding lectin 1 haplotypes influence serum MBL-A concentration, complement activity, and milk production traits in Chinese Holstein cattle. *Immunogenetics*, 63 (11): 727-742, 2011. DOI: 10.1007/s00251-011-0548-2

15. Wang C, Liu M, Li Q, Ju Z, Huang J, Li J, Wang H, Zhong J: Three novel single-nucleotide polymorphisms of MBL1 gene in Chinese native cattle and their associations with milk performance traits. *Vet Immunol Immunopathol*, 139 (2-4): 229-236, 2011. DOI: 10.1016/j.vetimm.2010.10.023

16. Prajapati BM, Gupta JP, Pandey DP, Parmar GA, Chaudhari JD: Molecular markers for resistance against infectious diseases of economic importance. *Vet World*, 10 (1): 112-120, 2017. DOI: 10.14202/vetworld.2017.112-120

17. Neth O, Jack DL, Dodds AW, Holzel H, Klein NJ, Turner MW: Mannose-binding lectin binds to a range of clinically relevant microorganisms and promotes complement deposition. *Infect Immun*, 68 (2): 688-693, 2000. DOI: 10.1128/iai.68.2.688-693.2000

18. van Emmerik LC, Kuijper EJ, Fijen CA, Dankert J, Thiel S: Binding of mannan-binding protein to various bacterial pathogens of meningitis. *Clin Exp Immunol*, 97 (3): 411-416, 1994. DOI: 10.1111/j.1365-2249.1994.tb06103.x

19. Eisen DP, Minchinton RM: Impact of mannose-binding lectin on susceptibility to infectious diseases. *Clin Infect Dis*, 37 (11): 1496-1505, 2003. DOI: 10.1086/379324

20. Yuan Z, Li J, Li J, Gao X, Xu S: SNPs identification and its correlation analysis with milk somatic cell score in bovine MBL1 gene. *Mol Biol Rep*, 40 (1): 7-12, 2013. DOI: 10.1007/s11033-012-1934-z

21. Muhasin Asaf VN, Bhushan B, Panigrahi M, Dewangan P, Kumar A, Kumar P, Gaur G: Association study of genetic variants at single nucleotide polymorphism rs109231409 of mannose-binding lectins 1 gene with mastitis susceptibility in Vrindavani crossbred cattle. *Vet World*, 7 (10): 807-810, 2014. DOI: 10.14202/vetworld.2014.807-810

22. Aksel EG, Arslan K, Özdemir F, Akyüz B: Investigation of the MBL-1 gene polyorphism in some cattle breeds raised in Turkey. *Mediterr Agric Sci*, 32 (1): 25-30, 2019. DOI: 10.29136/mediterranean.457231

23. Sambrook J, Fritsch EF, Maniatis T: Molecular cloning: A laboratory manual. 4th ed., 47, Cold-Spring Harbor, New York, US, 1989.

24. Alberts B, Johnson A, Lewis J, Raff M, Roberts K, Walter P: Molecular Biology of the Cell. 4th ed., 1456, Garland Science, New York, USA, 2002.

25. Murphy K: Janeway's Immunobiology. 9th ed., Garland-Northon, 2014.

26. Lewis CM, Knight J: Introduction to genetic association studies. *Cold Spring Harb Protoc*, 2012, 297-306, 2012. DOI: 10.1101/pdb.top068163

Kafkas Universitesi Veteriner Fakultesi Dergisi
ISSN: 1300-6045 e-ISSN: 1309-2251
Journal Home-Page: http://vetdergikafkas.org

Kafkas Univ Vet Fak Derg
27 (3): 397-401, 2021
DOI: 10.9775/kvfd.2021.25681

SHORT COMMUNICATION

Identification of a New MLST Subtype of *Cryptosporidium muris* from a Brown Rat *(Rattus norvegicus)* in China

Xuehan LIU [1,a (*)] Lei DENG [2,b] Zhijun ZHONG [2,c] Ziyao ZHOU [2,d] Xuefeng YANG [1,e] Zhixing AN [1,f]

[1] College of Animal Science and Veterinary Medicine, Henan Institute of Science and Technology, Xinxiang 453003, CHINA
[2] College of Veterinary Medicine, Sichuan Agricultural University, Chengdu 625014, CHINA
ORCIDs: [a] 0000-0002-8376-5580; [b] 0000-0003-0391-6180; [c] 0000-0001-8609-448X; [d] 0000-0002-8947-4303; [e] 0000-0002-7037-6607
[f] 0000-0001-7649-5626

Article ID: KVFD-2021-25681 Received: 03.03.2021 Accepted: 22.05.2021 Published Online: 23.05.2021

Abstract

Cryptosporidium muris is a zoonotic protozoan. Characterization of genetic differentiation can be exploited to trace the origins of the parasite. A *Cryptosporidium* isolate from brown rat was obtained by microscopy and genetically characterized. *C. muris* was identified with minor nucleotide differences. Further subtype analysis was performed using a multilocus sequence typing (MLST) tool. At each locus, the *C. muris* isolate was confirmed to be M12, M4, M1 and M2 subtype, representing as a new MLST subtype. Therefore, the results suggest that there was probably a new source of infection for *C. muris* in the study region.

Keywords: *Cryptosporidium muris, 18S rRNA, MLST, Subtype, Brown rat*

Çin'de Kahverengi Sıçanda *(Rattus norvegicus) Cryptosporidium muris*'in Yeni Bir MLST Alt Tipinin Tanımlanması

Öz

Cryptosporidium muris, zoonotik bir protozoondur. Genetik farklılaşmanın karakterizasyonu parazitin kökenini izlemek için kullanılabilir. *Cryptosporidium* izolatı kahverengi bir sıçandan mikroskopi ile elde edildi ve genetik olarak karakterize edildi. Küçük nükleotid farklılıklarla *C. muris* olarak tanımlandı. İleri identifikasyonu, çoklu lokus dizilim analizi (MLST) ile gerçekleştirildi. Her lokusta, *C. muris* izolatının yeni bir MLST alt tipini temsil eden M12, M4, M1 ve M2 alt tipi tanımlandı. Bu nedenle bu sonuçlar, çalışma bölgesinde *C. muris* için muhtemelen yeni bir enfeksiyon kaynağı olduğunu göstermektedir.

Anahtar sözcükler: *Cryptosporidium muris, 18S rRNA, MLST, Alt Tip, Kahverengi sıçan*

INTRODUCTION

Cryptosporidium is a ubiquitous zoonotic protozoan parasite that can infect a variety of vertebrate animals. Depending on the immunological status of hosts, the clinical symptoms of cryptosporidiosis commonly range from acute to chronic diarrhea. Epidemiologic studies indicate that multiple routes of transmission are likely, including direct, zoonotic, foodborne and waterborne transmission may occur in different areas [1,2]. To date, at least 45 valid species and a similar number of genotypes have been described based on molecular characteristics, revealing an extensive genetic diversity [3]. Among those, *C. muris* as gastric protozoa has a wide range of host-adaptations and is generally detected in various rodents [4,5]. Other animals including deer, Tasmanian devil, pig, camel, dog, cat, monkey, and bird can also be infected with *C. muris* at low frequency [6-10]. In addition, a few cases of human cryptosporidiosis have been attributed to *C. muris* in recent years, suggesting the potential for zoonotic transmission [11,12].

Numerous types of molecular diagnostic tools have been used to differentiate *Cryptosporidium* in host and environmental samples at the genotype and subtype levels to trace the likely source of infection [6]. Among those,

How to cite this article?

Liu X, Deng L, Zhong Z, Zhou Z, Yang X, An Z: Identification of a new MLST subtype of cryptosporidium muris from a brown rat *(Rattus norvegicus)* in China. *Kafkas Univ Vet Fak Derg,* 27 (3): 397-401, 2021.
DOI: 10.9775/kvfd.2021.25681

(*) **Corresponding Author**

Tel: +86-0373-3040718
E-mail: liuxuehan1986@126.com (X. Liu)

a multilocus sequence typing (MLST) tool was developed for *C. muris* by employing microsatellite and minisatellite markers with simple tandem repeats, which showed the capacity to distinguish various subtypes [13]. Currently, 14 MLST subtypes have been identified in diverse hosts and geographical regions [13,14]. Additionally, the MLST tool is also helpful for molecular epidemiology and population genetic studies [14].

Reports on *C. muris* infecting brown rats are limited, and subtyping *C. muris* was not conducted in those studies [15]. To our knowledge, there are no reports on brown rats being infected with *C. muris* in China [16]. In the present study, one *C. muris* isolate (BN01) from brown rat was genetically characterized by analysis of three genotyping and four MLST-subtyping genes for the purpose of further tracking of infection sources.

Material and Methods

Ethics Approval

This study was performed according to the recommendations of the Guide for the Care and Use of Laboratory Animals of the Ministry of Health, China. The research protocol was reviewed and approved by the Research Ethics Committee of the Sichuan Agricultural University.

Cryptosporidium muris Isolate

One brown rat was trapped in the suburbs of Ya'an city and kept in a sterilized mouse cage. Approximately 2-5 g of feces were collected for five consecutive days. The feces were dissolved into 50 mL double-distilled water via stirring. The Sheather's sugar flotation method was used for examining *Cryptosporidium* oocysts by microscopy at x400 magnification as previously described [17]. The specimen was found to be positive. Then, the concentrates containing oocysts were separated to 2.5% potassium dichromate solution and stored at 4°C.

DNA Extraction and PCR Amplification

Oocysts were rinsed twice in double-distilled water and pelleted at 5.000×g centrifugation to remove potassium dichromate. Genetic DNA was extracted using the E.Z.N.A.® Stool DNA Kit (OMEGA Biotek Inc D4015-02, USA) according to the manufacturer's protocol. The extracted DNA was stored at -20°C until the time of PCR analysis.

The nested-PCR was used to amplify the partial 18S rRNA, COWP and CpA135 genes to genotype identification. The primers and amplification conditions were adopted as previously described [17,18]. Premix Ex Taq™ (Takara, Dalian, China) was used for PCR amplification. The secondary PCR products at each genotyping locus were resolved using 1% agarose gel electrophoresis with ethidium bromide staining, and were identified by DNA sequencing (Sangon Biotech, Shanghai, China). Sequence accuracy was confirmed using bidirectional sequencing, and a new PCR product was re-sequenced if necessary.

MLST Subtype

Analysis using the MLST incorporated MS1 (coding for hypothetical protein), MS2 (coding for 90 kDa heat shock protein), MS3 (coding for hypothetical protein), and MS16 (coding for leucine rich repeat family protein) in order to subtype the *C. muris* isolated from a brown rat. Primers and amplification conditions were in accordance with those developed previously *(Table 1)* [13]. PrimeSTAR® DNA Polymerase (TaKaRa, Dalian, China) was used to ensure high sequence fidelity. To neutralize PCR inhibitors, 400 ng/mL of non-acetylated bovine serum albumin (TaKaRa, Dalian,

Table 1. *PCR primers for MLST subtype used in this study*

Genes	Primer	Sequence (5'-3')	Tm	Length	Tandem Repeat Sequence
MS1	F1 R1	ACCATCTAGAGATAACGAGCGA GAATCAGAAGATGAGCGACAA	55°C	~550 bp	GAACGAGATAGG
	F2 R2	CGTGATAGTGGGTATGAATTGGACA CGACTGCGATACTCACGTCCT	55°C		
MS2	F1 R1	TTGCAACTGTACCTAAATTAGTA GTGAGACTTCTGGGGTCCTGA	52°C	~460 bp	CCATATCCC
	F2 R2	TCATGACGCGTCATACCAACA ACTTAGACAGTTCTATGCTGA	55°C		
MS3	F1 R1	AACCAAGTGAATCACGAACTT TCAAGTACAGCAGTCTATTGCTT	55°C	~540 bp	TGTTGG /GCTGCA
	F2 R2	GCAATATCTTCGACGATCCCA ATGGGAATAATTCTTCATCATCAA	55°C		
MS16	F1 R1	GAAGAGGTCGAAGTTAAGCTA GACAATCATCTAAATCGTGTT	50°C	~600 bp	CTTCTTCAT
	F2 R2	AAGTTTCATCTAGGTACACTAAGA CACTACCTAATCTCGTGTACTT	55°C		

F and R: the forward and reverse primers, respectively; 1 and 2: the primary and secondary PCRs, respectively

China) was used in both PCRs at each MLST locus. The detection and DNA sequencing were performed identically to the above manipulations. Likewise, to ensure subtype accuracy, especially in the copy number of minisatellite repeats, PCR products in the subtype loci were sequenced at least twice.

Phylogenetic Analysis

Nucleotide sequences of all 7 genes were aligned with reference sequences in GenBank using ClustalX 1.83 *(ftp://ftp-igbmc.u-strasbg.fr/pub/ClustalX/)*. Phylogenetic analyses were performed using software PHYLIP v3.69 at each locus *(http://evolution.genetics.washington.edu/phylip.html)*. Neighbor-joining trees were constructed based on evolutionary distances calculated using the Kimura two-parameter model. Phylograms were drawn using MEGA4.0 *(http://www.megasoftware.net/)*. To assess the reliability of these trees, bootstrap analysis using 1,000 pseudo-replicates was carried out with values above 50% reported. Sequence identity was analyzed using MegAlign program in the DNAStar v6.0 software *(https://www.dnastar.com/software/DNASTAR-Cloud/)*.

Through adjustment, the partial nucleotide sequences obtained in this study were deposited in the GenBank under accession numbers: KF419208-KF419214.

Results

Through microscopic examination, it was observed that the oocysts were morphologically bigger than the intestinal *Cryptosporidium*, but similar to the gastric *Cryptosporidium* [4]. Thus, genetic analyses were necessary to distinguish genotypes.

An approximate 830 bp fragment of the 18S rRNA gene was successfully amplified. The resulting sequence was initially identified as *C. muris* with a maximum similarity of 100% when compared to reference *C. muris* isolates from hamster, ostrich, monkey, and human in GenBank. Phylogenetic analysis revealed that the current isolate was clustered with those *C. muris* isolates with high bootstrap values *(Fig. 1)*. In the present study, the observed CpA135 sequence was 99.8% identical to that from house rat-derived *C. muris* (RN66 isolate, HM358026) with a mutation of A to G at nucleotide 6 [18]. For the COWP gene, the isolate shared 100% homology with those *C. muris* reported in rock hyrax (AF161579), whereas 6 nucleotide changes were found compared to the RN66 isolate (DQ060430). Likewise, phylogenetic topology was similar to that in the 18S rRNA gene *(Fig. 1)*. These results demonstrated that this isolate was indeed *C. muris*.

At each MLST locus, the corresponding nucleotide sequences were obtained successfully. Sequence analysis of MS2, MS3 and MS16 genes identified M4, M1 and M2 haplotypes, respectively, which were homologous to those previously deposited in GenBank. However, the sequence at MS1 locus occupied max similarity to M5 haplotype with a single C insertion at nucleotide 471 in the nonrepeat region when compared to all known *C. muris* MS1 sequences. Based on the coding nature of MLST targets, nucleotide insertions and deletions commonly occur in trinucleotide

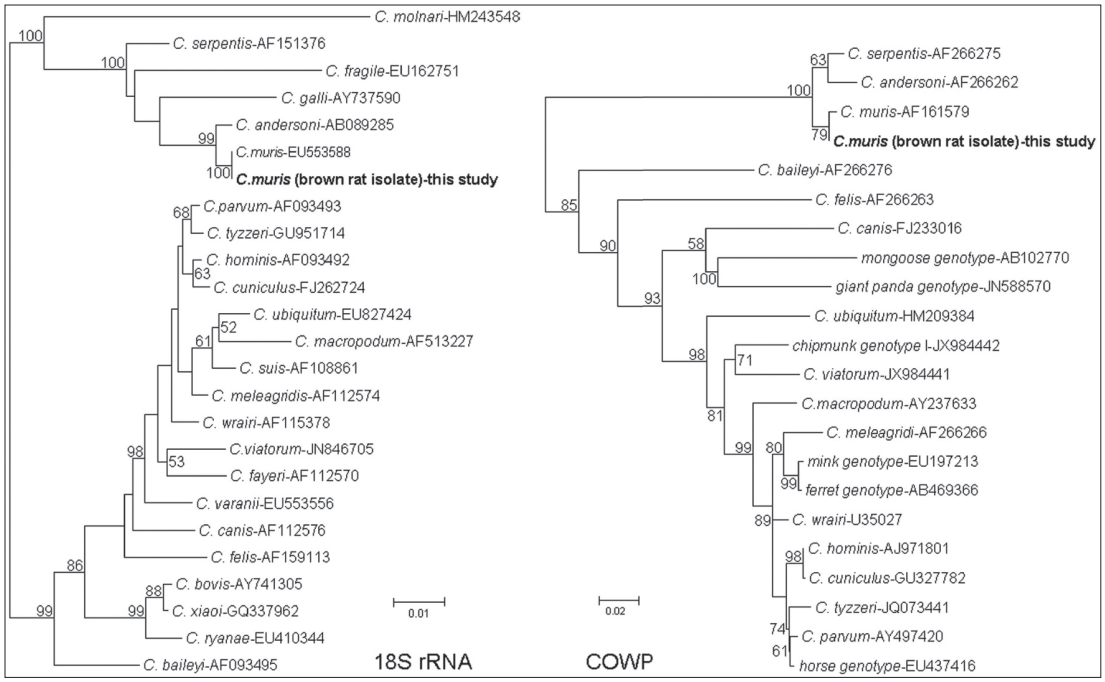

Fig 1. Phylogenetic relationship of *Cryptosporidium* isolated from a brown rat inferred by neighbor-joining analysis of the SSU rRNA and COWP genes based on evolutionary distances calculated using the Kimura two-parameter model. Bootstrap values above 50% are shown using 1.000 pseudoreplicates. Bar = substitutions/site

Table 2. *Subtype of C. muris brown rat isolate in this study and other representative C. muris isolates at four MLST loci*

No.	Specimen	Host	Source	MLST Subtype				Reference
				MS1	MS2	MS3	MS16	
1	RN66	Brown rat	Japan	M5	M4	M1	M5	[13]
2	6853	Human	Lima, Peru	M1	M2	M4	M5	[13]
3	7511	Bactrian camel	Czech Republic	M1	M1	M4	M5	[13]
4	14907	Rat snake	Czech Republic	M2	M2	M3	M5	[13]
5	13469	Camel via mice	Egypt	M5	M4	M2	M3	[13]
6	OH1	Ostrich	Henan, China	M5	M4	M6	M4	[14]
7	14714	Human	Nairobi, Kenya	M6	M4	M1	M2	[13]
8	14906	Lab mouse	Czech Republic	M6	M4	M2	M4	[13]
9	7379	Domestic mouse	Czech Republic	M7	M4	M2	M1	[13]
10	1666	Chipmunk	Czech Republic	M7	M4	M1	M5	[13]
11	7512	Mountain goat	Czech Republic	M8	M4	M2	M4	[13]
12	7380	Mara	Czech Republic	M9	M4	M1	M1	[13]
13	14243	SCID mice	Czech Republic	M10	M5	M5	M6	[13]
14	MC4	Hamster	Henan, China	M11	M4	M6	M1	[14]
15	**BN01**	**Brown rat**	**Sichuan, China**	**M12**	**M4**	**M1**	**M2**	**This study**

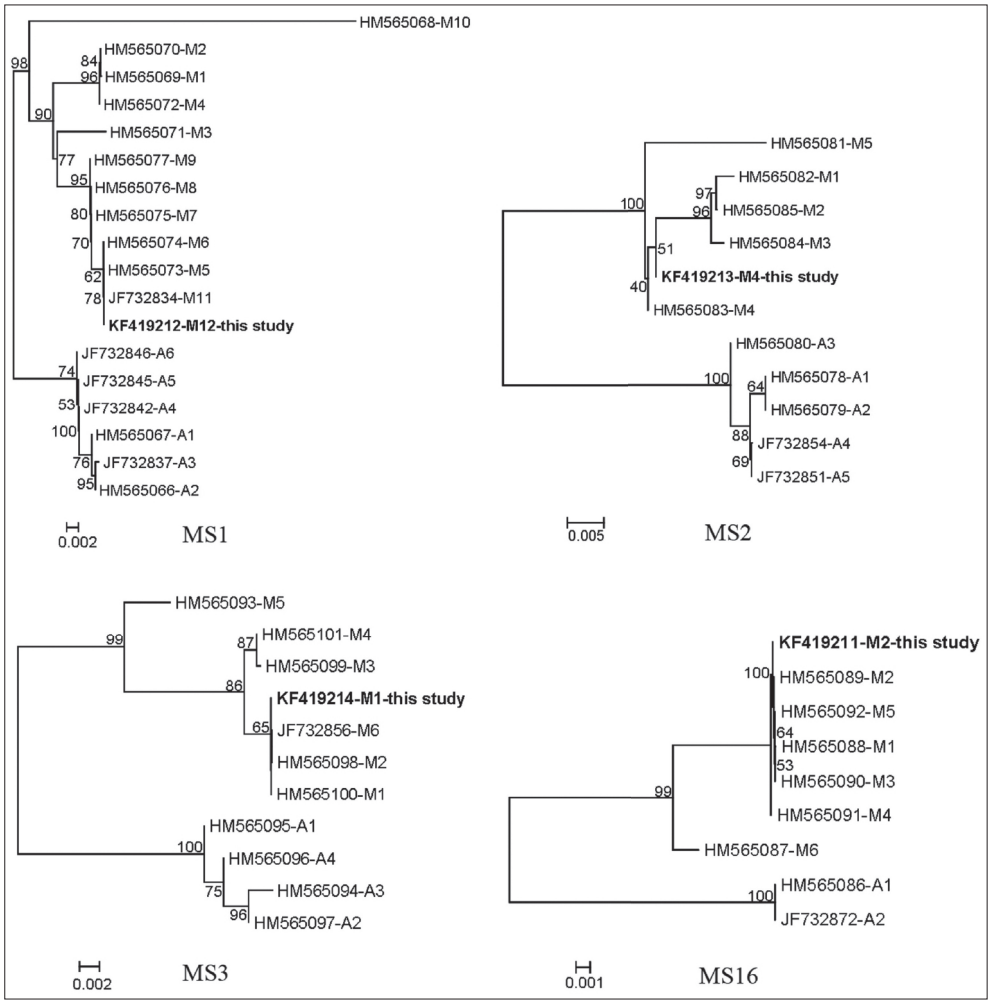

Fig 2. Phylogenetic relationships of *C. muris* and *C. andersoni* subtypes based on MS1, MS2, MS3, and MS16 sequences as assessed by a neighbor-joining analysis of the nucleotide sequences. Distances were calculated by the Kimura two-parameter model. Bootstrap values above 50% are shown using 1.000 pseudoreplicates. Bar = substitutions/site

sets [13]. The *C. muris* analyzed here was considered to be a new haplotype, M12, at MS1 locus and identified as MLST subtype M12, M4, M1 and M2. This characterization was supported by the phylogenetic relationship of each locus *(Table 2, Fig. 2)*.

Discussion

Previously, a total of 11, 5, 6 and 6 haplotypes comprising 14 MLST subtypes were identified for *C. muris* subtype loci *(Table.1; Fig. 2)*. However, the current subtype was distinct

from previous *C. muris*, especially isolate RN66 (subtype M5, M4, M1 and M5). Thus, the *C. muris* isolate in this study was evaluated as a novel MLST subtype.

Subtyping tools have proven useful in the tracing of sources of infection. Of those, the 60 kDa glycoprotein (gp60) gene is a frequently used subtype marker, and is extensively used for distinguishing intestinal *Cryptosporidium* [6,19,20]. In addition, the MLST tool with a high resolution could also accurately describe genetic diversity and perform subtype identification for *Cryptosporidium*, including *C. muris* [6,13,19]. Previous data indicated that genetic differences of *Cryptosporidium* were likely to be related to geographical restriction [6,19]. The presence of a new MLST subtype suggests a new infection source of *C. muris*. Moreover, subtype differences of *C. muris* were observed in different animal hosts. For example, the MLST subtypes from ostriches and other hosts are unique and distinct from each other [13,14]. Thus, the new subtype in this study may be indicative of host-specificity.

Cryptosporidium muris infection in a brown rat was first reported in China, and a new MLST subtype was identified. However, limited information about *C. muris* infection in current areas has been reported. Therefore, there was a need of surveying cryptosporidiosis in extensive areas and hosts to trace the infection sources and characterize the transmission dynamics of *C. muris*.

Acknowledgements

We thank the Xiaoxiao ZHOU and Wei LI for their assistance in feces collection during this study.

Funding

This study was supported by the Chengdu Giant Panda Breeding Research Foundation (No. CPF2012-01) and Program for Changjiang Scholars and Innovative Research Team in University (No. IRT0848).

Author Contributions

Conceived and designed the experiments: X. LIU, Z. ZHONG. Performed the experiments: L. DENG, F. YANG, Z. AN. Analyzed the data: X. LIU, Z. ZHONG, Z. ZHOU. Wrote the paper: X. LIU, L. DENG.

Declaration of Conflict of Interest

The authors declare that they have no competing interests.

References

1. Feng Y, Ryan UM, Xiao L: Genetic diversity and population structure of *Cryptosporidium*. *Trends Parasitol,* 34 (11): 997-1011, 2018. DOI: 10.1016/j.pt.2018.07.009

2. Ungar BL: Cryptosporidiosis in humans *(Homo sapiens)*. **In,** Dubey JP (Ed): Cryptosporidiosis of Man and Animals. 2nd edn., 59-82, CRC Press, Florida, 2018. DOI: 10.1201/9781351071260

3. Jezkova J, Prediger J, Holubova N, Sak B, Konecny R, Feng Y, Xiao L, Rost M, McEvoy J, Kvac M: *Cryptosporidium ratti* n. sp. (Apicomplexa: *Cryptosporidiidae)* and genetic diversity of *Cryptosporidium* spp. in brown rats *(Rattus norvegicus)* in the Czech Republic. *Parasitology,* 148 (1): 84-97, 2021. DOI: 10.1017/S0031182020001833

4. Ryan U, Fayer R, Xiao L: *Cryptosporidium* species in humans and animals: Current understanding and research needs. *Parasitology,* 141 (13): 1667-1685, 2014. DOI: 10.1017/S0031182014001085

5. Garcia-Livia K, Martin-Alonso A, Foronda P: Diversity of *Cryptosporidium* spp. in wild rodents from the Canary Islands, Spain. *Parasit Vectors,* 13:445, 2020. DOI: 10.1186/s13071-020-04330-9

6. Xiao L, Cama VA: *Cryptosporidium* and cryptosporidiosis. **In,** Ortega YR, Sterling CR (Ed): Foodborne Parasites. 2th ed., 73-117, Springer, Berlin, 2018. DOI: 10.1007/978-3-319-67664-7_5

7. Kvac M, Hanzlikova D, Sak B, Kvetonova D: Prevalence and age-related infection of *Cryptosporidium suis*, *C. muris* and *Cryptosporidium* pig genotype II in pigs on a farm complex in the Czech Republic. *Vet Parasitol,* 160 (3-4): 319-322, 2009. DOI: 10.1016/j.vetpar.2008.11.007

8. Pedraza-Diaz S, Ortega-Mora LM, Carrion BA, Navarro V, Gomez-Bautista M: Molecular characterisation of *Cryptosporidium* isolates from pet reptiles. *Vet Parasitol,* 160 (3-4): 204-210, 2009. DOI: 10.1016/j.vetpar.2008.11.003

9. Huang J, Zhang Z, Zhang Y, Yang Y, Zhao J, Wang R, Jian F, Ning C, Zhang W, Zhang L: Prevalence and molecular characterization of *Cryptosporidium* spp. and *Giardia duodenalis* in deer in Henan and Jilin, China. *Parasit Vectors,* 11:239, 2018. DOI: 10.1186/s13071-018-2813-9

10. Wait LF, Fox S, Peck S, Power ML: Molecular characterization of *Cryptosporidium* and *Giardia* from the Tasmanian devil *(Sarcophilus harrisii)*. *PLoS One,* 12 (4): e0174994, 2017. DOI: 10.1371/journal.pone.0174994

11. Guy RA, Yanta CA, Muchaal PK, Rankin MA, Thivierge K, Lau R, Boggild AK: Molecular characterization of *Cryptosporidium* isolates from humans in Ontario, Canada. *Parasit Vectors,* 14:69, 2021. DOI: 10.1186/s13071-020-04546-9

12. Ayinmode AB, Oliveira BCM, Obebe OO, Dada-Adgebola HO, Ayede AI, Widmer G: Genotypic characterization of *Cryptosporidium* species in humans and peri-domestic animals in Ekiti and Oyo States, Nigeria. *J Parasitol,* 104 (6): 639-644, 2018. DOI: 10.1645/17-74

13. Feng Y, Yang W, Ryan U, Zhang L, Kvac M, Koudela B, Modry D, Li N, Fayer R, Xiao L: Development of a multilocus sequence tool for typing *Cryptosporidium muris* and *Cryptosporidium andersoni*. *J Clin Microbiol,* 49 (1): 34-41, 2011. DOI: 10.1128/JCM.01329-10

14. Wang R, Jian F, Zhang L, Ning C, Liu A, Zhao J, Feng Y, Qi M, Wang H, Lv C, Zhao G, Xiao L: Multilocus sequence subtyping and genetic structure of *Cryptosporidium muris* and *Cryptosporidium andersoni*. *PLoS One,* 7 (8): e43782, 2012. DOI: 10.1371/journal.pone.0043782

15. Ng-Hublin JSY, Singleton GR, Ryan U: Molecular characterization of *Cryptosporidium* spp. from wild rats and mice from rural communities in the Philippines. *Infect Genet Evol,* 16, 5-12, 2013. DOI: 10.1016/j.meegid.2013.01.011

16. Lv C, Zhang L, Wang R, Jian F, Zhang S, Ning C, Wang H, Feng C, Wang X, Ren X, Qi M, Xiao L: *Cryptosporidium* spp. in wild, laboratory, and pet rodents in china: Prevalence and molecular characterization. *Appl Environ Microbiol,* 75 (24): 7692-7699, 2009. DOI: 10.1128/AEM.01386-09

17. Wang R, Zhang L, Feng Y, Ning C, Jian F, Xiao L, Zhao J, Wang Y: Molecular characterization of a new genotype of *Cryptosporidium* from American minks *(Mustela vison)* in China. *Vet Parasitol,* 154 (1-2): 162-166, 2008. DOI: 10.1016/j.vetpar.2007.12.038

18. Tosini F, Drumo R, Elwin K, Chalmers R, Pozio E, Cacciò SM: The CpA135 gene as a marker to identify *Cryptosporidium* species infecting humans. *Parasitol Int,* 59 (4): 606-609, 2010. DOI: 10.1016/j.parint.2010.08.011

19. Xiao L: Molecular epidemiology of cryptosporidiosis: An update. *Exp Parasitol,* 124 (1): 80-89, 2010. DOI: 10.1016/j.exppara.2009.03.018

20. Thompson RCA, Ash A: Molecular epidemiology of *Giardia* and *Cryptosporidium* infections - What's new? *Infect Genet Evol,* 75:103951, 2019. DOI: 10.1016/j.meegid.2019.103951

Kafkas Universitesi Veteriner Fakultesi Dergisi
ISSN: 1300-6045 e-ISSN: 1309-2251
Journal Home-Page: http://vetdergikafkas.org

Kafkas Univ Vet Fak Derg
27 (3): 403-407, 2021
DOI: 10.9775/kvfd.2020.25241

CASE REPORT

Septicemia and Multiple Abscesses Associated with *Pantoea agglomerans* in a Dog

Sinem İNAL [1,a (*)] Elif BAĞATIR [2,b] Nilüfer KURUCA [1,c] Merve Gizem SEZENER [3,d]
Kamil Serdar İNAL [2,e] Arzu FINDIK [3,f] Tolga GÜVENÇ [1,g]

[1] Ondokuz Mayıs University, Faculty of Veterinary Medicine, Department of Pathology, TR-55200 Samsun - TURKEY
[2] Ondokuz Mayıs University, Faculty of Veterinary Medicine, Department of Surgery, TR-55200 Samsun - TURKEY
[3] Ondokuz Mayıs University, Faculty of Veterinary Medicine, Department of Microbiology, TR-55200 Samsun - TURKEY
ORCIDs: [a] 0000-0002-2552-5159; [b] 0000-0002-0141-864X; [c] 0000-0001-5601-4952; [d] 0000-0003-0487-7515; [e] 0000-0003-0690-5743
[f] 0000-0002-9123-6160; [g] 0000-0003-1468-3415

Article ID: KVFD-2020-25241 Received: 08.12.2020 Accepted: 31.03.2021 Published Online: 31.03.2021

Abstract

A 2-year-old Anatolian Shepherd Dog was presented with lethargy and small abrasion wound on the left paw. The patient was diagnosed with phlegmon in his left arm and treatment was started. However, septicemia occurred and the dog died after fourteen days. At necropsy multiple white-colored foci was seen on the liver, lungs, kidney and heart. In these organs, abscesses formations with large areas of necrosis were seen in histopathologic examination. In samples taken from organs with abscess, the bacteria were identified morphologically and biochemically by Vitek II and *Pantoea agglomerans* was confirmed by PCR. *Pantoea agglomerans* has been previously isolated from humans and animals. However, the bacteria is rarely isolated from septicemia associated lesions in animals. In the presented report, *Pantoea agglomerans* was identified in a dog with septicemia and clinical, postmortal and histopathological findings caused by the bacteria were reported.

Keywords: *Bacteria, Dog, Pantoea agglomerans, Septicemia*

Bir Köpekte *Pantoea agglomerans* İle İlişkili Septisemi ve Multiple Apse Olgusu

Öz

İki yaşlı Anadolu çoban köpeği halsizlik ve sol patide küçük abrazyon yarası şikayetiyle getirildi. Hastanın sol ön kolunda bulanan yaraya flegmon tanısı konuldu ve tedaviye başlandı. Ancak septisemi meydana geldi ve tedavinin 14. gününde hasta öldü. Nekropside, karaciğer, akciğer, böbrek ve kalpte çok sayıda beyaz renkli odak görüldü. Bu organların histopatolojik incelemesinde, apse yapıları ile geniş nekroz alanları belirlendi. Organlardaki apselerden alınan örneklerde, bakteri morfolojik olarak ve Vitek II ile biyokimyasal olarak identifiye edildi. PCR ile etkenin *Pantoea agglomerans* olduğu doğrulandı. *Pantoea agglomerans* daha önce insanlarda ve hayvanlarda izole edilmiştir. Bununla birlikte bu bakteri, hayvanlarda nadiren septisemi ile ilişkili lezyonlardan izole edilmiştir. Bu olgu sunumunda, septisemili bir köpekte identifiye edilen *Pantoea agglomerans*'ın neden olduğu klinik, postmortal ve histopatolojik bulgular bildirilmiştir.

Anahtar sözcükler: *Bakteri, Köpek, Pantoea agglomerans, Septisemi*

INTRODUCTION

Pantoea agglomerans is a gram-negative opportunistic bacterium, belonging to the family *Enterobacteriacea*. The bacterium was called *Enterobacter agglomerans* or *Erwinia herbicola*. It was isolated from plant surfaces, seeds, water and humans [1]. *Pantoea agglomerans* is commonly known as nosocomial infection in human medicine. However, the bacteria is rarely isolated from clinical problems in animals [2].

Clinical outcomes of infection by *Pantoea agglomerans* in animals include fibrinonecrotic placentitis, equine abortion [3], and allergic lung disease in cows [4]. Also,

How to cite this article?

İnal S, Bağatır E, Kuruca N, Sezener MG, İnal KS, Fındık A, Güvenç T: Septicemia and multiple abscesses associated with *Pantoea agglomerans* in a dog. *Kafkas Univ Vet Fak Derg,* 27 (3): 403-407, 2021.
DOI: 10.9775/kvfd.2020.25241

(*) **Corresponding Author**

Tel: +90 362 3121919-2832 Fax: +90 362 4576922
E-mail: sinem.inal@omu.edu.tr (S. İnal)

Pantoea agglomerans related with pneumonia in a cat was reported [5]. The bacteria was isolated in fishes such as Brown Trout and Rainbow Trout [6,7]. *Klebsiella pneumoniae* is a gram-negative opportunistic bacterium. *Klebsiella* is known to cause enteritis, pneumonia and urinary tract infection in dogs [8].

In this case report, we aimed to present a case of *Pantoea agglomerans* related septicemia, and its postmortal and histopathological findings in a dog.

Case History

The patient was a 2-year-old Anatolian Shepherd Dog weighing 45 kg that was brought to Animal Hospital of Ondokuz Mayıs University due to lethargy and loss of appetite. Initial clinical examination revealed 4% dehydration, an increased white blood cell count (24.52 x 10^9/L) and mild anemia as well as a small abrasion wound on the left paw, about 1 cm in diameter. An intravenous catheter was introduced to the left cephalic vein in order to administer fluid therapy. On the following day, a fluctuating swelling formed in the arm and the patient was referred to the surgery department on day 3.

The patient was hospitalized due to his deteriorating condition. The hair over the swollen area which started from the cranial surface of the paw and extends over the scapula, some of the lateral thorax as well as, up to and including the 4th rib line was clipped. The skin over the swollen area was felt warm when touching and fluctuation was evident in the entire area. Antibiotic treatment with cefazolin-Na (Cezol® 20 mg/kg IV every 8 h, Deva, Istanbul, Turkey) and fomentation therapy was initiated along with daily IV fluid administration.

A pustule was opened at the mid-level of scapula at the 4th day and purulent content of the cavity was drained and irrigated using copious amounts of saline. After this, a drain was placed through the cavity, from the natural opening on the scapula, to an incision made laterally to the elbow. The drain was kept in place for 3 days, during this time, a wet to dry wound dressing was applied daily and a local antibiotic was rifamycin (Rif® 250 mg, Koçak Farma, Istanbul, Turkey) administered locally at each dressing change. The drain was changed once in 3 days.

Despite continuous antibiotic treatment, the WBC count (35.14 x 10^9/L) and the patient's condition has deteriorated. On day 10, hematuria was seen and the collected urine sample was evaluated under light microscope and calcium oxalate crystals were seen. Ceftriaxon (Novosef® 25 mg/kg IV, every 12 h, Zentiva, Prague, Czech) and metronidazole (Flagyl®, 10 mg/kg slow IV infusion, once a day, Eczacıbaşı, Istanbul, Turkey) was initiated at this point in favor of the other antibiotic treatment. In addition, vitamin K (Konakion® 2 mg/kg IV, single dose, Roche, Basel, Switzerland), vitamin C (Zinco-C® 750 mg PO, once a day, Berko İlaç, Istanbul, Turkey) supplements were administered and meloxicam (Maxicam® 0.2 mg/kg, SC inj, once a day for 3 days, Sanovel, Istanbul, Turkey) and ranitidine (Ranitab® 2mg/kg IV, twice a day, Istanbul, Turkey) was started. By this time the swelling has subsided, and only the drain's entry and egress wound openings were present, a dry-to-dry wound dressing was applied over them.

The dog started exhibiting respiratory distress on day 11, wheezing and wet sounds were heard during auscultation and a chest radiogram was taken and radiopaque areas were seen, confirming an empyema diagnosis *(Fig. 1)*. The patient's condition continued to deteriorate and he died at the 14th day. Informed consent form was obtained from the owner for the procedures to be applied to this case.

At gross examination, total of 5-6 perforated areas of 1-2 cm in diameter were determined on the left skin of the left forefoot *(Fig. 2-A)*. A yellow colored fluid was seen when the lesions were cut. In the liver, yellowish-white abscesses 2-5 cm in size were seen especially in lateral and medial lobules *(Fig. 2-B)*. It was seen that there were white colored foci of 2-3 cm diameter in the cortex of the cross-sectional area of the kidneys. In all lobules of the lungs, large and small yellowish-white diffuse foci ranging between 1-5 cm in diameter were found *(Fig. 2-C)*. A hemorrhagic fluid at a small amount was detected in the pericardium. The heart was seen to have a rounded shape, and the micro-abscesses were noticed on it. Left ventricular wall of the heart was thickened and the right ventricle was dilated. A white colored focus 2-3 cm in diameter attracted attention in the aorta exit of the heart *(Fig. 2-D)*. Tissue samples which

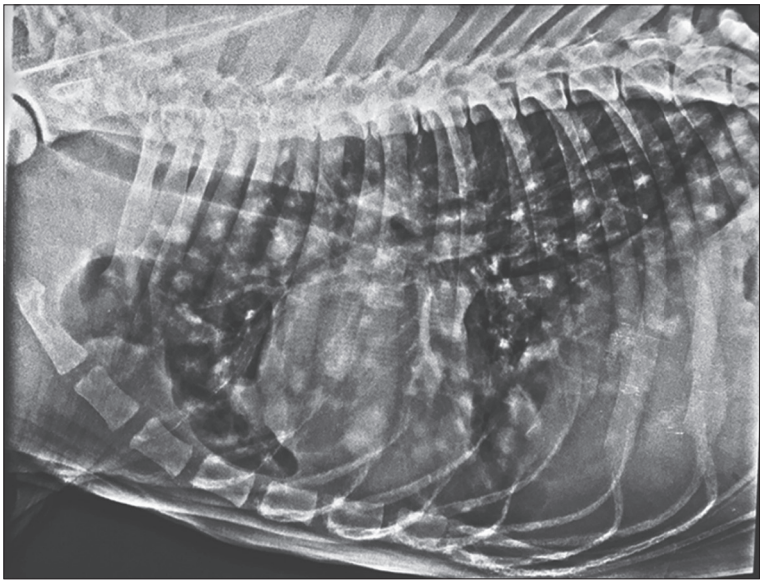

Fig 1. Diffuse nodular interstitial sign in the lateral radiograph of the dog

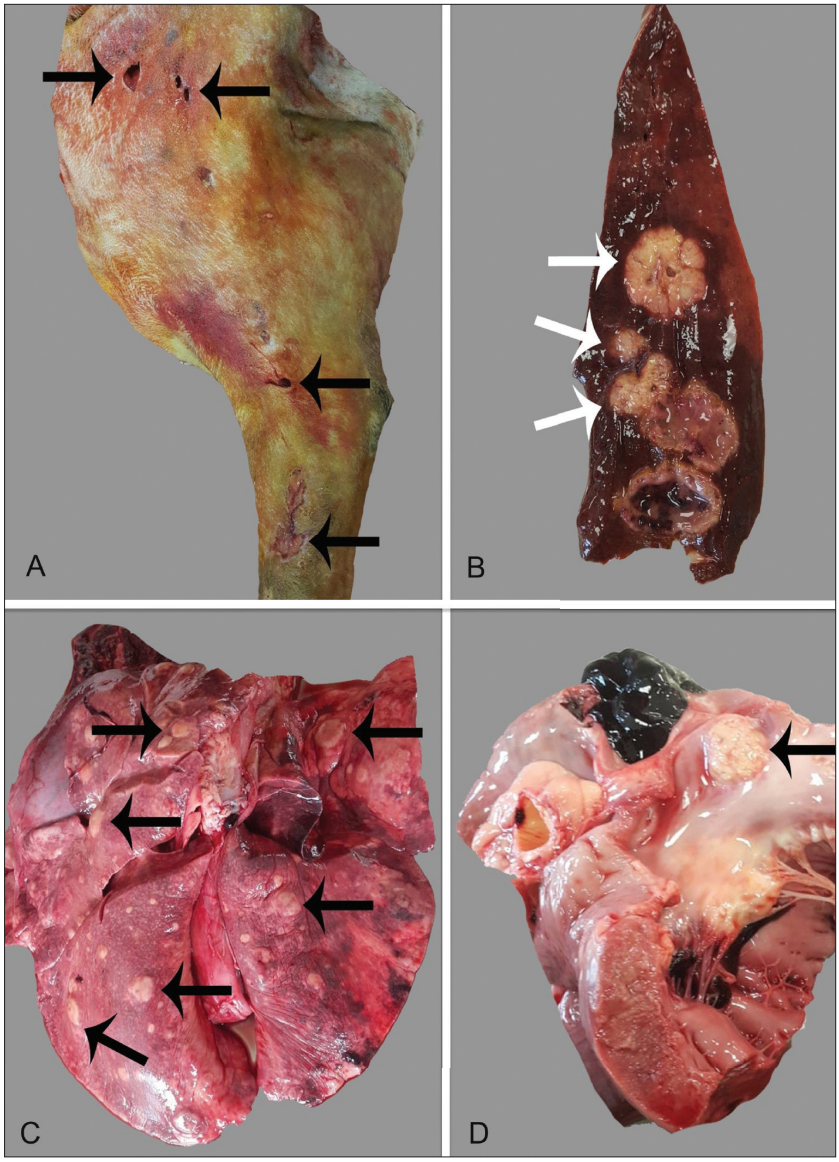

Fig 2. A- Perforated areas in skin of the left forefoot *(black arrows)*, **B-** Multiple yellowish-white colored abscesses in the liver *(white arrows)*, **C-** Different diameter yellowish-white foci in the lung *(black arrows)*, **D-** White colored focus in the aorta exit of the heart *(black arrow)*

were taken during necropsy were fixed in 10% formalin. Formalin fixed tissue samples were processed via paraffin embedding technique and sections were cut at 5 µm and stained with hematoxylin-eosine.

Microscopically, vacuolar and hydropic degeneration were detected in the hepatocytes together with congestion and edema in the liver. There were large abscesses with large areas of necrosis that were surrounded by connective tissue including macrophages and lymphocytes *(Fig. 3-A)*. Multifocal abscesses were observed with varying size and malacia areas in the brain. Meninges of the cerebellum was hyperemic and there were also diffuse cell infiltrations most of which were formed by polymorphic nuclear leukocytes, and the meninges were thickened *(Fig. 3-B)*. There was thickening and fibrotic areas in the kidney capsule. It was also noticed that the mesangial regions were enlarged in the renal glomeruli. Non-suppurative glomerulitis and periglomerulitis were seen in the kidney *(Fig. 3-C)*. Significant edema was observed in alveolar lumens in the lung. Many alveolar macrophages filled in the alveolar lumens with neutrophils *(Fig. 3-D)*. Widespread necrotic areas were seen in the stroma. Abscess formations separated to the septum by connective tissue was noticed in the heart *(Fig. 3-E)*. Mucoid degeneration was seen in the heart valves. Large necrotic areas were detected in pancreatic acini. Hypocellularity was also seen together with edema in the lymph follicles. Disseminated inflammatory changes, bleeding and necrosis were seen in subcutaneous tissues *(Fig. 3-F)*.

The lymph nodes, lung, liver of dog taken after necropsy for microbiological examination. The samples were inoculated into 5% sheep blood agar. The plate was incubated for 24 h at 37°C in aerobic conditions. After incubation period, the gram stained colonies of bacteria were shown microscopically as Gram negative rods. The bacteria were identified morphologically and biochemically by Vitek II with gram negative card as *Pantoea agglomerans*. *Pantoea agglomerans* was confirmed by PCR as described by

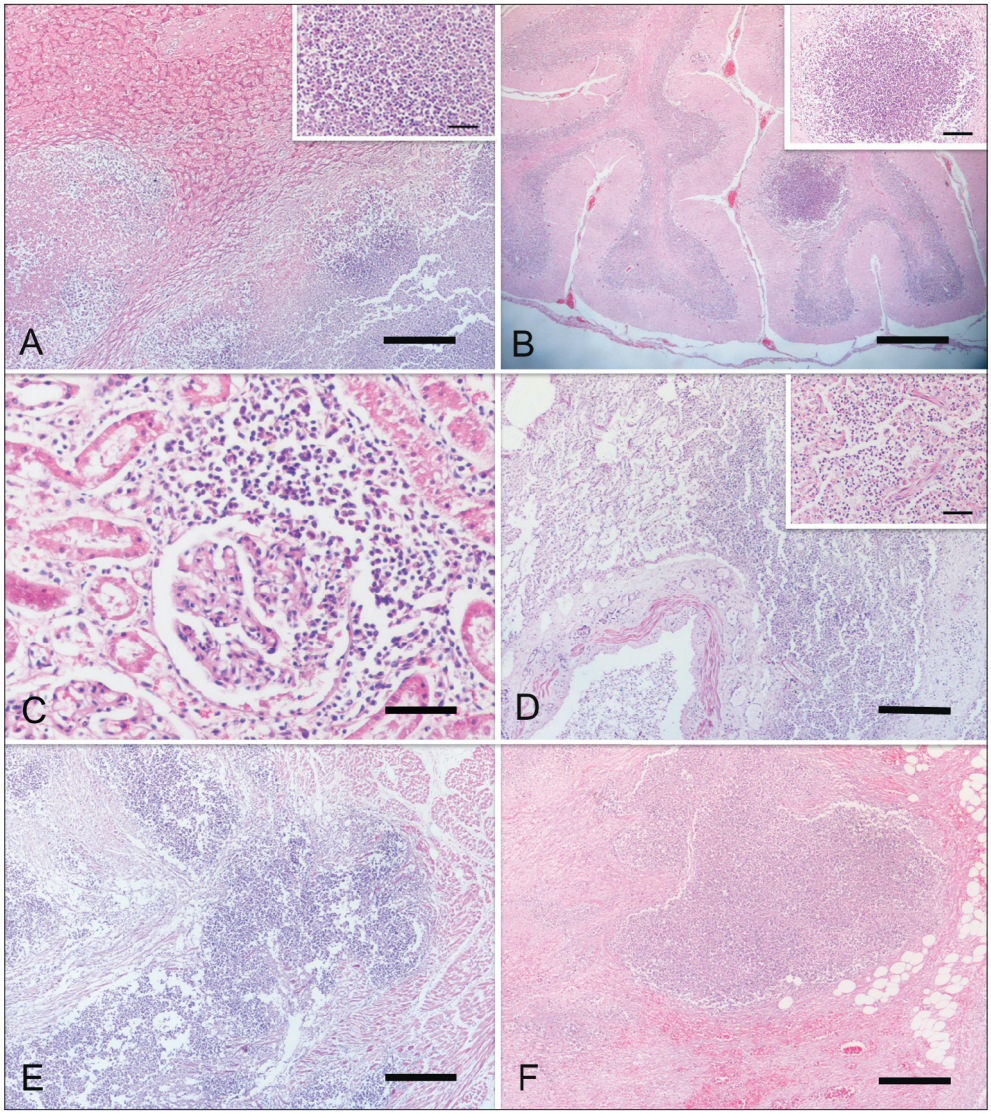

Fig 3. A- Degeneration in the hepatocytes with congestion and edema in the liver. H&E, Bar = 300 µm. Leukocyte especially neutrophil, macrophages and lymphocytes in the liver parenchyma. Inset shows a higher magnification of liver, H&E, Bar = 60 µm; **B-** Abscess foci in the cerebellum. H&E, Bar = 600 µm. Inset shows a higher magnification of cerebellum. H&E, Bar = 120 µm; **C-** Non-suppurative glomerulitis and periglomerulitis. H&E, Bar = 60 µm; **D-** Alveolar macrophages and neutrophils in the alveolar lumens in the lung. H&E, Bar = 300 µm. Inset shows a higher magnification of lung. H&E, Bar = 60 µm; **E-** Abscess formations in the heart. H&E, Bar = 300 µm; **F-** Bleeding, necrosis and inflammatory changes in subcutaneous tissue. H&E, Bar = 300 µm

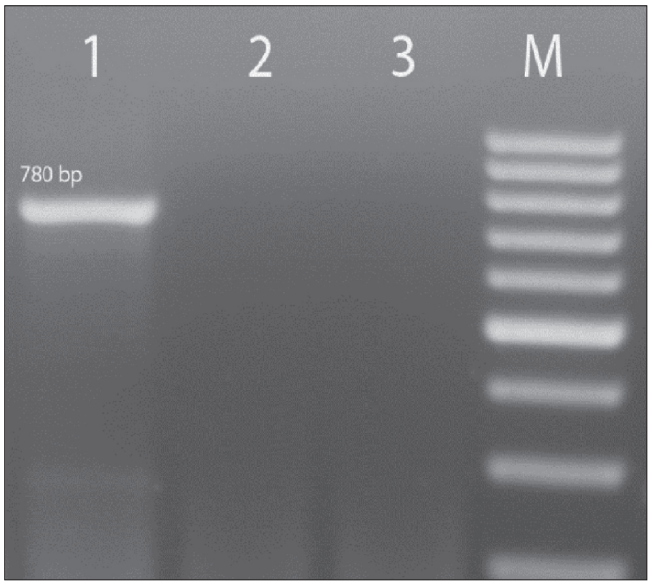

Fig 4. The PCR result of *Pantoea agglomerans*. M: marker (100-1000 bp); 1: *Pantoea agglomerans*; 2: *Escherichia coli*; 3: *Salmonella* spp.

previous study [9]. For this purpose, rep-F 5-TTGTGGGG GACATAAATTAACC-3 and rep-R5-AGGGCCATAGTGAGGA-AGGT-3 primer sets were used. In PCR, the band of 780 bp for rep gene were detected and the identification was confirmed as *Pantoea agglomerans (Fig. 4)*.

Discussion

Pantoea agglomerans is an opportunistic pathogen, and it has been reported especially in immunosuppressive patients. Infection are usually caused by infected plant parts that has penetrated the skin [2]. Septic arthritis [10], and muscle lesions [11], caused by plant thorn injury was reported in human medicine due to the bacteria that is found in plant surface. Reported diseases other than wound infection in humans include endophthalmitis [12], endocarditis [13] and osteomyelitis [14].

Infection caused by *Pantoea agglomerans* was infrequently reported in animals. In veterinary literature, abort, fibrinonecrotic placentitis in a mare [3], and pneumonia in a

cat were reported [5]. Also this agent was isolated in Brown Trout and Rainbow Trout [6,7].

In our case, *Pantoea agglomerans* was isolated in liver, subcutaneous tissues and lymph nodes and also *Klebsiella pneumonia* was isolated in lung on microbiological examination. Both *Klebsiella pneumonia* and *Pantoea agglomerans* bacteria are opportunistic pathogens. The presence of both bacteria in the dog may explain the increase in inflammatory activity, in particular neutrophils.

Abscesses have been identified in the liver, lung, heart, brain, cerebellum and subcutaneous tissues on macroscopic and microscopic examination in this case. In addition to this, widespread necrosis was observed, especially in the liver, lung, pancreas, heart and subcutaneous tissues.

Foreign body granuloma with giant cells that related with *Pantoea agglomerans* was reported in a human case. The authors were noticed that probable reason of these granuloma was penetration of plant thorn in to the muscle [11]. In our case, neutrophil infiltration and necrosis were the most prominent. Giant cells were not detected due to there have no foreign body penetration in the case history. Histopathological changes have been described in foetal lungs after equine abortion associated with *Pantoea agglomerans*. Interstitial inflammatory infiltrate of lymphocytes, macrophages, and neutrophils was seen in the lungs [3]. Similar histopathological changes were observed in our case.

Although *Pantoea agglomerans* mostly associated with infection in human medicine, the infection caused by this bacterium was uncommonly reported in animals. In this case report, a large number of abscesses included central nervous system and heart in a dog has been reported. Authors believe that these data would contribute to the veterinary literature.

Conflict of Interest

The authors declared that there is no conflict of interest.

Author Contributions

TG, Sİ and NK evaluated postmortal and microscopic examinations and wrote the manuscript. EB and KSİ are played role in the clinical examination and management of case. AF and MGS did phenotyping and molecular identification.

References

1. Gavini F, Mergaert J, Beji A, Mielcarek C, Izard D, Kersters K, De Ley J: Transfer of *Enterobacter agglomerans* (Beijerinck 1888) Ewing and Fife 1972 to *Pantoea* gen. nov. as Pantoea agglomerans comb. nov. and description of Pantoea dispersa sp. nov. *Int J Syst Evol Microbiol,* 39 (3): 337-345, 1989. DOI: 10.1099/00207713-39-3-337

2. Dutkiewicz J, Mackiewicz B, Lemieszek MK, Golec M, Milanowski J: *Pantoea agglomerans:* A mysterious bacterium of evil and good. Part III. Deleterious effects: Infections of humans, animals and plants. *Ann Agric Environ Med,* 23 (2): 197-205, 2016. DOI: 10.5604/12321966.1203878

3. Henker LC, Lorenzett MP, Keller A, Siqueira FM, Driemeier D, Pavarini SP: Fibrinonecrotic placentitis and abortion associated with Pantoea agglomerans infection in a mare. *J Equine Vet Sci,* 92:103156, 2020. DOI: 10.1016/j.jevs.2020.103156

4. Pomorski Z, Dutkiewicz J, Taszkun I, Woźniak M, Sitkowski W, Skórska C, Cholewa G: Studies on allergic conditioning of cattle pneumopathy, resulting from breathing in pneumoallergens comprised in organic dusts. *Ann Univ Mariae Curie Sklodowska Med,* 48, 183-193, 1993.

5. Decuadro A, Ruiz N, Martino P, Sala T, Benech A: Neumonía en gato causada por *Enterobacter (Pantoea) agglomerans*, reporte de un caso clínico. *Veterinaria (Montev),* 51 (198): 26-31, 2015.

6. Loch TP, Faisal M: Isolation of *Pantoea agglomerans* from brown trout *(Salmo trutta)* from Gilchrist Creek, Michigan, USA. *Bull Eur Assoc Fish Pathol,* 27 (5): 200-204, 2007.

7. Saticioglu IB, Duman M, Altun S: Antimicrobial resistance and molecular characterization of *Pantoea agglomerans* isolated from rainbow trout *(Oncorhynchus mykiss)* fry. *Microb Pathog,* 119, 131-136, 2018. DOI: 10.1016/j.micpath.2018.04.022

8. Roberts DE, McClain HM, Hansen DS, Currin P, Howerth EW: An outbreak of *Klebsiella pneumoniae* infection in dogs with severe enteritis and septicemia. *J Vet Diagn Invest,* 12 (2): 168-173, 2000. DOI: 10.1177/104063870001200215

9. Alobaidi LAH: Isolation, identification, and molecular detection of *Pantoea agglomerans* from nuts in commercial markets in Al Samawa City. *J Int Acad Res Multidiscip,* 2 (6): 235-241, 2014.

10. Demircan E, Kasap Demir B, Şahin H, Bayram A, Kanık A: *Pantoea agglomerans* as a cause of foreign body related septic arthritis in a child: Case report and review of the literature. *J Pediatr Infect Dis,* 15 (5): 265-268, 2020. DOI: 10.1055/s-0040-1709701

11. Jain S, Bohra I, Mahajan R, Jain S, Chugh T: *Pantoea agglomerans* infection behaving like a tumor after plant thorn injury: An unusual presentation. *Indian J Pathol Microbiol,* 55 (3): 386-388, 2012. DOI: 10.4103/0377-4929.101754

12. Seok S, Jang YJ, Lee SW, Kim HC, Ha GY: A case of bilateral endogenous *Pantoea agglomerans* endophthalmitis with interstitial lung disease. *Korean J Ophthalmol*, 24 (4): 249-251, 2010. DOI: 10.3341/kjo.2010.24.4.249

13. Williams AJK, Scott RJD, Lightfoot NF: Erwinia herbicola as a cause of bacterial endocarditis. *J Infect*, 12, 71-73, 1986. DOI: 10.1016/s0163-4453(86)94978-9

14. Vincent K, Szabo RM: *Enterobacter agglomerans* osteomyelitis of the hand from a rose thorn. A case report. *Orthopedics*, 11 (3): 465-467, 1988.

INSTRUCTION FOR AUTHORS

1- Kafkas Universitesi Veteriner Fakultesi Dergisi (abbreviated title: Kafkas Univ Vet Fak Derg), published bi-monthly (ISSN: 1300-6045 and e-ISSN: 1309-2251). We follow a double-blind peer-review process, and therefore the authors should remove their name and any acknowledgment from the manuscript before submission. Author names, affiliations, present/permanent address etc. should be given on the title page only.

The journal publishes full-length research papers, short communications, preliminary scientific reports, case reports, observations, letters to the editor, and reviews. The scope of the journal includes all aspects of veterinary medicine and animal science.

Kafkas Universitesi Veteriner Fakultesi Dergisi is an Open Access journal, which means that all content is freely available without charge to the user or his/her institution. Users are allowed to read, download, copy, distribute, print, search, or link to the full texts of the articles, or use them for any other lawful purpose, without asking prior permission from the publisher or the author. This is in accordance with the BOAI definition of Open Access.

The official language of our journal is **English**. Additionally, all the manuscripts must also have Turkish title, keywords, and abstract (translation will be provided by our journal office for foreign authors).

2- The manuscripts submitted for publication should be prepared in the format of Times New Roman style, font size 12, A4 paper size, 1.5 line spacing, and 2.5 cm margins of all edges. The legend or caption of all illustrations such as figure and table and their appropriate position should be indicated in the text. Refer to tables and figures in the main text by their numbers. Also figure legends explanations should be given at the end of the text.

The figures should be at least 300 dpi resolution.

The manuscript and supplementary files (figure etc.) should be submitted by using online manuscript submission system at the address of *http://vetdergi.kafkas.edu.tr/*

During the submission process, the authors should upload the figures of the manuscript to the online manuscript submission system. If the manuscript is accepted for publication, the **Copyright Transfer Agreement Form** signed by all the authors should be sent to the editorial office.

3- The authors should indicate the name of the institute approves the necessary ethical commission report and the serial number of the approval in the material and methods section. If necessary, the editorial board may also request the official document of the ethical commission report. If an ethical problem is detected (not reporting project information, lack of ethical committee information, conflict of interest, etc.), the editorial board may reject the manuscript at any stage of the evaluation process.

4- In the interests of brevity and standalone readability, Kafkas Universitesi Veteriner Fakultesi Dergisi strongly discourages the submission of multi-part manuscripts. Authors who feel that their topic requires an exception should obtain approval from the editor before submission of a multi-part manuscript. If submitted, multi-part manuscripts can be assigned to different editorial board members and independent outside expert reviewers. All parts of the manuscript are required to be loaded into the online system at the same time.

5- Types of Manuscripts

Original (full-length) manuscripts are original and proper scientific papers based on sufficient scientific investigations, observations and experiments.

Manuscripts consist of the title, abstract and keywords, introduction, material and methods, results, discussion, and references and it should not exceed 12 pages including text. The number of references should not exceed 50. The page limit does not include tables and illustrations. Abstract should contain 200±20 words.

Short communication manuscripts contain recent information and findings in the related topics; however, they are written with insufficient length to be a full-length original article. They should be prepared in the format of full-length original article but the abstract should not exceed 100 words, the reference numbers should not exceed 15 and the length of the text should be no longer than 6 pages in total. The page limit does not include tables and illustrations. Additionally, they should not contain more than 4 figures or tables.

Preliminary scientific reports are a short description of partially completed original research findings at an interpretable level. These should be prepared in the format of full-length original articles. The length of the text should be no longer than 4 pages in total.

Case reports describe rare significant findings encountered in the application, clinic, and laboratory of related

fields. The title and summary of these articles should be written in the format of full-length original articles and the remaining sections should be followed by the Introduction, Case History, Discussion and References. The length of the text should be no longer than 4 pages in total. The page limit does not include tables and illustrations.

Letters to the editor are short and picture-documented presentations of subjects with scientific or practical benefits or interesting cases. The length of the text should be no longer than 3 pages in total. The page limit includes tables and illustrations.

Reviews are original manuscripts that gather the literature on the current and significant subject along with the commentary and findings of the author on a particular subject. The title and summary of this manuscript should be prepared as described for the full-length original articles and the remaining sections should be followed by introduction, text (with appropriate titles), conclusion, and references. The length of the text should be no longer than 15 pages in total.

6- The necessary descriptive information (thesis, projects, financial supports, etc.) scripted as an italic font style should be explained below the manuscript title after placing a superscript mark at the end of the title.

7- At least 30% of the references of any submitted manuscript (for all article categories) should include references published in the last five years.

References should be listed with numerical order as they appear in the text and the reference number should be indicated inside the parentheses at the cited text place. References should have the order of surnames and initial letters of the authors, title of the article, title of the journal (original abbreviated title), volume and issue numbers, page numbers and the year of publication and the text formatting should be performed as shown in the example below.

Example: **Yang L, Liu B, Yan X, Zhang L, Gao F, Liu Z:** Expression of ISG15 in bone marrow during early pregnancy in ewes. *Kafkas Univ Vet Fak Derg,* 23 (5): 767-772, 2017. DOI: 10.9775/kvfd.2017.17726

If the reference is a book, it should follow surnames and initial letters of the authors, title of the book, edition number, page numbers, name and location of publisher and year of publication. If a chapter in a book with an editor and several authors is used, names of chapter authors, name of chapter, editors, name of the book, edition number, page numbers, name and location of publisher and year of publication and the formatting should be performed as shown in the example below.

Example: **Mcllwraith CW:** Disease of joints, tendons, ligaments, and related structures. **In,** Stashak TS (Ed): Adam's Lameness in Horses. 4th ed., 339-447, Lea and Febiger, Philadelphia, 1988.

DOI number should be added to the end of the reference.

In the references can be reached online only, the web address and connection date should be added at the end of the reference information. The generally accepted scientific writing instructions must comply with the other references. Abbreviations, such as "et al" and "and friends" should not be used in the list of the references.

Follow the link below for **EndNote Style of Kafkas Universitesi Veteriner Fakultesi Dergisi;**
https://researchsoftware.com/downloads/journal-faculty-veterinary-medicine-kafkas-university

8- Latin expression such as species names of bacteria, virus, parasite, and fungus and anatomical terms should be written in italic character, keeping their original forms.

9- The editorial board has the right to perform necessary modifications and a reduction in the manuscript submitted for publication and to express recommendations to the authors. The manuscripts sent to authors for correction should be returned to the editorial office within a month. After pre-evaluation and agreement of the submitted manuscripts by the editorial board, the article can only be published after the approval of the field editor and referee/s specialized in the particular field.

10- All responsibilities from published articles merely belong to the authors. According to the ethical policy of our journal, plagiarism/self-plagiarism will not be tolerated. All manuscripts received are checking by plagiarism checker software, which compares the content of the manuscript with a broad database of academic publications.

11- There is no copyright fee for the authors.

12- The authors are charged a fee on acceptance of the manuscript to cover printing costs and other expenses. This payment information can be found at *http://vetdergi.kafkas.edu.tr/*

13- Reprints (in multiples of 50) of the article are sent to the authors for free.

SUBMISSION CHECKLIST

Please use below list to carry out a final check of your submission before you send it to the journal for review. Ensure that the following items are present in your submission:

- Cover letter

• Importance and acceptability of the submitted work for the journal have been discussed (Please avoid repeating information that is already present in the abstract and introduction).

• Other information has been added that should be known by the editorial board (e.g.; the manuscript (or any part of it) has not been published previously or is not under consideration for publication elsewher.

- Title page

• Title, running title (should be a brief version of the title of your paper, no exceed 50 characters)

• The author's name, institutional affiliation, Open Researcher and Contributor ID **(ORCID)**

• Congress-symposium, project, thesis etc. information of the manuscript (if any)

• Corresponding author's address, phone, fax, and e-mail information

- Manuscript

• Title, abstract, keywords and main text

• All figures (include relevant captions)

• All tables (including titles, description, footnotes)

• Ensure all figure and table citations in the text match the files provided

• Indicate clearly if color should be used for any figures in print

Further considerations

• Journal policies detailed in this guide have been reviewed

• The manuscript has been "spell checked" and "grammar checked"

• Relevant declarations of interest have been made

• Acknowledgment and conflicts of interest statement provided